VNIVERSITAT DE VALÈNCIA
FACULTAT DE
CIÈNCIES BIOLÒGIQUES

Fundación para el Fomento de la
Investigación Sanitaria y Biomédica
de la Comunitat Valenciana

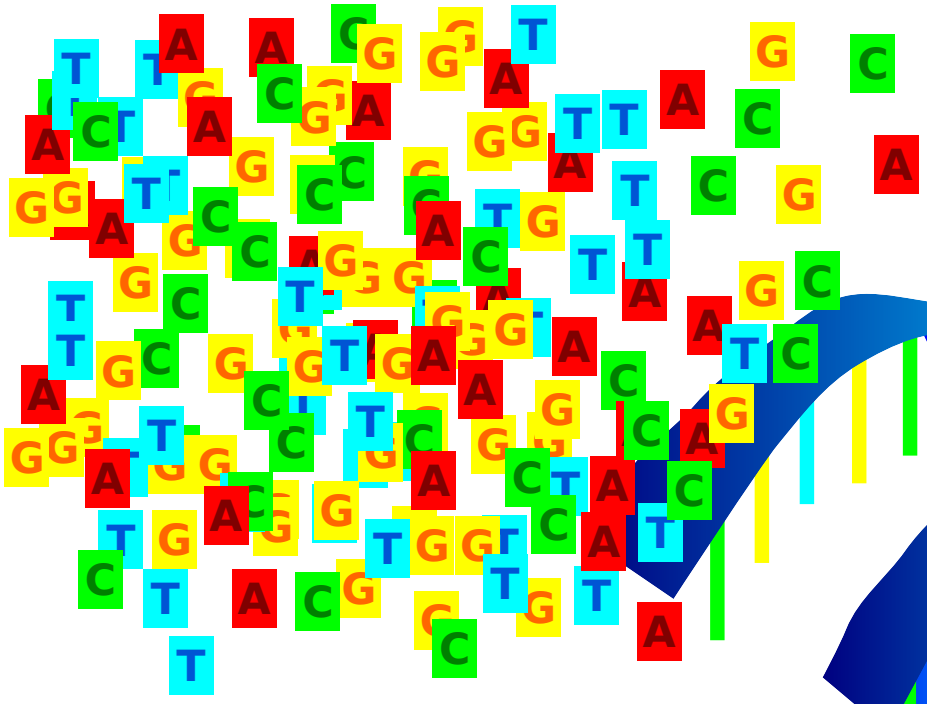

# Metagenomics of the Human Gut Microbiome Directed by the Flow Cytometry

PhD thesis of

**Mária Džunková**

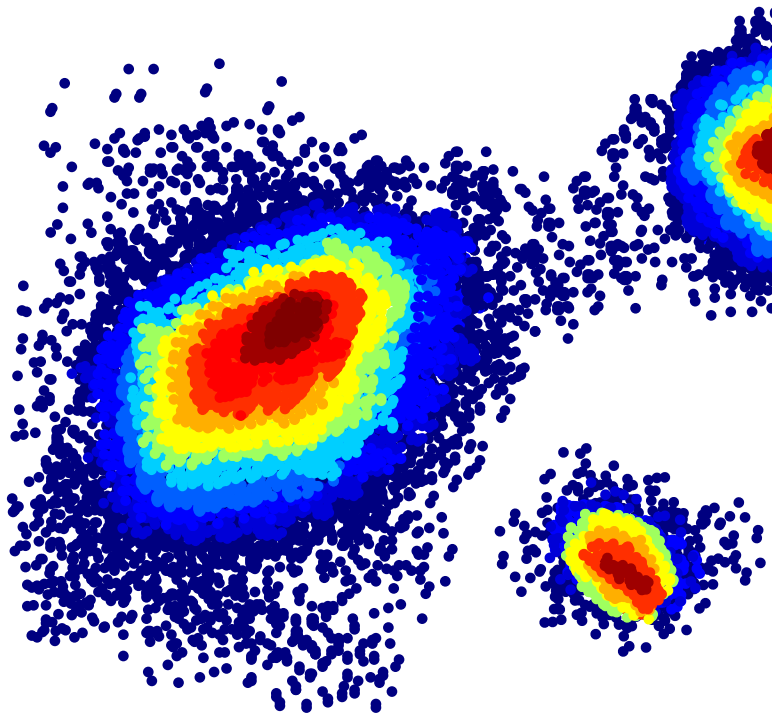

DIRECTORS:
Prof. Andrés Moya
Dr. Giuseppe D'Auria

Valencia, 2016

**UNIVERSITY OF VALENCIA**

Faculty of Biological Sciences

Valencian Region Foundation for the Promotion of Health and Biomedical Research (FISABIO) - Public Health


# METAGENOMICS OF THE HUMAN GUT MICROBIOME DIRECTED BY THE FLOW CYTOMETRY

PhD thesis of

**Mária Džunková**

Directors

Prof. Andrés Moya

Dr. Giuseppe D'Auria

Valencia, Spain, 2016

# Certificado

Prof. Andrés Moya, Catedrático del Departamento de Genética de la Universitat de València, y Dr. Giuseppe D'Auria, investigador del Área de Genómica y Salud de la Fundación para el Fomento de la Investigación Sanitaria y Biomédica (FISABIO) de la Comunidad Valenciana, certifican que la memoria titulada "Metegenomics of the human gut microbiome directed by the flow cytometry" ha sido realizada bajo su dirección por Mária Džunková para optar al grado de Doctor Internacional por la Universidad de Valencia. Y para que así conste, firman el presente certificado:

en Valencia, 4 de Marzo, 2016.

Prof. Andrés Moya

Dr. Giuseppe D'Auria

PhD student signature: Mária Džunková

# Acknowledgement

I would like to express my heart-whole gratitude to my supervisors Prof. Andrés Moya and Dr. Giuseppe D'Auria for guiding me during 5.5 years of my Ph.D. thesis. Dr. D'Auria was an excellent tutor and it is difficult to enumerate all the things I have learned from him. Especially, I am very grateful that he has taught me to enjoy working on challenging and apparently difficult projects. Prof. Moya was an excellent group leader role model for me. I was very lucky that I got the opportunity to do my PhD with them.

Moreover, I would like to thank the following people for:

- guidance during my temporary research stay on Harvard: Prof. Ciaran Kelly and Dr. Xianhua Chen from Beth Israel Deaconess Medical Center (BIDMC) of Harvard Medical School, Boston, USA
- assistance with my flow cytometry experiments: Ana Flores from the Faculty of Pharmacy, University of Valencia (UV) and John Tigges and Vasilis Toxavidis from BIDMC
- 454 and Illumina sequencing: Dr. Núria Jiménez and Llúcia Martínez from FISABIO - Public Health, Valencia
- assistance with Sanger sequencing: Dr. Manuela Torres from FISABIO; Central Service for Experimental Research team of UV and the DNA Sequencing Core team of Brigham and Women's Hospital of Harvard Medical School, Boston, USA
- assistance with programming scripts: Alejandro Artacho, Jorge Francisco Vázquez-Castellanos and Rodrigo García from FISABIO
- collection of fecal samples from patients: Kelsey Shields and Joshua Hansen from BIDMC
- assistance with preparation of culture media: Concepción Hueso from FISABIO
- providing bacterial isolates: Dr. Carles Úbeda, Ana Djukovic and Sandrine Isaac from FISABIO
- teaching me working with Digital Microdissector: Dr. Victoria Petkova from BIDMC
- collaboration on the article associated with the chapter about adaptation of sequencing protocols for sequencing of limited DNA samples: Dr. Marc Garcia-Garcerà from Institut Pasteur, Paris, France and Prof. Francesc Calafell from Institute of Evolution Biology, University Pompeu Fabra, Barcelona, Spain
- collaboration of the article associated with the chapter about selective inhibitory effect of 8HQ: Dr. Jitka Nováková, Dr. Šárka Musilová, Dr. Eva Vlková and Prof. Ladislav Kokoška from the Czech University of Life Sciences in Prague
- collaboration on the articles associated with the chapter about the active and IgA-coated cells sorting: Dr. Francecs Peris-Bondia from Université Libre de Bruxelles, Brussels, Belgium, Prof. Amparo Latorre, Dr. Alex Mira and Áurea Simón-Soro from FISABIO - Public Health, Valencia; Maria Carmen Collado from The Institute of Agrochemistry and Food Technology, Valencia and Dr. Shauna Culshaw from the School of Dentistry in Glasgow, United Kingdom
- emotional support: Erick Steve Giron Peña

This thesis has been written in the LaTeX environment. It contains hypertext links (marked by light blue color) connecting to the referred sections, figures, tables, acronyms glossary and bibliography within this thesis. The hypertext links are also connected to the on-line sources: the chemical product reference numbers are connected with the websites selling those products and the bibliography references are connected to the websites containing the cited articles.

The thesis contains appendix with detailed laboratory protocols and examples of programming scripts allowing the readers to follow the performed work.

# Contents

Chapter 1

# General Introduction

# 1.1 The human gut

## 1.1.1 Anatomy of the human intestinal tract

The human gastrointestinal tract (GI) is a one-way alimentary canal 7 m long. It begins at mouth, continues through organs pharynx, esophagus, stomach, small intestine (composed from duodenum, jejunum, proximal ileum and distal ileum), large intestine (composed from cecum, colon, rectum, and anal canal) and terminates at anus (Figure 1, panel A). In the GI tract, nutrients from food are being absorbed and at the same time toxin components or material that cannot be digested are being eliminated.

In the transversal section, the GI tract is composed of four tissue layers throughout its length: mucosa, submucosa, muscularis and serosa (Figure 1, panel B). The outer layer of mucosa is called epithelium, which is in direct contact with lumen - the inner part of the gastrointestinal tract. Interspersed among its epithelial cells are goblet cells, which secrete mucus and fluid into the lumen, and enteroendocrine cells, which secrete hormones. Under the epithelium tissue, the lamina propria layer can be found. It contains loose connective tissue and numerous blood and lymphatic vessels which transport absorbed nutrients to other cells of the body. It also has an immune function, as it houses lymphocytes. The lymphocyte clusters are particularly substantial in the distal ileum where they are known as Peyer's patches (Savage, 1977).

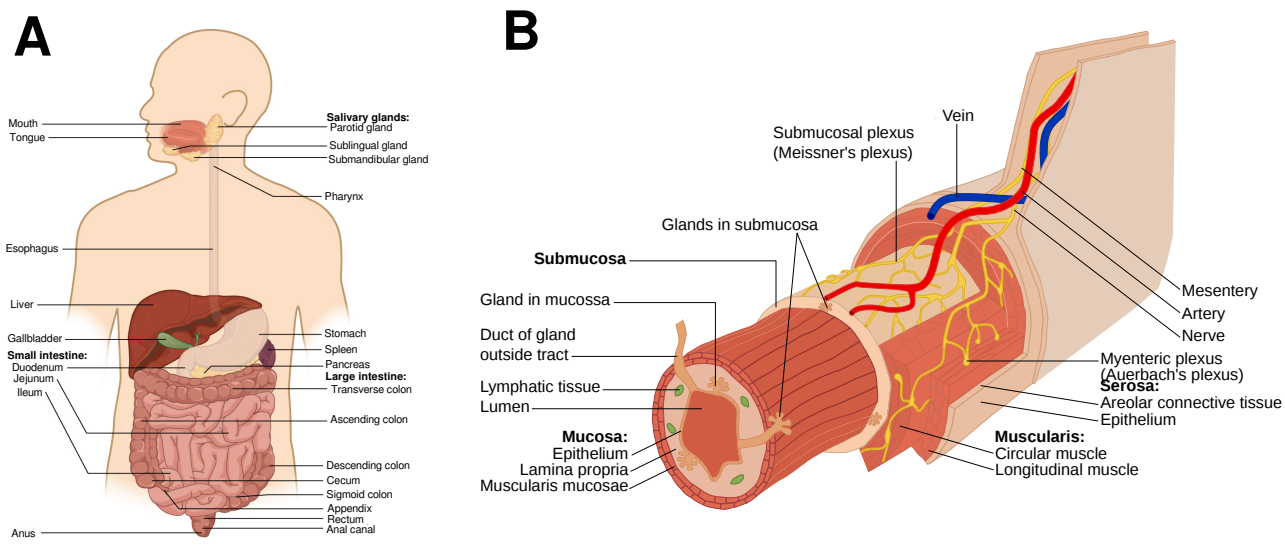


Figure 1: **Human intestinal tract. Panel A:** Components of the digestive system. **Panel B:** Layers of the alimentary canal. Source: OpenStax College

## 1.1.2 Gut microbiome

The organs of the GI tract are inhabited by numerous and diverse bacteria. They can be found in the mucosal structures of epithelium or either hidden deeper in so called crypts of Lieberkuhn (Savage, 1977). A layer of mucus on the epithelial surface protects against adhesion and invasion by many pathogenic species producing bacterial toxins (Macfarlane et al., 2005). Bacteria also form biofilms associated with food particles in the

lumen (Van Wey et al., 2011). The total microbial load of the intestine is $10^{13}$ - $10^{14}$ microorganisms, which collectively contain at least 100 × more genes than the human genome (Gill et al., 2006).

The interaction between humans and microorganisms inhabiting their bodies can be described as symbiotic relation in three different forms (Moya et al., 2008; Hooper and Gordon, 2001):

- Parasitic (pathogenic) bacteria: they increase their fitness (the ability to both survive and reproduce), while the fitness of human hosts is decreased.
- Mutualistic relationship: humans and the microorganism benefit from this relation.
- Commensal bacteria: their fitness is increasing without affecting humans.

In the human gut, numerous viruses can be found, too. The majority of them are bacteriophages, the viruses that attack bacteria (Minot et al., 2013). Rohwer (2003) estimated that if each of the bacterial host have at least 10 different phages, the number of phages in the human gut might be $10^9$.

The recent studies suggested that the colonization of the human gut has intrauterine origin (Gosalbes et al., 2013). The bacterial composition of the earliest microbiome is influenced by the way of delivery. The major compositional changes in early childhood occur when the breastfeeding frequency decreases and the milk is substituted by solid food (Koenig et al., 2011).

The species composition of the gut microbiota varies between individuals. However, the common basic microbial functions can be found in all humans (HMPC, 2012):

- **Metabolism of exfoliated epithelial cells and mucins:**
  Bacteria metabolize exfoliated epithelial cells and mucins to produce multiple metabolites that influence intestinal epithelial function (Macfarlane et al., 2005).
- **Metabolism of partially digested food:**
  The gut bacteria contain genes involved in metabolism of sucrose, starch, glycans, arabinose, mannose, xylose, etc. This metabolism results in synthesis of methane, vitamins, isoprenoids, and short-chain fatty acids, such as butyrate (Gill et al., 2006). It means that the gut bacteria influence energy balance of the host.
- **Detoxification of xenobiotics:**
  Bacteria can metabolize xenobiotics, including therapeutic drugs, antibiotics, and diet-derived bioactive compounds, such as plant-derived phenolics. It means that the bacteria may influence the absorption of medicaments (Gill et al., 2006). Unfortunately, microbial xenobiotic metabolism remains a largely underexplored component of the pharmacology (Haiser and Turnbaugh, 2013).
- **Modulation of intestinal architecture:**
  Bacteria also promote vessel formation in the intestinal epithelium by modulating tissue factor signaling (Reinhardt et al., 2012). The most prominent feature of germ-free animals is a greatly enlarged cecum (Wostmann, 1981).
- **Increase of the intestinal motility:**
  Bacterial metabolites are incorporated in the serotonine pathway modulating intestinal motility (Yano et al., 2015).

- **Protection against intestinal injury:**
  Bacterial metabolites enhance barrier integrity and facilitate wound repair after injury (Rakoff-Nahoum and Medzhitov, 2008). For example, *Bacteroides thetaiotaomicron* increases the resistance of the gut to injury by inducing the expression of molecules which are involved in maintenance of junctional complexes in the epithelium allowing cells to withstand shearing forces (Hooper et al., 2001). Also several *Lactobacillus* strains firm tight junctions between epithelial cells, resulting in reduced epithelial permeability (Lutgendorff et al., 2008).

- **Regulation of pathogen invasion:**
  It was demonstrated that some intestinal infections (e.g. caused by *Salmonella*) are regulated not only by human immune system, but also by the gut microbes which produces bacteriocins and other inhibiting metabolites, or by competition with the pathogens for nutrients and space (Endt et al., 2010).

- **Interaction with human immune system:**
  Peyer's patches, mesenteric lymph nodes and numerous lymphoid follicles form intestinal lymphoid tissues. They generate microbiome-reactive IgA-producing B cells. It was found that a peptidoglycan from Gram-negative bacteria (such as *Bacteroides fragilis*) is necessary to induce genesis of intestinal lymphoid tissues. The maturation of intestinal lymphoid tissues into B-cells clusters requires subsequent detection of bacteria by toll-like receptors. In the absence of intestinal lymphoid tissues, the composition of the intestinal bacterial community is profoundly altered. It means that the bacterial commensals and the human immune system communicate to generate adaptive lymphoid tissues and together maintain intestinal homeostasis (Bouskra et al., 2008; Mazmanian et al., 2005).

- **Modulation of behavior and brain functions:**
  Using measures of motor activity and anxiety-like behavior in germ-free mice compared to mice with controlled microbiota composition, differences in expression of genes in the brain metabolic pathways have been detected. Increased motor activity and reduced anxiety was observed in germ-free mice (Heijtz et al., 2011; Bercik et al., 2011). Probiotic bacteria were found to correct some behavioral alterations in autism (Hsiao et al., 2013).

# 1.2 Identification of gut bacteria and viruses

## 1.2.1 Sequencing approaches for gut microbiome studies

**Whole genome sequencing**

In bacterial genomics, whole genome sequence comes usually from DNA extracted from one colony considering it as the most reliable approximation to study the isolate or strain. The genetic information of bacteria is stored in a nucleoid (a bacterial chromosome) and in plasmids. During the DNA extraction process, the cells are disrupted by chemical agents and DNA is purified from proteins and other organic residues (Ausubel et al., 1992). For plasmid DNA recovery, protocols focused on circular DNA extraction must be applied (Birnboim and Doly, 1979).

The length of bacterial genomic DNA is several millions of base pairs (bp). The extracted DNA must be fragmented in order to fit the maximum read length achieved by the current sequencing platforms. The sequencing approach, in which fragmented genomic DNA is sequenced randomly, is called shotgun. The DNA fragmentation may be performed mechanically, using a sonicator, a nebulizer or the Hydroshear equipment (Digilab), or enzymatically, by restriction enzymes or tranposases. During sonication the vibration of the ultrasonic waves produce gaseous cavitations in the liquid that shears DNA molecules through resonance vibration. In nebulization, compressed nitrogen forces repeatedly the DNA to go through a small hole producing random mechanically sheared fragments (Knierim et al., 2011). The Hydroshear forces DNA diluted in liquid to pass through a tube with an abrupt contraction what is accompanied by fluid acceleration through a small hole leading to the DNA shearing. The enzymatic fragmentation is achieved by restriction enzymes cutting DNA at specific nucleotide sequences - restriction sites (Roberts and Murray, 1976). Different restriction enzymes may me combined for increasing randomness of the shearing (e.g. commercial kit NEBNext). Another type of enzymatic fragmentation is so called "tagmentation" (commercialized as Nextera), in which DNA is fragmented by transposase, while the sequencing adaptors are incorporated simultaneously (Syed et al., 2009). After sequencing the DNA fragments are aligned by computer programs and merged into longer units called contigs (genome assembly). The fragments must overlap each other and cover the genome several times. The required minimal genome coverage depends on error rate of the sequencing platform and on the genome complexity (Sims et al., 2014).

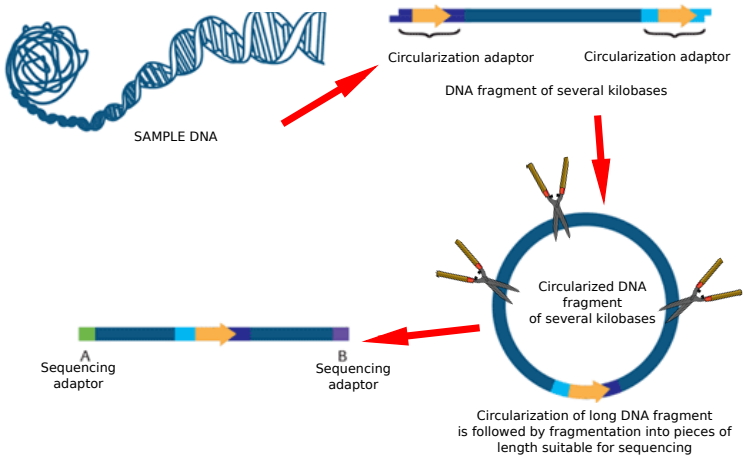


Figure 2: **Paired-end sequencing library preparation workflow.** Adapted from source: 454 sequencing library preparation protocol

Genomes may contain numerous repetitive fragments and genome rearrangements. Paired-end reads (Figure 2) may improve assemblies of such genomes (in the Illumina platform called mate-pairs). The original

genomic DNA is cut into longer pieces , e.g. 20 kbp long by the Hydroshear, and circularization adaptors allowing formation of DNA circles are attached to its ends. These circularized molecules are then fragmented as in the case of common sequencing library preparation. The specialized magnetic beads select the fragments than contain the circularization adaptor, while the fragments without this adaptor are removed. The fragments containing the circularization adaptors are ligated to the normal sequencing adaptors and sequenced. The pair-ends connected by the circularization adaptor are in the original genome sequence present with the distance of 20 kbp, what helps to order the contigs previously obtained by the common shotgun sequencing.

In the present time (2015), there are 54,468 genomes of 3,270 different bacterial species deposited in the National Center for Biotechnology Information (NCBI), from which 122 species are sequenced with the coverage and precision sufficient for labeling them as the reference genomes. The remaining genomes are partial assemblies containing genomic sequence covering 10-90 % of the whole genome sequence. The majority of the sequenced genomes belongs to the phyla *Proteobacteria*, followed by *Firmicutes* and *Actinobacteria* (Tatusova et al., 2014).

The genomes deposited in the databases can be used as backbone for mapping of obtained reads. Applications are very wide. Differences between sequenced bacterial strains can be studied on the level of the single nucleotide polymorphism (SNP) (Kuroda et al., 2010). In addition, comparison of different sequenced strains belonging to the same species can be performed, thus the species pan-genome would be calculated. It would be composed of a "core genome" containing genes present in all strains, and of a "dispensable genome" containing genes present in two or more strains and genes unique to the single strains (Medini et al., 2005).

### Metagenomics

The shotgun metagenomics allows researchers to sample DNA fragments from all organisms present in a given complex environmental sample, including the unknown or unculturable ones (Handelsman, 2004). The total environmental DNA is fragmented and ligated with the sequencing adaptors (Figure 3). In contrast to the sequencing of single organism genome, the metagenomics usually will does not end up with complete genomes due to the deep sequencing efforts required. Nevertheless, complete genomes can be obtained from environments containing low complexity communities (Vieites et al., 2009; Bhatt et al., 2013).

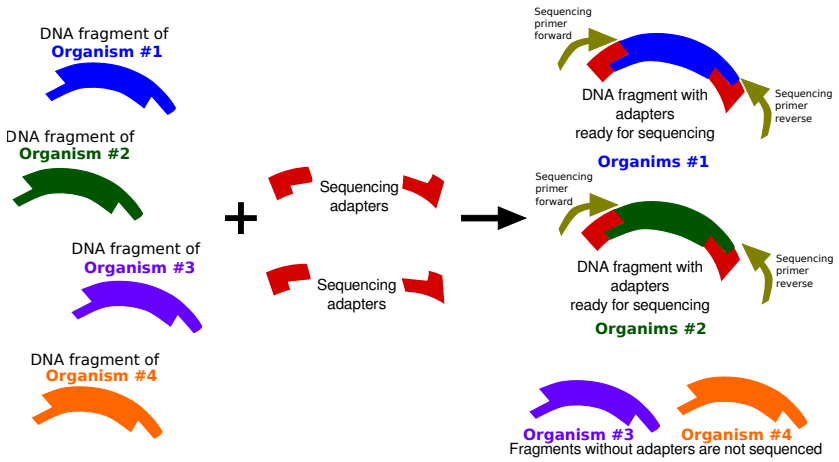


Figure 3: **Preparation of a sequencing library from an environmental sample**

The basic approach for analysing metagenomic dataset relies on functional or taxonomic annotation by

comparison with databases of completed bacterial genomes. However, when a metagenomic sequence is aligned to such a database, its sequence can match a large list of potential organisms especially when a conserved sequence is queried. Nowadays, numerous computational algorithms for estimation of the taxonomic content have been published (Huson et al., 2007). The species diversity in a metagenomic sample can be estimated also by grouping the sequences according to their GC content or oligonucleotide frequencies (short string of nucleotides, e.g. 4 or 6 bp) (Teeling et al., 2004). Theoretically, samples from the same genomic origin should present equivalent or similar oligonucleotide content, so analysis of oligonucleotides frequencies should allow the discrimination of samples with potential contamination (Willner et al., 2009). It is also possible to detect novel organisms (Dodsworth et al., 2013).

When the metagenomic sequences are assembled into contigs, a deeper analysis can be performed. For example, proteins encoded in open reading frames (ORFs) may be detected and compared with databases of protein sequences containing the information about their functions (Hunter et al., 2012). The comparison of the results of the taxonomic assignation and the annotation of ORF gives a more complete picture of the metabolic pathways in the microbial community. For example, the study of Human Microbiome Project (HMPC, 2012) revealed that most communities of the different human body sites consists of a single dominant phylum (such as *Firmicutes* or *Bacteroidetes*). However, conversely, most metabolic pathways are evenly distributed across all individuals and all body habitats (Figure 4).

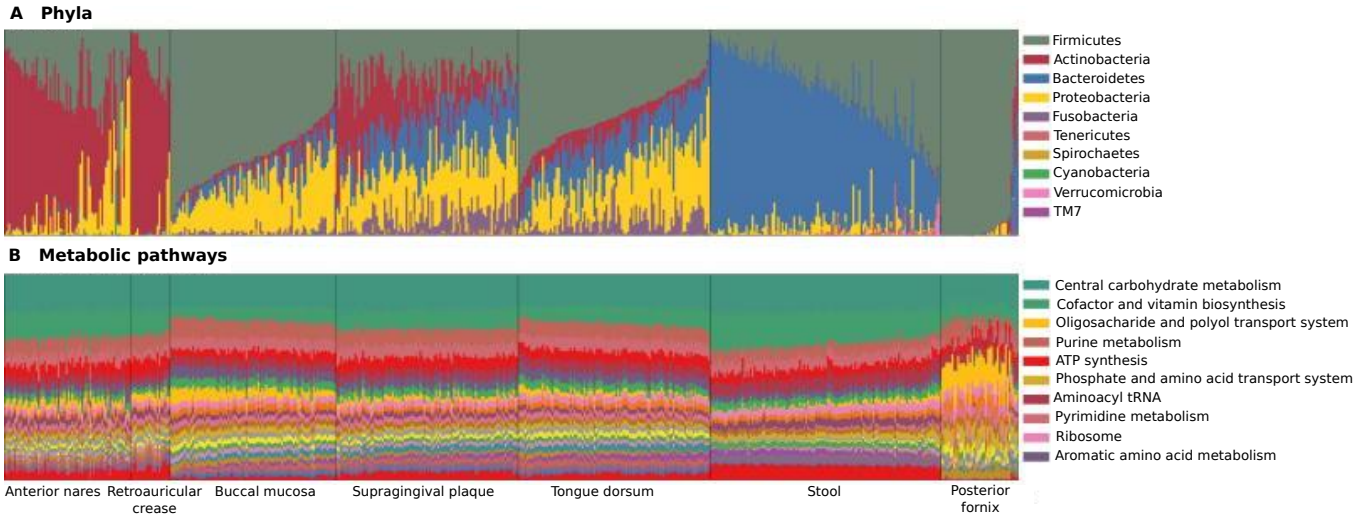


Figure 4: **Carriage of microbial taxa varies while metabolic pathways remain stable within a healthy population.** Author: HMPC (2012)

### Transcriptomics

The genome sequencing gives us information about the genetic potential of the sequenced organism. However, gene expression depends largely from environmental conditions and the growth stage. The gene expression is accomplished by RNA. The set of all RNA molecules including messenger RNA (mRNA), ribosomal RNA (rRNA), transfer RNA (tRNA) and other non-coding RNA, which are transcribed in one cell or a population of cells, is called a transcriptome. The size of a transcriptome is smaller than the size of a genome, because it contains only information about genes expressed in the moment of RNA extraction, and only the gene-coding regions of a genome (Okubo et al., 1992). For example, transcriptomics can be applied

to bacterial isolates cultured in certain conditions. Moroever, it can also reveal the dynamics of the gene expression in microbial communities over time (Vieites et al., 2009).

RNA must be converted to complementary DNA (cDNA) in a process called reverse transcription (Figure 5) for sequencing by the next-generation DNA sequencing platforms. The first step in the preparation of the bacterial RNA is the elimination of rRNA (and also tRNA), which usually forms the majority of extracted RNA (Sorek and Cossart, 2010). Prokaryots lack poly-A tail in their transcripts, therefore random hexamer priming (Perkins et al., 2009) or oligo-dT priming from artificially polyadenylated mRNAs (Frias-Lopez et al., 2008) must be applied for the initialization of conversion of RNA into cDNA by reverse transcriptase.

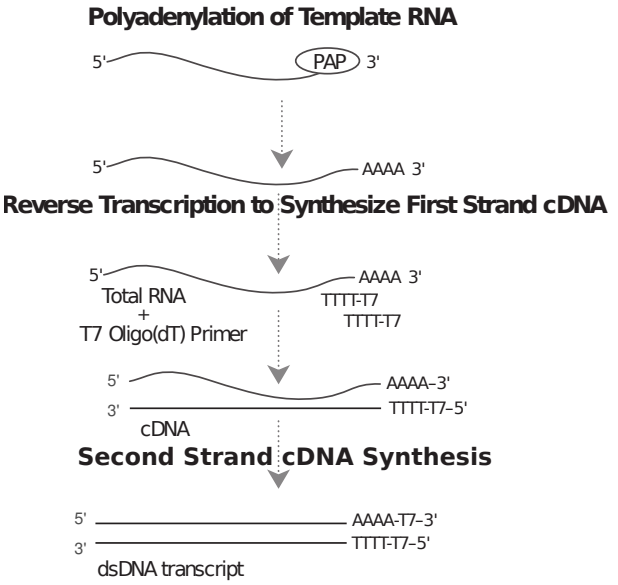


Figure 5: **Reverse transcription of prokaryotic RNA by MessageAmp II-Bacteria Kit.** Source: Thermo Fisher Scientific)

In transcriptomics, the sample collection, the storage and transport conditions are very important, because if bacteria are not appropriately fixed, they can continue growing or transforming themselves into sporulation stage, so the expression of genes can be influenced. In addition, it is important to avoid RNA degradation (Franzosa et al., 2014).

### 16S rDNA sequencing

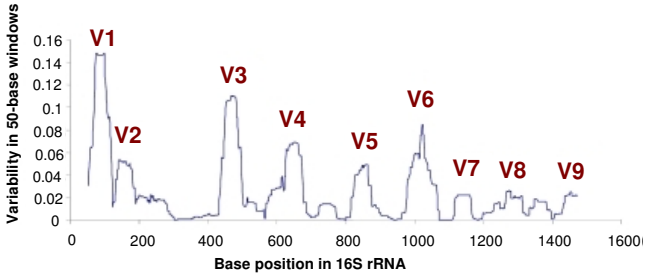


Figure 6: **Hypervariable regions within the 16S rRNA gene in 79 strains of *Pseudomonas*.** Author: Bodilis et al. (2012)

The most common tool for diversity estimation and environmental communities characterization is the analysis of bacterial ribosomal sequences (mainly 16S rDNA), which contain conserved sequences whose taxonomic signal allows to differentiate among bacterial species (Woese and Fox, 1977). 16S rDNA can be recovered from the original genomic sequence by PCR amplification using universal primers (Morris et al., 2002). The gene consists from 9 conserved regions (Figure 6). Klindworth et al. (2013) suggested the amplification of the regions V3 and V4 as the most reliable regions for taxonomic comparisons for sequencing by platforms generating reads of length up to 500 bp (such as Illumina MiSeq).

Figure 7 shows the work-flow for amplicon library preparation for the Illumina platform in two PCR steps. The first PCR is for 16S rDNA amplification, while the second PCR is for adding sequencing adaptors containing different specific index sequences. These index sequences consist of combinations of 8 nucleotides serving as a tag for individual samples that can be mixed on one sequencing plate (Wong et al., 2013).

Other sequencing platforms also employ tagging samples for combining them on one sequencing region (multiplexing). The reason, why sample multiplexing is so widely used, is that the current sequencing platforms are able to generate hundreds of thousands of amplicons per sample, however, sufficient overview of bacterial diversity in a sample can be reached with fewer sequences (Wooley et al., 2010).

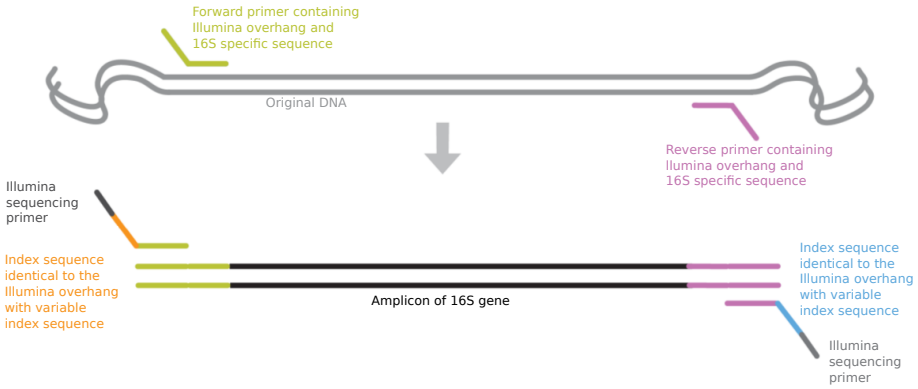


Figure 7: **Illumina amplicon sequencing work-flow.** Adapted from Illumina

The amplicon sequences can be aligned directly to the databases of 16S rDNA sequences, such as Ribosomal database project (Cole et al., 2009) or SILVA (Pruesse et al., 2007). However, many sequences may not be aligned to strain, species or genus level, but just to higher taxonomy levels, such as families or phyla. The final description in such cases includes unidentified species of one phylum, which have very different genomic content. Thus, the interpretation of such results may be complicated (Rasheed et al., 2013). Therefore, many researchers prefer to cluster obtained sequences by similarity into "operational taxonomic units" (OTUs). There are disagreements about which similarity level should be used for sequence clustering to the strain level (e.g. 99 %), because some "artificial" OTUs may be formed due to single-nucleotide sequencing errors if too high similarity level is set (Kunin et al., 2010).

For the investigation of microbiome of different human body sites, a large-scale surveys have been established, such as the Metagenomics of the Human Intestinal Tract (MetaHIT) consortium (Qin et al., 2010) and the Human Microbiome Project (HMP) (HMPC, 2012). Their results indicate that the estimation of bacterial community richness in the human body is bioinformatically challenging. According to the HMP, the human body contains between 3,500 and 35,000 OTUs depending on the sequence clustering parameter (HMPC, 2012). The taxonomic assignation of these OTUs showed that they belong to approx. 600 genera and covered 90 % of the phylogenetic range of microbes expected in this population (HMPC, 2012; Li et al., 2012).

### 1.2.2 Microbial taxonomic distribution of the gut

#### Bacteria of a healthy human gut

Various studies of the human gut microbiome based on the 16S rDNA reported high species diversity within and between individuals (Eckburg et al., 2005; Gill et al., 2006). Arumugam et al. (2011) joined fecal metagenomic sequences from different parts of the world obtained by different platforms. They identified three robust clusters (referred as enterotypes) which are not continent specific. Figure 8 shows the clustering of samples into *Bacteroides*, *Prevotella* and *Ruminococcus* enterotypes. Each enterotype contains also the main

bacteria from other two enterotypes, but in lower abundance. The results indicated that some markers, such as age or body mass index might be correlating with these enterotypes.

In the study comparing two large cohorts taking two different long-term diets, two enterotypes were identified: *Bacteroides* enterotypes was associated with protein and animal fat diet, while *Prevotella* was prevalent in people taking mainly high fiber diet. The enterotypes identity is so profound, that the minor differences caused by short-term diet do not overcome large variations among enterotypes (Wu et al., 2011). In contrast, the gut microbiota of elderly people, however, did not split into three nor two enterotypes, but the majority of them were found to be of *Prevotella* enterotype only (Claesson et al., 2012).

Interestingly, the enterotypes study of Arumugam et al. (2011) contains also a statement that the most important functions are not necessarily provided by *Bacteroides*, *Prevotella* or *Blautia*, but by the minority species. The ecological rules in the human gut let the minority species persist in the gut community, because they provide essential functions in the community (Lynch and Neufeld, 2015). It was found that the short-term diet changes do not influence the enterotypes, but they affect the microbial composition of the underrepresented species (David et al., 2014).

There are many factors that can influence the prevalence of the bacterial species in the gut, such as early colonization during first days of life (Cesarean vs. vaginal delivery, breastfeeding vs. formula feeding), heath/disease stage, host genetics, medication by antibiotics and other xenobiotics, general lifestyle and diet (Graf et al., 2015). It was found, that people living in tribes in isolated areas possess more diverse bacterial composition than Western people (Schnorr et al., 2014). For these reasons, it is difficult the define a general microbial composition applicable for every human.

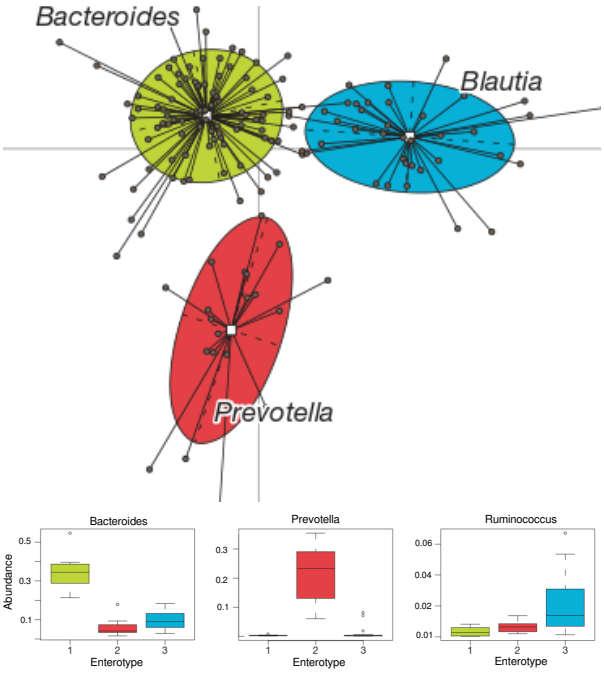


Figure 8: **Phylogenetic differences between enterotypes.** 154 metagenomes and abundances of the main contributors of each enterotype. Author: Arumugam et al. (2011)

### Bacterial dysbiosis and GI infections

The clinical manifestations of GI infections are usually diarrhea connected with other infection specific GI complications (Beeching et al., 2011). The causative agents for most of them have been discovered before the era of next generation sequencing by toxin identification. These pathogens may be either opportunistic or may be introduced to the GI tract by contaminated food, water or air, such as *Campylobacter*, *Clostridium difficile*, *Escherichia coli*, *Salmonella*, *Shigella*, etc. Another pathogenic bacteria, such as some Vancomycin resistant strains of *Enterococcus faecium*, come from the human gut, but penetrate the epithelium and infect other body parts (Willems et al., 2005).

Opportunistic pathogens take the advantage of microbial perturbation in the gut by environmental factors.

Such a perturbation can lead to the overgrowth ("bloom") of some of the underrepresented species (Segata et al., 2011). Figure 9 shows two possible scenarios occurring during microbial perturbation. If the perturbation leads to the positive selection of pathogens, the dysbiosis may end up in vicious cycle in which perturbation-induced blooms increase disease onset probability. In the more positive scenario, the first perturbation might result in a spread of perturbation-resistance genes among the intestinal microbiota, so the ecosystem gets stabilized with novel composition which is able to resist possible diseases (Stecher et al., 2013).

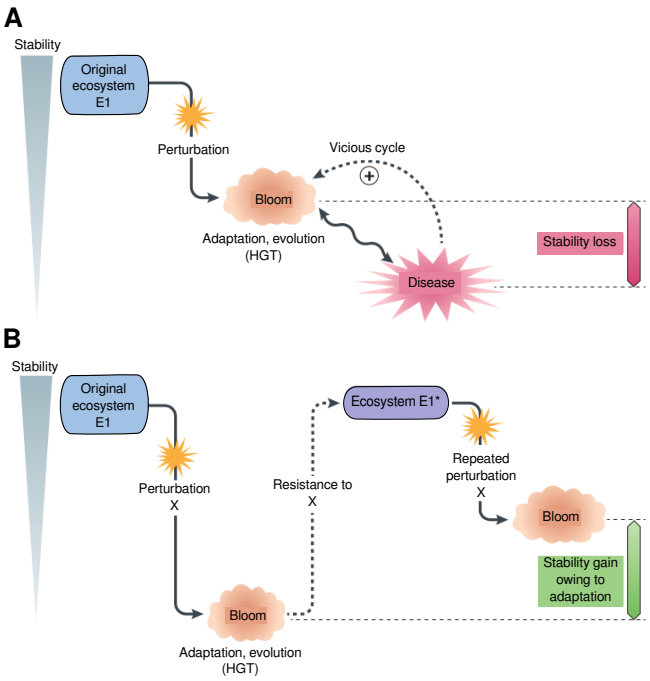


Figure 9: **Perturbation-induced destabilization (panel A) and stabilization (panel B) of intestinal ecosystems** Author: Stecher et al. (2013)

The single species GI infections can be treated by antibiotics, but they are useful only to a certain point. For example, in the case of *C. difficile* infection, it was observed that repeated treatments by Vancomycin and Metronidazole do not provide satisfactory treatment results and have caused the emergence of Vancomycin-resistant *Enterococcus* (Al-Nassir et al., 2008). The metabolomic analyses showed that antibiotic treatment decreases levels of secondary bile acids, glucose, free fatty acids and dipeptides, while it causes an increase of primary bile acids and sugar alcohols. Some opportunistic pathogens can take the advantage of specific metabolites which become more abundant after antibiotic treatment. They may use primary bile acid taurocholate for germination, and carbon sources such as mannitol, fructose, sorbitol, raffinose and stachyose for growth (Theriot et al., 2014). Microbiota disturbed by the antibiotic treatment may also produce increasing levels of sialic acid, which may be used for the expansion of opportunistic pathogens (Ley, 2014).

An alternative strategy for GI single-species infection treatment and prevention is the restoration of the gut microbiota by probiotics (and prebiotics) or fecal microbiota transplantation. Probiotics are microorganisms that are believed to provide health benefits when consumed. Prebiotics are nutritional compounds used to promote the growth of probiotics. In the fecal microbial transplantation, the healthy bacterial flora from a tested donor in the form of stool infusion is introduced to a recipient by enema, orogastric tube or orally in the form of a capsule containing freeze-dried material, as shown in the Figure 10 (Borody and Khoruts, 2012). Beneficial microorganisms probably prevent other luminal bacteria from reaching the lamina propria by competition. Moreover, they enhance mucus production and consistency which protects against pathogens. Beneficial bacteria also limit amount of metabolites which

Figure 10: **Fecal microbiota transplant capsules.** Author: (Youngster et al., 2014)

may be misused by pathogens. In addition, they stimulate the mucosal immune system to secrete protective secretory IgA, protective defensins and bacteriocins into the lumen (Fedorak, 2010). On the other hand, fecal transplantation therapy includes many unsolved issues, such as selection of the transplant donor selection. Recently undesired metabolical changes caused by introduced microorganisms by fecal transplantation have been reported (Gregory et al., 2014; Merenstein et al., 2014).

**Bacterial dysbiosis and GI disorders**

The metabolic pathways of the gut bacteria are connected to pathways of host's metabolism, meaning that bacteria may influence the onset of several human non-infectious diseases. There are numerous studies focused on associations between the composition of the human gut microbiota and the diverse diseases affecting different parts of human body (Sjögren et al., 2012), behavior (Hsiao et al., 2013) or onset of allergies (Trompette et al., 2014). In most of these studies, no single causative species are being identified, however, the differences in the overall bacterial composition have been found. The detection is mostly performed by comparison of bacterial composition of fecal samples of large cohorts of affected patients and healthy volunteers (Guinane and Cotter, 2013). The majority of these studies try to explain the onset of GI diseases, such as irritable bowel syndrome (IBS), inflammatory bowel disease (IBD), systemic diseases, such as type 2 diabetes and obesity, as well as the onset of colorectal cancer. The studies investigating bacterial dysbiosis and GI diseases reviewed in the study of Guinane and Cotter (2013) are shown in Table 1.

IBS is characterized by abdominal pain or discomfort and altered bowel habits. Recent studies have identified susceptibility genes for IBS. They are involved in the innate immunity and recognition of bacteria and also in maintaining the integrity of the intestinal barrier (Ohman and Simrén, 2013). A longitudinal study showed that quick shifts in the global pattern of gene expression is associated with acute diarrhea in IBS (Durbán et al., 2013). The IBS pathogenesis might be connected to the overgrowth of bacteria adhesing to the bowel wall (Ghoshal et al., 2012).

IBD has two forms: Crohn's disease (CD) and ulcerative colitis (UC) (Loftus, 2004). It is characterized by a chronic inflammation of the GI tract. The two forms of IBD differ in their symptoms and inflammation patterns. The GI inflammation in CD is more segmental and is probably a result of interaction of the host's genetics with the microbial population. UC is characterized by the inflammation of the lining of the colon. Both forms have been associated with overall dysbiosis in the gut, specifically by overgrowth of microbes involved in development of mucosal lesions (Lepage et al., 2011; Manichanh et al., 2012).

Intestinal bacteria may also promote colorectal cancer tumorigenesis. Mice infected by recombinant *E. coli* strain, which possessed a polyketide synthase pathogenicity island encoding a genotoxin, developed tumors, while mutants lacking this protein remained unaffected (Arthur et al., 2012). In addition, the tumorigenes of colorectal cancer may be enhanced by *Fusobacterium* through an inflammatory mechanism (Kostic et al., 2012).

Obesity is a syndrome that is caused by prolonged imbalance between energy intake and expenditure and is often connected to diabetes type 2. The causes are unhealthy lifestyle and diet, but also gut microbiota may play a role in its onset (Turnbaugh et al., 2006). The first study showed that increased ratios of *Firmicutes/Bacteroidetes* is connected to obesity, however, recent studies showed that the onset of obesity does not depend on prevalence of exact phylogenetic groups, but on the metabolites they produce (Murphy et al., 2010; Clarke et al., 2012; Fei and Zhao, 2012).

Table 1 demonstrates that further research is necessary to conclude which exact bacterial communities are causing studied GI diseases. Some researchers determine the bacterial taxonomy up to genus level, while others work only with phyla-level diversity, what results in discrepancies between studies. An example is the decreased *Bacteroidetes* proportion associated with obesity by phyla-level comparison, while in contrast genus-level analysis showed that increased *Bacteroides* proportion mat be linked to obesity. Another example is *Ruminococcus*: its increased proportion has been associated with IBS, while its decreased proportion has been associated with obesity. Therefore, according to the present stage of knowledge, the definition of a healthy microbiota is difficult (Guinane and Cotter, 2013).

Table 1: **Microbial associations with chronic intestinal diseases.** Author: Guinane and Cotter (2013)

| | **Increased** | **Decreased** |
|---|---|---|
| **Irritable bowel syndrome** | *Clostridium*<br>*Dorea*<br>*Firmicutes:Bacteroidetes* ratio<br>*Gammaproteobacteria*<br>*Haemophilus influenzae*<br>*Ruminococcus* | *Bacteroides*<br>*Bifidobacterium*<br>*Faecalibacterium* |
| **Inflammatory bowel disease** | bacterial numbers in mucosa<br>*γ-Proteobacteria*<br>*Clostridium*<br>*Enterobacteraceae*<br>adherent invasive *Escherichia coli* | bacterial diversity<br>*Bacteroidetes*<br>*Faecalibacterium prausnitzii*<br>*Firmicutes*<br>*Lachnospiracheae*<br>*Phascolarctobacterium*<br>*Roseburia* |
| **Colorectal cancer** | polyketide synthase containing *E. coli*<br>*Fusobacterium* spp. | |
| **Obesity** | *Actinobacteria*<br>*Bacteroides*<br>*Firmicutes:Bacteroidetes* ratio<br>*Prevotellaceae* | bacterial diversity<br>*Bifidobacterium*<br>*Methanobrevibacter*<br>*Ruminococcus flavefaciens* |
| **Diabetes type 2** | *Akkermansia muciniphilia*<br>*Bacteroides*<br>*Clostridium*<br>*E. coli*<br>*Eggerthella lenta* | *Eubacterium spp.*<br>*Faecalibacterium spp.*<br>*Firmicutes*<br>*Roseburia spp.* |

### 1.2.3 Taxonomic composition of the gut viruses

#### Viruses of the healthy gut

The human gut virome is composed from bacteriophages, prophages and also from eukaryotic viruses (Reyes et al., 2010), as shown in the Figure 11. Eukaryotic viruses form a minor part of the human gut virome. They may be ingested by food, as, for example, pepper mild mottle virus was found in about half of world's population (Zhang et al., 2005). Other groups of eukaryotic viruses, such as *Picobirnaviridae*, *Adenoviridae*, *Anelloviridae*, *Astroviridae* and bocaviruses, enteroviruses and sapoviruses are being found in the healthy human viromes (Minot et al., 2011), but the way how these viruses affect the human body is still unknown.

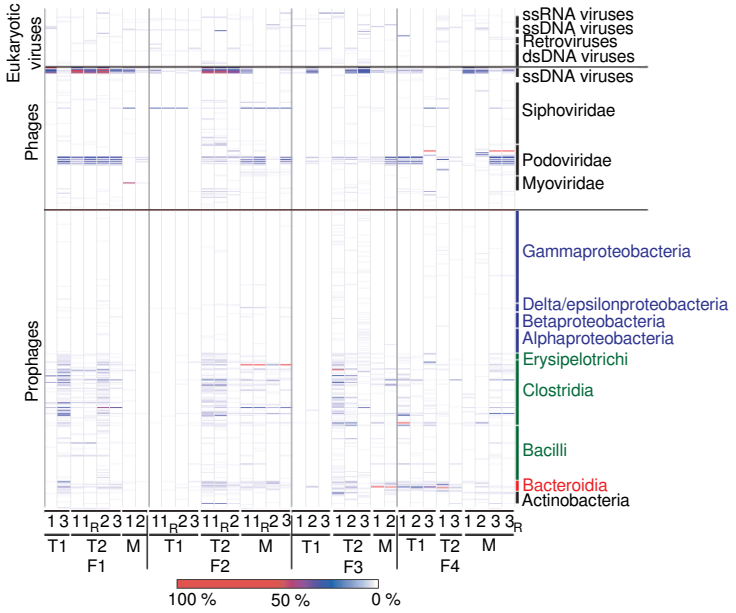


Figure 11: **Viral diversity of four families (F1-F4) of monozygotic twins (T1 and T2) and their mothers (M).** Author: Reyes et al. (2010)

Bacteriophages and prophages are more common in the human gut than the eukaryotic viruses. It is estimated that the number of bacteriophages outnumbers 10 × the number of bacteria. The genomes of bacteria and bacteriophages in the human gut form a complicated network in which one bacterial group can be predated by 1-5 different phages (Waller et al., 2014). Interestingly, the mutation rates of bacteriophages are orders of magnitude higher than in bacteria, so new phages are emerging constantly (De Paepe et al., 2014a) indicating that the GI tract hosts a dynamic community structure, characterized by predator-prey interactions connected to the horizontal gene transfer (Minot et al., 2011). Bacteriophages contribute actively to the emergence of a novel gene combinations in bacteria by the horizontal gene transfer (De Paepe et al., 2014a). Therefore, the composition of the bacterial and viral metagenomes are closely connected.

Diet can change the viral composition up to certain level (Minot et al., 2011), similarly as in the case of bacteria (Graf et al., 2015). Analysis of possible proteins encoded in ORFs detected in viromes revealed a high functional diversity which differs from the bacterial metagenome. ORFs detected in the gut viromes contain numerous proteins related to the horizontal gene transfer, mainly genes included in DNA replication and repair (Reyes et al., 2010).

Despite the fact that the viral composition among individuals is very different (Figure 11), 90 % of people have in common one recently discovered *Bacteroides* bacteriophage. It was assembled from joined sequence data from previously published viromes. Its genome is 97 kbp long and it encodes proteins that do not have matches to any known sequences in the databases, which is the reason why it had not been detected before (Dutilh et al., 2014).

### Viral dysbiosis and GI diseases

Eukaryotic viruses affecting directly humans hosts cause usually GI infections with wide variety of clinical presentations, usually diarrhea. The causative agents for the most common GI infections are rotavirus (Dennehy, 2000) and norovirus (Glass et al., 2009) which are transmitted by fecal-oral contact, by contaminated surfaces and hands and may be spreads also via air (Dennehy, 2000; Glass et al., 2009).

As the bacteriophages modulate the diversity of the human gut microbiota, they can also influence the development of the human immune system (Cario, 2013) and contribute to the health and disease of the host (Focà et al., 2015; Cario, 2013). There are four possible ways, how phages regulate the composition of gut

bacteria and so influence the onset of several GI disorders, described in the Figure 12.

In the "Kill the winner" way of action, the phages infect only those bacterial species which have overgrown and reached the threshold above which phages can predate them. These bacteria will be lysed, so the bacterial community will be shifted back to normal (Parsons et al., 2012). In the "Kill the relative" strategy, phages are growing within phage susceptible strain in lysogenic cycles. The bacteriophages will finally kill the relative bacterial strains (Brown et al., 2006).

In the moments when gut encounters environmental stress, phages can be induced more in mutualistic bacteria than in pathogenic bacteria, so finally the bacteriophage contribute to the intestinal dysbiosis by diminishing the ratio of mutualistic bacteria and pathogens (Mills et al., 2013). This theory is being confirmed by viral studies in different GI diseases, for example it was found that the mucus of CD patients has 30× fold enrichment of virus-like particles ($3\times10^{9}$) than the mucus of healthy controls (Lepage et al., 2008). Finally, the 4th model present a scheme where bacteriophages infect hosts, but without lysing them - the lysogeny is established so the way for horizontal gene transfer opens. Antibiotic treatment, for example, expands the interactions between phage and bacterial species, leading to a highly connected phage-bacteria network for horizontal gene transfer (Modi et al., 2013).

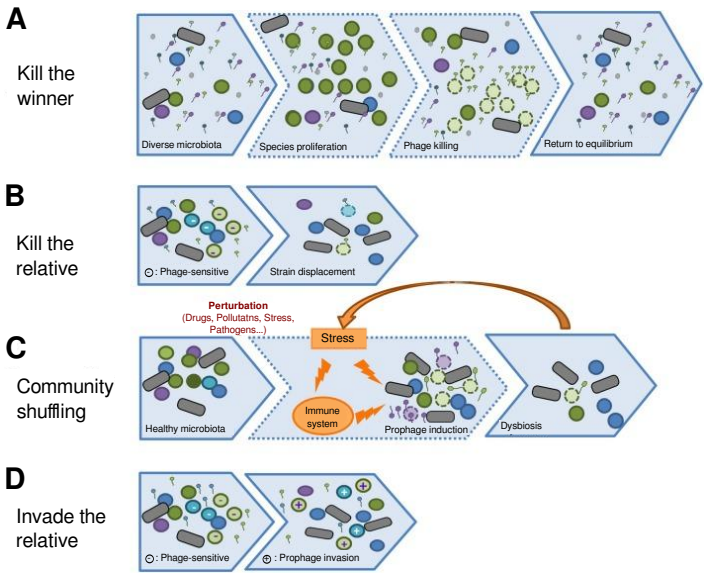


Figure 12: **Four different ways how bacteriophages influence bacterial composition of the human gut.** Author: De Paepe et al. (2014b)

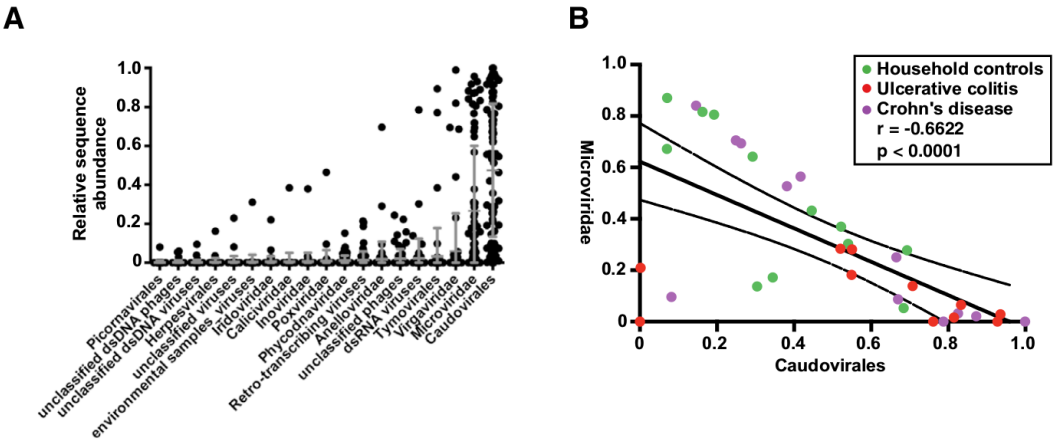


Figure 13: **Viromes of healthy volunteers and IBD patients. Panel A:** Relative abundance of sequences assigned to the indicated viral taxa. **Panel B:** Correlation plot of the *Caudovirales* and *Microviridae* relative abundance for all samples. Author: Norman et al. (2015)

The most prevalent bacteriophages in the healthy human gut belong to the order of double-stranded DNA

viruses *Caudovirales* (*Podoviridae*, *Siphoviridae* and *Myoviridae*) and *Microviridae* order of single-stranded DNA (Reyes et al., 2010; Minot et al., 2013; Reyes et al., 2010; Norman et al., 2015), as shown in the panel A of the Figure 13. The panel B of the Figure 13 shows that the altered ratio of *Caudovirales*/*Microviridae* may be the one of the factors involved in the pathogenesis of IBD (Lawlor and Moss, 2010). The increased richness of *Caudovirales* was associated with the both forms of IBD - CD and UC (Norman et al., 2015).

# 1.3 Fluorescent activated cell sorting (FACS) of the gut microbiome

## 1.3.1 Method description

Flow cytometry (FC) is a laser-based, biophysical technology employed in cell counting and sorting by suspending cells in a stream of fluid and passing them by an electronic detection apparatus. It allows simultaneous multiparametric analysis of the physical and chemical characteristics in the range of thousands of particles per second. The forerunner to today's flow cell sorters was the apparatus of M. J. Fultyler allowing to separate resuspended cells on basis of electronically measured volumes of droplets (Fulwyler, 1965). Kamentsky and Melamed (1967) have improved this equipment, so it was possible to separate the cells according to their optical properties measured simultaneously at four different wavelengths. Five years later, Bonner et al. (1972) published a report of the first fluorescence activated cell sorter sorting differently stained populations of cells.

### Fluorescent cell staining

Fluorescence is the emission of light by a molecule which absorbed light or other electromagnetic radiation. The emitted light has usually a longer wavelength and, therefore, lower energy than the absorbed radiation. Fluorescence occurs when an orbital electron of a molecule, atom or nanostructure relaxes to its ground state by emitting a photon of light after being excited to a higher quantum state by some type of energy. An example of the excitation and the emission wavelengths and their colors in the visible light spectrum is shown in the Figure 14.

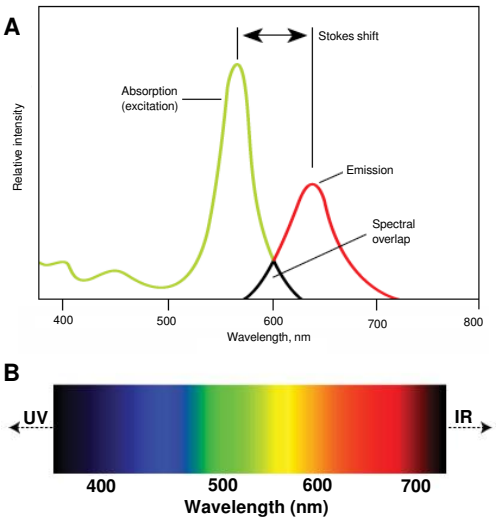


Figure 14: **Excitation and emission spectra of a fluorophore.** Source: BioRad (panel A) and Life Technologies (panel B)

Fluorescence can be found in minerals (abiotic fluorescence) but also in living organisms (biofluorescence). Some organic molecules in living cells also emit autofluorescence, such as tryptophan or chlorophyll. However, for research in biology, usually nonfluorescent molecules are labeled with an extrinsic fluorescent dye - a fluorophore.

Different fluorophores for molecular biology have been developed since the 1940's. The pioneers in this technique were Coons and collaborators, who used for the first time an anthracene-associated antibody to detect specific bacteria (Coons et al., 1941) and also described the first fluorescein isothiocyanate (FITC) association (Coons and Kaplan, 1950). Nowadays, there are numerous commercially available fluorophores (Figure 15). The current fluorophores used for cell staining can be divided into three general groups:

- Organic dyes:
  Synthetic organic dyes are, for example, fluorescein and its conjugates improving photostability and

solubility, e.g. fluorescein isothiocyanate (FITC) and rhodamine (tetramethyl rhodamine isothiocyanate, TRITC). These molecules are of small size so they can be conjugates with macromolecules, such as antibodies, biotin and avidin, without interfering with proper biological function.

- Biological fluorophores:
  Biological fluorophores come from organisms capable of biofluorescence. The green fluorescent protein, nowadays widely used for gene expression studies, was first isolated from jellyfish *Aequorea victoria* (Chalfie et al., 1994).

- Quantum dots:
  Quantum dots (developed in 1980's) are semiconductor nanocrystals of size 2-50 nm that when excited, emit fluorescence at wavelength based on the size of the particle. These nanocrystals can be produced with a great specificity of desired excitation and emission wavelength and have very long photostability. In addition, quantum dots can be coated for protein labeling and other applications (Ekimov et al., 1985).

**Labeling methods**

There are different cell labeling approaches. The cell staining can be:

- direct, by immediate staining of cell structures by a fluorescent dye,
- indirect, achieved by fluorophores conjugated with macromolecules (antibodies or probes).

The target localization can be:

- inside the cell, so the fluorophores must penetrate the cell surface,
- on the cell surface, so cell wall remain intact.

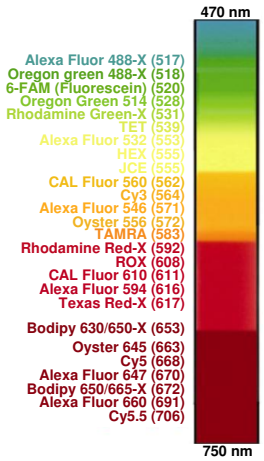


Figure 15: **The emission length of the most common fluorophores in visible light spectra.** Source: IDT

The labeling of specific DNA or RNA sequences inside the cell is called fluorescent in situ hybridization (FISH). For this application a probe with conjugated fluorophores is needed. The probe for RNA labeling is a synthesized string of about 20 nucleotides complementary to the known RNA sequence of interest. The cellular RNA must be stabilized before hybridization by a fixative agent, such as ethanol, glutaraldehyde or formaldehyde. The accessibility of RNA in the cell for hybridization is achieved by permeabilization of the cell surface by enzymes or chemical agents partially disrupting the cell wall (Amann and Fuchs, 2008).

It is also possible to stain the entire DNA or RNA content in the cells by specific fluorescent dyes, e.g. by acridine orange and ethidium bromide serve for detection of both RNA and DNA, while DAPI (4',6-diamidino-2-phenylindole) and SYTO®62 are DNA specific dyes. Other dyes, such as pyronin Y or other stains of the SYTO® family are RNA specific dyes.

For labeling of targets on the bacterial cell surface, a wide variety of antibodies conjugated to fluorophores can be used. This kind of labeling can be very specific, as bacterial strains of the same species differ widely by their cell surface protein structures (Waligora et al., 2001).

The key aspect in the selection of a fluorophore is the distance between excitation and emission wavelength, called Stokes shift (Figure 14, panel A). If a fluorophore has very small Stokes shifts, it would be difficult to

distinguish the emitted fluorescence from the excitation light, because the wavelengths greatly overlap. In the experiments with multiple fluorophore staining, the emission wavelengths of the fluorophores should not be overlapping.

Fluorophore detection in a given experiment can be obscured by high background fluorescence, which is mostly caused by insufficient removal of non-bound fluorescent probe or by the sample autofluorescence. The thorough washing or reducing the concentration of fluorescent probe may help to reduce background fluorescence.

The opposite problem is the low fluorescence which can be solved by adjusting the concentration of the fluorophore or by applying different amplification methods, which must be, however, performed carefully in the case of living cells, as extreme concentration of a fluorophore can induce death. Low fluorescence can be caused also by photobleaching which is an irreversible destruction of fluorophores due to prolonged exposure to the excitation light. If manipulation time with fluorophore detection equipment cannot be reduced, antifade reagents protecting against photobleaching can be used or the switching to a more photostable fluorophore should be considered.

### Fluorescence activated cell sorters

The present fluorescence activated cell sorters consist of 7 major parts shown in Figure 16.

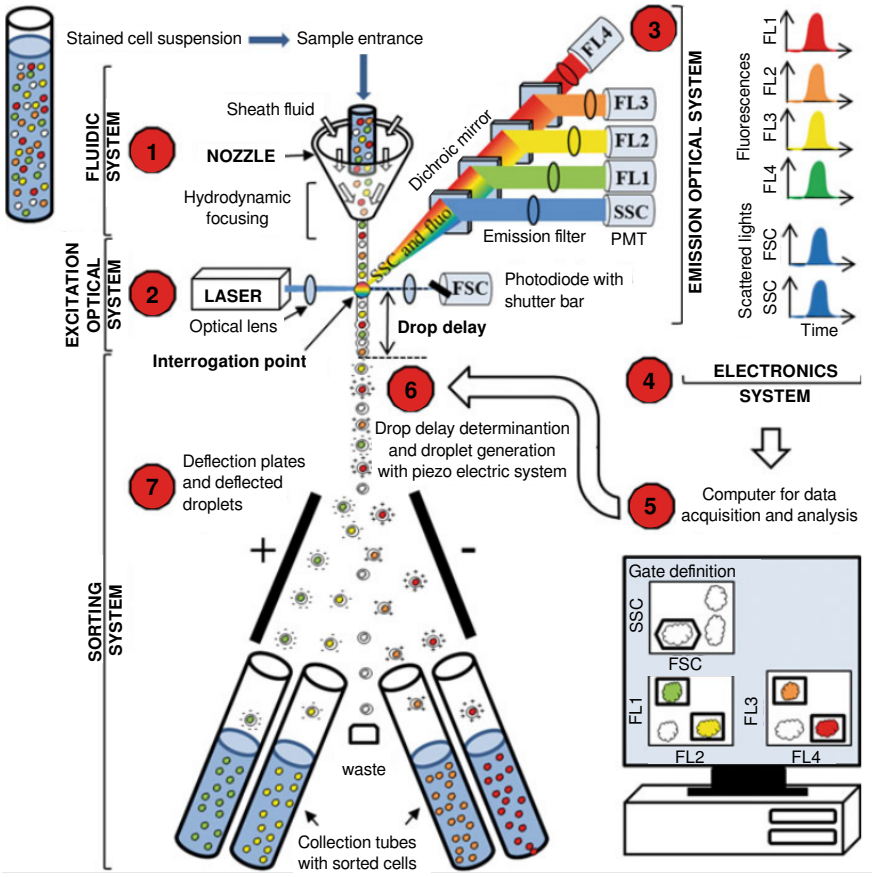


Figure 16: **Fluorescence activated cell sorting principle.** Author: Picot et al. (2012)

Cells in a salt buffer pass through a nozzle containing a unit for hydrodynamic focusing (Figure 16, point 1). In the next point - in the quartz chamber or in the air at the nozzle exit - the intersection between excitation light source and cells occurs (Figure 16, point 2). The majority of the current cytometers can be equipped with up to 4 different excitation sources, however some can have up to ten. The excitation light sources are mainly lasers, however some analyzers still use mercury arc-lamps for UV-excitation.

When a cell pass through the excitation source, the laser beam is refracted in all directions (Figure 16, point 3). Light diffusion at small angles is collected in the axis of the leaser beam by a photodiode or by a photomultiplier tube; it is called forward scatter light (FSC) and correlates with relative size of the cells. Light diffusion at small angels (side scatter light, SSC) is collected at 90 °of the laser beam, as well as fluorescent signals. SSC is a combination of diffusion, reflection and refraction caused by cell structural complexity. The emitted light is reflected by dichroic mirrors which transmit light signals to different detectors collecting specific fluorescence of different wavelengths. The light signal received by the detectors is amplified and digitalized.

The flow cytometer electronics (Figure 16, point 4) analyzes several thousand of cells per second. Analyzers digitalize signals by converting voltage value to digital values (from 0 to $2^{10} = 1024$) on logarithmic or linear scale. The resulting data are written in form of a table, an illustration example is shown in Table 2.

Table 2: **An example of flow cytometry data table.**

| | FSC | SSC | FL1 | FL2 | FL3 | FL4 | Time |
|---|---|---|---|---|---|---|---|
| Cell 1 | 382 | 77 | 618 | 0 | 225 | 286 | 1 |
| Cell 2 | 628 | 280 | 245 | 431 | 259 | 371 | 1 |
| Cell 3 | 1023 | 735 | 699 | 448 | 215 | 638 | 1 |
| Cell 4 | 373 | 128 | 202 | 354 | 94 | 149 | 1 |
| Cell 5 | 1023 | 1023 | 618 | 742 | 408 | 866 | 2 |
| Cell ... n | ... | ... | ... | ... | ... | ... | ... |

Cell sorters offer the possibility of isolating subpopulations of cells of interest with high recovery and high degree of purity from heterogeneous cell mixtures based on light scattering and fluorescent characteristics. The cells in a sample are visualized on FC bi-plots or single parameter histogram and the cells with properties of interest can be selected by drawing a "gate" (Figure 16, point 5). The cells in the stream matching the fluorescence ranges of the set gate will be separated into indicated tube or discarded.

After setting up the gating and sorting scheme, the cell suspension is directed into a stream, which emerges from a vibrating nozzle and breaks up into individual droplets. The system measures the drop delay - the milliseconds which droplets need to flow from detection unit to sorting unit (Figure 16, point 6). A droplet containing a cell of interest is positively or negatively charged and goes through an electric field between two deflection plates before being deflected into collection tubes (Figure 16, point 7).

## 1.3.2 Applications of flow cytometry in microbiology

### Selection of bacterial cell populations

#### Enumeration of microbes according to their size

FC has an advantage over laborious sample inspection by microscope, because it can scan thousands of cells per second (Müller and Nebe-von Caron, 2010). It has been applied, for example, for counting bacterial cells present in milk (Gunasekera et al., 2000), phytoplankton (DuRand et al., 2001) or soil samples (Bressan et al.,

2015) and for distinguishing of marine bacteria from marine viruses (Marie et al., 1999) (Figure 17). If forward and side scatter values are visualized in a FC bi-plot, the size of cells can be inspected, so eukaryotic cells or unicellular organisms can be counted and ratio of bacteria and protozoa in environmental samples can be determined. For example, this approach applied on phytoplankton provided an evidence for predator-prey interactions in the ecosystem changing over seasons (Martinez-Garcia et al., 2011; Sherr et al., 2002).

**Determination of viable cells**

Flow cytometry can be employed in studies of differential action of antibiotics on Gram-positive and Gram-negative bacteria: the cell membrane structures can be stained with fluorescent dyes and analyzed by FC (Novo et al., 2000; Silva et al., 2011). Another cell stains, such pyronins Y, target cellular RNA and so allow identification of highly active cells in environmental samples (Peris-Bondia et al., 2011). Propidium iodide provides additional information about damage levels of individual cells, distinguishing between damaged and integer cells in the culture (Ueckert et al., 1997; Héchard et al., 1992).

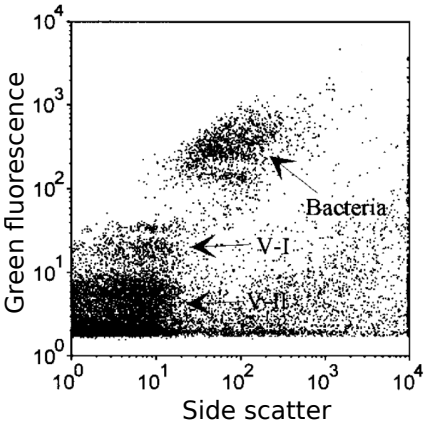


Figure 17: **FC biplot of marine viruses (areas V-I and V-2) and bacteria**. Author: (Marie et al., 1999)

**Metabolic activity measurement**

It is assumed that in the case of cell injury, dormancy or starvation, the metabolic functions will be below detection limit. The most commonly detected enzyme in metabolic activity studies is esterase. Esterase measurement is based on non-fluorescent compounds, such as dichlorocarboxy-fluorescein diacetate and calcein-acetomethyl ester, that become fluorescent when cleaved by the enzyme inside the cell demonstrating its metabolic activity (Vives-Rego et al., 2000).

The respiratory activity of cells can be assessed by tetrazolium salt reduction which capture electrons from oxidative metabolism, thus the resulting fluorescent products are detectable by FC. For cell starvation, this salt can be combined with other dyes, such as rhodamine or propidium iodide (López-Amorós et al., 1997). This method is very viable for studies of complex environments containing unculturable cells (del Giorgio et al., 1997; Günther et al., 2009).

It is also possible to detect bacterial toxins in samples. The antibodies specific to the studied toxins can be bound to fluorescent beads of a size that can be detected by FC, thus the amount of toxin in blood or stool sample can be detected quickly (Renner, 1994; Tazzari et al., 2004).

**Labeling of specific cell populations by fluorescent antibodies**

Monoclonal antibodies show high levels or specificity and are suitable for distinguishing among different bacterial genera in a co-culture or in an environmental sample. For example, specific cell surface antibodies were used for distinguishing between *Streptococcus mutans* and *Actinomyces viscosus* in samples from human oral cavity (Barnett et al., 1984).

FC can be also used as an alternative to the enzyme-linked immunosorbent assay (ELISA). In the study of Dietrich et al. (1991), *Brucella abortus* bound to bovine immunoglobulin in blood samples was labeled using a FITC conjugated anti-bovine immunoglobulin antiserum. The counts of immunoglobulin coated *Brucella* cells

were compared with non coated *Brucella* cells, thus the level of immunological responses was determined by direct visualization of immunologically recognized bacterial cells.

The labeling through antibodies with intracellular targets can be also performed. These kind of assays are commonly used for studies of gene expression (Vestvik et al., 2013).

The labeling by specific antibodies is more time effective and more specific than classical culture methods. The most difficult task in cell labeling through fluorescent antibodies is the laboratory preparation of lipopolysachharide monoclonal antibodies specific for cell surface of the bacterial species of choice (Evans et al., 1990).

**Labeling of specific cell populations by fluorescent oligonucleotides**

The gene for 16S rRNA subunit provides high level of conservation, which made it especially useful for recognition of specific bacteria in FC (Amann and Fuchs, 2008). However, the selection of 16S rRNA probes for FISH might be tricky, as the ribosome contains areas which are not equally accessible along the whole length of the sequence (Figure 18).

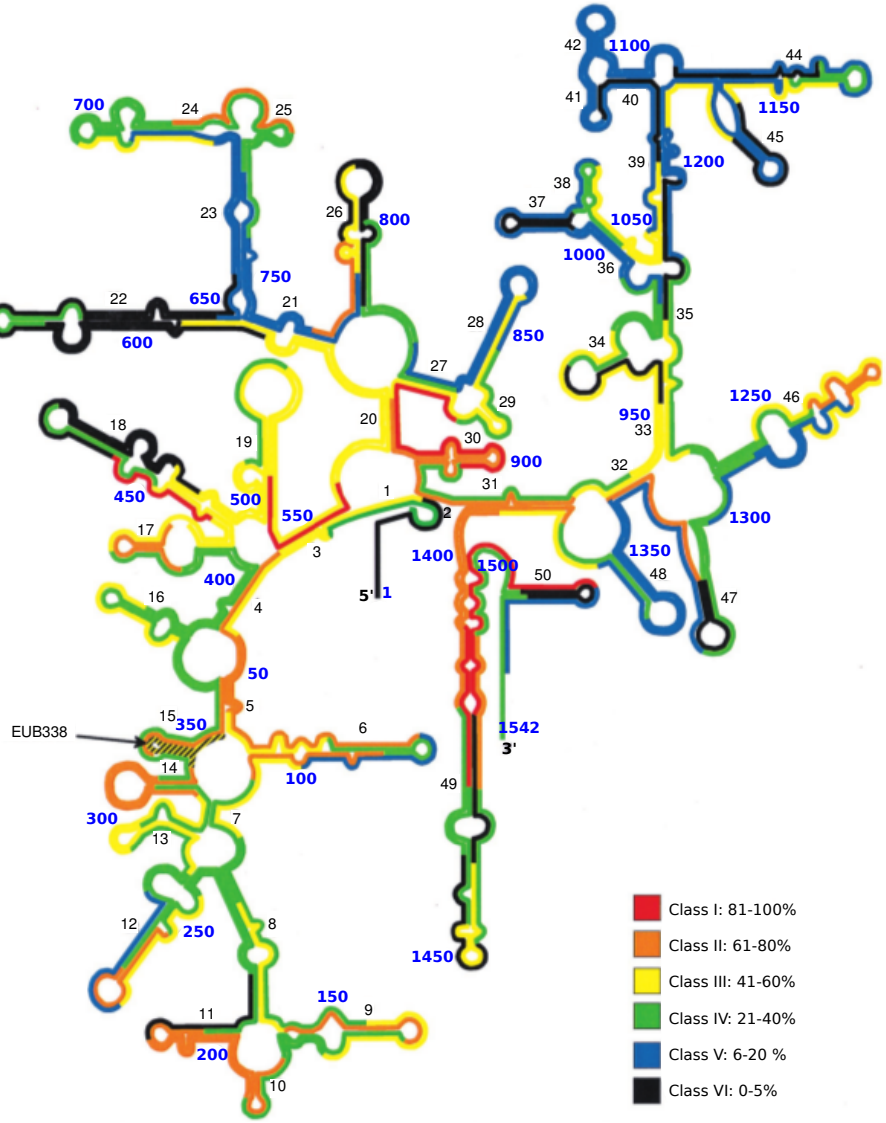


Figure 18: **Distribution of relative fluorescence intensities of oligonucleotide probes on a 16S rRNA secondary structure model.** It is standardized to that of the brightest probe Eco1482 and divided into brightness classes (I-VI). The standard bacterial probe Eub338 is also shown. Black numbers indicate structure helix and blue number nucleotide position of the gene. Author: Fuchs et al. (1998)

The Figure 18 illustrates the results of the study of Fuchs et al. (1998), in which performance of 171 oligonucloetide probes for *E. coli* FISH was tested. The probes were overlapping sets of adjacent oligonucleotides, shifted by 5-13 nucleotides and covering the whole length of 16s rRNA gene. It was found that the probes emit different levels of fluorescence and regions not suitable for probe design were identified. The best region for probe selection was found in positions 1482 to 1499 of the whole 1542 bp 16S rRNA gene length. The fluorescence of this region was 44 brighter than the worst region identified at 468-486 bp, as shown in the Figure 18.

The specificity of a probe can be adjusted by increasing of the hybridization temperature or adjusting hybridization time aiming to reduce number of false negative cells, coming from those target cells that did not get hybridized, and also to decrease the number of false positive bacteria which are not the target species (Amann and Fuchs, 2008).

The fluorescence of hybridized bacterial cells may be disturbed further by the fact that the number of ribosome copies in different cells is variable depending on bacterial species and its generation time. For example, *E. coli* can contain about 72,000 ribosomes during growth in the most optimal conditions with generation time 24 minutes. However, if the environmental conditions worsen, the generation times gets prolonged, so the number of ribosomes can drop to only 6,800 copies (Wagner, 1994). Furthermore, smaller bacteria, typically found in soil or water can have only few ribosome. This mean that the enumeration of cells belonging to different species based on this approach must be performed carefully (Amann and Fuchs, 2008).

There are several methods for increasing 16S rRNA probe fluorescence, for example the use of horseradish peroxidase-labeled probes in combination with catalyzed reported deposition (CARD) of fluorescently labeled tyramides where, instead of fluorophores, the probe is conjugated with horseradish peroxidase and the amplification of the fluorescence is achieved by radicalization of multiple tyramide molecules which permamently bind into cell (Schönhuber et al., 1997)

**Single cell analysis**

The above mentioned methods serve for separation of whole bacterial populations with selected characteristics. However, the flow cytometry sorter is an equipment that can perform selection of single cells, too. The cells can be placed for example in 96 well plates and cultured individually. Another option is to extract DNA from these single cells, which can be further used for applications such as amplification of selected genes or sequencing of the whole genome (Blainey, 2013). The advantage of single cell approach is that the novel genomes of unculturable organisms can be then assembled (Kalisky and Quake, 2011). Moreover, if 16S rDNA sequencing is applied to separated single-cells, the taxonomic structure of a bacterial community can be determined with high precision (Stepanauskas and Sieracki, 2007).

The main issue of working with single cell is the contamination which can be reduced by working with picoliter volumes of samples, trying to separate a single-cell using the smallest liquid volume possible. Therefore, miniaturized devices are being developed, they allow working with single-cells including separation of single cells, DNA extraction and amplification all in one (Marcy et al., 2007b).

The device shown in Figure 19 was developed by Leung et al. (2012). It is able to separate 95 microbial single-cells, amplify the whole genome and the reaction products can be recovered individually into standard microfuge tubes for downstream analysis. It has been tested for taxonomic diversity studies of bacteria from

marine enrichment culture, deep-sea sediments, and the human oral cavity (Leung et al., 2012).

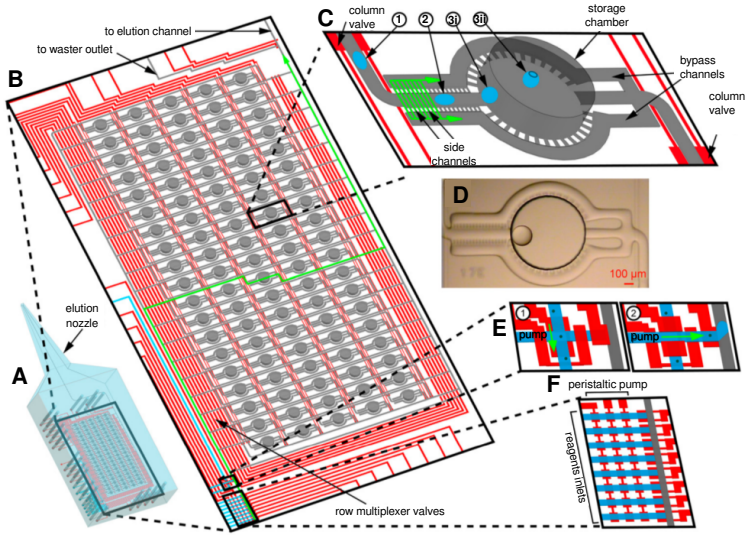


Figure 19: **Programmable microfluidic reaction array.** **A:** The device. **B:** Addressable array of 95 storage chambers. **C:** Storage element geometry: a lubricating thin film of oil (1) side channel reducing droplet velocity (2) cylindrical chamber entrance (3i), the droplet travels into the chamber and docks at the chamber ceiling (3ii). **D:** Micrograph of a 2.7 nL stored water droplet. **E:** Cell-sorting module: pumping positions (1 and 2). **F:** Reagent-metering module. Author: Leung et al. (2012)

Numerous devices for singe-cell separation, manipulation and amplification are offered on the market at the present time, e.g. Fluidigm. Their major feature is the possibility to distribute immediately single cells into microwells or microchannels. Some of them also offer PCR premix for targeted amplification of selected genes and fluorimetric detection of amplified products. Their disadvantage is that some wells can remain empty. If precise selection of cells is needed, it can be done for example by CellEctor which allows selection of cells in microdroplets from a microscopic slide (Figure 20, panel A). The fixed cells might be dissected from a microscopic slide by CellCut developed by Molecular Machines corporation (Figure 20, panel B).

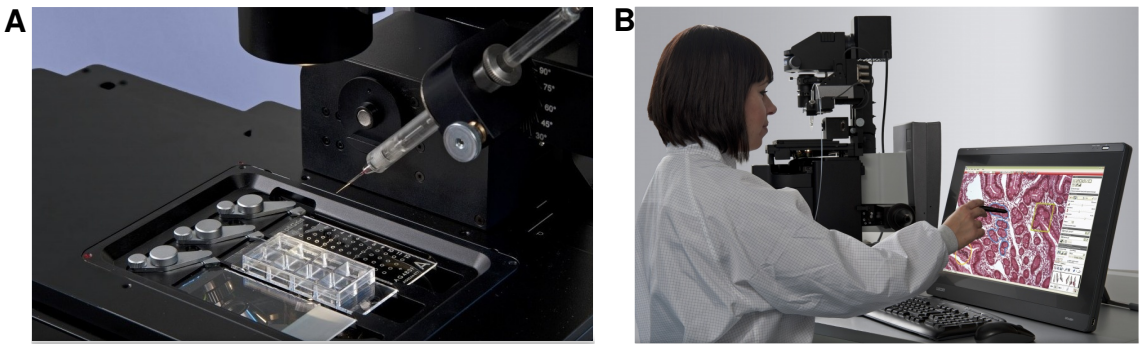


Figure 20: **Equipments for precise manual selection of single cells.** Panel A: CellEctor, panel B: CellCut. Source: Molecular Machines

Chapter 2

# Objectives of the thesis

The human gut microbiome is a very complex ecosystem. It consists of hundreds of thousands of bacteria, about half of them is still unknown and unculturable. There is a high interest in describing the genetic potential of bacteria and viruses inhabiting our gut, as the human gut microbiota acts in close relation with the human host.

One of the methods which allow to collect cells of unculturable microorganisms is fluorescence activated cell sorting (FACS). Cells with the specific features can be labeled with fluorescent dyes or probes, so the targeted bacteria can be separated from the unstained bacteria and sequenced. FACS followed by high-throughput DNA sequencing allows to decipher taxonomic diversity of bacteria with certain characteristic features and to describe the genetic potential of unculturable organism. The general objective of this thesis is to explore the bacterial and viral diversity of the human gut microbiota by sequencing of microbial fractions separated by FACS.

- **Objective 1: Active and IgA-coated cells sorting in *Clostridium difficile* infection**
  Not all the bacteria in the human gut are highly active, certain fraction is also dying or non-active. The composition of these two fractions may be influenced by different factors. The gut microbiota is also recognized by the intestinal immune system, so only a certain portion of the gut bacteria is covered by intestinal secretory immunoglobulin A. The objective of this chapter is to explore the taxonomic diversity of the active and the inactive fractions of the gut microbiota of patients infected by *C. difficile* and non-infected control patients. Also taxonomic distribution of bacterial fractions coated and non-coated by immunoglobulins A will be explained. Using this approach bacterial markers typical for *C. difficile* infection (CDI) might be determined.

- **Objective 2: Selective inhibitory effect of 8-hydroxyquinoline on *C. difficile***
  Hybridization of cells by fluorescent probes allows to detect bacterial species of choice in mixed co-cultures. Thus, selective effect of an antibiotic compound on different bacterial species can be then studied in more depth. The bacterial growth of different species can be monitored by FC along different time-points of growth in a culture media. In this chapter, one pathogenic *C. difficile* and one beneficial species *Bifidobacterium longum* is co-cultured and their growth in media with a natural antibiotic compound 8-hydroxyquinoline is monitored by FC.

- **Objective 3: Genetic diversity of *C. difficile* separated by FACS**
  Fluorescently labeled bacterial species of choice can be separated by the cell sorter and shotgun sequenced. Obtained genomic sequences would belong to a collection of all strains of the target organism. In many diseases, the strains present in one patient are identified by classical culture methods, but this method is biased by different growth rate of the strains in selective media, so an infection by multiple strains may remain uncovered. In this chapter, the cells of *C. difficile* from an infected patient are separated by FACS and the genetic diversity of the strains is explored.

- **Objective 4: Adaptation of sequencing protocols to limited DNA samples coming from FACS**
  The number of cells obtained after FACS is usually so low that DNA extracted from these cells does not reach the minimal concentration required for sequencing. The objective of this chapter is to optimize the sequencing library preparation protocols allowing to work with low DNA content samples proceeding from FACS.

- **Objective 5: Viral metagenomics directed by flow cytometry**
  Human gut virome remains still poorly explored. FACS has been previously applied to the study of

marine viral populations, but it has not been used for separation of viruses from human fecal samples yet. In this chapter, the viral sample previously filtered through 0.2 $\mu$m pores will be enriched. Selected viral particles will be sequenced on the 454 platform and annotated.

Chapter 3

# Active and IgA-coated cells sorting in *Clostridium difficile* infection

**Associated original articles:**

Džunková, M., Moya, A., Vázquez-Castellanos, J.F., Artacho, A., Chen, X., Kelly, C., D'Auria: Active and secretory IgA-coated bacterial fractions explain dysbiosis patterns in *Clostridium difficile* infection. Under revision.

Simón-Soro, Á., D'Auria, G., Collado, M.C., Džunková, M., Culshaw, S., Mira, A. (2015): Revealing microbial recognition by specific antibodies. BMC Microbiology15: 132.

D'Auria, G., Peris-Bondia, F., Džunková, M., Mira, A., Collado, M.C., Latorre, A., Moya, A. (2013): Active and secreted IgA-coated bacterial fractions from the human gut reveal an under-represented microbiota core. Scientific Reports 3: 3515.

# 3.1 Introduction

## 3.1.1 *C. difficile* infection

*Clostridium difficile* is a species of Gram-positive spore-forming bacteria. It can be found in nature in water, air, soil, human and animal feces and on most of surfaces (especially in hospitals). It is anaerobic and its optimal growth temperature is 37 °C. Under the microscope, it appears as long, irregular drumstick cells with a bulge at their terminal ends. The whole genome sequencing has resulted in new categorization of *Clostridium difficile*; it has been recently renamed as *Peptoclostridium difficile*.

*C. difficile* has been isolated from the gut of healthy neonates and asymptomatic patients. In both asymptomatic and symptomatic patients it forms only about 0.000 % of all intestinal bacteria (Matsuda et al., 2012). Despite being found to be present in such a low abundance, it is able to produce large amounts of toxins, which disturb the colon tissues. These toxins have been named toxins A (TcdA), toxin B (TcdB) and the binary toxin (Bartlett et al., 1978; Popoff et al., 1988; Stubbs et al., 2000).

The clinical outcomes of *C. difficile* infection (CDI) can range from mild diarrhea to more severe disease syndromes, including abdominal pain and fever. Fulminant or severe complicated CDI is characterized by inflammatory lesions and the formation of pseudomembranes in the colon, bowel perforation, sepsis and death. The classic appearance of *C. difficile* infection at colonoscopy is a yellowish pseudomembrane that can be washed off the inflamed mucosa (Figure 21) (Kelly et al., 1994; Rupnik et al., 2009).

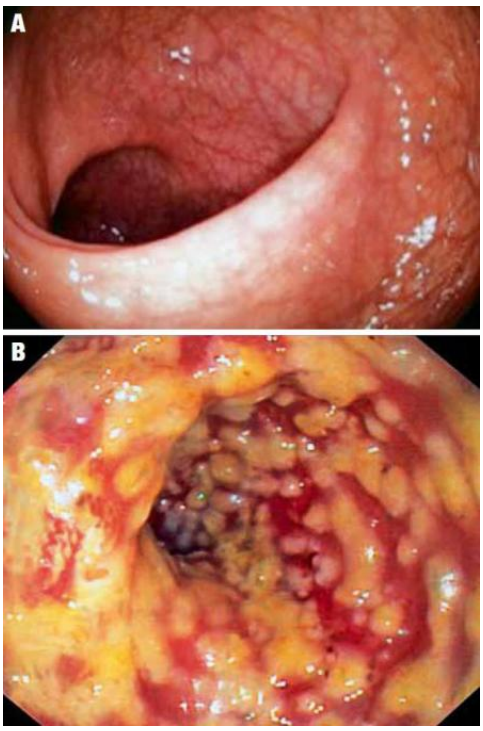


Figure 21: **Comparison of the normal colonic mucosa (Panel A) with the mucosa with CDI (Panel B).** The infected mucosa shows yellow pseudomembranes. Source: Student Oz Doc

Patients (especially elderly people) can get infected by *C. difficile* spores through contact with the hospital environment or health care workers. However, also cases in younger populations with no previous contact either with the hospital environment or with antibiotics are emerging. Patients who have acquired a toxigenic *C. difficile*, usually develop CDI if their gut microbiome is affected by dysbiosis and they are not able to mount an anamnestic serum immunoglobulin G (IgG) antibody response to the *C. difficile* toxin. If patients can mount an antibody response, they become asymptomatically colonized. Non-toxigenic strains do not cause infection symptoms (Kyne et al., 2000; Kelly and Kyne, 2011).

It is widely accepted that the onset of CDI is closely connected to the treatment with wide-spectrum antibiotics. After taking an antibiotic, the gut microbiota gets disturbed, so the proliferation of opportunistic pathogens, such as *C. difficile* can occur (De La Cochetière et al., 2008). The hamster models of CDI showed that the susceptibility to the colonization persists for several days after the administration of the last antibiotic dose; the time depends on the type of the antibiotic (Merrigan et al.,

2003).

*C. difficile* is resistant to fluoroquinolones, such as gatifloxacin and moxifloxacin (Pépin et al., 2004) and clindamycin (Kuijper et al., 2008). The only antibiotics, which may be still applied for *C. difficile* treatment, are Vancomycin and Metronidazole and the recently developed Dificlir (fidaxomycin) (Mullane et al., 2011). However, they are not so effective in relapsing patients. Moreover, the application of these antibiotics may be the cause of infections by resistant *Enterococcus*, which is a common resident of the human gut, but produces endotoxins which disrupt the epithelium, so it can cause infection in other body parts, such as endocarditis (Al-Nassir et al., 2008). Therefore, alternative treatment approaches, such as neutralization of *C. difficile* toxins by antibodies have been developed (Demarest et al., 2010). The probiotic treatment or fecal microbiota transplantation seem to be promising (Song et al., 2013; Rolfe et al., 1981). Recently, Buffie et al. (2014) used mouse models, clinical studies, metagenomic analyses, and mathematical modeling for prediction of probiotic candidates that correct the microbial deficiency occurring in the CDI.

### 3.1.2 Coating of gut bacteria by secretory immunoglobulin A

Secretory immunoglobulin A (SIgA) form the first line of immune defense in the gut. SIgA differ from serum antibodies specific to pathogens toxins. Both commensal bacteria and pathogens are coated by SIgA; it coats 25 - 75 % of gut bacteria (Kawamoto et al., 2012). Experimental pathogen free mice had 7.4±2.2 % of bacteria coated by SIgA. The genetically modified mice, that are not able to produce IgA, had only 0.5±0.3 % of intestinal bacteria stained (Palm et al., 2014).

SIgA is formed from the B cells in the mucosa-associated lymphoid tissues. In the pathway of SIgA formation, the dendritic cells sample intestinal bacteria and induce B cells to switch to the production of SIgA (Macpherson et al., 2012). This process may be performed with or without T cells (Pabst, 2012). It was demonstrated that the mice lacking classical B cell - T cell interaction can also produce SIgA (Macpherson et al., 2000). Experiments with immunodeficient mice infected by *Bacteroides thetaiotaomicron* demonstrated that the induction of SIgA is not regulated only by the host, but also the proper commensal bacteria induce the production of the SIgA (Peterson et al., 2007). Probiotic bacteria are also able to stimulate production of intestinal SIgA (Atarashi et al., 2011; Hapfelmeier et al., 2010; Galdeano and Perdigón, 2006).

SIgA does not interact with the pathogens and commensals in the same way (Kawamoto et al., 2014). When pathogens attempt to cross the epithelial barrier, the SIgA can cooperate with other elements of the immune system which should remove the pathogens from the gut (Macpherson et al., 2012). The immune system senses pathogen-associated activities or behaviors, such as adherence to the intestinal epithelium, tissue invasion or destruction, or the ability to colonize normally sterile mucosal environments, such as intestinal crypts. This sensing is provided by epithelial cells which use apical transporters for sampling of controlled amounts of bacterial pathogen associated molecular motifs or quorum-sensing autoinducers (McGuckin et al., 2011). The specific SIgA coating has not been investigated for particular intestinal infections yet, however, certain pro-inflammatory bacterial communities coated by IgA have been identified for inflammatory bowel disease (Palm et al., 2014).

The case of SIgA-coating of commensal bacteria is different. SIgA prevents the access of the beneficial bacteria to the proper human body, but maintains them within the gut lumen. In the case of commensal bacteria, the immune system is prepared for possible response action. This state may be called "physiological

inflammation". The pathogen produce molecular motifs which are probably more agonistic to pathogen-pattern recognition receptors than the molecules produced by commensals. Moreover, the commensals can dampen the innate immune responses, while the pathogens are not able to do so (Sansonetti, 2010).

There are multiple ways how the pathogens can escape the IgA coating and subsequent removal from the gut (Ng et al., 2013). One of the ways may be the covering of the cell surface by molecules which avoid opsonization by SIgA. During normal gut homeostasis, the gut lining expresses mucus molecules which have on their tips sialic acid. Sialic acid is found in animal tissues and bacteria, mostly forming part of glycoproteins and gangliosides. The normal gut microbiota cleaves the sialic acid by releasing sialidase (Ley, 2014). The pathogenic gut bacteria may coat themselves with sialic acid to inhibit or avoid host immune system responses. According to Vimr et al. (2004), there are four ways of bacterial cell surface covering by sialic acids. (i) Bacteria, such as *E. coli*, can synthetize the sialic acid by themselves (Figure 22). (ii) *Neisseria gonorrhoeae* has evolved a mechanism of using sialyltransferase which is present in small amounts as a normal constituent in human secretions. (iii) *Trypanosoma* species and *Corynebacterium diphtheriae* have endogenous trans-sialidase acceptors, which are mucin-like molecules that when sialylated may protect bloodstream trypanosomes from innate (antibody-independent) immunity. Moreover, host cell surface remodeling of glycoproteins facilitates parasite adhesion and invasion. (iv) *Haemophilus influenzae* scavenges host sialic acid and uses it for cell surface covering.

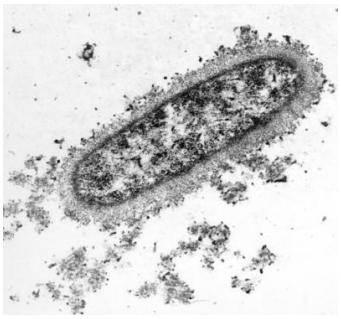

Figure 22: ***E. coli* coated by sialic acid.** Author: Vimr et al. (2004)

### 3.1.3 Activity of bacteria in the human gut

Bacteria in the human gut are continuously growing and dying, so not all bacteria in the human gut are active in the moment of sampling (Ben-Amor et al., 2005; Müller and Babel, 2003). The analysis of the taxonomic composition of the active bacterial fraction showed that the active bacteria differ among individuals (Peris-Bondia et al., 2011). It was concluded that one of the most active and antibiotic resistant taxonomic groups are the *Firmicutes*, which may be, on the other hand, the most damaged ones (Maurice et al., 2013). Interestingly, as shown in Figure 23 a great part of the most prevalent bacterial groups, such as *Bacteroidetes* is actually inactive (Peris-Bondia et al., 2011).

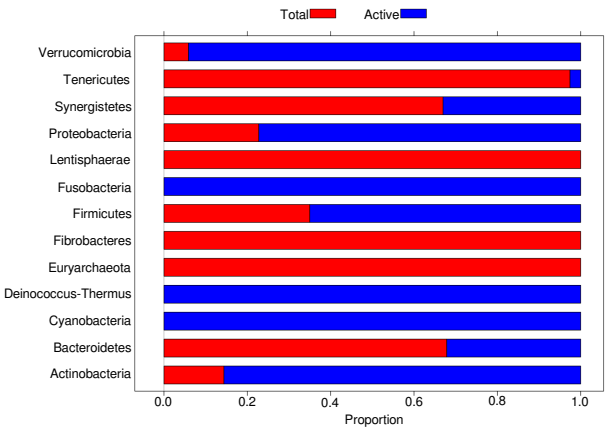


Figure 23: **The proportion of the active bacterial cells in each taxonomic group.** Author: Peris-Bondia et al. (2011)

The effect of the antibiotics may be reflected in the decreased activity of the bacteria or in the complete destruction of bacterial cells (Figure 24). This can be observed as the loss of membrane integrity, membrane polarity and in a decrease of the nucleic acid content (Maurice et al., 2013). At the same time, resistant bacteria may be substituting the susceptible ones. At the end of the antibiotic treatment, the bacterial species

composition may get changed, but the essential functions are being performed by community members which survived the treatment (Pérez-Cobas et al., 2012). These changes may be reflected in the increasing/decreasing proportion of the active bacteria during longitudinal studies including long-term antibiotic treatment.

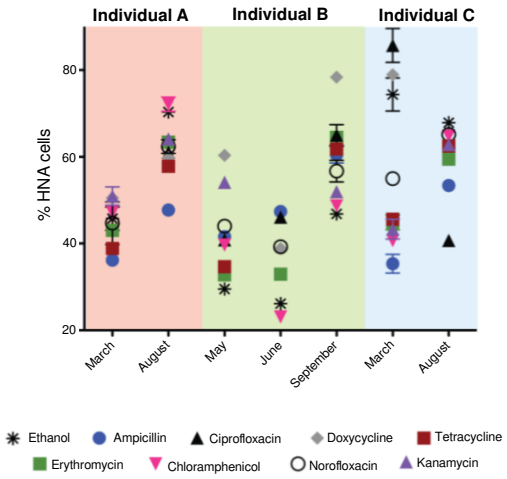


Figure 24: **The percentage of the active bacteria varies over time.** The different xenobiotics have differential effects on the cell activity. Author: Maurice et al. (2013)

It was also found that the host-targeted drugs do not influence the activity of the intestinal bacteria (Maurice et al., 2013). However, the proper bacteria in the gut may produce compounds that influence the activity of the other species present in the ecosystem. For example, there are speculations about the toxins produced by *C. difficile* which may also act against the bacteria in the community. It is based on the observation that two different toxinotypes of *C. difficile* have been associated with two different gut bacterial patterns (Ling et al., 2014; Skraban et al., 2013).

## 3.2 Objectives

CDI is associated with the use of the high-spectrum antibiotics, as it possesses several antibiotic resistant genes and is able to benefit from the metabolic changes occurring in the microbiome disrupted by antibiotics. In the daily clinical practice multiple combinations of antibiotics are applied to the patients and they often suffer from additional intestinal complications as well, so the microbial composition of the patient's gut can be disrupted by multiple additional factors. There have been attempts to define the taxonomic composition of the gut microbiota typical for CDI patients, however the results remain elusive. Interestingly, in the studies, in which the overall gut microbial composition of the CDI+ and CDI- groups are compared by metagenomics, the species of *C. difficile* is not differentiating the two groups, because *C. difficile* may be detected also in asymptomatic patients. Moreover, the proportion of *C. difficile* in the symptomatic and asymptomatic patients is very low, sometimes undetectable in metagenomic analysis. It suggests that despite being one of the minority species in the infected gut, *C. difficile* is able to produce significant amounts of toxin and damage the gut tissues.

As it seems that the overall bacterial composition typical for CDI cannot be defined, we aimed to determine microbial patterns typical for CDI by studying active gut bacteria and bacteria coated by unspecific intestinal SIgA. We hypothesized that *C. difficile* might be distinguishing CDI+ and CDI- patients in some these microbial fractions, independently on the antibiotic treatment taken.

We aimed to detect which bacteria are active during the antibiotic treatment which consequently leads to the development of CDI. We hypothesized that even if different kinds of antibiotics have been used, the patients with CDI must have a common bacterial cores of active and dead intestinal bacteria. Similarly, the patients without CDI may have a community of active bacteria which protect them from the CDI. We aimed to detect which of gut bacteria are recognized by SIgA. Hypothetically, if some of them are able to escape immune responses, they would be present in the fraction of bacteria not opsonized by SIgA. In contrast, bacteria recognized by the immune system will be coated by SIgA.

FACS will be used for sorting of bacteria which are opsonized by SIgA in the work presented in this chapter. The taxonomic composition of IgA opsonized and non-opsonized bacterial will be detected by 16S rRNA sequencing. Our objective is to find statistically relevant correlations between microbial composition of these fractions and the patients' medical data.

# 3.3 Methods

## 3.3.1 Samples preparation

**Patients medical data**

The participants of this study were 24 hospitalized patients from Beth Israel Deaconess Medical Center, Harvard Medical School, MA, U.S.A. with CDI symptoms or within the risk category for CDI and therefore tested for CDI by routine Illumigene assay (Meridian Biosiences, Ref. 280050). The study was approved by the institutional review board, and informed consent was obtained from all patients. Twelve patients have been diagnosed to be CDI negative (CDI-) and 12 CDI positive (CDI+). Patients' total dose of antibiotics taken is shown in Table 3.

Table 3: **Patients medical data**

| Patient number | Patient | Antibiotic CDI treatment | Antibiotics associated with onset of CDI | Antibiotics with no reported association to CDI |
|---|---|---|---|---|
| 1 | CDIneg01 | Vancomycin (2 g), Metronidazole (12 g) | - | Tigecyclin (0.05g) |
| 2 | CDIneg02 | Vancomycin (7 g) | Cefepime (54 g) | - |
| 3 | CDIneg03 | Vancomycin (6 g) | Cefepime (12 g) | Cefazolin (6g) |
| 4 | CDIneg04 | Vancomycin (12 g), Metronidazole (9 g) | Cefepime (36 g) | Ampicillin - Sulbactam (48 g), Amoxicillin - Clavulanic acid (3.5 g) |
| 5 | CDIneg05 | - | - | - |
| 6 | CDIneg06 | - | - | - |
| 7 | CDIneg07 | Rifamixin (0.25 g) | Ciprofloxacin (0.25 g) | - |
| 8 | CDIneg08 | Vancomycin (1.25 g) | Cefepime (2 g) | - |
| 9 | CDIneg09 | Metronidazole (5 g) | Ciprofloxacin (5 g) | - |
| 10 | CDIneg10 | - | - | - |
| 11 | CDIneg11 | - | - | - |
| 12 | CDIneg12 | - | - | Piperallicin - Tazobactam (9 g) |
| 13 | CDIpos01 | - | - | - |
| 14 | CDIpos02 | - | - | - |
| 15 | CDIpos03 | Metronidazole (12 g), Vancomycin (16 g) | Ciprofloxacin (7.2 g) | - |
| 16 | CDIpos04 | - | - | - |
| 17 | CDIpos05 | - | - | - |
| 18 | CDIpos06 | - | - | - |
| 19 | CDIpos07 | Vancomycin (2 g) | Ceftraxone (2 g), Cepefime (6 g) | Piperallicin - Tazobactam (27 g), Amoxicillin - Clavulanic acid (5 g) |
| 20 | CDIpos08 | - | - | - |
| 21 | CDIpos09 | - | - | - |
| 22 | CDIpos10 | - | Ciprofloxacin (1 g) | Nitrofurantoin (1.6 g), Cephalexin (3 g), Piperallicin - Tazobactam (27 g) |
| 23 | CDIpos11 | - | Levofloxacin (0.5 g) | - |
| 24 | CDIpos12 | - | Clindamycin (7.2 g) | - |

The amounts of *C. difficile* genes of toxin A and toxin B and *C. difficile* specific 16S rDNA gene quantified by quantitative PCR (qPCR, Qiagen, Ref. BPVF00463AF, BPVF00464AF, BPID00110AF) were taken into account, too. The protocol for quantification of toxin A, toxin B and 16S rRNA of *C. difficile* is explained in the protocol section 11.11.

**Fractions of the total bacteria population**

The bacterial fecal suspension was collected and fixed with formaldehyde as described in the protocol section 11.3.

The fecal bacterial suspensions were divided into 4 tubes; all of them were stained with DNA stain (SYTO®62 at concentration 50 $\mu$M from Life Lechnologies, Ref. S11344) for distinguishing the bacteria from the cytometer electrical noise (described in more details in the protocol section 11.13).

The second staining was performed with one of the following:

- IgA-human labeled with FITC (Life Technologies, Ref. M31001)
- IgA-mouse labeled with FITC as isotype control (Life Technologies, Ref. A24459)
- pyronin Y for staining RNA for active cell sorting (10 $\mu$l of pyronin Y at concentration 0.1 mM (Sigma-Aldrich, Ref. P9172-1G)
- The 4$^{th}$ tube was left as a negative control

The IgA staining is described in more details in the protocol section 11.14.

The FACS was performed on S3 cell sorter (Bio-Rad) by setting the cytometer emission filters to green light emission (FL1) for FITC-labeled IgA antibodies, to the orange light emission (FL2) for pyronin Y stained cells and to the red emission light (FL4) for SYTO®62 stained cells detection.

Two rounds of sorting were performed.

The SIgA-coated cell sorting resulted in 2 tubes:

- SIgA coated bacteria (IgA-pos-F)
- Bacteria not coated by human IgA (IgA-neg-F)

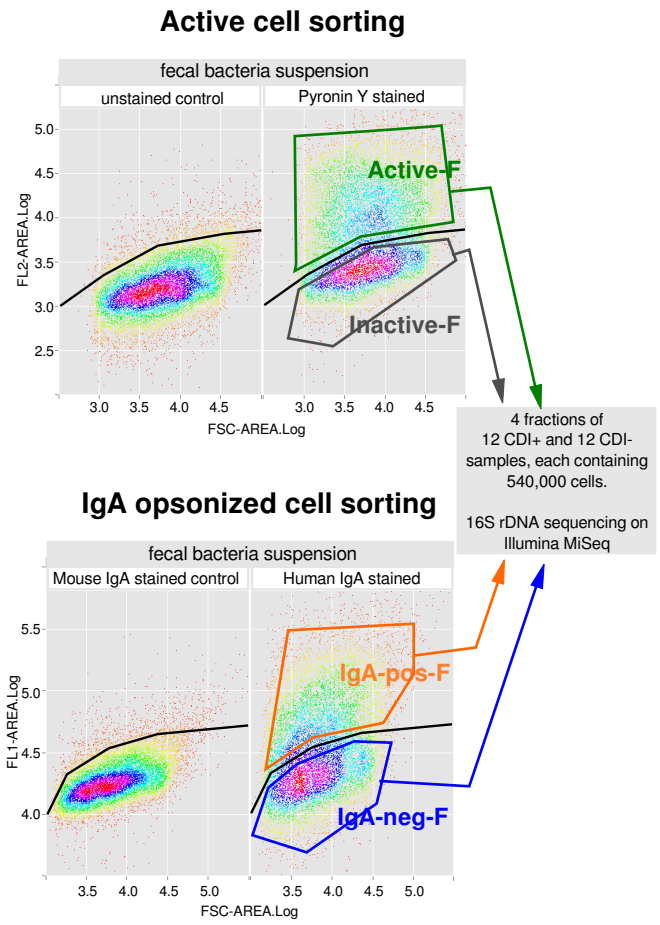


Figure 25: **FACS bi-plots showing the set-up of sorting gates by comparison with negative controls.** Each sample was used for two separated sorting rounds: active bacteria sorting and human-IgA coated bacteria sorting

Similarly, from the active cell sorting 2 separate tubes were obtained:

- Active bacteria (active-F)
- Bacteria with low RNA amounts (inactive-F)

Each tube contained 540,000 cells (Figure 25). The proportion of cells in bacterial fractions was calculated using "flowViz" package from R statistics environment (R Development Core Team, 2008).

**In vitro culture test of antibiotic influence on bacterial cell activity**

In order to detect the differences of bacterial composition of the active and the inactive bacterial fractions, antibiotics were applied to the bacterial culture of fecal bacteria suspension.

One ml of fecal bacterial suspension was inoculated in 10 ml of anaerobic media reported to recover wide diversity of human gut microbiota (Goodman et al., 2011), containing no antibiotics or Metronidazole (40mg/l). The culture tubes with media were prepared similarly as for *C. difficile* culture described in the protocol section 11.4. Culture samples of volume 0.5 ml were taken every hour from each flask.

The cells for active cell sorting were fixed and stained with pyronin Y as described above for patients' fecal samples (protocol section 11.13). They were also amplified by the same primers (protocol section 11.1). The 16s rRNA gene amplicons were sequenced by Sanger method (laboratory protocols section 11.2).

The FC bi-plots of these growth curves are shown in Figure 26. Finally the following cells fractions were sorted:

- 63,096 cells for the time-point 0 hours in media with antibiotics
- 84,683 cells for the active fraction at the time-point 10 hours in media with antibiotics
- 95,241 cells for the inactive fraction at the time-point 10 hours in media with antibiotics
- 81,857 cells for the active fraction at the time-point 10 hours in media without antibiotics

## 3.3.2 Sequencing and data analysis

**Sequencing and sequence processing**

DNA from all the 96 samples (active-F, inactive-F, IgA-pos-F, IgA-neg-F fractions for each of the 24 patients) was extracted at once in sterile conditions by phenol-chloroform extraction (Ausubel et al., 1992), as described in more details in the protocol section 11.5. The regions V3 and V4 of 16S rDNA (Klindworth et al., 2013) were amplified and prepared for sequencing in one MiSeq Illumina run. In order to confirm the results, replicates of 24 samples were sequenced.

Short, low quality and chimeric sequences were removed by Prinseq program (Schmieder and Edwards, 2011). Sequences of length $< 200$ nt have not been considered; 5' trimming was performed by cutting out nucleotides with a mean quality $< 30$ in 20 bp windows. Eventual chimeric 16S amplicons have been removed by USEARCH program (Edgar, 2010) as described in the programming scripts section 12.6, what resulted in

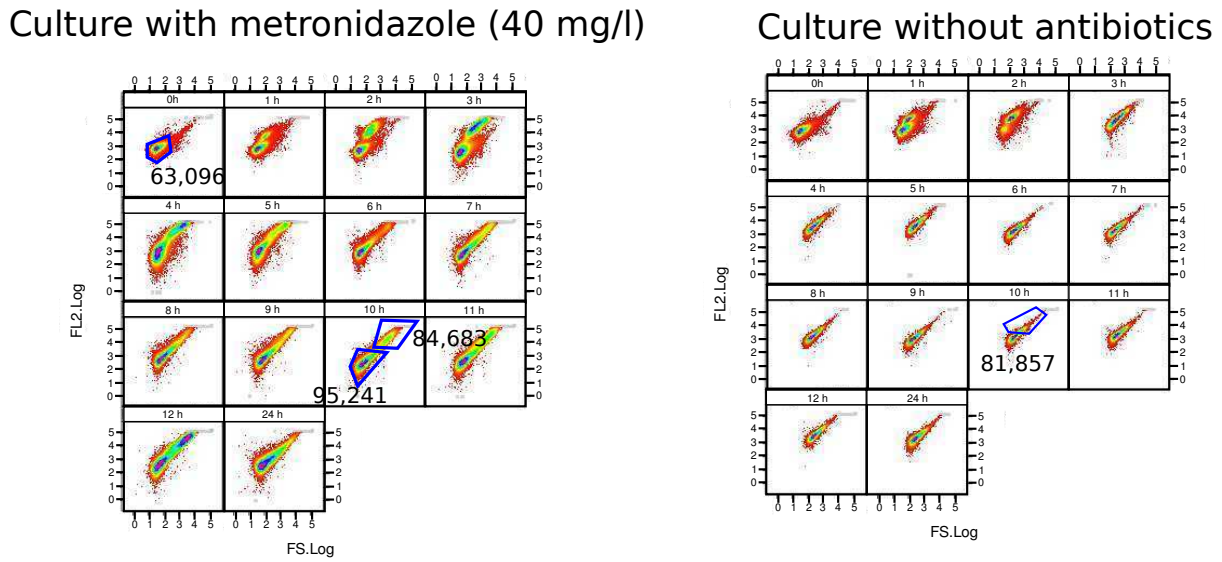


Figure 26: **Flow cytometry bi-plots of the growth curves of fecal suspension with and without Metronidazole.** The gates for cell sorting and number of sorted cells are shown

an average of 163,519 sequences per sample. The sequences have been deposited in European Nucleotide Archive database with study accession number PRJEB8416.

**Analysis of the overall bacterial composition**

Obtained sequences were taxonomically classified by RDP_classifier (boostrap cut-off 0.8) program from Ribosomal Database Project up to genus taxonomic rank (Cole et al., 2009). Genera represented for less than 10 reads in average among all samples were not considered.

The canonical correspondence analysis was used for the ordination of the 24 samples (for each fraction separately) in which the bacterial composition was tested for fitting on medical data using the "envfit" function from "vegan" R package (programming script section 12.2). As categorical medical data were considered:

- CDI
- Antibiotics categorized into 3 groups: (I) antibiotic against CDI, (II) antibiotics promoting CDI and (III) antibiotics with neutral effect on CDI onset

As numerical data we considered:

- Amounts of toxin A
- Amounts of toxin B
- Amounts of specific *C. difficile* 16S rDNA gene
- Total doses of each of the three antibiotic types

**Comparison of the frequency of the bacterial genera in the separated fractions**

Fold-change frequency tests between

- active-F and inactive-F

- IgA-pos-F and IgA-neg-F

were performed by the R package "edgeR", shown in programming scripts section 12.4.

Statistically significant associations of the medical data with the statistically significant fold-change increase of bacterial genera in one of the compared fraction pairs ($p < 0.01$, Benjamini-Hochberg correction) have been visualized in a Bayesian network (a graphical probabilistic model) by R package "bnlearn", explained in details in the programming scripts section 12.1. The nodes of the network (Figure 32) corresponded to the occurrence of bacterial genera in the four fractions, CDI and the three types of antibiotic treatment (excluding antibiotics started on the day of the sample collection). Only bacterial genera increased significantly in at least 5 patients in one of the compared fraction pairs were included in the network. The connecting arcs represented a mutual associations rather than causality. In order to determine which bacteria predict the behavior of a selected node, a subset called Markov blanket can be extracted (Pearl, 1988), in our case the nodes corresponding to the three types of antibiotics and CDI were dissected. The dissection of Markov blankets is also shown in the programming scripts section 12.1.

# 3.4 Results

## 3.4.1 Load of *C. difficile* specific 16S rDNA, toxin A and toxin B genes detected by qPCR

The qPCR assay detected specific *C. difficile* 16s rDNA sequences in 16 samples of the patients cohort; it formed 0.0001 % - 0.881 % of total gut microbiota.

Four of these patients were considered clinically CDI- by Illumigene assay and the absence of toxin genes was confirmed also by qPCR, indicating that these patients were colonized by non-toxigenic *C. difficile* strains. In six CDI+ patients, the burdens of toxin A gene were 1.4 - 5 times lower than burdens of toxin B genes, suggesting that these patients might be colonized by A+B+ and A-B+ toxinotypes Table 4.

Table 4: **Proportion of cells belonging to *C. difficile* and containing toxin A genes or toxin B genes**

| Sample name (CDI negative samples) | 16S rDNA | Toxin A | Toxin B | | Sample name (CDI positive samples ) | 16S rDNA | Toxin A | Toxin B |
|---|---|---|---|---|---|---|---|---|
| **CDIneg01** | - | - | - | | **CDIpos01** | 0.0972 | 0.0012 | 0.0012 |
| **CDIneg02** | - | - | - | | **CDIpos02** | 0.1091 | 0.0003 | 0.0010 |
| **CDIneg03** | 0.0002 | - | - | | **CDIpos03** | 0.8580 | 0.0055 | 0.0054 |
| **CDIneg04** | 0.0008 | - | - | | **CDIpos04** | 0.0013 | 0.0010 | 0.0012 |
| **CDIneg05** | - | - | - | | **CDIpos05** | 0.0044 | 0.0002 | 0.0010 |
| **CDIneg06** | 0.0002 | - | - | | **CDIpos06** | 0.8881 | 0.0071 | 0.0100 |
| **CDIneg07** | 0.0001 | - | - | | **CDIpos07** | 0.0262 | 0.0002 | 0.0001 |
| **CDIneg08** | - | - | - | | **CDIpos08** | 0.0406 | 0.0004 | 0.0010 |
| **CDIneg09** | - | - | - | | **CDIpos09** | 0.0021 | 0.0002 | 0.0001 |
| **CDIneg10** | - | - | - | | **CDIpos10** | 0.0029 | 0.0002 | 0.0010 |
| **CDIneg11** | - | - | - | | **CDIpos11** | 0.0001 | 0.0001 | 0.0001 |
| **CDIneg12** | - | - | - | | **CDIpos12** | 0.0284 | 0.0002 | 0.0010 |

## 3.4.2 Proportions of active and IgA coated bacteria

The results of fluorescent cell counting indicated that not all active bacteria were coated by IgA: the proportion of cells belonging to the IgA-pos-F was lower (39.67 ± 7.73 %) than the proportion of cells belonging to the active-F (63.02 ± 5.56 %). The outlying samples for IgA-pos-F were more homogeneous in active-F proportion (Figure 27). The mouse-IgA control allowed to remove non-specifically labeled bacteria (31.05 ±2.43 % of all bacteria).

Despite the fact that the proportion of active-F was significantly lower in the patients undertaking antibiotic treatment (56.79 ± 4.79 %) than in the patients without antibiotics (69.25 ± 4.24 %, t-test, p = 0.0473, Figure 27, panel C), the active-F proportion range was wide in the both groups (40.26 - 83.87 % and 48.46 - 87.7 %, respectively).

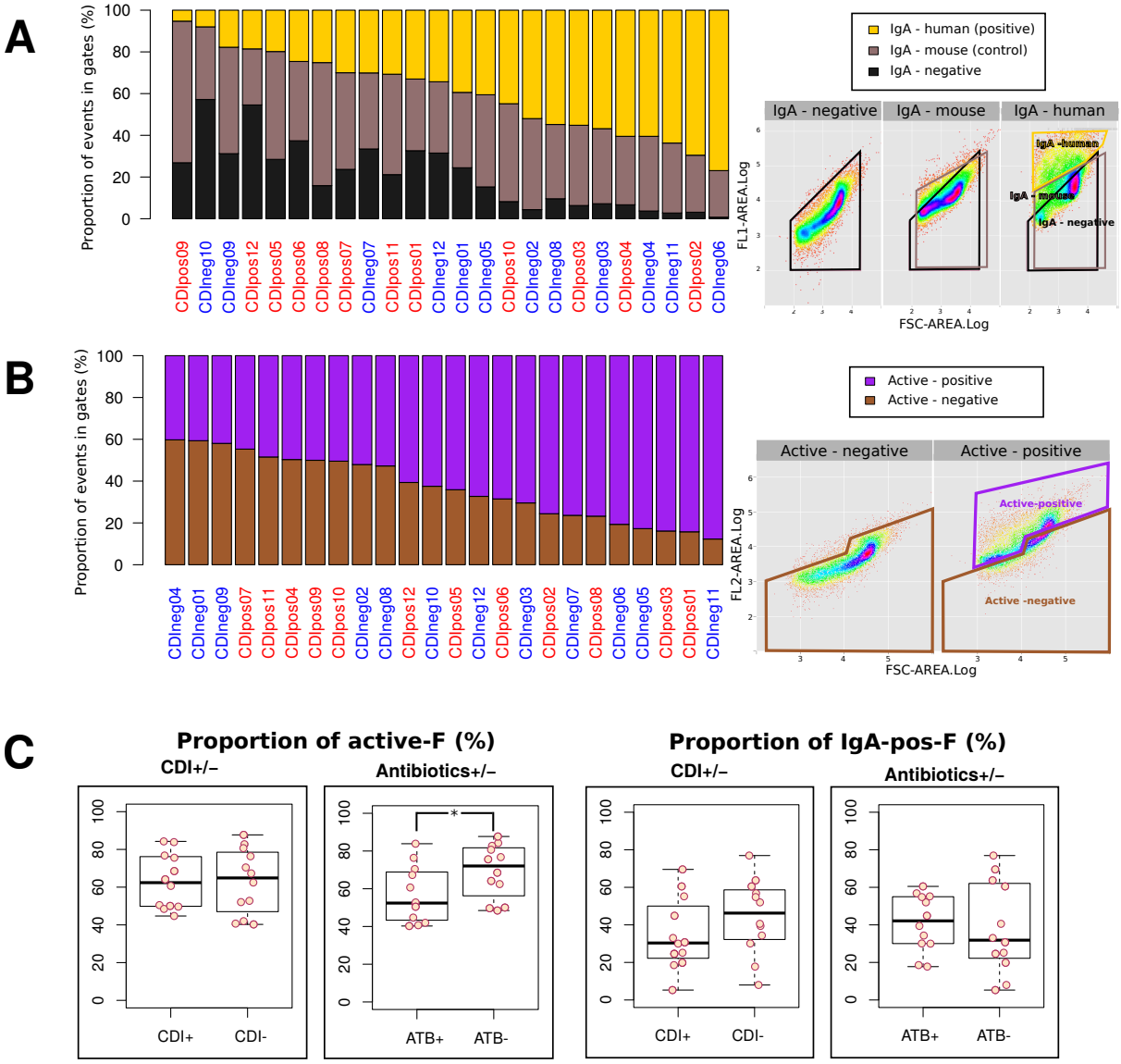


Figure 27: **Proportion of events in set gates. Panel A:** Cells not stained by IgA, mouse-IgA isotype control and human IgA staining. **Panel B:** Cells in active-F and inactive-F **Panel C:** Comparison of proportions of bacteria in active-F and IgA-pos-F in CDI+/- groups and antibiotics +/- groups of patients' samples

### 3.4.3 The overall bacterial composition of the active fraction of the bacterial cell culture

The *in vitro* fecal bacteria culture experiments in this study confirmed that antibiotics alter the species composition of active-F (Figure 28).

The media with Metronidazole was characterized by high diversity of bacteria at the time-point 0 hours, typical for any fecal sample. As the media itself has also influence on bacterial composition, *Escherichia/Shigella* was the most dominant species (76.2 %) of the active-F after 10 hours of this culture without antibiotics. Other detected species were *Enterococcus* and *Alcaligenes* and *Rhodanobacter*, however forming less than 15 % of total microbial composition.

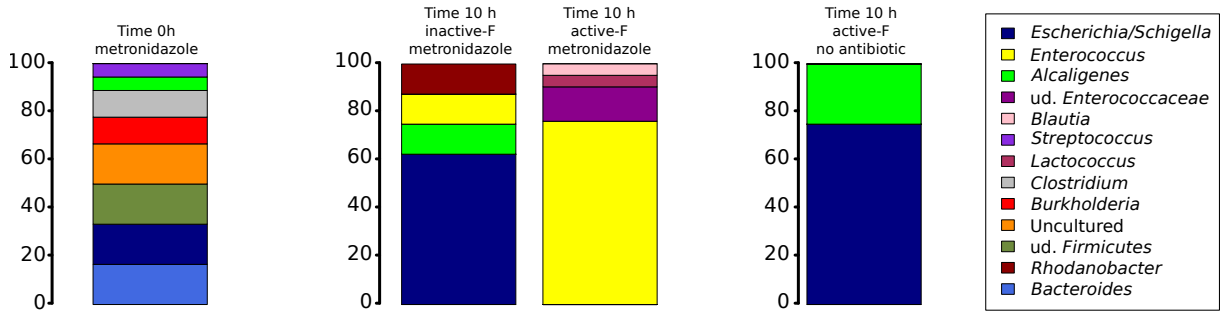


Figure 28: **Results of 16S rDNA gene sequencing of microbial culture sample cultivated with and without antibiotics**

In contrast, at the time-point of 10 hours in the culture with Metronidazole, *Escherichia/Shigella* (62.5 %) was found in the inactive-F (dying). Figue 28 shows that Metronidazole in this media did not affect *Enterococcus* which formed 76.2 % of the active-F at the same time point. The increase of proportion of *Enterococcus* in the culture with Metronidazole in comparison with the media without Metronidazole is caused by its antibiotic resistance. Similar results were expected from *in vivo* experiments with the patients cohort.

### 3.4.4 Bacterial composition of the four separated fractions

*Enterococcus*, *Ruminococcus*, *Faecalibacterium* and undetermined species of *Lachnospiraceae* were the most dominant genera detected. However, they did not distinguish clearly the CDI+ and CDI- groups, as they were present in abundance in some patients of the both groups.

The detected bacterial genera were found to have different proportions in the four separated fractions. Therefore, the four fractions in the present study had significant influence on ordination of the 96 samples ($p < 0.001$) in the canonical correspondence analysis (CCA) (Figure 29).

The patients in the present study showed very different microbial patterns, probably beacuse they had different medical history. Therefore, the influence of different medical factors on ordination of samples was tested. It is shown in the CCA in the Figure 30.

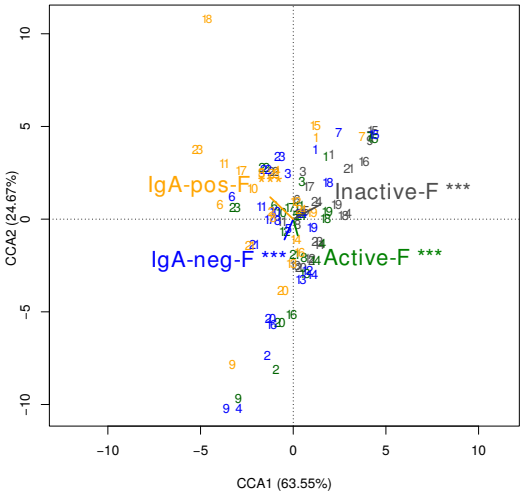


Figure 29: **CCA of samples, fitting into 4 fractions**

Antibiotics were found to shape significantly the overall bacterial composition of the four separated fractions ($p < 0.05$). In contrast, the diagnosis of CDI+/- and the quantified amounts of toxin A and toxin B did not have significant influence on the overall bacterial composition of the bacterial fractions.

*Enterococcus* was typical for patients undergoing antibiotic CDI treatment (Metronidazole and Vancomycin) in the four fractions. The proportion of *Enterococcus* in the active-F and IgA-pos-F samples was rising with the increasing dose of antibiotic CDI treatment. Also the dose of antibiotics associated with the onset of CDI, such as cephalosporins and Clindamycin, had significant influence on ordination of active-F samples. The

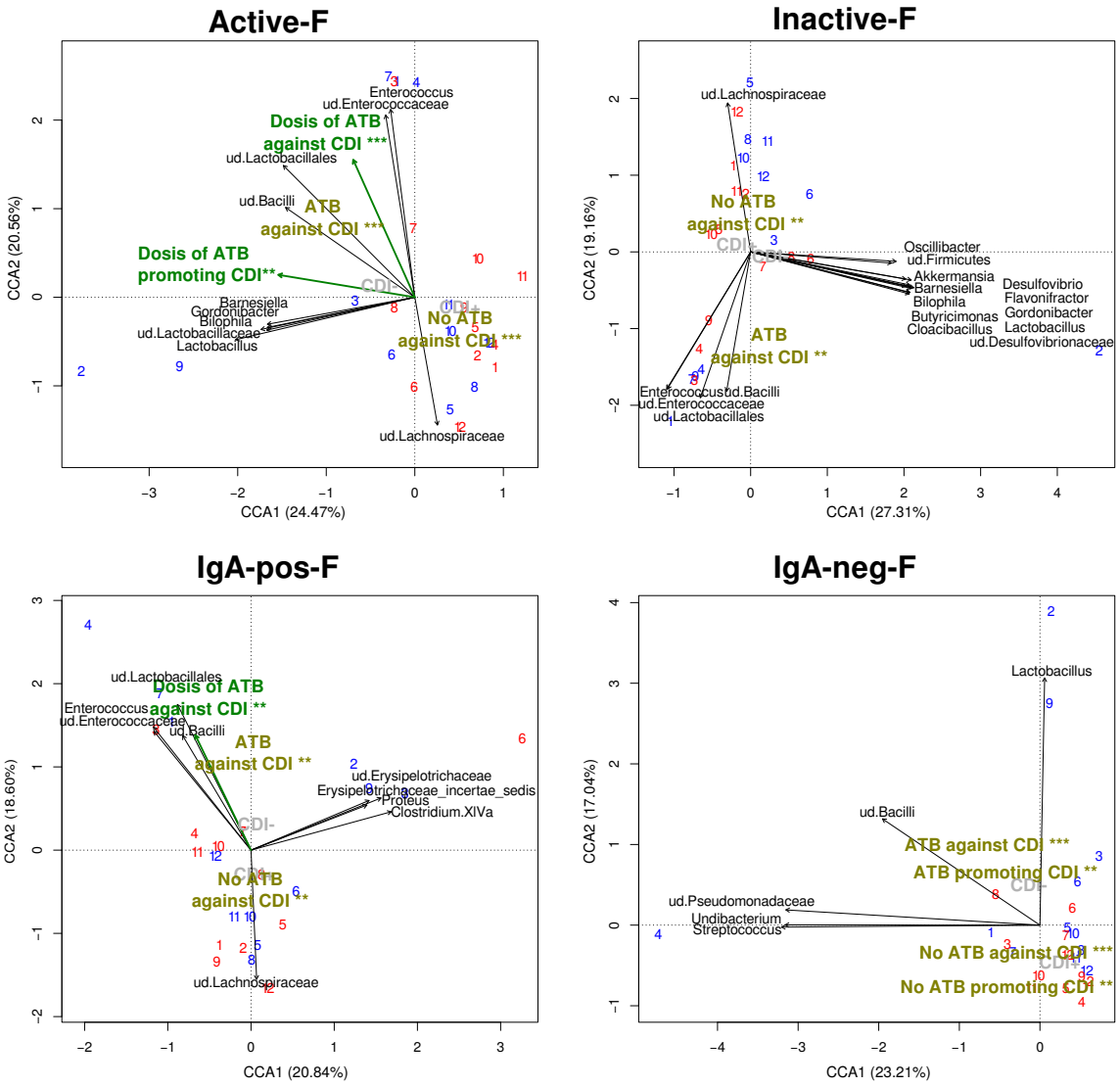


Figure 30: **Ordination of the 24 samples shown separately for each separated fraction, tested for fitting on medical data.** As numerical factors were taken into account the total dose of antibiotic treatment and the load of toxin A and toxin B genes quantified by qPCR. As the categorical medical data were taken into account the diagnosis of CDI and the type of antibiotic treatment ((i) antibiotic against CDI, (ii) antibiotics promoting CDI and (iii) antibiotics with neutral effect on CDI onset). The bacterial species (black) and numerical variables (bold green) with significant influence on the ordination of samples are shown ($p < 0.01$). The categorical medical data (olive green) are shown with the stars corresponding to the p-value (** $p<0.01$, *** $p<0.001$). The diagnosis of CDI as a categorical factor did not have significant influence on the ordination of samples ($p>0.05$), however, its ordination effect is shown in light gray just for illustration. Samples are marked by numbers in red or blue corresponding to CDI+ or CDI- patients

antibiotics associated with the onset of CDI and the antibiotics used for CDI treatment have been applied concurrently in several patients in our cohort (Table 3), what was reflected in their similar influence on the ordination of the IgA-neg-F samples (Figure 30). The variable of "antibiotics" affected the microbial composition in a direction which was contrary to the variable of "no antibiotics". In general, the bacterial composition of patients without antibiotic treatment was so divergent that no common characteristic bacterial

pattern could be defined for them, except from the *Lachnospiraceae* group.

When the proportion of bacterial genera in the active-F was compared with the inactive-F and similarly, when the proportion of genera in the IgA-pos-F was compared with the IgA-neg-F, significant fold-change differences (p-value < 0.01) were detected (Figure 31). *Bifidobacterium*, *Lactobacillus* and *Nesterenkonia* could be labeled as genera typical for active-F, as the proportion of the inactive cells was never greater than the proportion of the active cells. In patients undertaking antibiotic CDI treatment, the *Enterococcus* cells were equally distributed among the active-F and the inactive-F. However, in the patients without antibiotic CDI treatment, a significant part of *Enterococcus* cells were inactive.

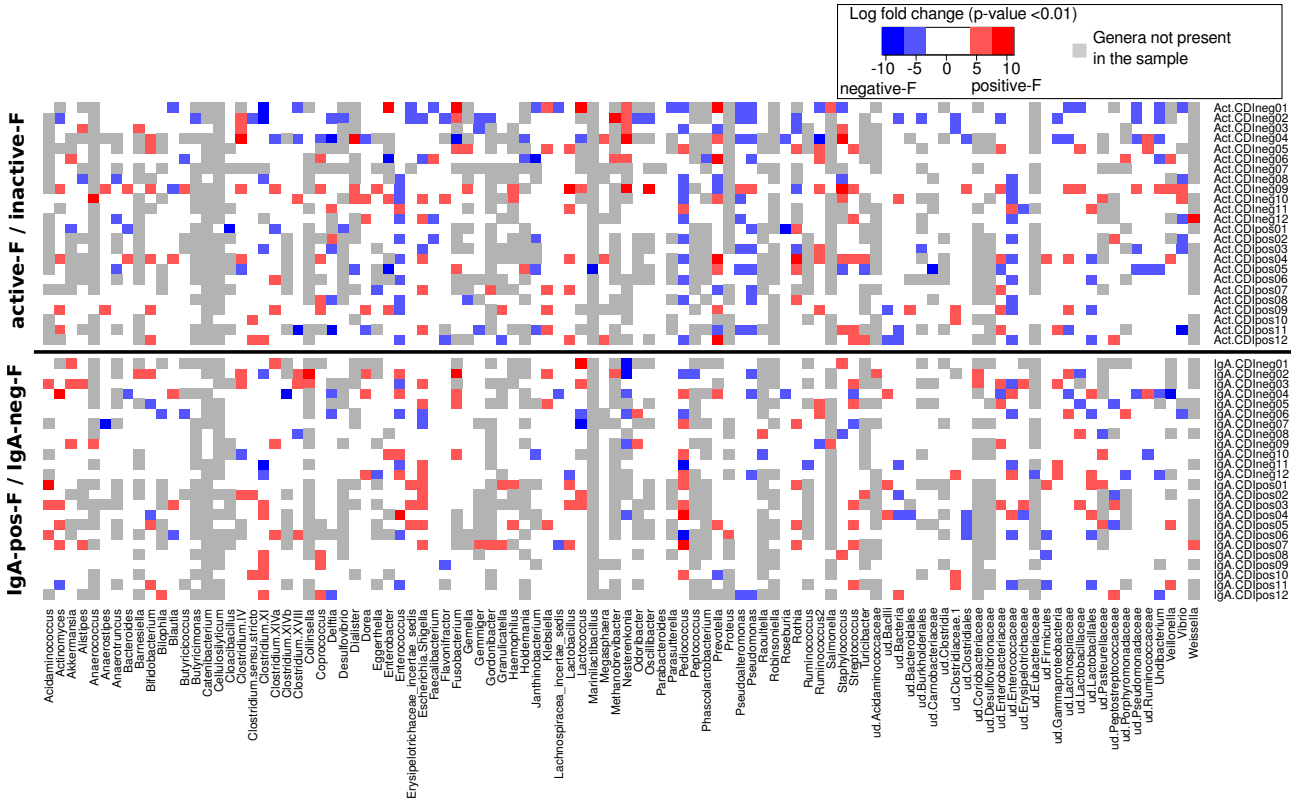


Figure 31: **Heatmap comparing proportion of each genus in active-F with its proportion in inactive-F, as well as its proportion in IgA-pos-F with its proportion in IgA-neg-F.** Genera which appeared to be significantly increased (p < 0.01) in active-F or IgA-pos-F are marked by red color, while the genera significantly increased in inactive-F or IgA-neg-F are marked by blue. The intensity of red or blue depends on fold of increase. White fields mean that no significant increase in none of the compared fractions was detected. Gray fields mean that the genus was not detected in the sample at all

Statistically significant associations of the medical data (the three types of antibiotic treatment and CDI) with the statistically significant fold-change increase of bacterial genera in one of the compared fraction pairs (p < 0.01), have been visualized in a Bayesian network (a graphical probabilistic model shown in Figure 32). By extraction of Markov blankets from the network, we determined the nodes that predict the behavior of nodes corresponding to the three types of antibiotics and CDI.

The three types of antibiotics had overlapping Markov blankets and were directly connected to the active or to the inactive bacteria. Their synergistic effect was reflected for example in the decreased activity of

*Staphylococcus* cells. The majority of *Rothia* cells has increased activity in patients that did not take antibiotics promoting onset of CDI. CDI- patients taking preventive antibiotic treatment of CDI had typically increased *Nesterenkonia* and *Clostridium* cluster IV in the active-F. *Clostridium* cluster XI (the cluster where *C. difficile* belongs (Collins et al., 1994)) was the one differentiating clearly intestinal SIgA coating in CDI+ and CDI- patients. In CDI+ patients, *Clostridium* cluster XI was increased in the IgA-pos-F, while in CDI- patients it was increased in the IgA-neg-F.

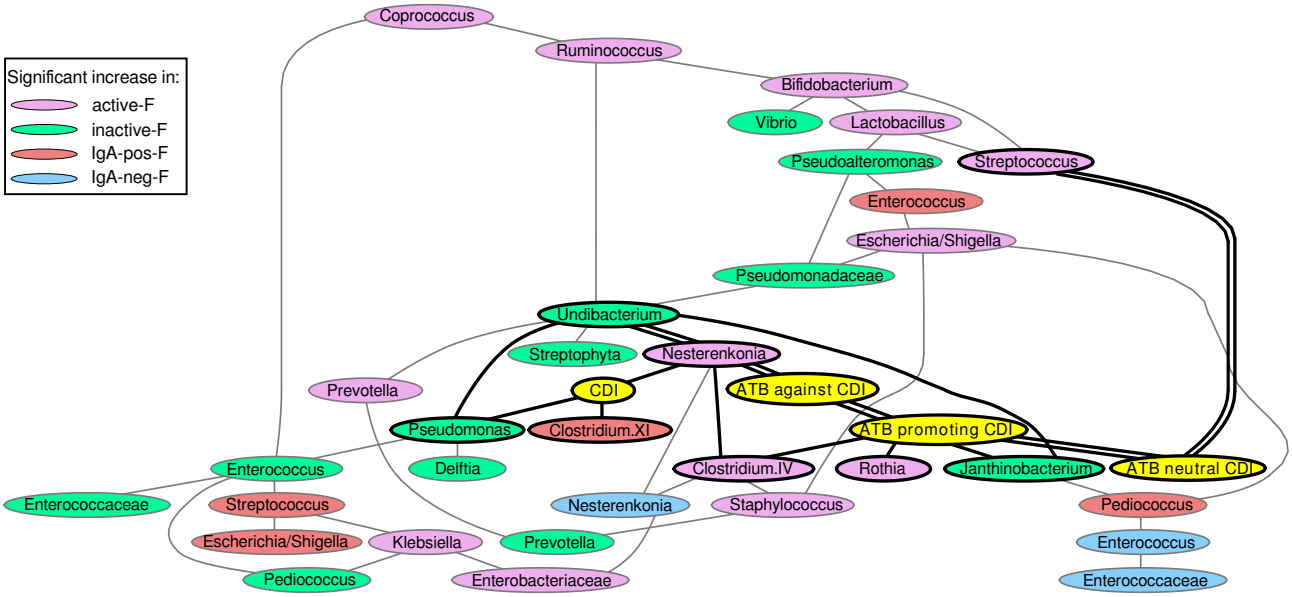


Figure 32: **The Bayesian network with Markov blankets.** The Markov blankets (marked by bold strikes) show the most significant correlations of medical data (the three types of antibiotic treatment and CDI) and the significant increments of proportions of bacterial genera in the bacterial fractions from the panel A. The overlapping Markov blankets are marked by double strikes

In the following comparison of genera typical for CDI+ and CDI- we considered only genera whose fraction-specific position was confirmed by more than 4 patients in a given CDI group, while in the same CDI group these genera should not be specific for the opposite bacterial fraction. Similarly, as in Bayesian networks in the previous step, also this simple comparison of species related to CDI+ and CDI- showed that the majority of *Clostridium* cluster XI cells were coated by IgA in CDI+. The differentiating factor between CDI+ and CDI- were also *Lactobacillales* which was inactive in CDI+. In CDI- patients *Fusobacterium* was a genus typically increased in IgA-pos-F and *Nesterenkonia* in active-F.

# 3.5 Discussion

The literature review of Seekatz and Young (2014) indicates that in general there are no clear differences between the taxonomic profiles of CDI+ and CDI- patients assessed by 16S rDNA amplicon sequencing. In the present study, *C. difficile* was detected in low proportions (0.0001-0.8881 %) in both CDI+ and CDI- patients. In general, the proportion of *C. difficile* detected in this study by qPCR was similar to previous studies (Tonooka et al., 2005; Koo et al., 2014; Matsuda et al., 2012). Tonooka et al. (2005) determined that 1 g of feces of healthy infants contains the 1.04 - 5.2 $\times$ $10^5$ cells of *C. difficile*. According to Matsuda et al. (2012), asymptomatic carrier and symptomatic patients have similar proportion of *C. difficile* in feces, ranging from $10^{2.4}$ to $10^4$. If the total number of bacterial cells present in 1g of a fecal sample is $10^7$ - $10^8$ (Franks et al., 1998), the proportion of *C. difficile* detected in the mentioned studies may be 0.002 - 1 % of all bacteria. It is also important to mention, that the results of the studies based on 16S rDNA quantification of *C. difficile* include also non-toxigenic *C. difficile* strains. The low proportion of *C. difficile* may be due to the its low presence in fecal samples, as *C. difficile* acts in the colon mucosal tissues. Durbán et al. (2011) demonstarted that the taxonomic composition of fecal samples differ from the colon mucosa biopsies of the same individual; especially the proportions of the genera of the *Clostridia* families were in higher proportion in the biopsies. Such a study has not been performed in CDI+ patients yet.

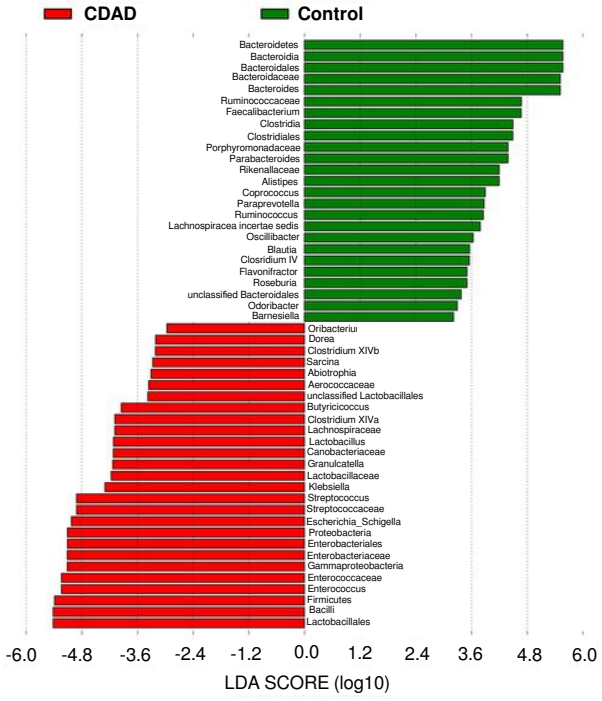


Figure 33: **Differentially abundant taxa between CDI+ and CDI- patients.** Author: Ling et al. (2014)

Not *C. difficile* itself but other bacterial species differentiate between taxonomic composition of feces of CDI+ and CDI- patients (Ling et al., 2014), as shown in the Figure 33. It suggests that other members of the human gut are providing optimal conditions for *C. difficile* growth. The results of the in vitro studies indicated that the germination of *C. difficile* spores is induced by primary bile acids, such as taurocholate (Heeg et al., 2012). In contrast, other secondary bile acids, such as chenodeoxycholate, inhibit the germination of *C. difficile* spores (Sorg and Sonenshein, 2009). The gut microbiota have an important role in bile acid metabolism, however, the information about their metabolism cannot be accessed by simple 16S rDNA amplicon sequencing, as it does not provide information about the genetic potential of each baterial strain. The individual strains are usually grouped into OTUs or simple assessed by taxonomic assignation on the genus level, therefore, the production of bile acids cannot be assed by 16S rDNA sequencing. The question is complicated by the fact that different *C. difficile* strains respond differently to the bile acids in culture media (Heeg et al., 2012), thus a lower proportion of taurocholate producing bacteria may be sufficient for induction of spores of those *C. difficile* strains which are easilly induced by this kind of secondary bile salts.

As the 16S rDNA amplicon sequencing cannot provide direct information about the genetic potential of

the sequenced bacterial cells, we decided to assess at least their SIgA-opsonization and activity patterns by fluoresent labelling. The results of fluorescent cell counting in our study indicated that the proportion of the active bacteria and the bacteria coated by SIgA is very variable, in accordance with previous studies on active bacterial fraction (Ben-Amor et al., 2005; Peris-Bondia et al., 2011; Maurice et al., 2013) and of the SIgA-coated fraction (Palm et al., 2014; van der Waaij et al., 2004). An example is shown in the Figure 34. The proportions of active and SIgA-coated cells detected in our study did not correlate with CDI+/- diagnosis neither with antibiotic treatment. The similar proportion of active cells in patients with and without antibiotic treatment may be due to the fact that the bacteria susceptible to antibiotics are being replaced by the resistant bacteria which keep maintaining the metabolic functions of the gut (Pérez-Cobas et al., 2012). A similar very wide proportion of SIgA coated cells in CDI+ and CDI- patients may be the reflection of the individual SIgA coating pattern of each patient. The proportion of SIgA coated cells is individual and may be changing over time, as it serves for accomodation of new bacterial phylotypes coming to the gut everyday with the food (Peterson et al., 2007). In general, the proportion of the bacteria opsonized by SIgA in our study was lower than the proportion of the active bacteria (in 22 out of 24 patients), indicating that not all newly formed active bacteria were opsonized by SIgA in the moment of sampling. This unbalance may be due to the low amount of available SIgA in the gut and also due to the accelerated growth rate of the active bacteria resisting antibiotic treatment, suggesting that not all recently formed bacterial cells can be coated by SIgA immediately.

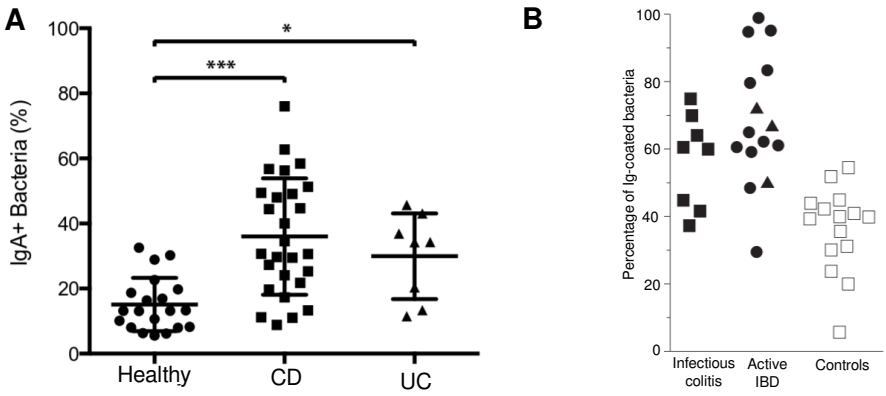


Figure 34: **IgA coating of fecal bacteria from healthy kumans and IBD patients. Panel A:** healthy controls, CD patients, UC patients. Author: Palm et al. (2014) **Panel B:** Infectious colitis patients, IBD patients (black triangle UC, black dot CD) and healthy controls. Author: van der Waaij et al. (2004)

The intestinal SIgA coating is rather strain-specific than genus-specific (Palm et al., 2014). Therefore, always only a part of a single bacterial genus is coated by SIgA, while the other part is not. The comparison of the proportions of *C. difficile* cells in IgA-pos-F with cells in IgA-neg-F helped to detect preferential SIgA opsonization of *C. difficil*e in CDI+ patients. The same analysis of fold change of cells in IgA-pos-F and IgA-neg-F performed individually for each genus was used for the identification of a bacterial community typical for the inflammatory bowel disease in the study of Palm et al. (2014), shown in the Figure 35.

In contrast to the fold change analysis of the separated fraction pairs, the analysis of the overall bacterial composition of the individual separated fractions reveals less information. In our study, the description of the overall bacterial composition for each bacterial fraction only confirmed the strong effect of antibiotics on the human gut microbiome, however, it did not detect any correlation of CDI+/- diagnosis with the bacterial composition, while the fold change approach did. The preferential coating of *C. difficile* by SIgA confirmed that the intestinal immune system of CDI+ patients recognizes *C. difficile* and it is probably trying to eliminate

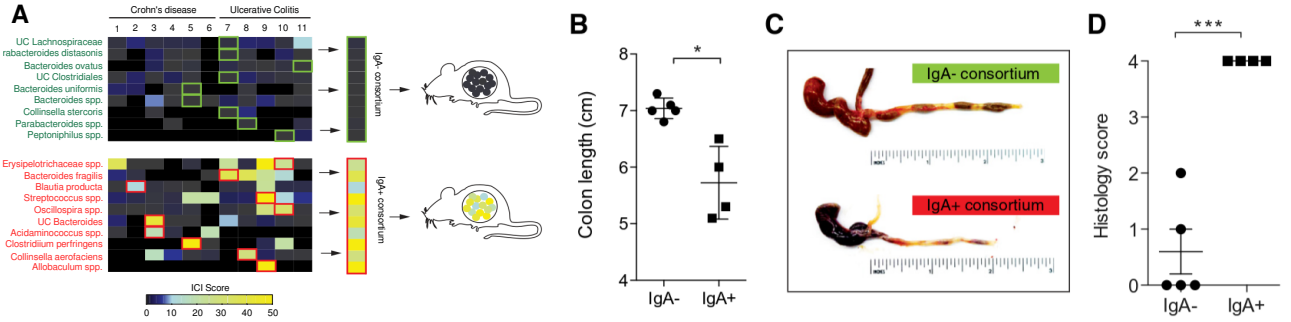


Figure 35: **Taxonomic composition of the IgA coated and non-coated bacteria and results of the nice colonization. Panel A:** Selection of individual bacterial isolates comprising IgA+ and IgA- consortia and colonization of germ-free mice. Specific isolates that were included in the consortia are boxed in green (IgA-) or red (IgA+). **Panel B, C, D:** Influence on IgA+ and IgA- bacterial consortia on DSS-induced colitis in gnotobiotic mice. **Panel B:** Colon length, **Panel C:** Gross pathology of large bowel, **Panel D:** Colon histopathology score. Author: Palm et al. (2014)

it from the gut. This result also indicates that *C. difficile* is not coating its cell surface with molecules avoiding SIgA opsonization, as some pathogens do (Ng et al., 2013; Vimr et al., 2004).

In the clinical practice, the hospitalized patients are under different types of antibiotic treatment, from which especially cephalosporins, fluoroquinolones and Clindamycin are associated with the onset of CDI. These divergent antibiotics perturb the gut microbiome composition of CDI patients in different ways (Rojo et al., 2015; Knecht et al., 2014). The patients under risk of CDI are often treated with Metronidazole or Vancomycin which are usually still effective against CDI, even though they have been associated with CDI recurrence and with the increased prevalence of nosocomial *Enterococcus* infections (Al-Nassir et al., 2008; Ozaki et al., 2004). The canonical correspondence analysis with the "envfit" function in present study showed that the antibiotics influence the composition of the gut microbiota in such an extent that the influence of CDI toxins on the gut microbiota is not observable.

*Enterococcus* was exclusively dominating the four fractions of patients under antibiotic CDI treatment. This is in accordance with the results of the culture experiment, in which fecal bacteria were cultivated in the rich gut microbiota medium with and without Metronidazole. *Enterococcus* dominated the active-F of the culture with antibiotics, however, a smaller portion of *Enterococcus* was found to be in the inactive-F, too. The antibiotic resistant bacteria in the gut are quickly growing, but their smaller portion is also dying. Therefore, *Enterococcus* had significant influence on the ordination of both active-F and inactive-F samples in the canonical correspondence analysis. Previous studies also showed that certain part of the most dominant genera of the human gut, e.g. *Bacteroides*, is actually inactive (Peris-Bondia et al., 2011; Maurice et al., 2013). Accordingly, *Enterococcus* cells were mostly inactive in the gut of the patients without antibiotic CDI treatment, while in the patients undertaking CDI antibiotic treatment *Enterococcus* was mostly active.

The bacterial resistance or susceptibility to multiple antibiotics, which are applied in combinations in the clinical practice, were detected by the extraction of Markov blankets from the Bayesian network connecting the increased prevalence of bacterial genera in the four individual fractions with the medical data. Bayesian networks have been previously used to reveal probabilistic relationships between bacterial communities and clinical markers (Vazquez-Castellanos et al., 2014). In the present study, the antibiotic combinations had

synergistic effect on decreased activity of *Staphylococcus* and *Rothia*, what reflected antibiotic susceptibility of these genera (Liu et al., 2011; von Eiff et al., 1995). Bayesian network also revealed that the CDI- patients had typically increased activity of cells belonging to *Clostridium* cluster IV. This cluster is formed mainly by commensal Clostridia which have been found to maintain gut homeostasis and often mark the difference between CDI+ and CDI- gut microbiomes (Lopetuso et al., 2013). The immune system of CDI- does not have to fight against *C. difficile*, therefore other bacteria, such as *Fusobacterium*, have been found typically increased in their SIgA coated fractions. Despite the fact that the presence of *Fusobacterium* was associated in some studies with various diseases, including inflammatory bowel disease or colon cancer, its role remains unexplained, because it also belongs to the most prevalent genera of the gut of healthy individuals (Sommer and Bäckhed, 2013). Interestingly, *Lactobacillus* was found to be inactive in CDI+ patients. It has been found to have an inhibitory effect against *C. difficile* growth and therefore it was selected for the probiotic CDI treatment for clinical studies (Gao et al., 2010; Rolfe et al., 1981). The results of the present study indicated that one of the factors allowing proliferation of *C. difficile* may be the absence of active *Lactobacillus* in the gut.

## 3.6 Conclusions

In clinical practice, hospitalized patients take different types of antibiotics. Despite being on the same risk of CDI onset (being hospitalized at the same department, taking similar antibiotics) some of the patients develop CDI and some do not. The detection of *C. difficile* from feces is not a marker for CDI patients, because also non-toxigenic *C. difficile* strains exist. Therefore, after numerous metagenomic studies the definition of a microbiome susceptible to CDI remains elusive.

Our results indicate that the differences in microbial composition of CDI+ and CDI- patients cannot be detected by a simple comparison of the proportion of the most prevalent bacterial groups, because the overall bacterial composition is influenced more significantly by antibiotics than by CDI. However, the fractionation of the gut microbiota according to their activity and SIgA opsonization provides more information on bacterial dysbiosis during CDI. When the proportions of SIgA-coated and non-SIgA-coated bacterial cells were compared for each genus, we have found that the abundant SIgA-coating of *Clostridium* cluster XI (the *C. difficile* cluster) is a marker for CDI+ patients. When the proportions of active and inactive gut bacteria for each genus were compared, a greater part of beneficial *Lactobacillales* and *Clostridium* cluster IV were found dying in CDI+ patients.

The excessive coating of *C. difficile* (*Clostridium* cluster XI) by intestinal SIgA and decreased activity of beneficial bacteria are the markers of CDI, independently on the overall bacterial composition of gut microbiota which is, on the other hand, shaped mostly by antibiotics. The results showed that *C. difficile* is being recognized by the intestinal immune system, meaning that this pathogen does not use the metabolites of the proliferating antibiotic resistant bacteria for covering its cell surface against SIgA opsonization. On the other hand, the CDI onset is connected to decreased activity of bacterial species which under normal conditions produce molecules inhibiting growth of *C. difficile*.

Chapter 4

# Selective inhibitory effect of 8-hydroxyquinoline on *C. difficile*

**Associated original articles:**

Novakova, J., Džunková, M., Musilova, A., Vlkova, E., Kokoska, L., Moya, A., D'Auria, G. (2014) Selective growth-inhibitory effect of 8-hydroxyquinoline towards *Clostridium difficile* and *Bifidobacterium longum* subsp. *longum* in co-culture analyzed by flow cytometry. Journal of Medical Microbiology 63: 1663-9.

JN and MD contributed equally to work

# 4.1 Introduction

## 4.1.1 Effects of antibiotics on bacterial growth

The rate of growth of a bacterial population can be described in form of a growth curve (Figure 36). The growth rate in a batch culture is usually described by measuring the optical density of cells (OD600) of samples taken in certain time intervals, e.g. every hour, or every 30 min. The cell growth in a batch culture may be monitored by FC (Skarstad et al., 1983). The bacterial growth curve consists of four phases:

1. **Lag phase:** When a bacterium is transported to a new environment, it needs some time to adapt to new conditions, so the usual replication time, which is in *E. coli* about 20 min, may be prolonged into several hours. This phase is called lag phase and it depends on the metabolic activity of the surviving cells. They must grow in size, synthesize essential enzyme and duplicate the cell constituents in order to prepare for division.

2. **Log phase:** When the number of surviving daughter cells outnumbers the number of cell in the parental generation, the bacterial population enters to the exponential phase of the growth.

3. **Stationary phase:** When the available nutrients become scarce and the waste products accumulate, the vigor of the population changes and, as the reproductive and death rates equalize, the population enters a plateau, called the stationary phase.

4. **Decline phase:** When the quantities of nutrients became extremely low, the population enters to a decline phase. The number of death cell exceeds the number of newly formed cells. The sporoforming bacteria may enter to the sporulation phase.

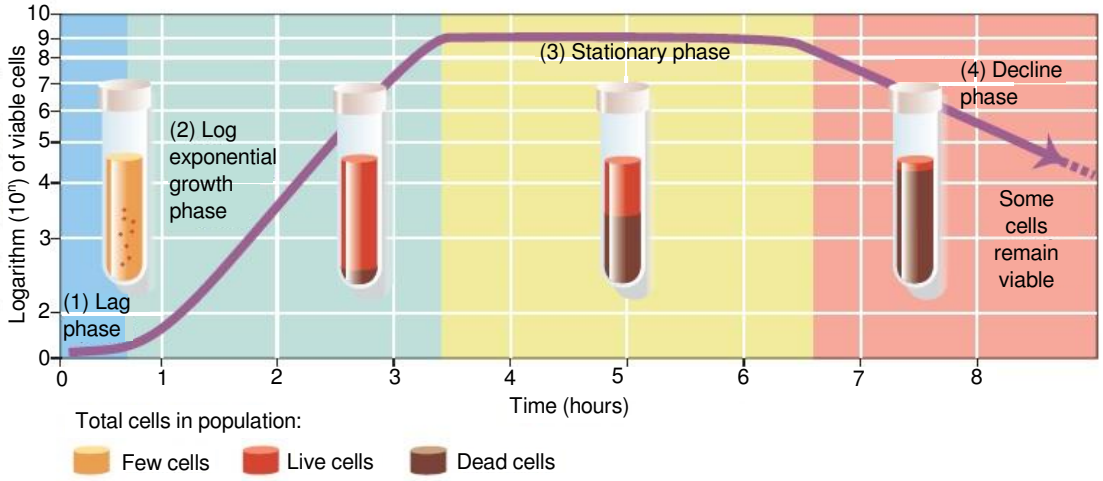


Figure 36: **Bacterial growth curve.** Source: Mendel University of Brno

Bacterial growth curves are influenced by antibiotics. Bactericidal antibiotics directly kill the bacteria, while bacteriostatic antibiotic inhibit their growth. According to the way of the production and the origin, the antibiotics may be classified into natural, semisynthetic and synthetic. The natural antibiotics are product of secondary metabolism of organism, so they actually serve for enhancing their survival in the nature. According to Berdy (2005), there are about 17,000 bioactive natural products with antibiotic properties found in higher

organism, from which the majority (11,500) come from plants. It is estimated that there is about 2,900 antibiotic compounds in *Bacteria*, 8,700 natural antibiotics in *Actinomycetales* and 4,900 in *Fungi* (Berdy, 2005). Most modern antibacterials are semisynthetic modifications of various natural compounds (von Nussbaum et al., 2006). For example, penicillins produced by fungi of the genus *Penicillium* is the base for the current beta-lactam antibiotics.

In antibiotic treatment, the dose of antibiotic must be considered. In microbiology, a frequently measured parameter is the minimal inhibitory concentration (MIC), defined as the lowest concentration of a drug that will inhibit the visible growth of an organism after overnight incubation (this period is extended for organisms such as anaerobes, which require prolonged incubation for growth). The range of antibiotic concentrations used for determining MICs is generally set by doubling dilution steps up and down from 1 mg/l (Andrews, 2001).

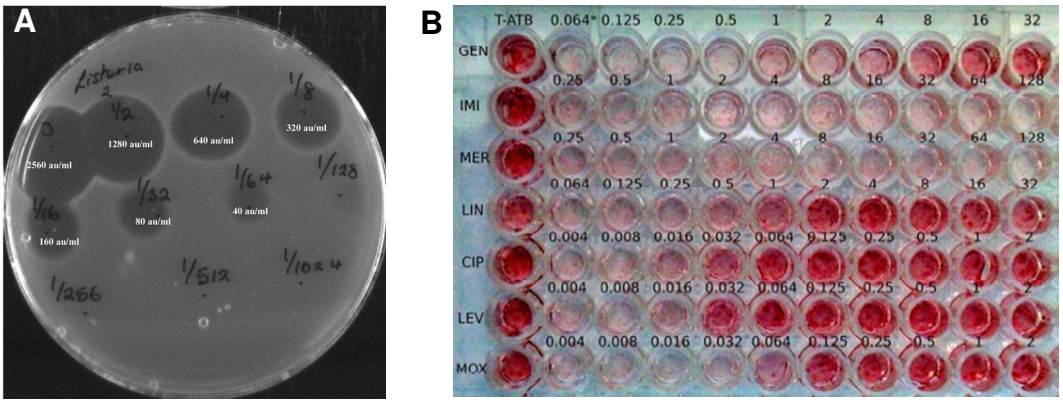


Figure 37: **MIC measurement methods. Panel A:** Petri's plate. Author: Mills et al. (2011). **Panel B:** 96 well plate. Author: Sutera et al. (2014)

There are several methods for MIC measurement. One option is the impregnation of the paper disks with different concentration of tested antibacterial compound, which are placed on the Petri's plate on which bacterial culture is spread and let grow overnight. The diameter of the zone of visible inhibition are measured, as shown in Figure 37, panel A. Another option is to distribute the cells from the liquid culture into a 96 well plate and add increasing concentrations of antibiotics. After overnight incubation, the cell optical density is measured. The growth can be also measured spectrophotometrically using dyes which are added to the cells as growth indicator, such as neutral red (Borenfreund and Puerner, 1985) as shown in Figure 37, panel B.

The strains of the same species may have different MIC, which is given by their level of resistance. The strains may differ in their antibiotic resistances due to the differences in outer membrane permeability, development of OXA-type $\beta$-lactamases and levels of carbapenem-specific porins, etc. (Strateva and Yordanov, 2009). Another types of antibiotic resistances may be acquired by plasmids, e.g. those decreasing the binding affinity of the modified antibiotics to the target 30S ribosomal subunit or different types of metallo-$\beta$-lactamases (Llano-Sotelo et al., 2002; Xiong et al., 2006).

When the antibiotics are applied for the treatment of infections in different human body organs, they do not affect only the susceptible pathogen but also the human gut bacteria which are not the target of this treatment. The counts of susceptible gut bacteria will decrease, so resistant gut bacteria will get the opportunity for proliferation. These resistant bacteria may be opportunistic pathogens, such as *Clostridium difficile*, which

causes CDI (Rupnik et al., 2009). *C. difficile* is still resistant to Vancomycin and Metronidazole, but elevated use of these antibiotics is the origin of infections by Vancomycin resistant *Enterococcus* (Al-Nassir et al., 2008). Moreover, certain strains of *C. difficile* also became resistant, so hypervirulent strains are appearing worldwide (Goorhuis et al.). Therefore, there is a call for preventive measures in the treatment strategies against CDI that would not harm or unbalance the resident gut microbiota. One of the options is the use of selective agents that inhibit pathogens with neutral impact on beneficial bacteria.

### 4.1.2 Selective antibacterial effect of 8-hydroxyquinoline

The antibiotics with selective inhibitory effect are of great interest in the current medicine, as the negative consequences of wide-spectrum antibiotics are widely known. One of such antibacterial compounds is 8-hydroxyquinoline.

8-hydroxyquinoline (8HQ) is a simple quinoline alkaloid detected in roots of *Sebastiana corniculata* (Figure 38). Its derivatives are chloroxine, clioquinol, iodoquinol and nitroxoline. In pharmacology, they serve as antimicrobial agents, whereas in agriculture they serve as fungicides and insecticides. The 8HQ molecule is also used in antiseptics, deodorants, antiperspirants, as a preservative in cosmetics and tobacco, and as a chemical intermediate in dye synthesis. 8HQ and its derivatives are also good chelating agents and therefore they are used both in analytical chemistry and in pharmaceutical chemistry as a complexing agents (Karpińska et al., 2010).

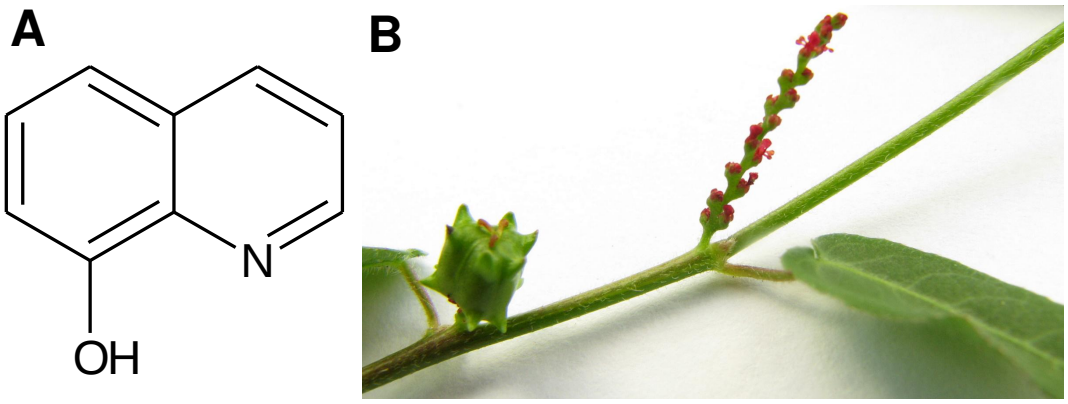


Figure 38: **8HQ extracted from *Sebastiana corniculata*. Panel A:** Chemical structure of 8HQ. Author: Paginazero (Wikipedia). **Panel B:** The plant. Author: Alex Popovkin (Flickr)

It has been demonstrated to be very effective against several bacterial pathogens, while it seems that it does not affect beneficial bacteria. The selective antibacterial effect of 8HQ towards clostridial strains has been firstly shown using disk diffusion method (Jeon et al., 2009). 8HQ exhibited strong or moderate growth inhibition against *C. difficile*, *C. perfringens* and *E. coli*, whereas no growth inhibition was observed against *Bifidobacterium bifidum*, *Lactobacillus acidophilus* and *L. casei*. Novakova et al. (2013) confirmed selective activity of 8HQ; its MIC toward bifidobacteria was 13-fold higher compared to that of clostridia, as shown in Table 5, where the MIC of 8HQ is compared with MIC of Penicillin and Tetracycline. For this reason it may be considered as a potential antibiotic treatment against *C. difficile* infections, which at the same time promotes restoration of beneficial bacteria whose counts had decreased during original antibiotic treatment

with large-spectrum antibiotics promoting the onset of *C. difficile* infection.

Table 5: **The selective antimicrobial effect of 8HQ.** Data are median values of MIC ($\mu$g/ml) of three independent experiments, each performed in triplicate. Author: Novakova et al. (2013)

| **Bifidobacterium strain** | **8HQ** | **Penicillin G** | **Tetracycline** |
|---|---|---|---|
| *B. adolescentis* infant H1 | 512 | 0.13 | 0.5 |
| *B. animalis* CCM 4988 | 512 | 0.25 | 2 |
| *B. bifidum* infant JKM | ≥ 2048 | 2 | 0.5 |
| *B. breve* ATCC 14700 | 1024 | 0.5 | 0.5 |
| *B. breve infant* FE | 256 | 0.13 | 0.5 |
| *B. catenulatum* CCM 4989 | 512 | 0.25 | 2 |
| *B. dentium* infant AP | 1024 | - | - |
| *B. infantis* ATCC 17930 | 256 | 0.06 | 2 |
| *B. longum* ATCC 15707 | 512 | 0.5 | 2 |
| *B. longum* infant J2 | 512 | 0.25 | 16 |

| **Clostridium strain** | **8HQ** | **Penicillin G** | **Tetracycline** |
|---|---|---|---|
| *C.acetobutylicum* DSM 792 | 64 | 0.016 | 0.5 |
| *C. acetobutylicum* infant L4 | 128 | 0.25 | 0.25 |
| *C. butylicum* infant AS3 | 128 | 0.13 | 0.5 |
| *C. butyricum* infant CM14 | 32 | 0.06 | 0.25 |
| *C. butyricum* DSM 10702 | 32 | 0.25 | 0.031 |
| *C. clostridioforme* DSM 933 | 16 | 0.5 | 16 |
| *C. difficile* infant KK4 | 32 | 0.25 | 0.06 |
| *C. paraputrificum* DSM 2630 | 64 | 0.13 | 16 |
| *C. perfringens* DSM 11778 | 32 | 0.13 | 8 |
| *C. ramosum* DSM 1402 | 32 | 0.016 | 0.25 |
| *C. ramosum infant* HH3 | 64 | 0.25 | 0.25 |
| *C. tertium* DSM2485 | 8 | 0.5 | 0.031 |

## 4.2 Objectives

There are thousands of antibiotic compounds in the nature. Some of them, as 8HQ, have been demonstrated to have selective antibacterial properties. These selective properties are usually tested on individual cultures of different bacterial species and strains, however it is impossible to determine the selective action of these antibiotics to different strains growing in a co-culture.

If it is not possible to distinguish between two bacterial species grown in co-culture by simple microscopical observation of their morphology, their 16S rRNA may be hybridized by fluorescently labeled probes and so the proportion of each species may calculated by visualization by the fluorescent microscope. However, counting of cells by FC is more effective than microscopic visualization of a small aliquot of cells, because FC is more sensitive and can process large number of cells per second. Small populations of distinct cells in a sample containing thousands of cells can be detected by FC.

The selective antibacterial effect of 8HQ will be studied on a co-culture of *C. difficile* with *Bifidobacterium longum* subsp. *longum* monitored by FC. Since the culture methods commonly used for selectivity testing (e.g. agar dilution or broth microdilution method) do not allow detailed study of this aspect, FC combined with FISH may be useful for the monitoring of the two populations dynamics in individual and mixed cultures. The experiment will be performed in media with and without 8HQ. For evaluation of the FC results, the growth rate data will be compared with measurements of optical density of the cultures.

This work aims to explain in more detail growth dynamics of co-culture of two species in media with antibiotic agent with selective activity against one of them.

# 4.3 Methods

## 4.3.1 Bacterial strains, growth conditions and inoculum

*C. difficile* CECT 531 was obtained from The Spanish Type Culture Collection (CECT). After cultivation according to CECT instructions described in details in the protocol section 11.4, *C. difficile* was stored in Clostridial Reinforced Medium (Oxoid, Ref. CM0149) with glycerol at -80 °C.

*B. longum* subsp. *longum* was isolated from infant faces according to Rada and Petr (2000) and identified according to Vlková et al. (2005). It was cultivated in Wilkins-Chalgren broth (Oxoid, Ref. CM0643) supplemented with soya peptone and glycerol (20 % v/v) at -20 °C.

The stock cultures were activated by anaerobic growth at 37 °C overnight in Wilkins-Chalgren broth with 5 g/l of soya peptone and 0.5 g/l of L-cysteine (Sigma, Ref. C1276-10G). Both strains were cultivated on 96-wells microtiter plates in the anaerobic workstation Whitley DG 250 (Don Whitley Scientific). The inoculum of each strain was adjusted to receive $1 \times 10^6$ cells.

In vitro broth microdilution method was used to determine MIC of 8HQ towards both strains tested in anaerobic conditions. A stock solution of 8HQ was prepared in dimethyl sulfoxide (Lach-Ner, Ref. 30161). Two-fold dilutions were carried out, starting from an initial concentration of 256 $\mu$g/ml for *Clostridium*, and 1024 $\mu$g/ml for *Bifidobacterium*, employing 96 wells microtiter plates. Tetracycline hydrochloride (Applichem, Ref. A2228) was employed as positive control of antibiotic activity.

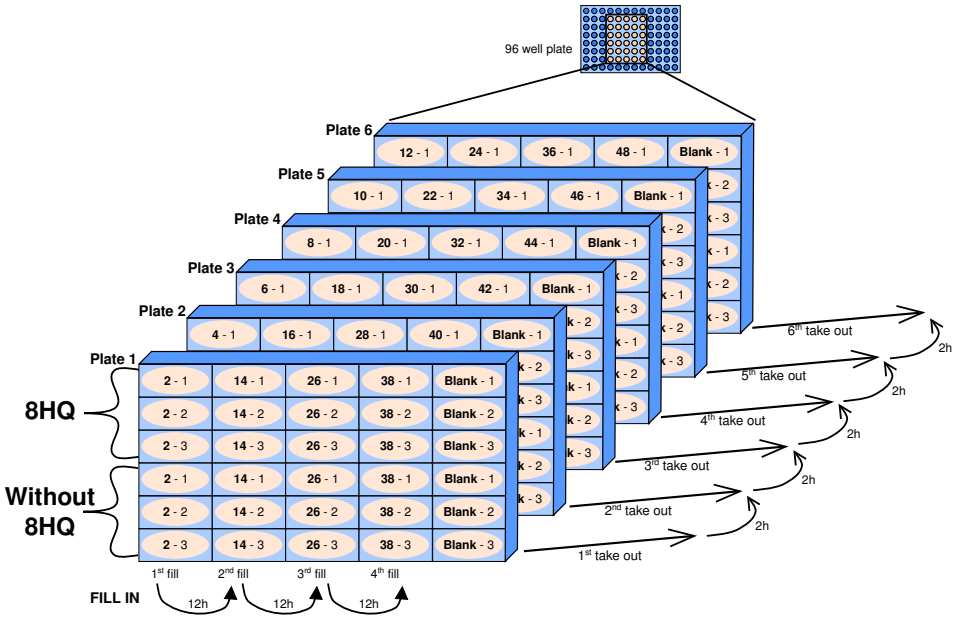


Figure 39: **Preparation of 96 well plates for OD measurement and sample collection**

The plates were incubated in anaerobiosis at 37 °C for 48 h. The turbidity in the wells was determined spectrophotometrically using a Tecan® Infinite 200 Pro at 405 nm to evaluate the growth. MIC was defined as the concentrations resulting in a ≥ 80 % inhibition of growth relative to the growth control. The tests were performed in triplicate in three independent experiments and median values were used for MIC calculation.

### 4.3.2 Hybridization of the co-culture with specific fluorescent probes

For the co-culture experiments, 100 $\mu$l of *B. longum* inoculum were mixed with 100 $\mu$l of *C. difficile* inoculum (both containing $1 \times 10^6$ cells). In the trial, 8HQ was tested at 16 $\mu$g/ml, what is higher than MIC towards *C. difficile*, to demonstrate its complete inhibition. Wilkins-Chalgren broth supplemented with 5 g/l of soya peptone and 0.5 g/l of L-cysteine was used as liquid growth medium. Viable cell count analysis was performed as described by Coconnier et al. (1997) to check inoculum density of viable cells able to form colonies.

For the FC detection of fluorescently hybridized cells, 100 $\mu$l were taken every 2 hours from the microtiter plate in the anaerobic chamber and transferred to a fresh tube (Figure 39) containing formaldehyde as described in the protocol section 11.3.

FISH probes for *C. difficile* were designed by the Primrose software 2.17 (Ashelford et al., 2002) using 16S rDNA bacterial sequences from Ribosomal Database Project (Cole et al., 2009), from April 2011 and synthesized at Integrated DNA technologies. The FISH probe for *Bifidobacterium* spp. comes from the kit of RiboTechnologies (Ref. 10-ME-H001). The FISH scheme for each sample was the following:

- ***C. difficile* individual detection:**
  CD174 probe: 5'-/56-FAM/ GCCTCTCAAATATATTATCCCG-3'
  CD60 probe: 5'-/56-FAM/TTTACCGAAGTAAATCGCTCAAC-3'
- ***B. longum* subsp. *longum* individual detection:**
  Bif662 probe labeled by cy5: 5'-CCACCGTTACACCGGGAA -3'
- **Co-detection of *C. difficile* and *B. longum* subsp. *longum*:** hybridized with probes for the both species
- **A negative control:** containing no hybridization probes, but undergoing the same hybridization protocol

The hybridization was performed according to the modified protocol of Fuchs et al. (1998), detailed in the protocols section 11.6. Briefly, the cell membrane was permeabilized with short lysozyme treatment. The hybridization buffer contained very low concentration of SDS a NaCl (for adjusting proper hybridization pH and accessing the ribosomal RNA) and formamide (for enhancing the hybridization specificity). The final concentration of 0.5 $\mu$g/ml for each probe. The hybridization was performed in 100 $\mu$l volumes by incubation at 54°C in a termoblock and after 3 hours, the non-hybridized cells were removed by adding 1ml of the washing solution preheated to 56°C. Afterwards, the washing solution was replaced by the salt solution and stored in dark at 4°C until processed on FC. The fluorescence was checked before FC by fluorescent microscope, as shown in Figure 40.

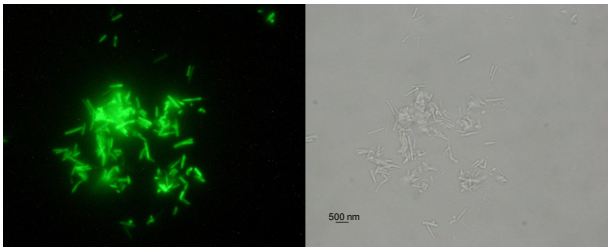


Figure 40: ***C. difficile* culture hybridized with fluorescent probes**

The samples were processed on the flow cytometer Cytomics FC 500 (Beckman Coulter, Ref. 626553). Gates were set using FL1 channel (x-axis, Cy3 probe specific for *C. difficile* versus FL3 channel (y-axis, *B. longum* subsp. *longum* Cy5 probe). FC data were analyzed using R packages "FlowCore" and "FlowViz" (Hahne et al., 2009) and ggplot2 (Wickham, 2009) as described in the programming script section 12.7.

# 4.4 Results

## 4.4.1 Microbiological assays

Control experiments without 8HQ showed that both bacterial strains grow similarly when individually cultivated. Considering the total amount of cells, the optical density data of monoculture experiments shown in Figure 41 demonstrated the significant reduction of *C. difficile* in presence of 8HQ (8 $\mu$g/ml, $p<0.01$). In this case the lag phase of the whole bacterial culture was prolonged up to 12 hours in comparison to control experiment without 8HQ where lag phase was only 2 hours. On the contrary, in the data for *B. longum* subsp. *longum* BL1 shown on Figure 41 there was no significant difference between experiments with and without 8HQ (8 $\mu$g/ml, $p>0.05$).

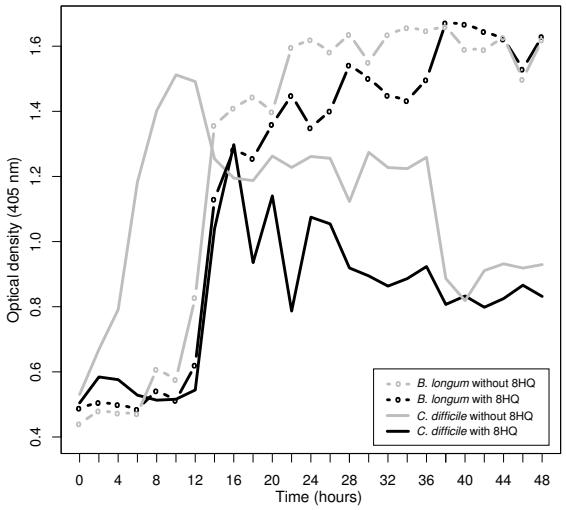


Figure 41: **Optical density based growth curves of monoculture experiments.** The average of 3 replicates

In the microtiter plate assay 8HQ inhibited *C. difficile* in vitro with MIC of 8 $\mu$g/ml. In contrast, MIC of *B. longum* subsp. *longum* BL1 was 512 $\mu$g/ml. These data show a 64-fold higher MIC of 8HQ towards *B. longum* compared to *C. difficile* demonstrating a selective inhibitory effect of 8HQ.

## 4.4.2 FC analysis of a mixed co-culture

The samples along the growth curves were hybridized with probes for *B. longum* subsp. *longum* (fluorescence on FC channel FL3) and with probes for *C. difficile* on (detectable on channel FL1).

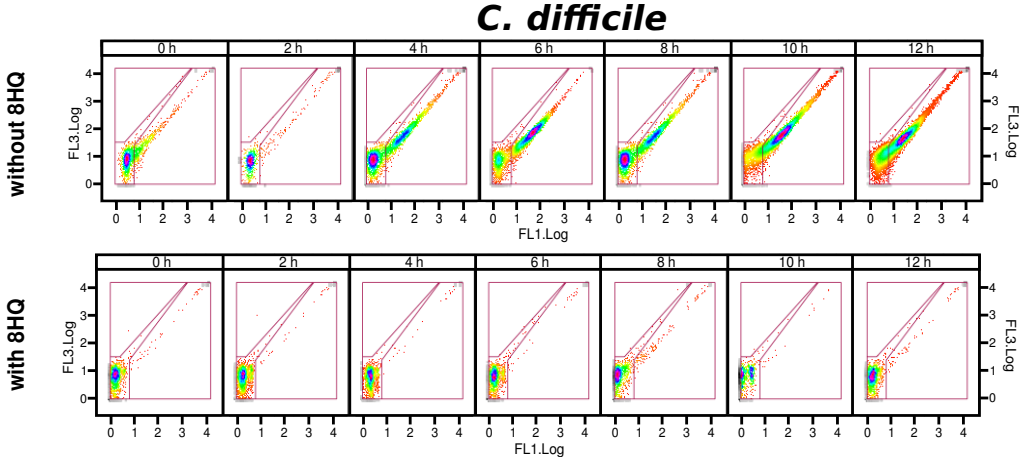


Figure 42: **FC plots of hybridized cells of individual culture of *C. difficile***

In the individual culture of *C. difficile* (Figure 42) in media without 8HQ, the active *C. difficile* formed up

to 70.10 % of all FC events. If 8HQ (16 $\mu$g/ml) was present in the media of individual cultures, almost no clostridial positive events were observed (maximally 5.9 % of all FC events). The remaining events were actually culture media residues or decomposed *C. difficile* cells already containing almost no RNA.

In the individual culture of *B. longum* without 8HQ 58.36 % of all recorded FC events belonged to *B. longum* cells with high RNA content. In the case of culture with 8HQ, in contrast to *C. difficile*, any decrease in the proportion of positive bifidobacterial events was observed: 71.01 % of all FC events, as shown in Figure 43. Thus, the growth of monoculture of *B. longum* was highly similar in the conditions with and without 8HQ (Welch Two Sample t-test p-value=0.626; Wilcoxon test p-value=0.522).

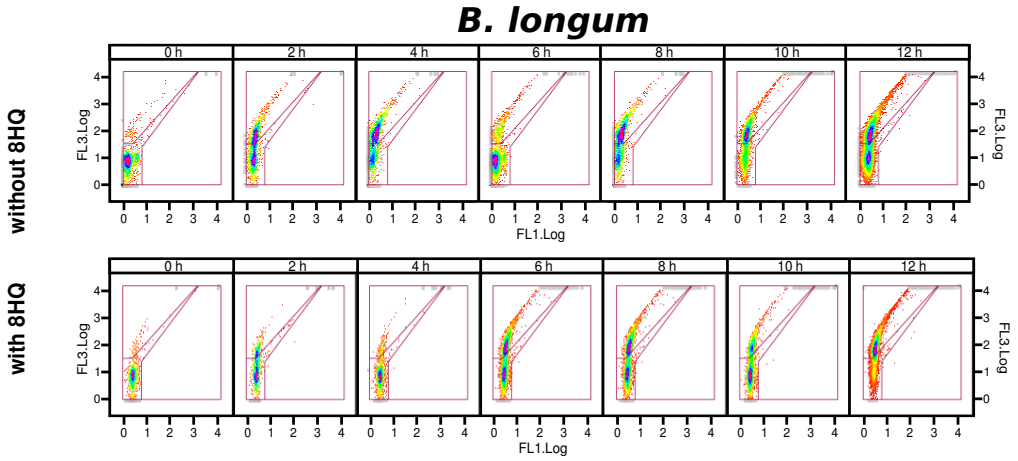


Figure 43: **FC plots of hybridized cells of individual culture of *B. longum***

Similar behavior was observed in the control mixed cultures without 8HQ where hybridized strains of *C. difficile* and *B. longum* subsp. *longum* were equally distributed (Figure 44). The proportion of the strains of *C. difficile* and *B. longum* subsp. *longum* oscillated during the growth between 22.66 - 77.88 % and 27.11 - 77.17 % of all hybridized cells, respectively. In contrast, in the mixed culture experiment in presence of 8HQ (16 $\mu$g/ml) the proportion of the 2 strains was in equilibrium only during first 2 hours of growth. After 4 hours, clostridial positive events significantly decreased, forming only 8.8-17.5 % of all hybridized cells (2.59 - 6.52 % of all FC events).

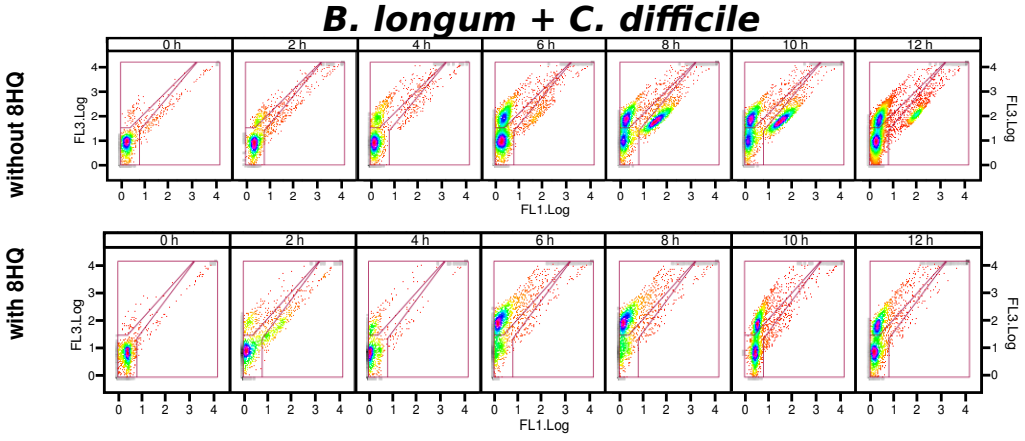


Figure 44: **FC plots of hybridized cells of mixed culture of *B. longum* and *C. difficile***

Figure 45 resumes the proportion of FC events belonging either to *C. difficile* or *B. longum* in media with and without 8HQ.

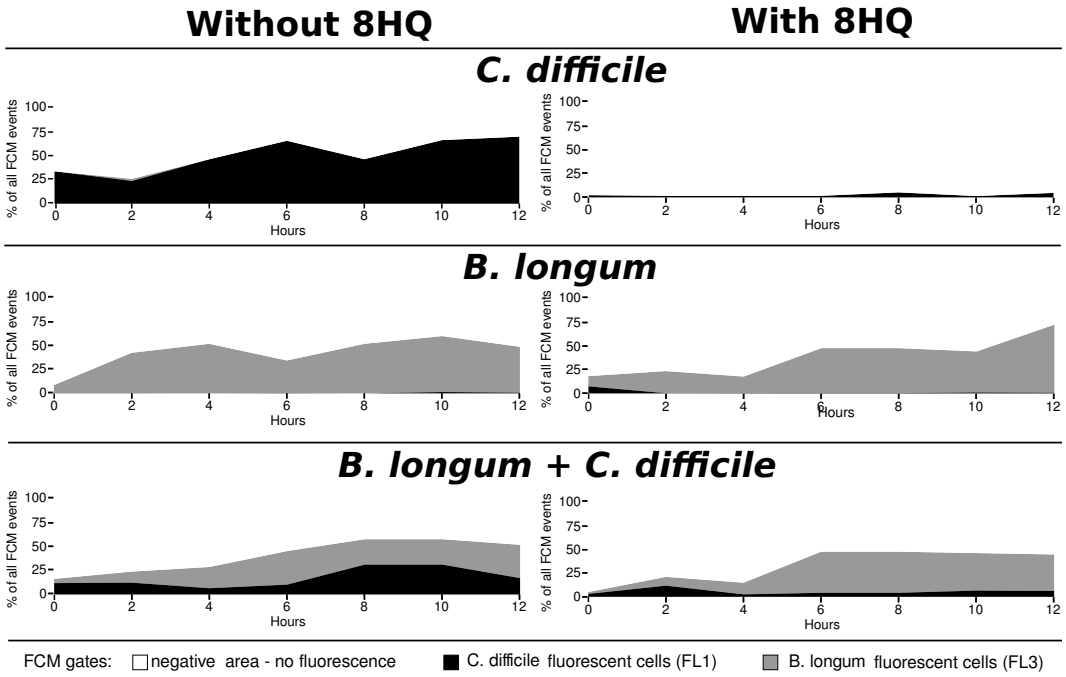


Figure 45: **Proportional distributions of bacterial strains during growth in mixed co-cultures with and without 8HQ.** The area scattered plots show the proportion (in % of all FC events) of *C. difficile* and *Bifidobacterium longum* subsp. *longum* and non-fluorescent events present in their corresponding areas of FC plots

## 4.5 Discussion

The present study represents an extension of the previous work of Novakova et al. (2013) where the selective inhibitory activity of 8HQ towards 10 bifidobacterial and 12 clostridial strains in monocultures was shown. The MIC of *B. longum* strains in both studies was 512 $\mu$g/ml whereas *C. difficile* infant isolate tested in the previous study showed MIC of 32 $\mu$g/ml while the MIC of its type strain in the present study was even lower, 8 $\mu$g/ml.

In the present work, the selective action of 8HQ was confirmed also in a co-culture of one bifidobacterial and one clostridial strain. The present findings supports the potential use of this molecule for therapeutic use against CDI. 8HQ does not have negative effects on bifidobacterial strains which are considered as part of the resident microbiota and being employed for CDI treatment (Selinger et al., 2013).

Up to now, the mechanism of 8HQ selectivity has not been elucidated. 8HQ has chelating activity, it scavenges the metallic cations from its environment meanwhile the reactive oxygen species are formed. The chelated metals become unavailable for enzymes and so certain metabolic processes are inhibited (Chobot et al., 2011). 8HQ was found to inhibit polymerase activity by chelating the dissociate cations $Mn^{2+}$ and $Mg^{2+}$, what results of inhibition of synthesis of ribosomal and polydisperse RNA. These are inhibited more than 5S RNA and tRNA which may be the explanation why protein synthesis is not inhibited inmediatelly (Fraser and Creanor, 1975). In relation to our results it could be suggested that 8HQ causes the selective RNA polymerase inhibition because of the different ability of bifidobacteria and clostridia to accumulate metallic ions.

Most likely the oxidative stress defense systems of the *C. difficile* and *B. longum* strains are also different. The genome sequencing of *C. difficile* showed that it has several proteins putatively involved in the oxidative stress response, such as putative manganese superoxide dismutase (CD1631), several putative manganese catalases (CD1567, CD0598, and CD2401), even though vegetative cells of *C. difficile* display no catalase activity (Sebaihia et al., 2006). On the other hand, *B. longum* usually does not possess manganese catalase activity (He et al., 2012), however, these properties are strain dependent. The role of metalloenzymes in these systems should be exploited profoundly in connection with the different acquisition of metallic ions by these bacterial species to explain the mechanism of 8HQ selective antibacterial action.

## 4.6 Conclusions

8HQ has selective inhibitory activity against *C. difficile*, while it does not affect the growth of *B. longum*. It suggest that 8HQ can be potentially used as a molecule for *C. difficile* infection treatment. Molecules with selective activity against *C. difficile* have a great potential in CDI treatment, as the protection of the normal gut microbiota is the key factor for CDI recurrence prevention. In contrast, broad spectrum conventional antibiotics currently used for CDI treatment perturb the normal microbiota and often cause CDI recurrence or infections by other antibiotic resistant opportunistic pathogens.

FC analysis of cells hybridized with specific probes was used to study selective action of antibacterial substance 8HQ towards beneficial and pathogenic bacterial strains grown in vitro in a mixed co-culture. The combination of the sensitivity and specificity of fluorescent probes with FC analysis of thousands of bacterial cells in seconds seems to be a powerful approach for studying bacterial population growth dynamics. FC confirmed that 8HQ does not influence negatively the growth of beneficial *B. longum* at the same time as it inhibited the opportunistic pathogen *C. difficile* for its first 12 hours of growth.

Chapter 5

# Genetic diversity of *C. difficile* separated by FACS

**Associated original articles:**

Džunková, M., Moya, A., Chen, X., Kelly, C., D'Auria, G.: Infection by multiple *Clostridium difficile* strains detected by whole genome sequencing of FACS-separated bacteria. In preparation.

# 5.1 Introduction

## 5.1.1 Methods for identification of *C. difficile* strains

The genetic diversity of *C. difficile* is very wide. There are different methods for identification of *C. difficile* strains based on diversity of specific genes (Rupnik et al., 2009):

- **PCR ribotyping** is based on PCR amplification of the spacer regions of 16S and 23S ribosomal RNA. The method generates patterns of few DNA bands called ribotypes (Bidet et al., 1999).
- **Pulsed field gel electrophoresis** (PFGE) involves using an enzyme that cuts the bacterial genome infrequently. The large fragment patterns separated in a polyacrylamide gel are called pulsovars (Klaassen et al., 2002).
- **Multilocus variable number tandem repeat analysis** (MLVA) is a method of counting the numbers of repeat alleles in the genome for a series of conserved loci amplified by PCR (van den Berg et al., 2007).
- **Restriction endonuclease analysis** (REA) relies on more frequent cutting of the bacterial genome than PFGE. Resulting numerous DNA fragments may be difficult to interpret and reproduce (Clabots et al., 1993).
- **Amplified fragment length polymorphism** (AFLP) uses restriction enzymes to cut genomic DNA, followed by ligation of adaptors which serve for subsequent amplification (Klaassen et al., 2002).
- **Multilocus sequence typing** (MLST) facilitates isolate discrimination using nucleotide sequences of housekeeping gene fragments. Each unique combination of alleles is assigned a sequence type number. There are searchable Internet-accessible MLST databases, such as PubMLST (Griffiths et al., 2010) including 7 housekeeping genes of *C. difficile* 630, the pathogenicity locus PaLoc and the binary toxin genes. The genes considered in the database are: adk (adenylate kinase), atpA (ATPase A), cdtA, cdtB (binary toxin), dxr (1-deoxy-D-xylulose 5-phosphate reductoisomerase), glyA (serine hydroxymethyltransferase), recA (recombinase A), sodA (spore coat protein-superoxide dismutase), tcdA (toxin A on the PaLoc), tcdB (toxin B on the PaLoc), tcdC (repressor of toxins A and B on the PaLoc), tpi (triose phosphate isomerase), which are shown in the Figure 49.

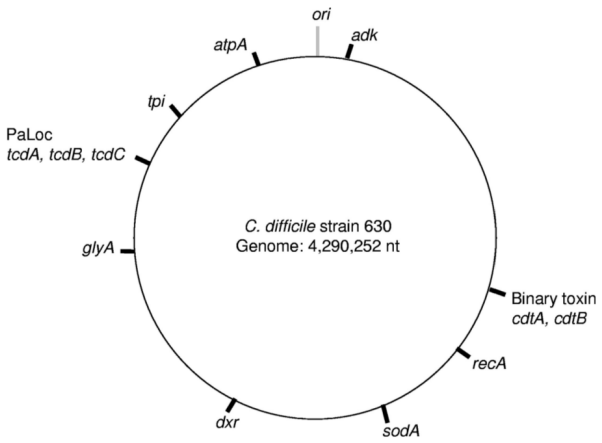


Figure 46: **Multilocus sequence typing sites of *C. difficile*** Author: Griffiths et al. (2010)

### 5.1.2 *C. difficile* virulence genes

Toxinotyping is a RFLP-PCR (AFLP) based method for differentiating *C. difficile* strains according to changes in their toxin genes when compared to the reference strain VPI 10463 which does not have toxins. A toxinotype is a group of strains with identical changes in pathogenecity locus (PaLoc). PaLoc includes the genes for the toxin A and for the toxin B and the three additional genes tcdC, tcdR and tcdE. tcdC is the negative regulator of toxins and tcdR is the positive regulator (Braun et al., 1996). Thirty-one toxinotypes are known (Rupnik, 2010). The toxinotypes may have only toxin A, toxin B, none or both of them. Nontoxigenic strains contain a 127 bp sequence instead of this 19,641 bp PaLoc, but other variations are also possible (Hammond and Johnson, 1995). An example of the variants found in the *C. difficile* clade 5 is shown in the Figure 47. The majority of variant strains produce also a third toxin, the binary toxin CDT. Toxinotyping correlates with other molecular typing methods, such as ribotyping or REA (Dingle et al., 2011; Rupnik et al., 2001).

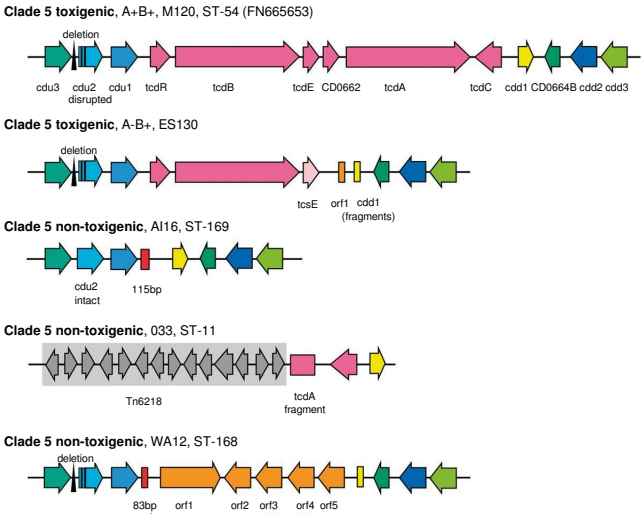


Figure 47: **Distinct variants of the PaLoc found in clade V** Author: Elliott et al. (2014)

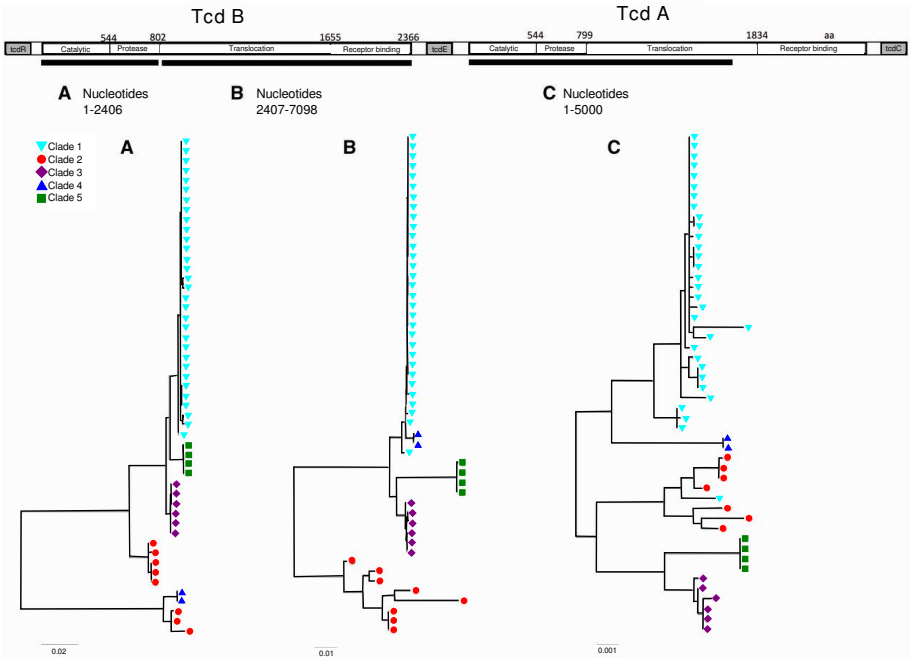


Figure 48: **Cross-population phylogeny of the PaLoc.** Phylogenies constructed from the catalytic and protease domains of tcdB (A), from the translocation and receptor binding domains of tcdB (B), and from the catalytic, protease, and part of the translocation domain of tcdA (C). Breaks in assembly caused by repetitive sequences in the receptor-binding domain of tcdA precluded its inclusion. Colored shapes indicate clade. Author: Dingle et al. (2014)

Deletions are found mostly in tcdA and up to date no form of significant deletion in tcdB is known. In contrast, the point mutations are more common in the tcdB gene than in the tcdA gene (Rupnik, 2008). An insertion of about 2,000 bp were observed in tcdA of toxinotypes XIV, XVII, XXII and XXIII (Mehlig et al., 2001; Geric et al., 2004). tcdC, which encodes a negative regulator of toxin expression, is highly variable. In total there are 17 different tcdC genotypes (Curry et al., 2007). Insertions larger than one codon are observed upstream of tcdR (150 bp in several toxinotypes) and between tcdB and tcdE in the toxinotype X (Song et al., 1999).

When whole genomes of *C. difficile* isolates are clustered, five different clades are formed. Comparison of the *C. difficile* core genome and PaLoc phylogenies of 1,693 isolates (shown in the Figure 48) demonstrated an eventful evolutionary history, with distinct PaLoc variants acquired clade specifically after divergence. In the clade 4 the PaLoc was acquired just recently. Exchanges and losses of the PaLoc DNA have also occurred, via long homologous recombination events involving flanking chromosomal sequences. The most recent loss event occurred 30 years ago within the clade 1 genotype. The genetic organization of the clade 3 PaLoc is unique, as it contains a stably integrated novel transposon, variants of which were found at multiple chromosomal locations (Dingle et al., 2014).

The binary toxin locus CdtLoc (Figure 49) consists of two genes, cdtA and cdtB, which are regulated by cdtR (Popoff et al., 1988; Carter et al., 2007). This binary toxin (ADP-ribosyltransferase toxin) disrupts or rearranges the cytoskeleton of the host cell (Schwan et al., 2009; Carter et al., 2012). Not more than a half of the toxigenic isolates possess binary toxin genes, but their presence is associated with more severe disease outcomes (McEllistrem et al., 2005). For example, the binary toxin genes are typical for ribotype 027, while the reference strain 630 contains a sequence deletion resulting in frameshift mutation (Stabler et al., 2009).

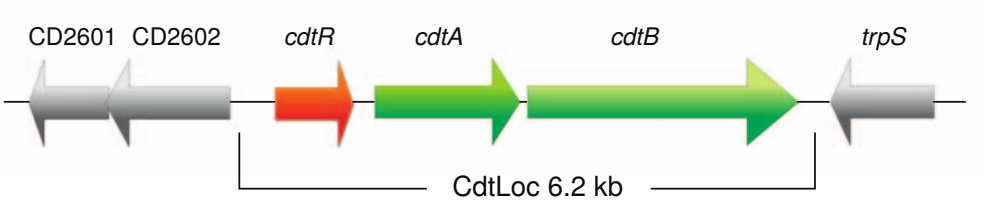


Figure 49: **The structure of the binary toxin locus** Author: Carter et al. (2012)

Stabler et al. (2009) compared the whole genome sequences of the reference strain 630 with a hypervirulent strain ribotype 027 and revealed differences in antibiotic resistance genes. The reference strain 630 has two copies of erythromycin resistance gene (ermB1 and ermB2) on a mobile transposon Tn5398 and tetracycline resistance gene tetM, which are absent in the hypervirulent ribotype 027. The ribotype 027 is highly resistant to fluoroquinolones due to point mutations in the DNA gyrase genes, which is absent in the reference strain 630 (Drudy et al., 2007). Moreover, ribotype 027 acquired the conjugative transposon CTn-027 encoding the chloramphenicol resistance gene. By whole genome sequencing two separate lineages of 027/BI/NAP1 were identified, which probably acquired the fluoroquinolone resistance in two separate events between years 1984-1999. Their fluoroquinolone resistance is related to the CTn5-like conjugative transposon (He et al., 2013).

He et al. (2010) constructed a phylogenetic tree from whole genome sequences of 21 isolates belonging to the hypervirulent ribotype 027 (e.g. strains BI-1, 2007855, CD196, R20291) and the ribotypes 001 (strain BI-9), 012 (strain 630), 017 (strain M68 and CF5) and 078 (strain M120). The phylogenetic analysis explained the origin of the mobile elements introducing antibiotic resistances genes for tatracycline, chloramphenicol,

erythromycin and aminoglycosides in different *C. difficile* lineages (Figure 50). It was calculated that the common ancestor of the *C. difficile* dates back millions of years (He et al., 2010).

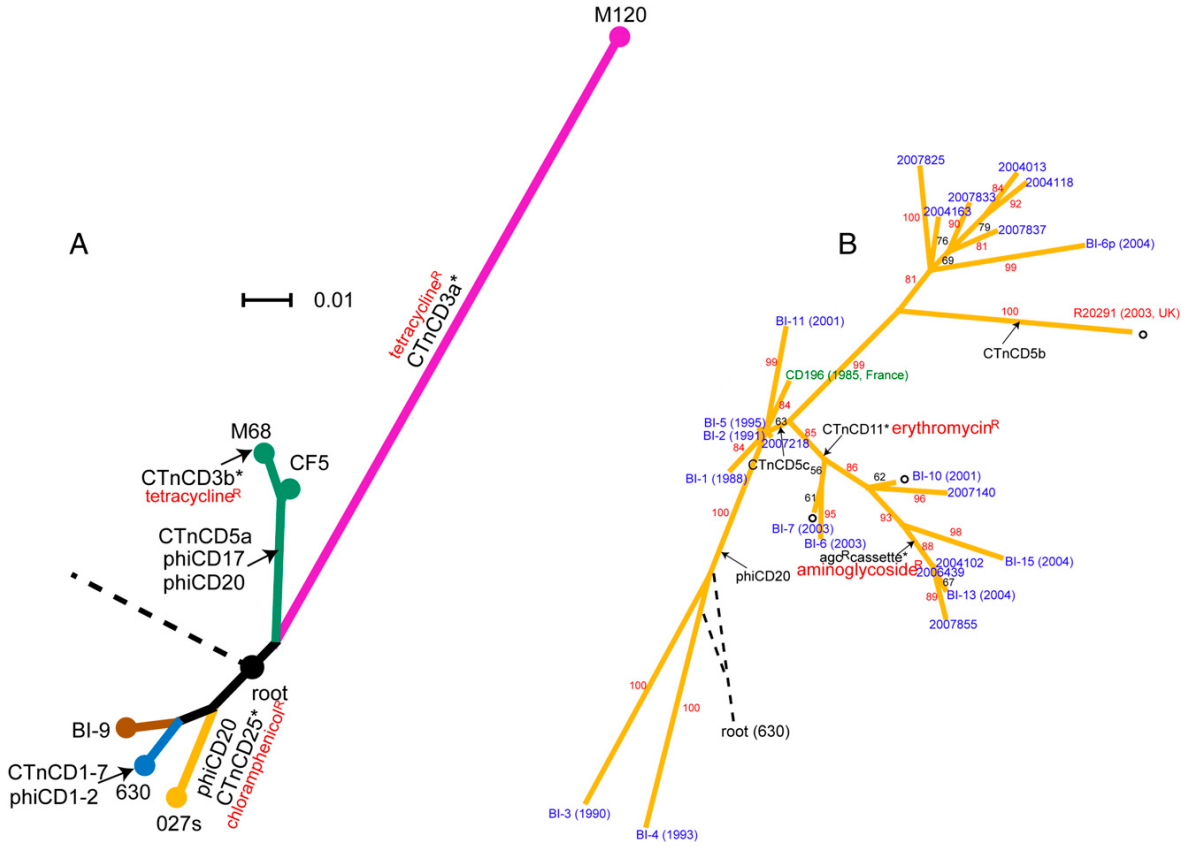


Figure 50: **Phylogenetic trees of *C. difficile* based on whole-genome sequence. Panel A:** Deep-branching phylogeny between different lineages/ribotypes. Scale bar indicates number of substitutions per site. The root connects to *C. bartlettii* and *C. hiranonis*. **Panel B:** Split decomposition network indicating microevolution within the hypervirulent lineage. Strain names are colored according to countries of isolation (blue USA; red UK; green France). Bootstrap values are labeled along branches. The root connects to strain 630. Arrows = insertions, unfilled circles = deletions, asterisks = genomic islands carrying drug resistance genes. Author: He et al. (2010)

There are also other genes than increases the virulence of *C. difficile*. Flagella enhance its motility in mucus-rich environments (Tasteyre et al., 2000). Diversity within flagellin genes is high, especially in flagellin monomer and the flagellar cap protein (Tasteyre et al., 2001; Twine et al., 2009; Stabler et al., 2009). Putative pilus type IV and capsule coding genes belong to the genes responsible for the motility of *C. difficile* (Varga et al., 2006; Stecher and Hardt, 2008). Moreover, *C. difficile* produces proteins which are employed in binding to host cell surface proteins, such as fibronectin (Barketi-Klai et al., 2011; Lin et al., 2011; Hennequin et al., 2003), collagen (Sebaihia et al., 2006) and fibrogen (Vedantam et al., 2012; Sebaihia et al., 2006).

The cell wall proteins have an important role for survival in the gut environment. The cell wall protein of *C. difficile* has at least 12 genetically divergent variants (Dingle et al., 2013; Reynolds et al., 2011; Martin et al., 2011). Two cystein proteases Cwp84 and Cwp13 are involved in assembling *C. difficile* surface layer (ChapetónMontes et al., 2011; de la Riva et al., 2011; Janoir et al., 2007; Calabi et al., 2001). *C. difficile* has a original peptidoglycan structure in the cell wall, which may provide resistance to lysozime (Peltier et al.,

2011).

### 5.1.3 Whole genome comparison of *C. difficile* strains

By comparison of different sequenced strains a species pan-genome can be derived. A pan-genome is composed from a "core genome" containing genes present in all strains, and a "dispensable genome" containing genes present in two or more strains and genes unique to single strains (Medini et al., 2005). The comparison of 73 *C. difficile* strains from different hosts showed that the core genome consists of only 586 genes, representing only 16 % of all 3,674 genes of the reference strain 630 (Janvilisri et al., 2009). Similar data was obtained by comparison of 75 strains, which shared only 19.7 % of genes (Stabler et al., 2006).

When the genomes of an "historic" non-epidemic ribotype 027 (CD196), a recent epidemic ribotype 027 (R20291) and a previously sequenced PCR-ribotype 012 strain (630) were compared, the core genome consisted of 3,247 genes (Figure 51). There were 505 genes unique to the strain 630, 47 genes unique to R20291 and 3 unique to CD196. The epidemic strain R20291 differed from its non-epidemic counterpart CD196 by a unique approximately 20-kbp phage island of high G+C content DNA (SMPI1) inserted into a 027 unique conjugative transposon (Stabler et al., 2009).

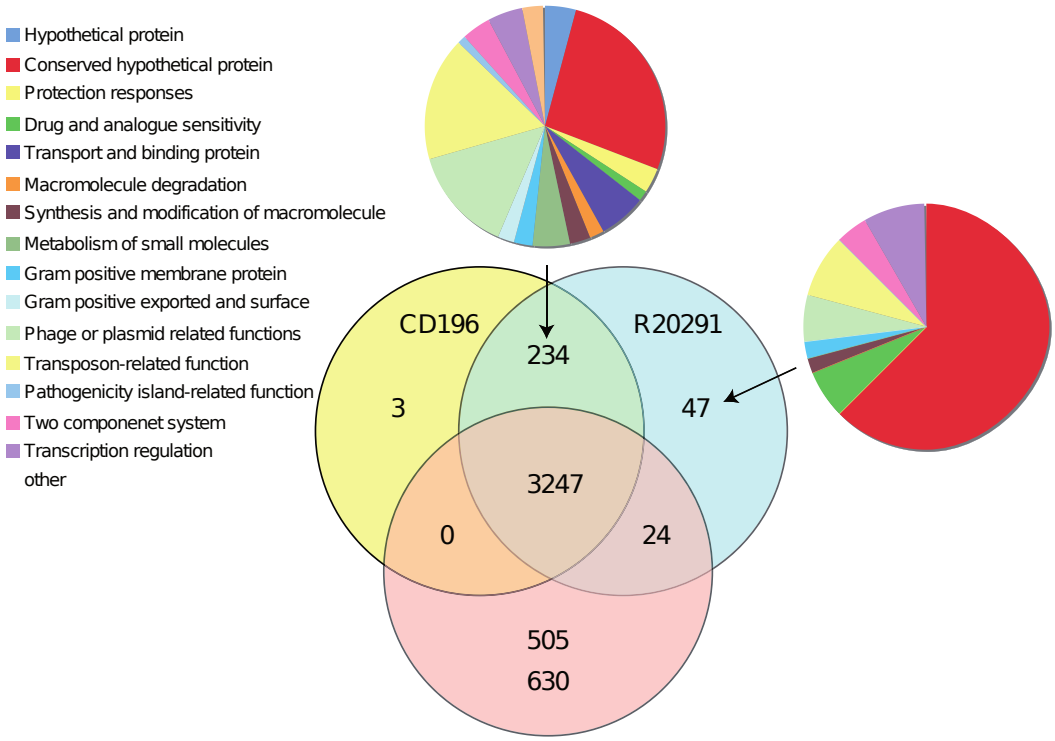


Figure 51: **Distribution of orthologues CDSs in *C. difficile* strains 630, CD196 and R20291.** The Venn diagram shows the number of genes unique, shared or core between the three strains. The associated pie charts show the breakdown of the functional categories assigned to these CDS. Author: Stabler et al. (2009)

The results of two studies comparing 73 and 75 divergent isolates from humans, cattle and pigs based on DNA microarrays combined with Bayesian phylogenies showed that the core genome of *C. difficile* may consist from 16-19.7 % of all of the 3,674 genes of the reference strains 630. The isolates were clustered into clades

and their genetic differences were detected in several genetic islands related to virulence and niche adaptation, including antibiotic resistance, motility, adhesion, and enteric metabolism (Janvilisri et al., 2009; Stabler et al., 2006).

*C. difficile* contains numerous mobile genetic elements, resulting in the potential for a highly plastic genome. It was estimated that 11 % of its genome is formed by genome rearrangements. The reference strain 630 possesses a conjugative transposon Tn5397 and six putative conjugative transposons CTn1, CTn2, CTn4, CTn5, CTn6, CTN7. From them, CTn4 and CTn5 are capable of excision (Sebaihia et al., 2006). The conjugative transposons CTn1, CTn2 CTn4, CTn5 and CTn7 were shown to excise from the genome of strain 630 and transfer to the Canadian isolate QCD-37X79 (Brouwer et al., 2011). Recently, van Eijk et al. (2015) compared the genomes of the reference strain 630 with its spontaneous erythromycin sensitive derivative 630Δerm and revealed that in the 630Δerm the mobile element CTn5 is present in the gene encoding the methyltransferase rumA, while in the reference strain 630 this transposon is present in the adhesin CD1844 (Figure 52). Interestingly, it was experimentally demonstrated that the non-toxigenic strains are capable of acquiring PaLoc toxigenic variants by horizontal gene transfer, what would convert them into toxigenic strains (Brouwer et al., 2013).

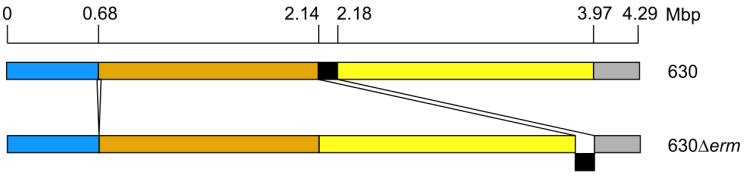


Figure 52: **Mobile genetic elements in the strain 630 compared with 630Δerm.** Segments between breakpoints are indicated with different colors. The putative transposed element is indicated in black. Author: van Eijk et al. (2015)

The mutation rate for *C. difficile* hypervirulent clade 027/BI/NAP1 was estimated to be between $1.47\times10^{-7}$ and $5.33\times10^{-7}$ (95 % confidence interval) substitutions per site per year, equivalent to 1-2 mutations per genome per year.

It was found that the hospital outbreaks may actually differ by 2,000 - 16,000 nucleotides, which may be detected by whole genome sequencing only. In the study of Eyre et al. (2012a), eight strains of *C. difficile* obtained from the same hospital within 3 weeks period were sequenced and divided into clades. Afterwards, the analysis of sequence types and SNPs showed that the isolates differ and should not be considered as one outbreak (Figure 53). The analysis of two isolates per patients/day performed on the cohort of 109 patients showed that 3 % of isolate pairs had different genotype. When samples with time-lapse 0-7 days were analyzed by whole genome sequencing, it was found that 10 % of cases were mixed infections with more than 1 strain (Eyre et al., 2012b). Similar results were obtained by MLST analysis of specific locus (van den Berg et al., 2005; Tanner et al., 2010).

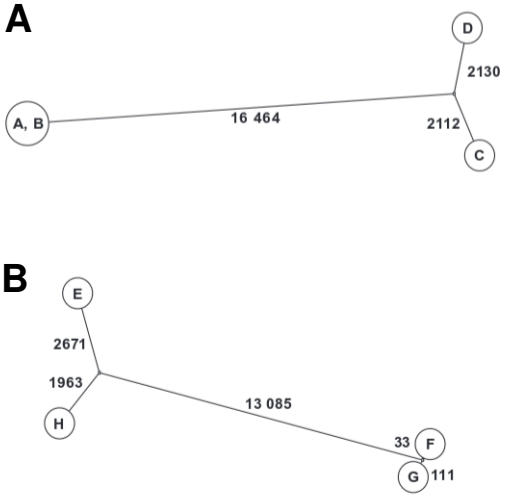


Figure 53: **The genetic relationships of isolated of *C. difficile* cluster 1 (panel A) and 2 (panel B).** Author: Eyre et al. (2012a)

The coexistence of multiple strains in one patients explains why less than 25 % of CDI cases can be linked

to a previous case with the same strain type within the same hospital (Walker et al., 2012). For that reason, if a genome epidemiological study is based on comparison of only one isolate from each patient, exclusion of transmission and determination of a origin of an outbreak may be impaired (Eyre et al., 2013a; Didelot et al., 2012).

## 5.2 Objectives

It has been shown that about 3-10 % of CDI patients are infected by multiple *C. difficile* strains. The presence of multiple strains in the previous studies has been detected by isolation of numerous colonies followed by MLST or by the whole genome sequencing (van den Berg et al., 2005; Tanner et al., 2010; Eyre et al., 2012b). It has been found that if only one colony per patient is collected, only less than 25 % of CDI cases can be linked to the previously isolated strains within the same hospital. The analysis based on sequencing of numerous microbial isolates would be very expensive for everyday clinical practice, especially because the infection by multiple strains is not known *a priori*, so numerous colonies isolated from patients infected in fact by a single strain would be sequenced uselessly. Moreover, the analysis of the microbial culture isolates may be biased by the different growth rate of the strains, so that not all strains may be sampled.

However, culture-independent cell separation methods for bacterial cells are also available. A bacterial species of interest can be hybridized with fluorescent probes based on 16S rRNA gene and separated by FACS (Podar et al., 2007).

The objective of the work presented in this chapter was to collect *C. difficile* cells present in one CDI patient by FACS, obtain their genomic sequence (a natural pan-genome) and determine the diversity of virulence genes. This approach allows to obtain whole genetic sequence of strains present in a fecal sample as they naturally are (without the cultivation bias). Their real proportions in one patients can be determined. This approach would have an advantage over the PCR based methods, where several unexpected mutations in virulence genes might be omitted.

In addition, the spread of the detected strains within the hospital will be analyzed by sequencing of the amplicons capturing the characteristic sequences of the strains detected in the first collected fecal sample.

# 5.3 Methods

## 5.3.1 Sample preparation

**Patient's fecal samples collection**

The fecal sample for the *C. difficile* natural pan-genome analysis was collected from a patient hospitalized in Beth Israel Deaconess Medical Center, Harvard Medical School, MA, U.S.A. Moreover, the fecal samples from the patients hospitalized with CDI at the same department in the following weeks ($29^{th}$ of May 2014 - $19^{th}$ of June 2014) were collected for analysis of the spread of strains present in the first patient.

The patients were diagnosed to be positive to the *C. difficile* infection (CDI) by routine Illumigene assay (Meridian Biosiences). The study was approved by the institutional review board, and informed consent was obtained from the participant.

About 5 ml of the fecal sample was resuspended in 30 ml of PBS by vortexing and centrifuged for 2 min at 2,000 g, afterwards the supernatant was centrifuged at 4,000 g for 10 min and resuspended in 30 ml PBS and fixed by formaldehyde as described in the protocol section 11.3.

As a positive control, *C. difficile* ATCC 9689 was cultured in anaerobic conditions in Difco cooked meat media (BD Diagnostic Systems). After 24 hours of anaerobic culture, the culture was fixed by formaldehyde (3.7 % final concentration).

**Quantification of *C. difficile* specific 16S rRNA genes and toxin A and toxin B genes by qPCR**

One ml of the bacterial suspensions for analysis and 1 ml of *C. difficile* culture (OD600= 0.1) as a positive control were used for the phenol-chloroform DNA extraction (Ausubel et al., 1992), as described in more details in the protocol section 11.5.

DNA concentration of the fecal sample and the *C. difficile* positive control were adjusted to contain equal amounts of amplificable 16S rRNA sequences by qPCR quantification assay with universal 16S rRNA primers (Klindworth et al., 2013) shown in the protocol section 11.1 employing KAPA SYBR FAST qPCR premix (Kapa, Ref. KK4610) on the Roche Light Cycler 480 Instrument (Roche, Ref. 05015278001).

Commercial qPCR kits of Qiagen was used to quantify sequences of according to the protocol described in protocol section 11.11:

- 16S rRNA gene specific for *C. difficile*,
- toxin A gene,
- toxin B gene.

The proportion of *C. difficile* in the fecal sample was calculated by comparison with a positive control sample containing DNA coming from 100 % of *C. difficile* ATCC 9689 culture.

**Hybridization with fluorescent probes and FACS**

The optical density at 600 nm (OD600) of the fecal bacteria suspension and the *C. difficile* culture was measured. These values were used for preparation of a control sample spiked with 10 % of *C. difficile*.

Three types of samples were prepared for the hybridization which is described in more details in the protocol section 11.6:

- fecal sample of the patient P1,
- fecal sample of the patient P1 spiked with *C. difficile*,
- culture of *C. difficile*.

In order to obtain also negative hybridization controls, each sample was divided in three parts:

- fluorescent probes + SYTO®62,
- no fluorescent probes but SYTO®62,
- no fluorescent probes, no SYTO®62.

FACS was performed on S3 cell sorter (Bio-Rad) by setting the cytometer emission filters to 520/30 (FL1) and 680/30 (FL4) for hybridization probes and SYTO®62, respectively. The first gate for FACS sorting was set to remove aggregated cell by comparison with the 6 $\mu$m calibration beads. The second gate was to distinguish cells containing DNA; it was set according to the sample which was not stained with SYTO®62 neither was hybridized with fluorescent probes. The hybridized *C. difficile* culture was used for localization of positive gate for *C. difficile* cells. The area of sorting of *C. difficile* was set according to this gate, but with respect to the fluorescence threshold of the non-hybridized P1 fecal bacteria sample, as the fluorescence threshold of fecal samples is usually a slightly higher that the threshold of bacterial cultures. The FC bi-plots of P1 fecal sample spiked with 10 % of *C. difficile* is shown in Figure 54. The bi-plot of sorting of non-spiked (original) P1 fecal samples is not shown, as the .fcs file size was too large due to the low abundance of events in *C. difficile* area.

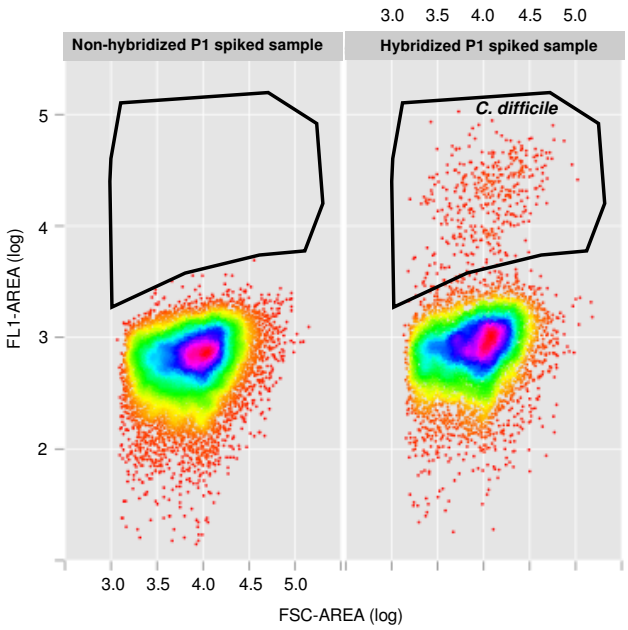


Figure 54: **FC bi-plots of non-hybridized and hybridized P1 sample spiked with 10% of *C. difficile* culture**

**Bacterial composition study**

DNA extracted from the P1 fecal sample was used for amplification of the regions V3 and V4 of 16S rDNA gene with Takara ExTaq polymerase (TakaraRef. RR001A) using primers designed for sequencing on MiSeq Illumina platform (Klindworth et al., 2013), as described in the protocol section 11.1.

Three fractions containing cca 10,000 cells resulting from the FACS of the P1 fecal sample with fluorescently hybridized *C. difficile* were also amplified and sequenced by Sanger methods, as described in the protocol section 11.2, concretely:

- fluorescent area of the P1 fecal sample spiked with 10 % of *C. difficile*,

- fluorescent area of the P1 fecal sample (*C. difficile* sample = CD-sample),
- non-fluorescent area of the P1 fecal sample.

Sequence quality assessment was carried out by using PRINSEQ program (Schmieder and Edwards, 2011). Sequences of length < 200 nt have not been considered; 5' trimming was performed cutting out nucleotides with a mean quality < 30 in 20 bp windows. Eventual chimeric 16S amplicons have been removed by USEARCH program (Edgar, 2010). After sequence processing, the sequences were taxonomically classified by RDP classifier program from Ribosomal Database Project up to genus taxonomic rank (Cole et al., 2009).

**Sequencing of the *C. difficile* FACS separated sample**

DNA coming from the FACS fraction containing 10,000 *C. difficile* cells separated from the P1 fecal sample was extracted according to the protocol described in details in the protocol section 11.5. The sample was processed with Nextera XT (Illumina) sequencing library preparation protocol, despite the fact that it contained DNA amount indetectable by Picogreen assay (Life Technologies, Ref.P11496).

DNA amount present in the library was quantified employing KAPA SYBR FAST qPCR premix (Kapa, Ref. KK4610) on the Roche Light Cycler 480 Instrument (Roche, Ref. 05015278001), using the following Illumina sequencing adaptor primers amplifying the fragments of the sequencing library:

- PCR premix:

  12.5 $\mu$l Kapa SYBR® mix 2 ×

  1 $\mu$l 10 mM Illumina forward primer: 5' - AAT GAT ACG GCG ACC ACC GAG A - 3'

  1 $\mu$l 10mM Illumina reverse primer: 5'- CAA GCA GAA GAC GGC ATA CGA G - 3'

  9.5 $\mu$l water

  1 $\mu$l DNA / water

- PCR program:

  Initialization step:

  95 °C 3 min

  Denaturation, annealing and elongation steps in 40 repetitions:

  95 °C 15 sec

  65 °C 20 sec

  72 °C 45 sec

  Cool down to 40 °C

The concentration of the prepared Illumina library was compared with control samples which have been previously sequenced successfully on MiSeq platform. It was confirmed that the library contained sufficient DNA amount for sequencing.

Afterwards, the sample has been sequenced on one entire flowcell on Illumina MiSeq platform.

### 5.3.2 Sequence data analysis

The paired-end reads were joined by fastq-join program from "ea-utils" package (Aronesty, 2013), while the non-joined reads were also used in the following analysis. Short sequences (< 50 bp) and low quality sequences (entropy < 70; quality in 10 bp windows < 25; presence of N per read > 5) were removed from the analysis, as shown in the programming script section 12.6.

The sequences were mapped to the genome of *Peptoclostridium* (*Clostridium*) *difficile* reference strain 630 (GenBank assembly accession GCA_000009205.1) by Bowtie2 using the parameters default for "very-fast" mapping of only the most similar reads, requiring that the entire read align from one end to the other (Langmead and Salzberg, 2012). The exact command is shown in the programming script section 12.5, where the resulting output is converted into "bam". Information in the .bam file was used for plotting the whole genome coverage by R package "RSamtools" (Li et al., 2009; Morgan et al., 2015) as shown in the programming script section 12.9. In addition, the resulting mapping was visualized in Integrative Genomics Viewer software (Robinson et al., 2011), where the potential SNPs sites were spotted.

Moreover, the reads were also mapped to the complete genomes representing the different clades identified by whole genome sequencing in the study of (He et al., 2010) shown in the Figure 50. These strains were the only complete *C. difficile* genome assemblies available at that moment (April 2015) in public databases (NCBI):

- BI9 (ribotype 001)
- CF5 (ribotype 017)
- M68 (ribotype 017)
- R20291 (ribotype 027)
- 2007855 (ribotype 027)
- BI1 (ribotype 027)
- CD196 (historical ribotype 027)
- M120 (ribotype 078)

The reads, which were not mapped to the reference strain 630, were assembled by Ray metagenome assembler (Boisvert et al., 2012) by the following command:

```
1 $ ray -k 31 -minimum-contig-length 300 -p forward.fastq reverse.fastq -o name
```

The obtained assembled sequences were aligned with e-value $1{\times}10^{-100}$ to the database containing all the 262 complete or partial genome assemblies of *C. difficile* available on NCBI in June 2015. The strain with the major number of hits was considered to be the potentially most genetically similar to the obtained sequences. The original whole genome shotgun reads were mapped to the resulting most similar strain by bowtie2, as explained above (see also the script in the sections 12.5 and 12.9).

### 5.3.3 Confirmation of the SNPs

One pair of primers was desiged to confirm the presence of the SNPs detected in the genomic sequence of the FACS-sorted *C. difficile* cells. The online tool Primer-BLAST was used for design of primers suitable for Illumina MiSeq amplicon sequencing (amplicon size 300-550 bp). The setting for primer melting temperatures (Tm) were the following: minimal Tm 60 °C, optimal Tm 62 °C, maximal Tm 65 °C. The primers contained Illumina-specific adaptor sequences allowing multiplexing. The specificity of the primers was checked by comparison with the "nr" database of NCBI.

The DNA extracted from the original patients' fecal samples was used as template for the PCRs. The amplicons were prepared according to the Illumina amplicon sequencing protocol with slight modifications:

- PCR premix:

  2.5 $\mu$l DNA (or water for the negative control)

  5 $\mu$l forward B primer 1$\mu$M 5'- TCG TCG GCA GCG TCA GAT GTG TAT AAG AGA CAG TCA ACG TAG AGG AGA CTT ATC CTG G -3'

  5 $\mu$l reverse B primer 1$\mu$M 5'- GTC TCG TGG GCT CGG AGA TGT GTA TAA GAG ACA GCA ATC CTT TCC TCA ACA ATT TGC GT -3'

  12.5 $\mu$l 2× KAPA HiFi HotStart ReadyMix

- PCR program:

  Initiation step:

  95 °C for 3 min

  Denaturation, annealing and elongation steps in 35 cycles:

  95 °C for 30 sec

  55 °C for 30 sec

  72 °C for 30 sec

  Final elongation:

  72 °C for 5 min

  Final hold at 4 °C

Two replicates of each PCR were prepared and were pooled in order to capture more genetic diversity and avoid effect of PCR amplification bias.

The PCR products have been purified and the sequencing index adaptors have been added by secondary PCR according to manufacturer's instruction described in Illumina MiSeq sequencing library preparation protocol.

The obtained Illumina amplicon paired-end reads were joined by fastq-join program from "ea-utils" package (Aronesty, 2013). Low quality sequences (entropy < 70; quality in 10 bp windows < 25; presence of N per read > 0) were removed from the analysis, as shown in the programming script section 12.6. In addition, amplicons were filtered for their length, keeping only sequences with the exact amplicon length and +/- 1bp of the expected amplicon length: 410-412 bp.

For the amplicon analysis, the reference amplicon was prepared by excision from the reference *C. difficile* 630 genome. The obtained amplicon sequences were mapped to the reference amplicon by Bowtie2 program, as described in the programming script section 12.5 and analyzed by the program VarScan (Koboldt et al., 2012) using the following command:

```
$ samtools mpileup -f amplicon.fasta amplic.bowtieveryfastsorted.bam | java -jar VarScan.
    v2.3.9.jar pileup2snp --min-var-freq 0.01
```

PCR of the site where SNP variations were detected were performed with the remaining 11 CDI positive samples from BIDMC collected within three weeks after the collection of the first investigated patient P1.

# 5.4 Results

## 5.4.1 An increase of the proportion of *C. difficile*

**Low load of *C. difficile* in the feces**

The proportion of *C. difficile* in the original (not FACS-sorted) fecal sample was quantified by qPCR of the *C. difficile* specific 16S rDNA sequences to be 0.10 %.

Illumina 16S rDNA amplicon sequencing confirmed the low load of *C. difficile* in the patient's feces detected by qPCR. From the 500,302 Illumina amplicons, only 0.10 % sequences could be aligned to the *Clostridium* clade XI, which *C. difficile* species belongs to (Collins et al., 1994).

**Bacterial composition of the samples**

Figure 55 shows bacterial composition of the FACS-processed P1 sample, of the P1 fecal sample spiked with 10 % *C. difficile* and of the non-fluorescent fraction of the P1 fecal sample.

The three FACS-sorted samples differed in the proportion of *Clostridium* cluster XI. No sequences of *C. difficile* were detected in the non fluorescent FACS fraction. In contrast, the sample spiked with *C. difficile* contained 54.84 % of *Clostridium* XI, although 100 % of *Clostridium* XI was expected, suggesting that FACS of such a low frequent bacterial species brings the risk of contamination by non-hybridized bacteria. The positive *C. difficile* FACS fraction contained 12.90 % of *Clostridium* XI, what represents 129× enrichment of *C. difficile* by FACS in comparison with the original non-sorted fecal sample (0.1 %).

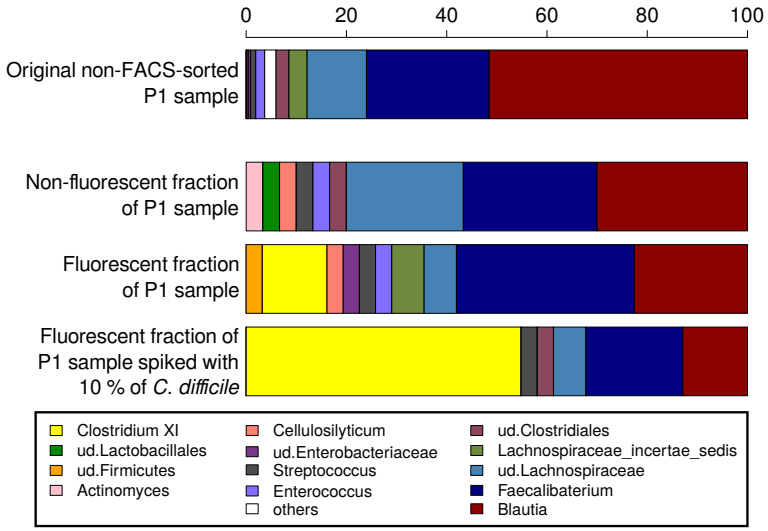


Figure 55: **Results of 16S rDNA sequencing.** The bacterial composition of the original P1 fecal sample, non-fluorescent part of the P1 fecal sample and of the *C. difficile* fraction of this sample is shown, as well as composition of *C. difficile* fraction of P1 sample spiked with *C. difficile*

### 5.4.2 Comparison with *C. difficile* reference genomes

#### *C. difficile* reference strain 630

From the total number of 4,935,947 processed reads (mean length 182,32 bp), 55,490 reads were mapped to the reference genome of *C. difficile* 630. The average coverage per a base pair was 2.12× (Figure 56). The reads were uniformly distributed along the genome, with the exception of three areas with coverage over 400× representing ribosomal RNA genes, where phylogenetically similar species present in the sample were also mapped, similarly as in the case of two peaks with coverage around 80× representing conjugative transposons.

Ten gaps of length > 5,000 bp totaling for 238,344 bp have been detected in comparison with the strain 630. These large missing regions contained especially strain-specific surface layer proteins and strain-specific sequences introduced by bacteriophages. For example, the erythromycin resistance gene ermB1 found on mobile transposon Tn5398 of strain 630 was missing, as well as the area containing putative CTn5-like conjugative transposon. Proteins employed in binding to host cell surface proteins, such as adhesin (cwp66) and proteinaceous cell surface layer (SlpA) were not covered. *C. difficile* present in the sequenced sample may also contain the binary toxin, as it was also covered.

Tetracycline resistance gene tetM of the strain 630 was covered by the obtained reads, but contained numerous mutations. Highly divergent area was detected also in cystein proteases Cwp84 and Cwp13, which are involved in assembling the surface layer and also in fiboronectin-binding proteins (Fbp68 and FpbA).

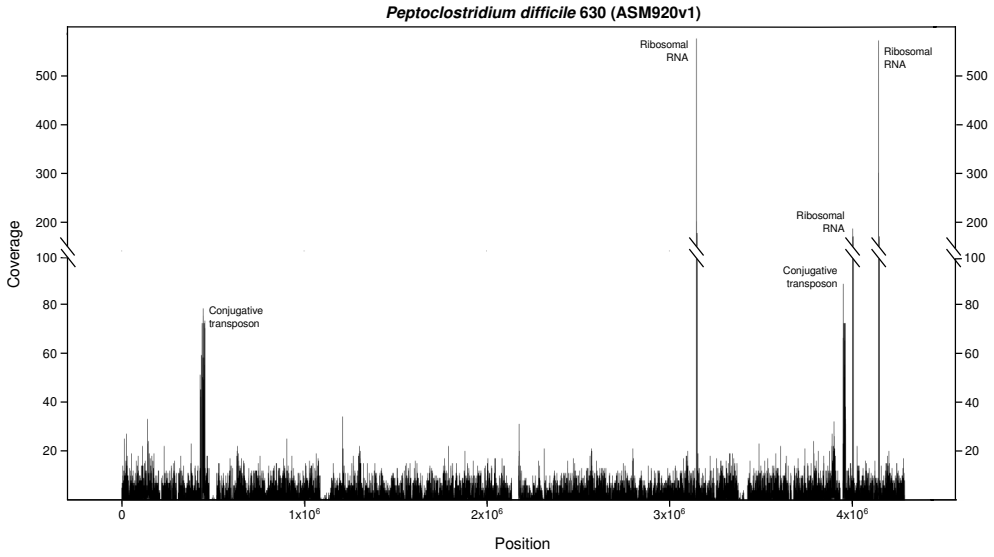


Figure 56: **Coverage of the genome of *C. difficile* strain 630.** The areas with higher coverage were identified to be ribosomal 16S rRNA and conjugative transposon-related sequences

#### Other complete genomes of *C. difficile*

The mapping of the reads to the remaining genomes representing the clades in the study of He et al. (2010) resulted also in uniform coverage with several high peaks representing either rRNA genes or conjugative transposomes-like sequences (Figure 57).

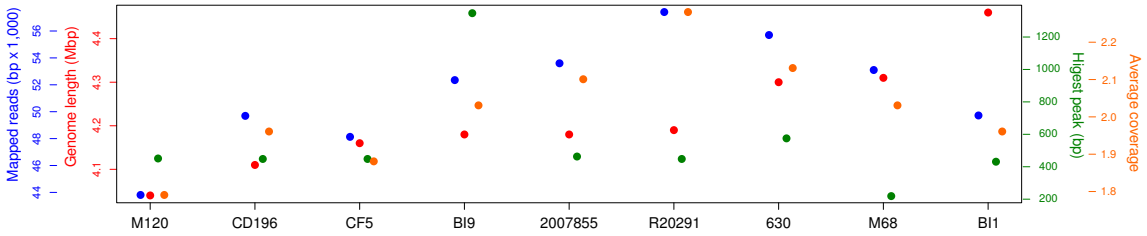


Figure 57: **Read mapping on nine *C. difficile* strains.** Total reference genome length, number of mapped reads, highest coverage peak and the average coverage data are shown for each strain

The highest peak was observed in the strain BI9 (1347 bp), while the strain with the lowest maximal peak was the M68 (219 bp). However, the highest average coverage had the strain R20291 (2.27 ×), while the lowest was of the strain M120 (1.78 ×). The highest number of reads was mapped to the genome of strain R20291 (57,407) while the lowest of the strain M120 (43,813). The low number of mapped reads and low coverage of strain M120 may be influenced by the fact that it was the coverage with the shortest genome (4,047,729 bp). The genome with the longest genome was BI1 strain (4,464,700 bp), however not the highest number of reads was mapped to it, but to the strain R20291.

From the above mentioned it can be suggested that the patient was not infected by the strain 630, neither by any of the 8 complete *C. difficile* genomes available on NCBI sequence database. Therefore, the sequences were compared with the remaining 262 *C. difficile* partial genomes available in the NCBI sequence database (April 2015). For this purpose, the reads that were not mapped to the genome of the strain 630 were assembled. The assembly of these reads resulted into 50,340 contigs of mean length 711.13 bp (±182.429 bp). The longest contig was 14,4031 bp long.

The major number of contigs (48) was mapped to the strain F665 (assembly name ASM47370v1). However, the mapping of all original whole genome shotgun reads back to the strain F665 showed again large gaps (gaps >5,000 bp) which were totaling 143,457 bp (Figure 58). The presence of the toxigenic genes tcdA and tcdB was confirmed by qPCR in the patient P1, however, the strain F665 should not contain these sequences. This suggests that despite the fact that the strain F665 was the closest to the the strains collected from the patient P1, the collected strains could not be indentified as the strain F665.

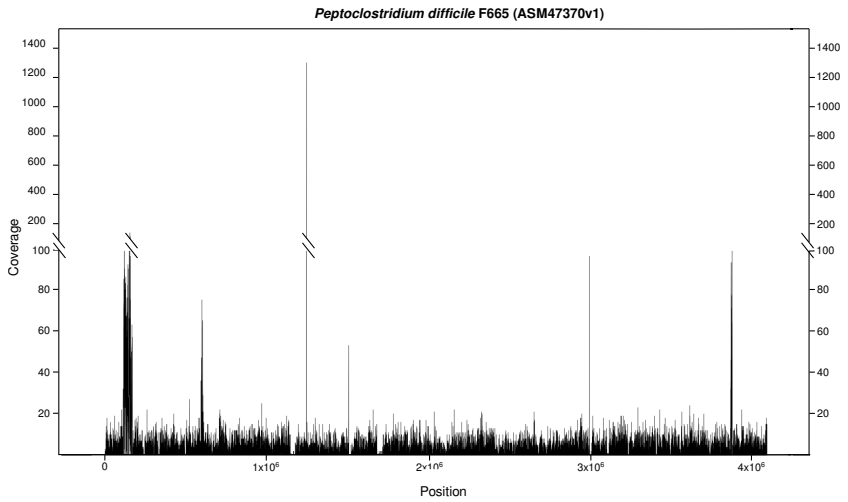


Figure 58: **Coverage of the genome of *C. difficile* strain F665**

### 5.4.3 Detection of SNPs in PaLoc region

Apart from the missing regions, the mapping of the obtained shotgun sequences also revealed single nucleotide mismatches in comparison with the reference genome 630. In addition, in numerous cases two or more variants of the obtained sequences mapped to the reference genome 630 were detected. The potential inclusion of *C. difficile*-inspecific matches in the non-conserved genome regions did not allow us to perform advanced SNP analysis on the whole-genome bases. Therefore, we focused in the deeper analysis only on the potential SNPs detected in the PaLoc region, which is *C. difficile* specific (is not found in other bacterial species). The presence of the both toxigenic genes tcdA and tcdB contained within the PaLoc region were confirmed by qPCR. The amounts of these genes in the metagenomic sample of the analyzed patient was detected to be 0.0012% for the both toxin genes.

The mapping of the shotgun reads to the reference strain 630 showed that the whole PaLoc region contains 12 sites with two variants (herein called potential SNPs). Figure 59 shows the PaLoc region and the site which was amplified by primers B. Primers B were designed to cover the region with two possible SNPs and one sequence mismatch which differed from the reference strain 630 genome (position 5,667 - 6,053 of the whole PaLoc region shown in the Figure 59). In the position 152 of the amplicon B cytosine was detected once, while reference guanine was detected 2 ×; in the position 155 cytosine was detected in one sequence, while the reference thymine was found in two sequences. In the position 176, cytosine was detected in the one shotgun sequence, while thymine in reference sequence had no sequence coverage. These nucleotide changes would not cause any changes in the amino acid string.

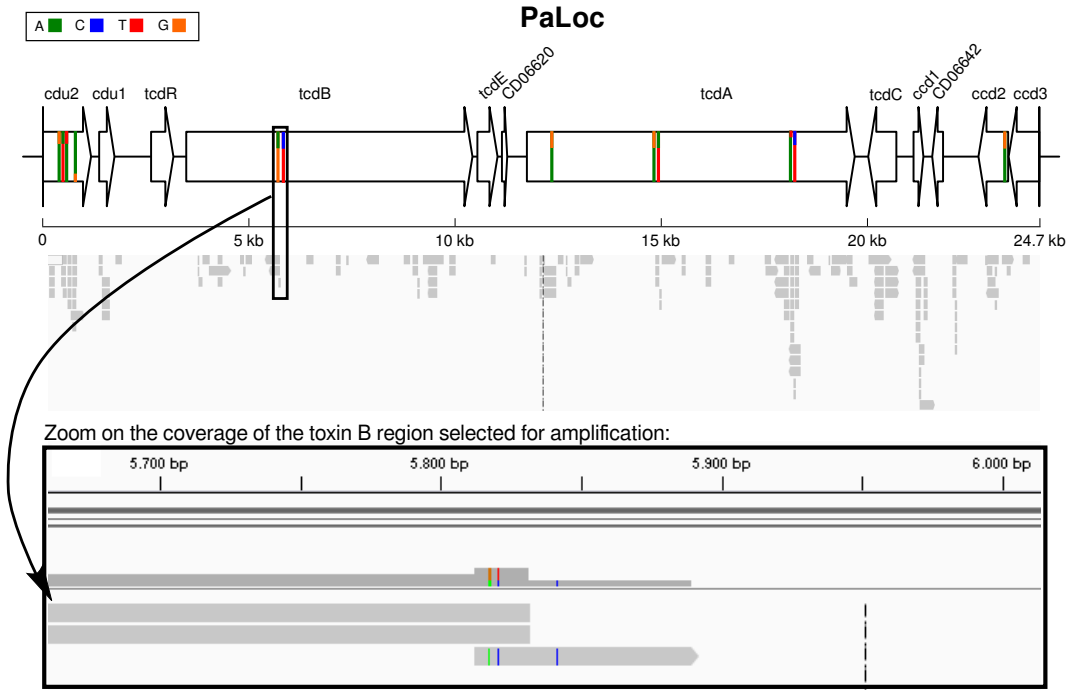


Figure 59: **SNPs identified in PaLoc locus and flanking regions totaling 24.7 kbp in comparison with *C. difficile* strain 630.** The proportion of the nucleotides detected in the mapped reads is shown by color bars within the PaLoc scheme: the reference nucleotide is shown below the substituting nucleotide. The position of the amplicon within the PaLoc and itscoverage visualized by the IGV software is marked by a black rectangle. The panels below represents the zoom into the amplified regions of the PaLoc visualized in the IGV software

MiSeq platform generated 574,694 filter passed reads of the amplicon B. The analysis of the amplicon sequences mapped to the reference amplicon B (excised from the reference genome of the strain 630) by program VarScan confirm the SNPs within the amplicon B. In the position 152 of the amplicon B, the reference variant G was detected in 0.1 % of the amplicon sequences, while the variant A was found in 99.9 % of all amplicons. In the positions 155 and 176 the reference variant thymine were found in 0.1 % of the amplicons, while the cytosine was found in 99.99 % of all obtained amplicons (Figure 60). In addition, one part of the amplicon B which was not covered by shotgun sequences but was included in the amplicon sequence contained an additional SNP: 7.17 % of the amplicon had guanine variant, while 92,83 % of amplicons had the reference thymine variant.

The amplicon B sequence containing the most prevalent variants was aligned to the "nr" database of NCBI. The only one 100 % identity match was with the toxin B sequence of strains isolated in China submitted by Du et al. (2014) in September 2014: strains of toxin B sequence types B07 and B08. The complete genomes of these strains were not available, thus mapping of the previously obtained shotgun sequences to this strains could not be performed.

Primers B were used for amplification of the 5,667 - 6,053 bp position of the PaLoc in the next 11 patients hospitalized at the same department during the next three weeks, in order to detect spread of these detected strains. The amplicon B region of three of the 11 patients was not amplified, probably because of the mismatches present in the primer annealing regions. Patient P2, P9 and P10 contained the same variants of the patient P1, but in slightly different rates. The prevalence of the non-reference nucleotide variants in the patient P1 and P2 were about 99.9 %, however in the posterior patients it was slightly less: 94.5 % in patient P9 and 99.7 % in patient P10. Interestingly, in patient P10 a novel variant in the position 354 was detected - this SNP was not detected in the patient P1.

In contrast, patients P4, P8 and P12 did not contain the above mentioned SNPs, but their sequence matches with 100 % similarity the reference amplicon. It suggests that these patients had single strain infection. Interestingly, similarly as the patients P4, P8 and P12, neither the patients P5 and P6 contained the above mentioned SNPs detected in the patient P1, but their contained novel variants detected by the amplicon sequencing: the patient P6 had two novel variants in the positions 275 and 276 at the frequency about 99.9 % and patient P5 one novel variant at the position 278 (99.86 % frequency).

In summary, as shown in the Figure 60, from 9 patients, in which the selected region of the toxin B was amplified succesfully, 8 were infected by at least two strains. The variants at the positions 152,155 ad 176 in the patient P1 were at frequency 99.9 %, while there was a SNP at the position 380 at frequency 7.17 %. Probably, aprox. 7 % of the cells containing mismatches at positions 152, 155 and 176 contained also a mismatch in the position 380, while aprox. 93 % of this population contained the reference nucleotide in the position 380. Theoretically, the minority population forming 0.1 % of all strains may be also divided in two parts: one part containing the mismatch at the position 380 and an another part containing at the position 380 the reference nucleotide. It means that the patient P1 may contain 4 different strains. Similarly, patient P10 may be also infected by 4 different strains, as at the position 354 a SNP with frequency 13.98 % was detected in addition to the SNPs at positions 152, 155 and 176. Patients P2, P9 were possibly infected by two strains: one strain was possessing SNPs in the positions 152, 155 and 176, which have been detected in the patient P1, while the second strain had the same sequence as the reference strain 630. The reference strain was in minority, forming only about 0.1 and 5.4 % of all *C. difficile* cells in patients P2 and P9, respectively. Patients P5 and P6 were also possibly infected by two strains, the minority strains had the same sequence as

the reference strain 630, while the more prevalent strain had a novel mismatch which was not detected in the patient P1.

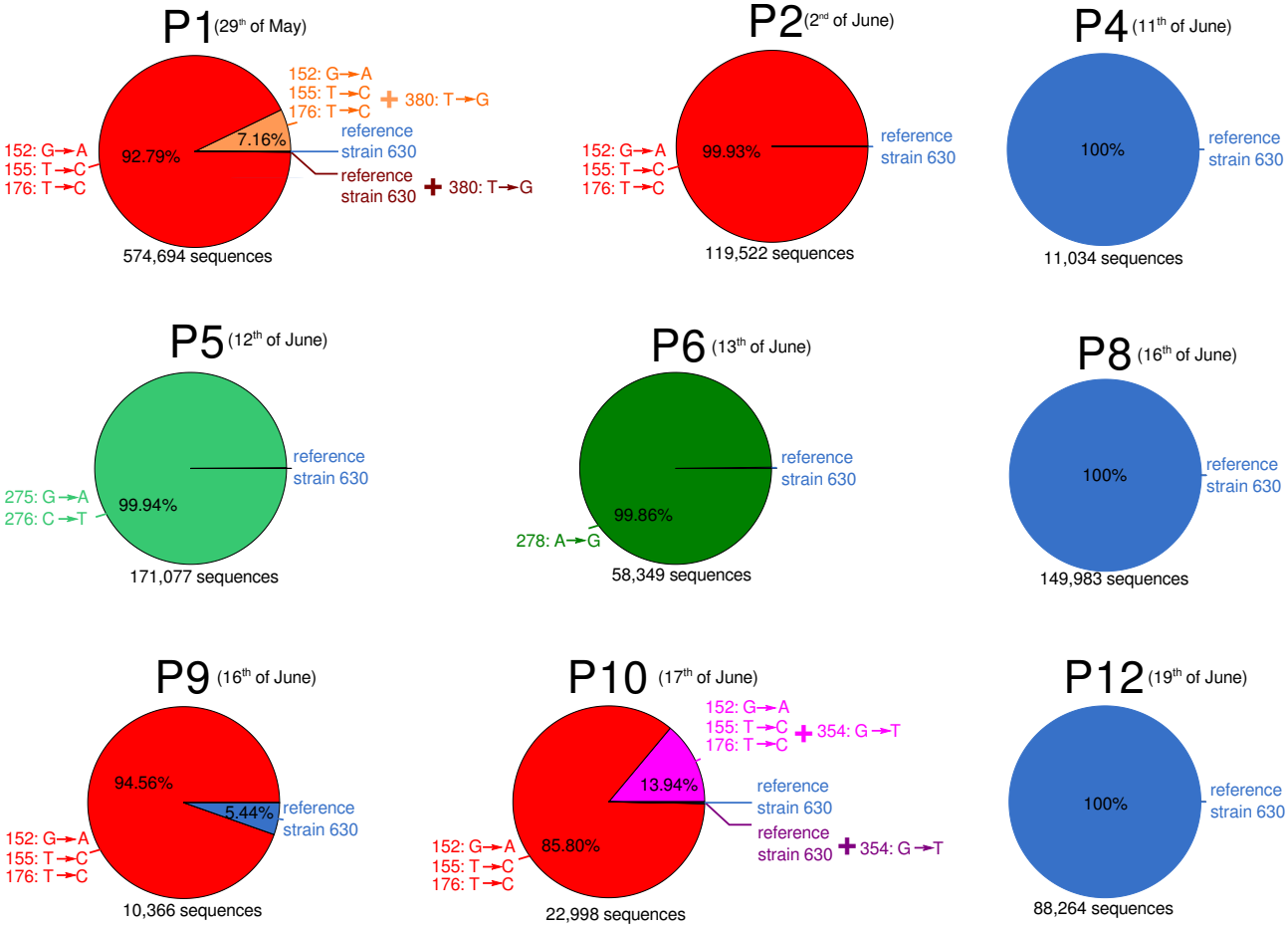


Figure 60: **An estimation of the proportion of strains found in analyzed patients based on amplification of selected region of the toxin B.** The numbers 152, 155, 176, 275, 276, 278, 354 and 380 refer to the positions within the amplicon B in which SNPs have been detected

## 5.5 Discussion

The infection by multiple *C. difficile* strains is quite common. Eyre et al. (2013b) and Didelot et al. (2012) claimed the strains present in one patient usually differ in thousands of SNPs, which may be detected by whole genome sequencing only. They claimed that for exact analysis of the origin of an infection spread, tens of isolated colonies must be sequenced with high genome coverage. Despite the decreasing costs of genome sequencing, this approach represents still important expenses which makes genome sequencing impossible to be applied the routine diagnostics (Eyre et al., 2012b).

Different growth rate of the strains and their different requirements on nutrient and environmental conditions are the major obstacle for retrieving isolates of different strains by the conventional microbial culture. The major advantage of the FACS approach used in the herein presented work is that it recovers multiple *C. difficile* strains at their real proportion, independently of their growth rate. Another advantage of FACS is the reduction of the diagnostic time, as there is no need for microbial culture.

The herein presented approach serves as a preliminary screening of fecal samples whether they contain multiple *C. difficile* strains or not. It operates with low genome coverage, which is, however, sufficient for detection of possible SNPs sites. The presence of multiple strains was confirmed by a PCR amplifying a region within the toxin B gene which contained SNPs detected by mapping of the shotgun sequences. FACS-based isolation of *C. difficile* cells may reduce the cost of sequencing numerous isolated colonies without previous certainty of multiple strain infection. However, if the FACS-separated samples were sequenced by sequencing platform with higher throughput, such as Illumina HiSeq, complete genomes of the present strains could be recovered, too.

The low genome coverage obtained in this study was sufficient for detection of possible SNPs positions. The SNPs were confirmed by deep amplicon sequencing and showed that the patient P1 contains variants in the toxin B that have been previously sequenced by Du et al. (2014) (Figure 61). The strains containing the same SNPs come from the collection of 70 patients isolated in China. Du et al. (2014) in their study prepared custom amplicons covering the whole sequence of the toxins A and B genes and created custom system for sequence type clusterization. Their amplicons were of the length from 700 to 1,800 bp and were sequenced by Sanger method from single culture isolates. It cannot be concluded that the collected strains of the sample P1 belong to some of the Chinese isolates, as the full genomes of the Chinese collection were not available.

The multiple-strain infection screening based on whole genome shotgun sequencing of FACS-separated *C. difficile* cells from patient's feces is important, as the positions of SNPs in a genome are never known *a priori*. Evidently, amplicons for standard MLST analysis may be also used (Griffiths et al., 2010), however multiple strains infection may remain undetected, as the strains may differ by SNPs present in genome regions which are not covered by the standard MLST amplicons (Didelot et al., 2012). It is also important to mention possible PCR bias. The primers designed for amplification of the regions containing possible SNPs in one patient, may not serve for amplification of the same region in other patients, as they may contain some additional nucleotide variants in the primer annealing sites, what would result in no PCR amplification product or some sequence variants may be omitted. This is probably the reason why no amplification product was obtained for the patient P3, P7 and P11. Similarly, the strain proportions in individual patients calculated in this study may be also biased by primer annealing sites differences. Therefore, the shotgun sequencing should be taken as a gold standard for SNPs detection and strains proportion estimation.

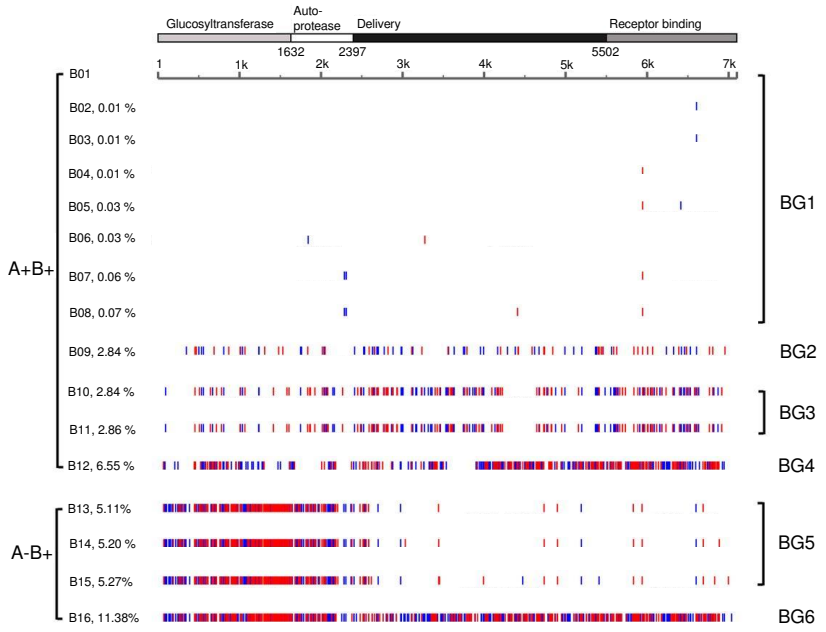


Figure 61: **Identification of SNPs in tcdB sequences of 95 isolates (70 patients and 25 GeneBank sequences) using VPI 10463 as reference.** The rates of SNPs in each tcdB type are given in brackets after the type name on the left; the names of groups are marked on the right. Nonsynonymous SNPs (red lines) and synonymous SNPs (blue lines) are identified. Author: Du et al. (2014)

FACS increased the proportion of *C. difficile* from the 0.1 % in the initial fecal sample of the patient P1 to 12.9 % in the FACS-collected sample. It seems that 100 % recovery of the target species without any contaminant is very difficult. Samples with higher concentration of the target species also contains contamination - the fecal sample spiked with 10 % of *C. difficile* contained finally 45,16 % of contaminating species. The taxonomic analysis showed that the contaminating bacteria were similar to the original fecal sample. It suggest that the contamination comes from the sorting equipment processing the fecal bacteria suspension sample and it suggests that the 16S rRNA probes were *C. difficile*-specific.

For more precise cell sorting, cell single-cell collectors or dissectors may be used, such as CellEctor equipment for collection of single cells in a suspension (shown in Figure 20). CellEctor is widely used for selection of human cells, especially for cancer research, where single-cell transcriptomics is of the major interest (Pachmann, 2015), however there are no studies focused on selection of bacteria. Blainey laboratory at the Broad Institute (MIT, Boston) is developing a microfluidic device, in which DNA from single bacterial cells will be extracted and Nextera libraries will be constructed. The resulting pool will be sequenced directly on Illumina platform (Soohong Kim, MIT, personal communication on Single Cell Analysis Congress, Boston, USA; May 2014).

The contamination of the sorted sample impairs the genome coverage analysis. The regions covering conjugative transposon and ribosomal DNA had high coverage in the present study, as these sequences have high similarity with genomes of other bacteria. If these regions are not taken into account, no other peaks of extremely high coverage were observed. The uniform coverage in this study was achieved by direct preparation of the sequencing library from the 10,000 FACS-separated cells, meaning that the cells were not enriched by whole genome amplification (WGA) methods, which is commonly applied to the samples with low DNA

concentration. WGA is prone for development of chimeras and GC amplification bias (Lasken and Stockwell, 2007), which is unacceptable in sequencing project in which SNPs and genome rearrangements differentiate the studied bacterial strains. Due to WGA some genome regions may be overamplified with coverage of hundreds or thousands, while other regions are unamplified. This discrepancy was not observed in the present study. As no WGA were used, it may be concluded that the gaps observed after mapping of the shotgun sequences to the reference genomes were due to their natural absence in the collected strains. Larger gaps in the 630 genome indicated that the patient was not infected by the strain 630. It was difficult to determine which of the 263 strains available in the online databases (August 2015) was genetically the most similar one to the strains of the patient P1. Even the strain F665, which had the highest number of hits, was not completely covered. Unfornatelly, the strains from China, determined by high-throughtput amplicon sequencing to be the most similar to our patient's strains, could not be used for mapping of our whole genome shotgun reads, as the whole genome assemblies of these Chinese isolates were not available.

## 5.6 Conclusions

The work performed in this section showed that sequencing of FACS-separated cells belonging to the target *C. difficile* species may serve as a method for fast screening of the fecal samples for the presence of the multiple strains. FACS allows to screen a great number of target cells, while in the culture-based methods, only one colony is usually sequenced. The recent studies, in which more isolates were sequenced from one patients, showed that the strains in one fecal sample may differ in thousands of SNPs. These mutations may not be detected by ribotyping of toxinotyping methods and therefore may lead to the false conclusion that patient is infected by only one strain.

On the other hand, the whole genome sequencing of tens of isolates as a diagnostic method may be expensive if considered as a standard diagnostic procedure for the future. However, if the *C. difficile* cells are sorted by FACS and sequenced as a metagenome enriched for the target species of *C. difficile*, the obtained sequences may show whether SNPs variations are present in the strains. If the presence of multiple strains in one sample is confirmed by PCR, the origin of the epidemiological outbreak may be tracked more easily.

In the studied sample, the infection by three of four *C. difficile* strains was detected by identification of SNPs in the whole genome sequence of the cells separated by FACS. Possible SNPs in the selected region of the toxin B were confirmed by PCR. Theoretically, the genomes of these *C. difficile* strains could be completed if a deeper sequencing were performed.

The primers designed for amplification of the selected region of the toxin B were used for analysis of the presence of the same variants in other patients hospitalized with *C. difficile* infection within the following three weeks. Five of the 8 additionally amplified samples contained variants suggesting presence of 2-4 different strains. Three of these five patients were probably infected by the same strain as the first patient (which was used for FACS-seq analysis). Three of the 8 additionally analyzed patients were probably infected by only one strain.

Chapter 6

# Adaptation of the sequencing protocols to limited DNA samples coming from FACS

**Associated original articles:**

Džunková, M., Garcia-Garcerà, M., Martínez-Priego, L., D'Auria, G., Calafell, F., Moya, A. (2014) Direct sequencing from the minimal number of DNA molecules needed to fill a 454 picotiterplate. PLoS One. 9: e97379+

MD and MGG contributed equally to the work

# 6.1 Introduction

## 6.1.1 DNA amount needed for sequencing

In many cases, e.g. biopsies, laser dissection experiments and FACS, the amount of DNA available for sequencing is limited. The protocols for sequencing library preparation have restrictions for the starting DNA amount, so not all the samples can be sequenced easily. For example, the rapid library preparation protocol for shotgun sequencing by 454 FLX + technology requires 1 $\mu$g of starting material. One *E. coli* cell contains 4.96 femtograms of DNA. If theoretically no losses during DNA extraction occurred, for starting sequencing library preparation protocol 2.01 $\times 10^8$ *E. coli* cells would be needed. This number of cells is easy to obtain by standard culture methods, but difficult to collect by FACS.

The major steps of the shotgun library preparation protocol by 454 platform are the following:

1. Shotgun library preparation:
   - fragmentation into 700 bp of DNA by nebulization,
   - removal of fragments which do not have required length by spin columns,
   - enzymatic reparation of fragment ends and ligation of sequencing adaptors,
   - removal of unligated sequencing adaptors by magnetic beads, taking the advantage of an extraordinarily high affinity of biotin (vitamin H) to streptavidin,
   - library concentration measurement and dilution to the working stock for starting emPCR titration.
2. Titration of the emulsion PCR (emPCR), testing 4 different concentrations of the prepared library. The mixed DNA fragments are separated into microreactors by emPCR. These microdroplets serve as microscopical laboratory tubes for PCR. DNA fragment in each microdroplet is copied thousand times in order to amplify the light signal which is to be detected by the machine. The objective of the emPCR titration is to find the correct ratio between library volume and beads.
3. Final emPCR with the most suitable amount of DNA selected by titration.
4. Sequencing run preparation. Loading of the beads to the picotiter plate (PTP) shown in the Figure 62.

Figure 62: **Picotiter plate.** Bead deposition device with divisions for two 1/2 regions and the used PTP divided into four 1/4 regions. Source: Roche and D. P. Lyle' blog

The pyrosequencing reaction is performed on the PTP (Figure 62). The method is schematically shown in Figure 63. The surface design of the PTP contains thousands of microwells and it allows accommodation of only one bead per well. Each bead contains clonally amplified DNA molecule from the previous emPCR step. Individual nucleotides and pyrosequencing reagents are flowed across the wells. Nucleotides are being added to a single-stranded DNA template in cycles. The synthesis of a complementary strand is accomplished by DNA polymerase which starts synthesis from the point where a primer is attached to the template DNA strand. The system detects pyrophosphate released in the moment of addition of a nucleotide during second DNA strand

synthesis; it measures the quantitative conversion of pyrophosphate to ATP by sulfurylase and the subsequent production of visible light by firefly luciferase. Unincorporated nucleotides are degraded between each cycle by a nucleotide-degrading enzyme apyrase. Each incorporation of a nucleotide complementary to the template strand results in a chemiluminescent light signal recorded by the camera (Ronaghi et al., 1998).

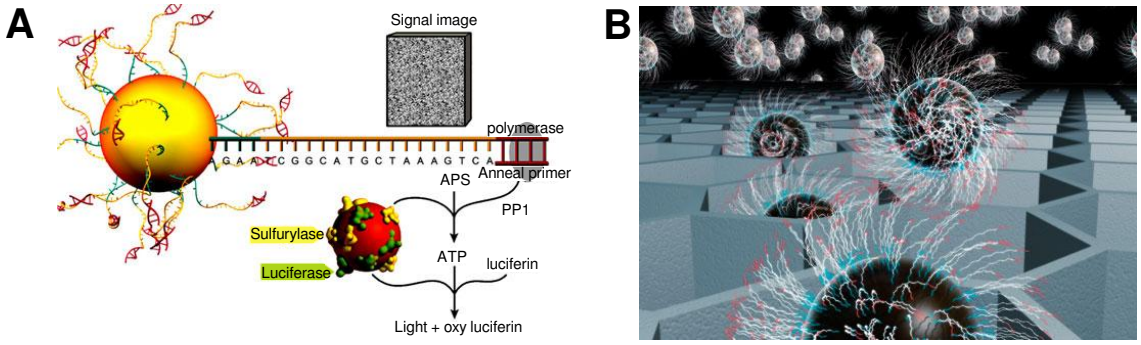


Figure 63: **454 pyrosequencing. Panel A:** Scheme of the pyrosequencing chemistry. **Panel B:** Illustration of "one bead = one read" notion. Adapted from 454 Life Sciences

The Rapid library preparation protocol of Roche has several control points, where the DNA amounts must be measured and the library quality must be checked. The prepared library concentration is measured by the fluorometer, which detection limit is 0.25 pg/$\mu$l. In addition, the quality of the prepared library can be checked by Agilent Bioanalyzer which analyzes the length distribution of the fragments and the presence of remaining sequencing adaptors. The protocol requires that a prepared library must contain at least 6,340 pg of total DNA amount (Figure 64). If the required DNA amount if reached, the remaining amount of a library can be stored in the freezer, so that it can used in the case when a repetition of the sequencing is required.

The protocol further requires that the library must be diluted to the stocks of different concentrations. The final DNA concentration of a library is converted to the number of molecules - the minimal library dilution should contain at least $10^7$ molecules, which is actually 7.6 pg (Figure 64). As every library contain DNA from different origin having different GC content, the performance of a emPCR may be different for each library. The producer claims, that some small variations between products with different lot numbers may also occur.

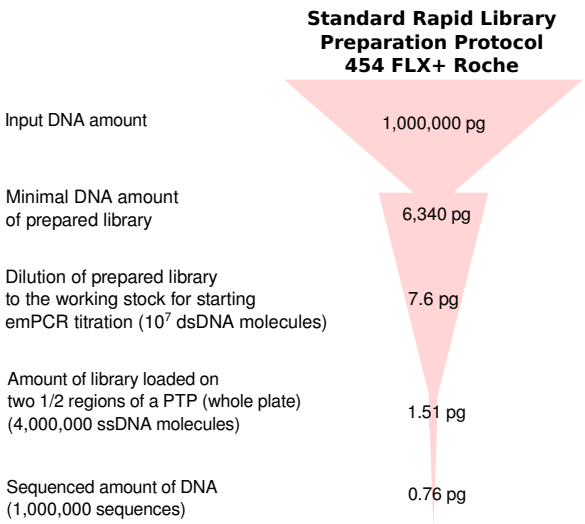


Figure 64: **Amount of DNA needed in subsequent steps of sequencing library preparation protocol of 454 platform**

The PTP can be divided into 16, 8, 4 or 2 segments, allowing combination of different libraries (Figure 62). The emPCRs for libraries which will be sequenced on 1/16 and 1/8 regions of the PTP must be prepared using small volume kit (SV-emPCR), the samples to be sequenced on 1/4 region must be prepared in medium volume kit (MV-emPCR) and samples for 1/2 regions required large volume kit (LV-emPCR). The titration emPCR is always performed in SV-emPCR kit. Four different dilution are prepared for this titration, but it is also possible that

the dilution selected as the most suitable for final emPCR will be incorrect when performed by MV-emPCR or LV-emPCR kits, so the titration must be repeated with different volumes. Therefore, the reasons why such a high amount of prepared library is required are the possible repetitions of emPCR and the possibility of repeating the sequencing run with frozen library stock if needed.

The purpose of the emPCR titration is to determine the exact volume of library needed for amplification of exact number of molecules which must be loaded on a selected region of the PTP. One tube of SV-emPCR volume contains 2.4 $\times 10^6$ beads. The correctly amplified bead must contain just one amplified fragment. If the library concentration is too high, it is possible that into the oil drop formed by shaking during emPCR preparation will get two or more DNA fragments. These fragments will be amplified on one bead, resulting in a mixed signal during the sequencing, what will cause the failure of the sequencing run. In the opposite situation, when too few molecules are present in the library, the resulting run will give poor sequencing results, as the major part of the PTP will contain empty wells. The producer claims, that from 2.4 $\times 10^6$ beads present in the SV-emPCR kit tube, 7-15 % must contain correctly amplified fragments. This proportion ensures that the PTP will be uniformly covered by beads containing amplified fragments and the probability that one contains mixture of two fragments is very low. The minimal number of fragments (molecules) required for loading on one region of the PTP is the following: 1/16: 125,000 fragments, 1/8: 340, 000 fragments, 1/4: 790,000 fragments, 1/2: 2,000,000 fragments.

The following equation will be used for calculation of the DNA amounts actually loaded on one whole PTP plate (two 1/2 PTP regions) corresponding to 2 × 2,000,000 ssDNA molecules = in total 4,000,000 ssDNA molecules of length 700 bp (2,000,000 dsDNA molecules):

$$DNA\ amount = \frac{Conversion\ to\ pg \times Length\ (bp) \times Average\ weight\ of\ bp \times Number\ of\ dsDNA\ molecules}{Avogadro\ constant} =$$

$$= \frac{10^{12} \times 700 \times 650 \times 2{,}000{,}000}{6.023 \times 10^{23}} = 1.51\ pg$$

The result indicate that on one PTP, actually 1.51 pg of DNA is loaded. Actually, the sequencing does not recover all the fragments loaded on the PTP plate, so finally maximally 1,000,000 sequencing reads will be obtained from the whole PTP. These sequences are equivalent to 0.76 pg of DNA (153 cells of *E. coli*). This result indicates that 2.01 $\times 10^8$ *E. coli* are needed for starting with the protocol, while the obtained sequences correspond only to 153 cells.

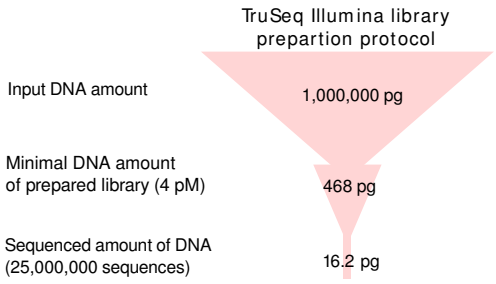


Figure 65: **Amount of DNA needed in subsequent steps of Illumina TruSeq sequencing library preparation protocol**

The high amount of the inpiyt DNA is required not only by the 454 platform, but also by Illumina platforms in the protocols in which mechanical fragmentation is used in library preparation protocol. Illumina platform allows use of different library preparation protocols. Nextera is the most common protocol. It requires only 1 ng, because it is based on enzymatic fragmentation of template DNA by transposase which incorporates sequencing adaptors. an another sequencing library protocol, TrueSeq, is based on DNA fragmentation by sonication which is followed by ligation of sequencing adaptors. This protocol is preferable, if the sample requires random shearing. TrueSeq requires 1 $\mu$g, similarly as Rapid 454 library preparation (Figure 65), because both are based on mechanical fragmentation. The Illumina platform requires 4 pM concentration of the library to be loaded on a

sequencing plate (called flow cell), what corresponds to 468 pg. However, finally only 25 $\times 10^6$ sequences will be recovered from one sequencing run. These sequences are theoretically equivalent to 16.19 pg (3,260 *E. coli* cells). Interestingly, one sequencing run on the Illumina MiSeq platform produces 25 × more sequences than 454, but the final amount of sequenced *E. coli* cells is only 21 × higher. Waste amounts of Illumina libraries dilutions are also stored in a freezer for cases when a sequencing run fails and it must be repeated.

The shotgun sequencing library protocols based on mechanical DNA fragmentation require 1 $\mu$g of DNA, while enzymatic fragmentation protocols requires less DNA (1 ng). There are also alternative protocols for cDNA sequencing - transcriptomics, in which even less DNA amount is required, as cDNA can be amplified by primers which have been used for reverse transcription from RNA. However, these protocols are not considered in this chapter, as it is focused on whole genome sequencing only. Paired-end libraries require even more input DNA, because great DNA losses occur when unpaired fragments are removed, e.g. 20 kbp paired-end library of 454 platform requires 30 $\mu$g.

### 6.1.2 Whole genome amplification methods

Despite the fact that the final amount of library loaded on the sequencing plate is far lower than the required input amount for library construction, the automatization of the library preparation process has forced the scientists to artificially enrich the low input DNA amount samples. For whole genome amplification (WGA) various approaches are currently used.

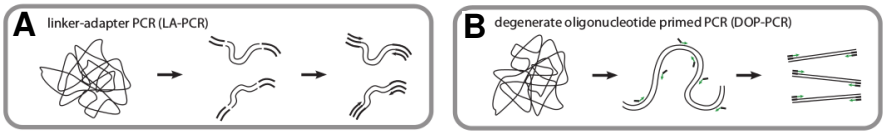


Figure 66: **Whole genome amplification methods.** Modified from Blainey (2013)

In the linker adaptor WGA (also known as ligation-anchored) PCR (LA-PCR), randomly sheared DNA is ligated with adaptors and amplified by PCR targeting the adaptors with the aim to reach the concentration required for starting with shotgun library preparation, as shown in Figure 66, panel A (Troutt et al., 1992; Klein et al., 1999). This method was used also for amplification of unknown microorganisms from environmental samples (Breitbart et al., 2004; Duhaime et al., 2012; Williamson et al., 2012). Another method is degenerated oligonucleotide-primed PCR (DOP-PCR, Figure 66, panel B), which uses hybrid oligonucleotides with degenerated bases to allow dense priming of the template by low initial annealing temperature (Telenius et al., 1992).

The multiple displacement amplification (MDA) is the most commonly used WGA method (Binga et al., 2008). Random hexamers are hybridized to the genomic DNA and isothermal polymerase from the $\phi$29 phage of *Bacillus subtilis* (Vlček and Pačes, 1986) which forms displaced strands. Secondary hexamer annealing occurs on the displaced product strands. This reaction (Figure 67) was originally designed to amplify circular DNA templates (Dean et al., 2001). It was later also tested on non-circularized templates (Dean et al., 2002; Lage et al., 2003). Later, MDA was used for partial genomes recovery of marine protists (Yoon et al., 2011), of the phylum TM7 isolated from soil (Podar et al., 2007; Marcy et al., 2007b), of *Proteobacteria* cluster SAR324 inhabiting ocean (Swan et al., 2011) or of single viruses (Allen et al., 2011).

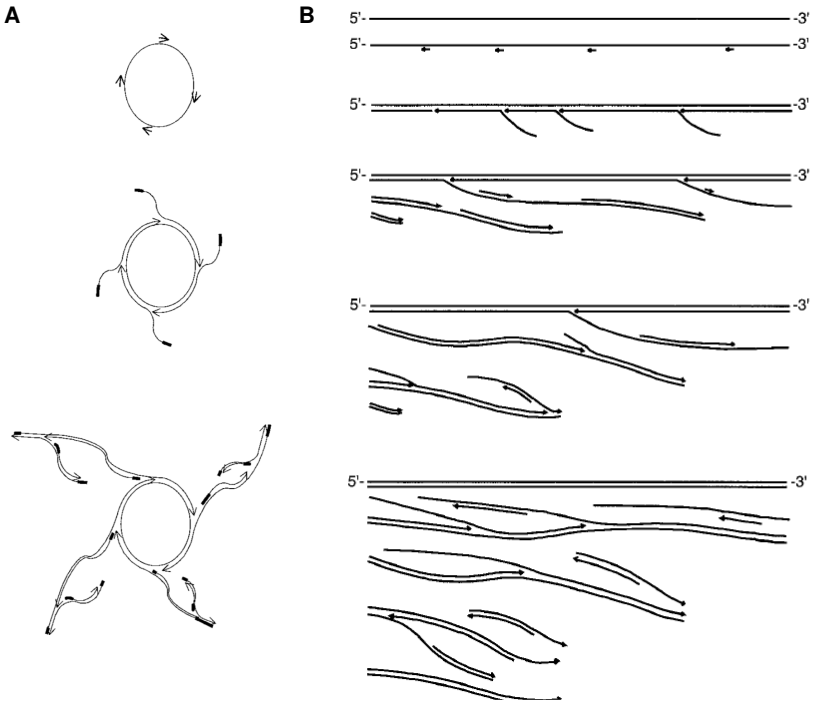


Figure 67: **MDA. Panel A:** The schematic of the multiply-primed rolling circle amplification. The polarity of polymerization is indicated an arrows. The location of the original primers is marked by thickened lines. Author: Dean et al. (2001). **Panel B:** Schematic of the hyperbranched strand-displacement amplification reaction. Author: Lage et al. (2003)

An improvement of MDA was developed by the team of Ch. Zong in 2012 (Lu et al., 2012; Zong et al., 2012). It is called looping-based amplification cycles (MALBAC). Amplified fragments form loops what avoids excessive amplification resulting in more uniform genome coverage than the coverage achieved by MDA. Despite MALBAC was demonstrated to be very effective, Lasken (2013) presented an opinion that MALBAC, as any other WGA methods, can have numerous limitations, which must be evaluated, too.

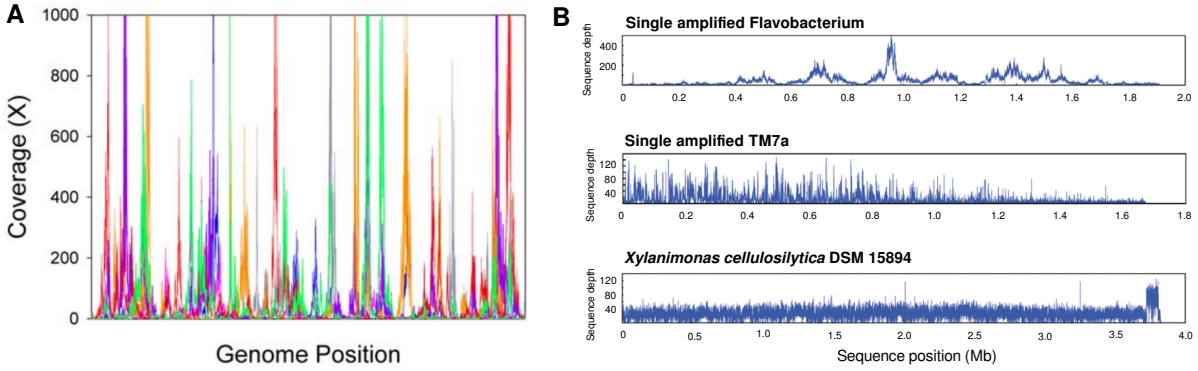


Figure 68: **Genome coverage distribution of MDA enriched single-cells. Panel A:** Variation in coverage depth among replicate single-cell WGA libraries of the same bacterial species. Author: Rodrigue et al. (2009). **Panel B:** Genome coverage of MDA enriched single-cells from three different species. Author: Ishoey et al. (2008)

Genome coverage bias is the most important limitation of the WGA methods. The inventors of MDA admitted that smaller chromosomes might be amplified more uniformly than larger ones (Dean et al., 2001). The amplification bias in MDA is also specifically associated to the GC-rich regions or chromosome ends (Bredel et al., 2005). The coverage among regions can variate from 0 to 2,500 ×, as shown in Figure 68, panel

A, and is independent from sequencing platform (Rodrigue et al., 2009; Paez et al., 2004; Hosono et al., 2003; Lage et al., 2003). Preferential overamplification of some bacterial species has been detected (Abulencia et al., 2006; Raghunathan et al., 2005). Some species might be amplified uniformly, while others can have coverage variations from 0 to 500 × (Ishoey et al., 2008), shown in Figure 68, panel B.

There are numerous studies reporting improvements for MDA coverage-related issues. For example, Zhang et al. (2006) and Hutchison et al. (2005) proposed a method in which the branched structures are debranched by S1 nuclease digestion and only double-stranded fragments are kept. However, this method was reported to recover typically only 75 % of the genome from a single bacterial cell (Marcy et al., 2007a). Bredel et al. (2005) and Zhulidov et al. (2004) presebted another improvement, they suggested to compensate genome coverage distortions by cDNA microarrays.

In many cases, template independent amplification products have been reported. These amplifications are largely oligonucleotide-derived, but exogenous DNA contamination can also contribute. For example, the GenomiPhi v2 kit from GE Healthcare Life Sciences was reported to form up to 10 ng/$\mu$l of template independent amplifications (Spits et al., 2006b; Le Caignec et al., 2006; Iwamoto et al., 2007). Also other studies reported that more than 70 % of the reads obtained from MDA enriched samples could not be classified neither by comparison with NCBI "nr" database (Woyke et al., 2011; Rodrigue et al., 2009). Even if the volume of reaction is reduced down to nanoliters, a single-cell amplification can contain up to 53-62 % of these artifacts (Marcy et al., 2007a). These artifacts may assemble together with the correctly amplified genome sequences, creating corrupted sequences of a novel organism.

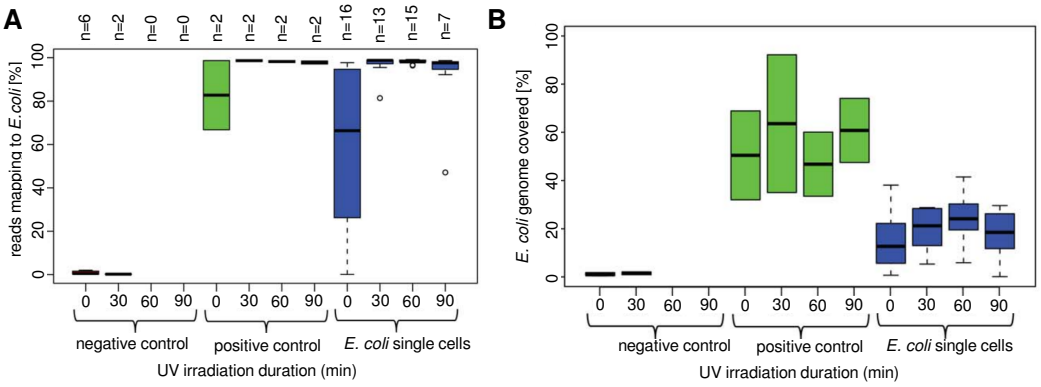


Figure 69: **Sequence analysis of single-cells of *E. coli* enriched by MDA reagents decontaminated by UV irradiation. Panel A:** Reads mapping to *E. coli*. **Panel B:** Proportion of *E. coli* genome covered. Positive control contained 10-100 cells. Author: Woyke et al. (2011)

Treholase or single-stranded DNA binding protein from *Thermus thermophilus* have been proposed for removal of template independent amplification products (Pan et al., 2008; Inoue et al., 2006). It was also demonstrated that reduction of MDA reaction time to 2 hours is effective in reducing nonspecific amplification products (Spits et al., 2006b). Woyke et al. (2011) reported that the MDA reactives already contain non-target DNA and they proposed UV irradiation as the best method for kit decontamination (Figure 69). Interestingly, some of the 16 replicates of non-irradiated samples of single-cell of *E. coli* in their study contained 0 % of sequences mapping to *E. coli* genomes. UV irradiation helped to increase number of sequences matching *E. coli* genome, but the non-uniformed genome coverage issues remained unsolved.

The low specificity of the random hexamers together with an amplification temperature of 30 °C make the MDA reaction prone to development of chimeras (Lasken and Stockwell, 2007), shown in Figure 70. A chimera is a sequence which has been formed during amplification by joining two sequences which are not following the correct sequence order in the template DNA. They can be joined together in the moment when polymerase creates secondary amplicon from the previously formed amplicons. Lasken and Stockwell (2007) calculated that in 85 % of detected chimeras, sequence inversion (Figure 70, panel A and C) takes place. If DNA from other organism is accidentally present in the MDA reaction, it can be incorporated in the process of chimera formation. In *de novo* applications, such chimeric sequences may be accepted in reconstructions of the true sequence, so the resulting sequence of a novel microorganism will be corrupted.

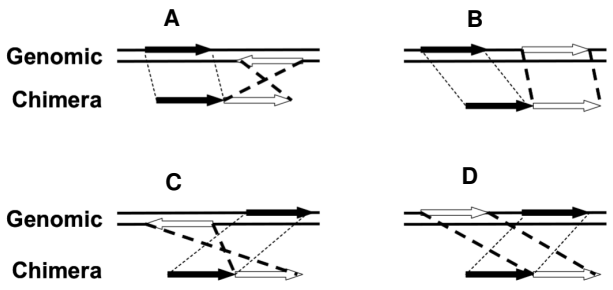


Figure 70: **Chimera formation by MDA.** Author: Lasken and Stockwell (2007)

### 6.1.3 Attempts to sequence less DNA

Some research started to speculate that if WGA has many limitations, the attention must be focused to the reduction of input DNA needed for sequencing, so that the limited DNA samples could be sequenced directly, without previous WGA step.

For 454 pyrosequencing, 1 $\mu$g of DNA is required for starting with the library preparation yielding picograms of the prepared library. Most of that library is spent for the titration of the emPCR. Meyer et al. (2008) and Zheng et al. (2010) presented the idea that the exact quantification of the number of molecules in the prepared library is the key for the reduction of the input DNA amount. Meyer et al. (2008) used qPCR to quantify the prepared library and they calculated the exact template/bead ratio avoiding emPCR titration steps, consequently reducing the input DNA amount for starting with the library preparation protocol. Zheng et al. (2010) described an approach for qPCR quantification of library amplificable molecules based on MGB Taqman probes which is even more exact than the method of Meyer et al. (2008). These probes allow quantification of small amounts of DNA down to a few zeptograms ($10^{-21}$ grams), even below the minimum amount needed for proper sequencing (Huang et al., 2011). The low DNA amounts in these studies were derived from a highly concentrated sample DNA diluted to the zeptogram concentrations.

Unfortunately, samples quantification by qPCR was never officially included in Roche sequencing library preparation protocols. Similarly, qPCR is not obligatory for Illumina sequencing library quantification.

## 6.2 Objectives

Sequencing platform require high amounts of DNA for preparation of a shotgun library, what is a limitation for sequencing of samples containing low amounts of DNA, as those coming from FACS containing few hundreds or few thousands of cells.

The most common method for overcoming this limitation is the enrichment of the input DNA by WGA, which is usually MDA. However, MDA is prone to development of chimeric sequences, formation of non-target amplifications and genome coverage bias, so the resulting genome assembly is usually presented in an incomplete form, probably including erroneously assembled reads originated from non-target species.

Some investigations have been made for modification of the sequencing library preparation protocols with the objective to allow sequencing of samples with lower DNA concentration. The most important point is the exact quantification of the DNA molecules present in the prepared libraries, aiming to work with the minimal number of molecules which might be loaded on a sequencing plate.

In the previously performed experiments of low DNA amount sequencing, even zeptogram amounts of input DNA have been tested for quantification and sequencing, however these samples were actually dilutions from a highly concentrated samples.

This work aims to obtain a 454 shotgun library for direct sequencing starting from the amount of DNA needed for reaching exactly the minimal number of molecules required for filling the target region of the sequencing plate. This will be performed starting from few thousand of *E. coli* cells obtained from FACS. DNA from these cells will be extracted and the shotgun sequencing library will be prepared. In order to perform a successful sequencing run, some modifications of the standard 454 protocol will be made. The steps, in which DNA loss in the standard 454 protocol occurs, will be replaced by more sparing alternatives. The resulting library will be quantified by qPCR, as the quantification limit of the standard quantification methods recommended by 454 protocols will be probably above the concentration of the prepared library. Moreover, qPCR is needed for quantification of exact number molecules which is important in avoiding DNA losses in emPCR titration.

To assess whether direct sequencing can be proposed as an alternative to MDA, the same number of cells will be enriched by MDA and processed by the same sequencing protocol. In order to avoid sampling bias, 20,000 *E. coli* cells will be separated by FACS, the DNA will be extracted and then split into halves to MDA and direct sequencing samples. A replicate of this will be also prepared. Thus, the amplification bias caused by MDA can be evaluated by comparison with direct sequencing.

# 6.3 Methods

## 6.3.1 Sequencing library preparation

### DNA preparation

The *E. coli* strain K12 was cultured overnight in a liquid LB medium at 37°C and fixed as described in protocol section 11.3. The cells were stained with SYTO®62 (Life Lechnologies, Ref. S11344), as described in the protocol section 11.13.

Flow cytometry sorting was performed using MoFlo XDP Cell Sorter (Beckman Coulter, Ref. ML99030). Wavelength emission was set at 635 nm, and absorption at 670 nm, to detect signal from the *E. coli* DNA stain. Gates were set using the side-scatter vs. fluorescent signal to separate the cells. Sorted cells were placed in 1.5 ml sterile LoBind tubes (Eppendorf, Ref. 0030 108.051) to reach 20,000 cells. One replicate of 20,000 sorted cells was also prepared.

DNA was extracted according to the protocol of Ausubel et al. (1992) in sterile conditions, described in details in the protocol section 11.5. DNA was resuspended in 20 $\mu$l nuclease- free water and divided in two sub-samples, one for direct sequencing (DSsample) and the second for enrichment by MDA (MDAsample). The experimental design is shown in Figure 71.

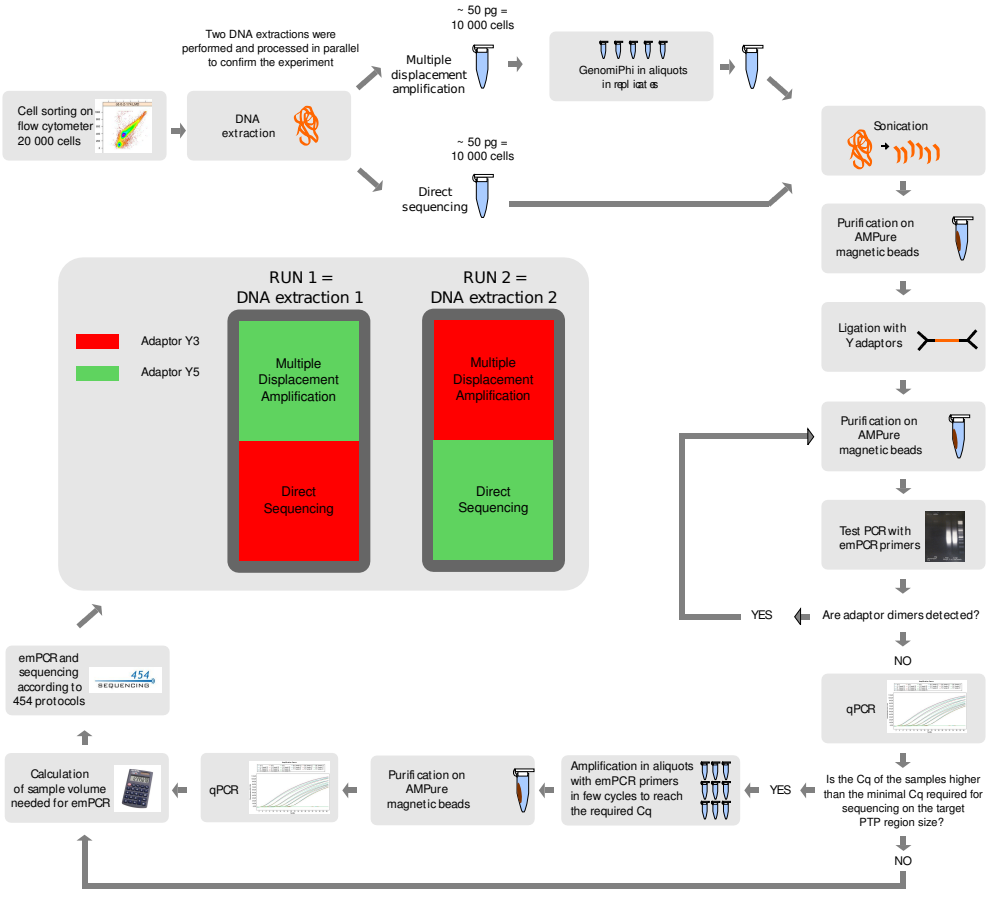


Figure 71: **Flowchart of the minimal library preparation protocol**

MDA was performed with the GenomiPhi V2 amplification kit (GE Healthcare Waukesha, Ref. 25-6600-30) following manufacturer's instructions with incubation at 30°C for 2.5 hours. In order to reduce amplification bias, the amplification was performed in 5 replicates using 2 $\mu$l of extracted DNA per tube, and the aliquots were finally pooled back after the reaction finished. After this step, this DNA sample (MDAsample) was processed in parallel with its unamplified counterpart (DSsample), as shown in Figure 71.

**Library preparation work-flow**

The protocol for minimal library preparation is described in details in protocol section 11.12. Figure 72 shows the changes to the standard Roche FLX+ Rapid Library preparation protocol proposed here.

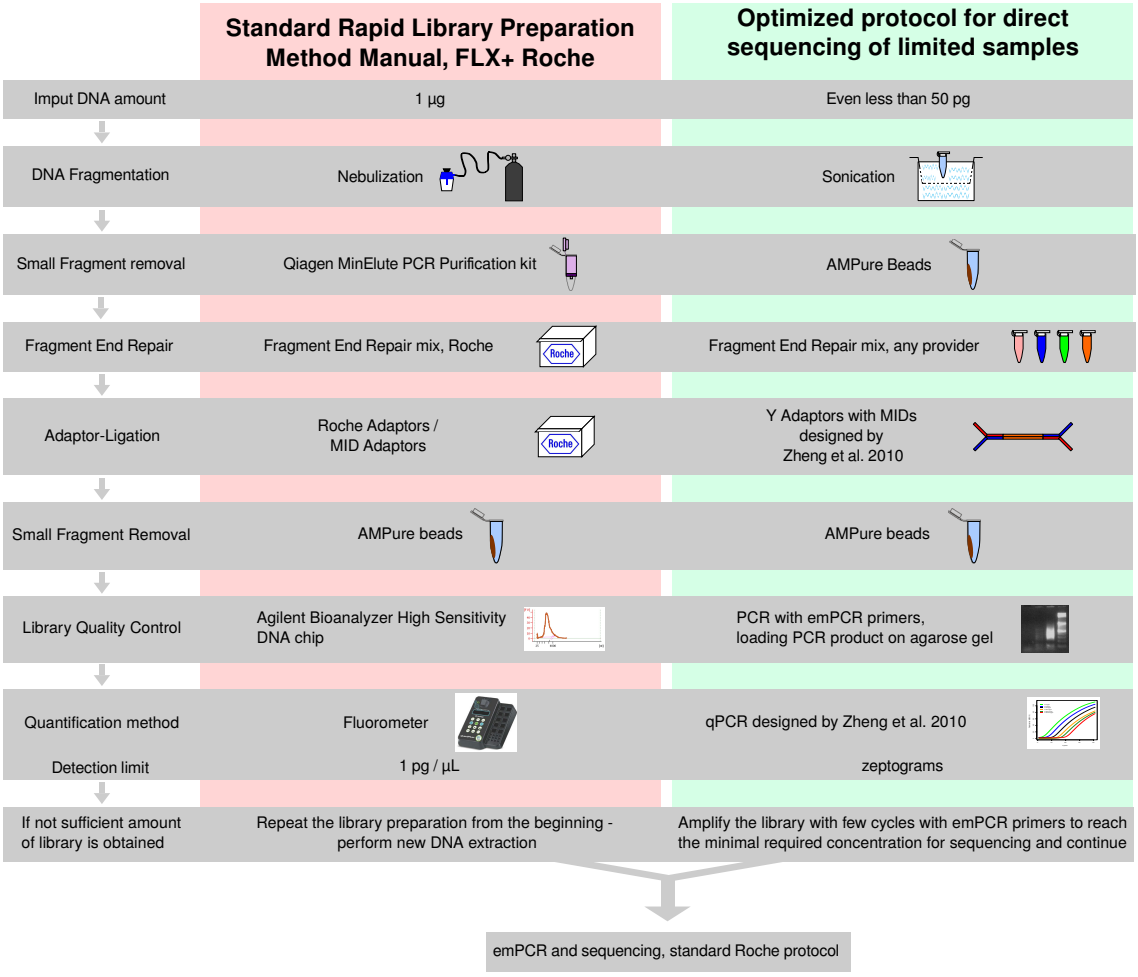


Figure 72: **Steps in standard 454 library preparation compared with optimized protocol for minimal libraries.**

In the standard Roche protocol, the samples are fragmented by nebulization in which DNA is forced through a small hole in a nebulizer. It results in the formation of a fine mist which is collected by a pipette. Fragment size is regulated by the pressure of the gas used to push the DNA through the nebulizer, the speed at which the DNA solution passes through the hole, the viscosity of the solution, and the temperature (Sambrook and Russell, 2006a).

In contrast, the sonicator used in this study allows to shear DNA placed in closed 1.5 ml tubes used along

the whole protocol. Sonicator shears extracted DNA hydrodynamically. The time of sonication, the volume of the sample and the temperature influence the DNA fragmentation (Sambrook and Russell, 2006b). Different sample volumes (Figure 73, panel A), temperature of water in the sonicator container (Figure 73, panel B) and time of sonication (Figure 73, panel C) were tested with the aim to obtain fragments distribution 200-1000 bp. High sonication temperature has been found to distort the sonication results, therefore, the experiments were performed in water cooled with ice which was removed before sonication. Finally, as the best option for 454 sequencing, the samples in volume 100 $\mu$l were sonicated at 4 °C for 3 minutes.

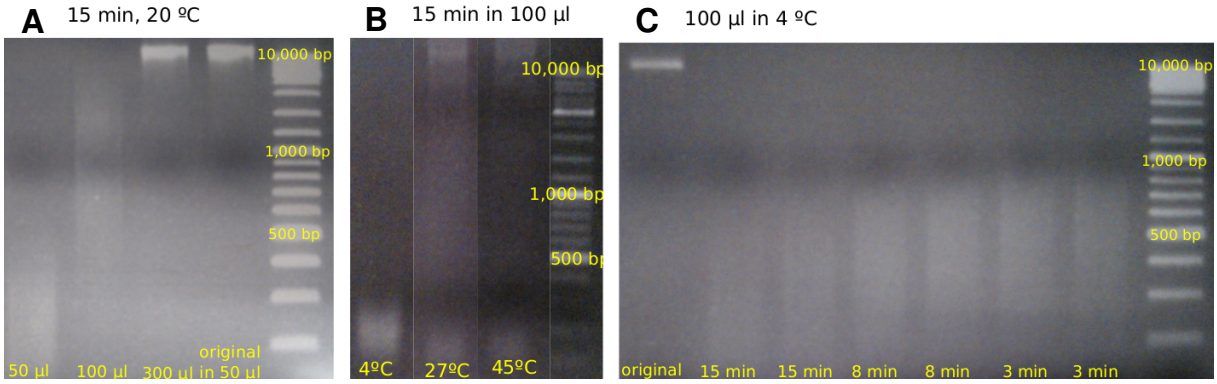


Figure 73: **Sonication optimization. Panel A:** The sample volume was tested at 20 °C with sonication duration for 15 min. **Panel B:** The water in the sonicator container was tested with sample volume 100 $\mu$l by sonication for 15 min. **Panel C:** The time of sonication was tested with the sample volume 100 $\mu$l and water temperature 4 °C

DNA fragments shorter than 400 bp were removed by magnetic beads. This is also a modification of the original Roche's sequencing library preparation protocol (Figure 72), where the nebulized fragments are purified by MinElute PCR Purification kit from Qiagen (Ref. 28004 ).

The 454 adaptor ligation was performed according to the protocol proposed by Zheng and collaborators (Zheng et al., 2011), where custom adaptors in form of "Y" are used. They already contain a MID tag for distinguishing the samples pooled in one region of the PTP. The Y adaptors also contain a sequence which serves as a template for MGB probe hybridization in qPCR. Two different MIDs, Y3 and Y5 were used in the present study. The primer sequences are shown below, the asterisks (*) indicate a phosphorothioate-modified bond, p indicates a phosphorylation. The experiment replicate was carried out inverting MID tagging in order avoid a possible MID-based bias (Fig. 71).

- Y3:

  5'- C*C*A* T*C*T* CAT CCC TGC GTG TCT CCG ACG ACT ACA CT*A* C*T*C* G*T -3'

  5'-p C*G*A* G*T*A GTG TGA CAC GCA ACA GGG GAT AGA CAA GGC ACA CAG GG*G* A*T*A* G*G -3'

- Y5:

  5'- C*C*A* T*C*T* CAT CCC TGC GTG TCT CCG ACG ACT ACG AG*T* A*G*A* C*T -3'

  5'-p G*T*C* T*A*C TCG TGA CAC GCA ACA GGG GAT AGA CAA GGC ACA CAG GG*G* A*T*A* G*G -3'

The possible self-ligated adaptors were removed with magnetic beads, which is a step in common with the Roche's protocol (Figure 72). In order to confirm the correct adaptor ligation, the correct fragment size and the elimination of self-ligated adaptors, a PCR using emPCR primers was performed, as described in the protocol section 11.12. It is also a modification of the Roche's protocol, where the Agilent 2100 Bioanalyzer is used for the sample size checking and it may be used also for library quantification (Figure 72). This step is important, as self-ligated adaptors might abolish the sequencing run. Theoretically due to the A overhang present on one of the adaptors, no self-ligated adaptors should be formed, however, the practice showed that the self-ligation occurs quite frequently in low concentrated DNA samples. The self-ligated adaptors may be observed as a band around the 100 bp region. In this case, the purification by magnetic beads was repeated 5 times until the band became undetectable (Figure 74). After the first purification, usually only self-ligated adaptors are visible, because they are shorter than the library and therefore amplify better. After each of these purification steps, the amount of self-ligated adaptors is reduced and the library fragments become more visible.

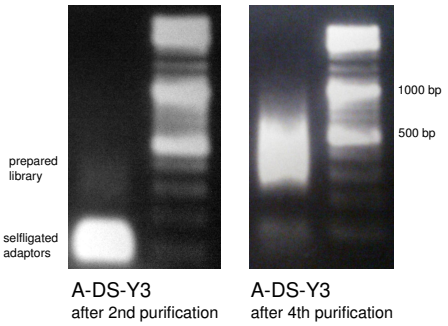


Figure 74: **Quality control of minimal 454 libraries after the 2nd and 4th purification steps**

## 6.3.2 Quantitative PCR

**Preparation of a quantification standard**

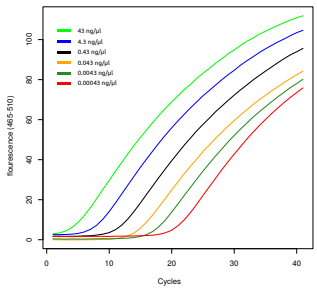


| Concentration | Cp | Number of molecules | Logarithm |
|---|---|---|---|
| 43 | 3.65 | 62,452,134,072.82 | 11.80 |
| 4.3 | 6.33 | 6,245,213,407.28 | 10.80 |
| 0.43 | 9.84 | 624,521,340.72 | 9.80 |
| 0.043 | 12.70 | 62,452,134.07 | 8.80 |
| 0.0043 | 15.47 | 6,245,213.40 | 7.80 |
| 0.00043 | 18.90 | 624,521.34 | 6.80 |

Figure 75: **qPCR of the dilutions of the sample with standard concentration**

For determination of the exact number of molecules, qPCR was performed with a MGB-TaqMan probe, according to Zheng and collaborators (Zheng et al., 2011), described more details in the protocol section 11.12. The concentration of the sample selected for the standard curve construction was measured by Picogreen (Life Technologies, Ref.P11496). The construction of the standard is described in the protocol section 11.7. Briefly, the 16S rDNA amplicon was gel-purified and then it was ligated with "Y" adaptors designed by Zheng et al. (2011) (adaptor Y5 in this case). After removal of self-ligated adaptors, the sample was amplified with emPCR primers and gel-purified. This amplicon was cloned into blunt-end vector pJET (Thermo Scientific, Ref. K1231) and sequenced by Sanger sequencing method, as showed in the protocol section 11.2. The sequencing revealed that the insert is exactly 547 bp long. The amplicon length was confirmed by Agilent 2100 Bioanalyzer. The concentration of the control sample was determined by Picogreen assay (Life Technologies, Ref.P11496) to be 43 ng/$\mu$l. Ten fold dilutions of the standard sample were prepared and a qPCR was run as described in the protocol section 11.12.

The values obtained from the qPCR were used for the exact library quantification. First, the number of

cycles where no molecules are present was calculated from the standard curve (Figure 75) and the following equations:

$$Number of molecules = \frac{Concentration \times Avogadro\ constant}{10^9 \times Length\ (bp) \times Average\ weight\ of\ a\ base\ pair} = \frac{Concentration \times 6.023\times10^{23}}{10^9 \times 638 \times 650}$$

$$Logarithm = log_{10}(\text{Number of molecules})$$

The amplicon length in the equation is 638 bp, as it is the sum of the original amplicon of 547 bp with ligated adaptor A (41 bp) and adaptor B (50 bp).

Afterwards, slope and intercept (Point 0) of arrays in **Cp** column (y-axis) and in the **Logarithm** column (x-axis) must be calculated.

$$\text{Slope} = \frac{\sum(x-\bar{x}).(y-\bar{y})}{\sum(x-\bar{x})^2} = -3.08 \qquad Point\ 0 = \bar{y} - Slope.\bar{x} = 36.63$$

**Quantification of the samples**

In the first step, the minimal number of molecules required for loading on a picotiter plate must be calculated. MDAsample and DSsample in this study were prepared using combination of two different MIDs, in order to be combined on the same 1/8 picotiter plate. The number of beads required to be loaded on one 1/8 size region of the sequencing plate is 340,000, however when two tagged samples are combined in one region, the number of beads required per sample is only 170,000 (single stranded molecules) per sample. If the final volume of the prepared libraries was 44 $\mu$l, the number of required beads/molecules per $\mu$l was 3,863.54 (170,000 ÷ 44). As fragments used for the qPCR are in the form of double stranded molecules , it means that 1,931.82 dsDNA molecules (3,863.54 ÷ 2) were introduced to the qPCR.

$$\text{Minimal required Cp} = log_{10}\left(\frac{Molecules\ in\ qPCR}{Sample\ volume}\right) . Slope + Point\ 0 =$$

$$= log_{10}\left(\frac{1{,}931.82}{44}\right) . (-3.08) + 36.63 = 26.52$$

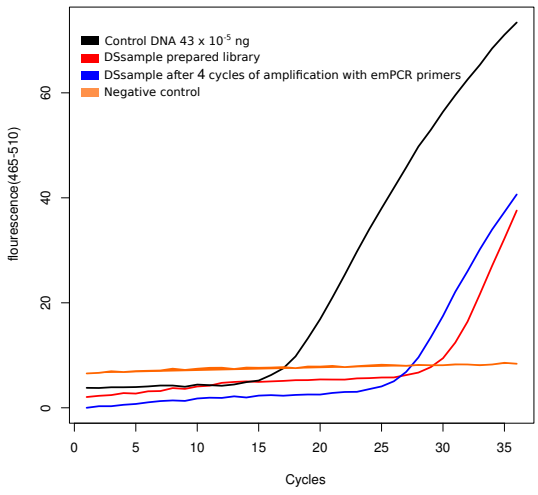


Figure 76: **qPCR of prepared library before and after amplification with low number of cycles**

The real obtained Cp of qPCR (the number of cycles which are needed to generate enough molecules with detectable fluorescence) of the DSsample was 29.96 (Figure 76), meaning that it contained less molecules than required for sequencing - the Minimal Cp required for this library was calculated to be 26.52. The difference was 3.44 cycles (29.96 - 26.52). Therefore, the DSsample and also the MDSsample (in order to apply the same method to the both samples) were further enriched with PCR using the emPCR primers in 4 cycles, as explained in details in the protocol section 11.12. In order to avoid amplification bias, the samples were aliquoted in separate PCR tubes, which were pooled afterwards. Some remaining primers were purified by magnetic beads and again quantified by qPCR. The Cp of the DSsample has

decreased to 25.97 (Figure 76), meaning that the concentration has increased. If the Cp of the DSsample was 25.97, the number of molecules per $\mu$l can be calculated by the following equation:

$$\text{ssDNA molecules}/\mu\text{l} = 10^{\left(\frac{sample\ \ Cp\ -\ Point\ \ 0}{Slope}\right)} \times 2 = 10^{\left(\frac{25.97\ -\ 36.63}{(-3.08)}\right)} \times 2 = 5{,}781.88$$

The following example shows the calculation of volume of sample needed for SV-emPCR, for obtaining exactly 5-15 % bead enrichment for 170,000 beads corresponding to one of the two samples loaded on a 1/8 PTP. The emPCR was prepared with the Small Volume emPCR kit (Roche Applied-Science, Ref. 05618444001) and later sequenced using a GS FLX Titanium Sequencing XLR70 Kit (Roche Applied Science, Ref. 5233526001).

$$\text{Volume of the sample for emPCR} = \frac{Number\ \ of\ \ beads\ \ required\ \ per\ \ sample}{ssDNA\ \ molecules\ \ /\ \ \mu l} = \frac{170{,}000}{5{,}781.88} = 29{,}40\ \mu\text{l}$$

The following equation shows the calculation of the actual DNA amount loaded on the PTP plate:

$$\text{Concentration fg}/\mu l =$$

$$= \frac{ssDNA\ \ molecules/\mu l\ \times\ ssDNA/ddDNA\ \times\ library\ \ length\ \times\ ng/gf\ \times\ average\ \ weight\ \ of\ \ a\ \ base\ \ pair}{Avogadro\ \ constant} =$$

$$= \frac{5{,}781.88\ \ \times\ 2\ \times\ 400\ \times\ 10^{15}\ \times\ 650}{6.023\times10^{23}} = 4.9\ \text{fg}\ /\ \mu\text{l}$$

### 6.3.3 Sequence analysis

The obtained sequences were filtered and trimmed by quality. They were also checked for the presence of Y adaptors in the 3' end using the Blast program (Altschul et al., 1990) using a match e-value below $10^{-3}$. Thus, eventual adaptor sequences were trimmed out using the Biostrings v.2.11 package (Pages et al., 2014) written in the R programming language (R Development Core Team, 2008), as described in the programming script section 12.3. Low complexity reads (entropy < 70), low quality reads (< 25), short reads (< 50bp) and erroneous reads (> 5 % N bases) were removed using PRINSEQ (Schmieder and Edwards, 2011), shown in details in the script section 12.6. The bioinformatics downstream analysis pipeline is shown in Figure 77.

Reads from both experiments were mapped against the genome of *E. coli* K12 (gi:49175990) using SSAHA 2.5.4 (Ning et al., 2001) with the following command settings:

```
1 $ssaha2 -output sam -kmer 13 -skip 1 -seeds 2 -score 30 -cmatch 10 -ckmer 10 Ecoli.fna
    sample.fasta > sample.sam
```

The .sam file was converted to .bam file by samtools program (Li et al., 2009) by the commands shown in the programming script section 12.5. From the produced .bam file, the coverage was obtained by applying the R packages Rsamtools (Li et al., 2009), ShortRead and Chipseq (Morgan et al., 2009; Sarkar et al., 2015) as shown in the programming section 12.9.

The distribution of coverage differences between MDAsample and DSsample was checked using Cramer von Mises test with the CvM2SL2Test R package (Xiao et al., 2006) and also the normality of the coverage and the differences between coverage distributions among both sequencing methods was tested by subsampling the datasets 100 times 1000 reads each.

Reads that did not match *E. coli* were aligned using NCBI-blast against the "nr" database using the Megablast algorithm. The presence of read clusters (duplicated reads) was explored using CD-HIT software on a range of stringency values (Li and Godzik, 2006) changing the minimal length similarity (-s) and sequence identity threshold (-c) from 99 to 75 by the following command:

```
$ cd-hit -i sample.fasta -o sample-cd-hit99 -c 0.99 -s 0.99
```

In order to examine the origin of reads not matching any "nr" database entry, a hexamer distribution analysis was carried out by applying the Cramer von Mises test (Xiao et al., 2006). Hexamer distribution of unassigned reads generated by DSsample and MDAsample was compared with the hexamer distributions of complete genomes chosen from best matches of non-*E. coli* reads. As a null distribution, an artificial genome based on an average purine-pyrimidine ratio of 0.5 was constructed, and the hexamer distribution for that genome was calculated. Hexamer relative abundance statistics was estimated by applying the R package Vegan (Dixon, 2003). To assess similarities between the different groups, ANOVA was performed using the correlation eigenvalues and the different theoretical clusters. The robustness of hierarchical grouping among different groups was measured with a bootstrap analysis with 1,000 generations. Hierarchical clustering was performed using the R packages "hclust" and "pvclust" (Suzuki and Shimodaira, 2014).

Sequences were deposited in EMBL-EBI Sequence Read Archive (SRA) with study number ERP003418.

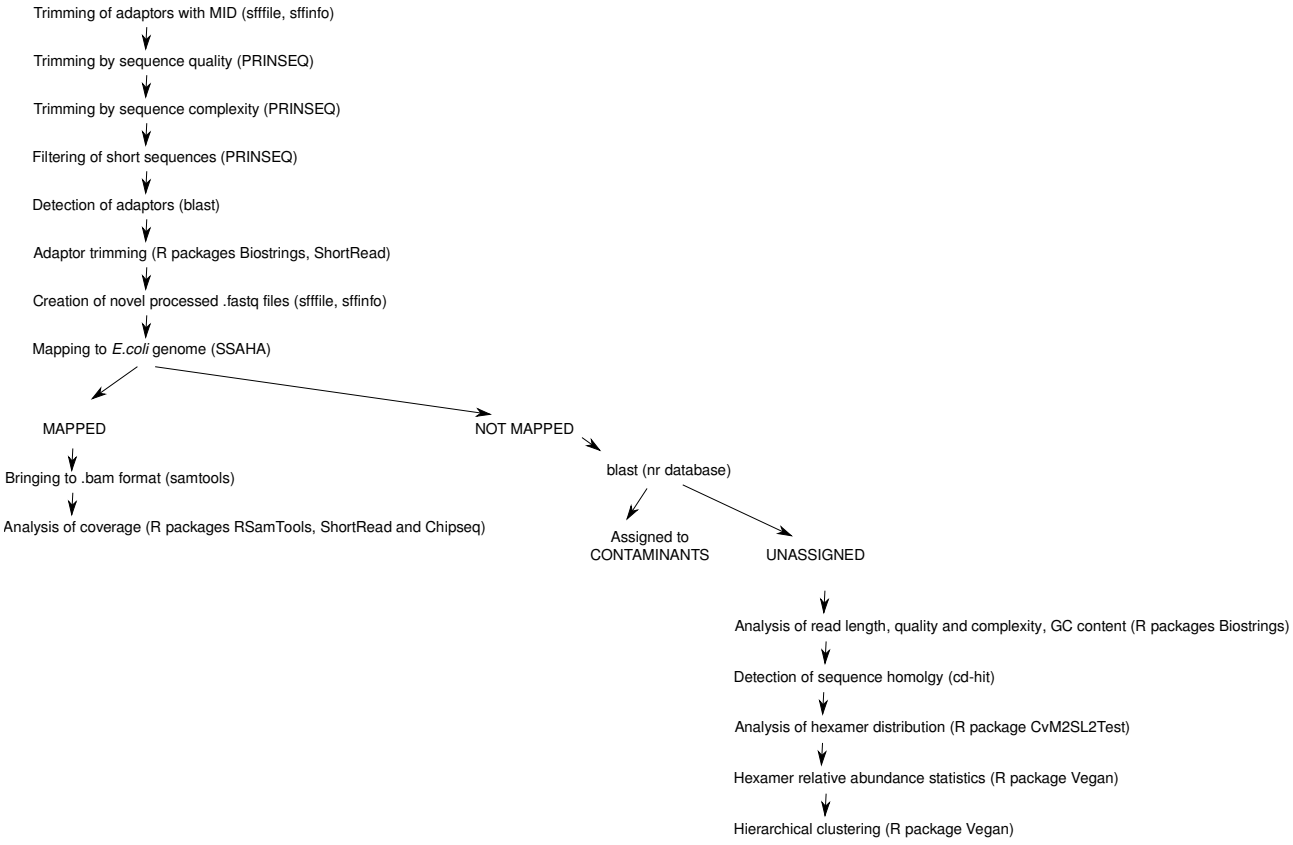


Figure 77: **The scheme showing bioinformatics analysis pipeline used in this work**

# 6.4 Results

## 6.4.1 *E. coli* genome mapping

Sequence quality assessment of the run1 had an output of 63,305 sequences (average quality score 36.05). Run2 sequencing did not work properly providing only 5,762 reads that passed quality assessment filters. A sequencing overview after quality assessment is shown in Table 6. After pool splitting by MIDs and dataset joining, the two methods resulted in 20,927 and 48,140 for DSsample and MDAsample, respectively. A significant decrease in GC content in the MDAsample (46.10 %) compared to the DSsample (48.74 %, t-test, p-value = 0.0021) was observed.

Table 6: **Sequencing results of MDAsample and DSsample in two runs.**

| | | **Direct sequencing** | **Multiple displacement amplification** |
|---|---|---|---|
| **Total number of reads** | Run1 | 16,758 | 46,547 |
| | Run2 | 4,169 | 1,593 |
| **Total Mbp** | Run1 | 3,853,532 | 12,891,425 |
| | Run2 | 582,005 | 253,376 |
| **Average read length** | Run1 | 229.95 ± 137.26 | 276.96 ± 165.51 |
| | Run2 | 139.60 ± 89.85 | 159.06 ± 111.82 |
| **Average read quality** | Run1 | 36.18 ± 3.48 | 35.91 ± 3.52 |
| | Run2 | 31.12 ± 3.41 | 30.84 ± 3.41 |
| **GC content ( %)** | Run1 | 48.94 | 46.05 |
| | Run2 | 48.54 | 46.15 |
| **Theoretical *E. coli* coverage of all processed reads** | Run1+ Run2 | 0.96 | 2.83 |
| **Theoretical *E. coli* coverage of all reads mapped to *E. coli*** | Run1+ Run2 | 0.77 | 0.07 |
| **Actual obtained *E. coli* coverage** | Run1+ Run2 | 0.76 | 0.05 |

Although there were three times more sequences in the MDAsample than in the DSsample, both methodologies were theoretically sufficient to cover the whole *E. coli* genome (Table 6). However, the DSsample covered a greater part of the reference genome (47.43 %) than the MDAsample (2.45 %). Moreover, only 2.10 % of the sequences of the MDAsample matched the *E. coli* genome, whereas this was 80.59 % for DSsample (Figure 78). The genome coverage associated with the MDAsample was characterized by peaks of overrepresented regions up to 121 × with an average coverage of 0.05 ×; by contrast, the DSsample showed a maximum coverage of 15 × but followed a uniform distribution with an average value of 0.76

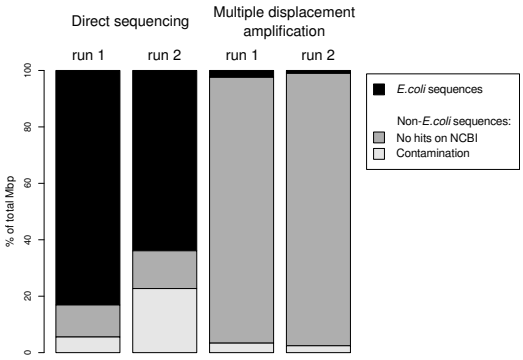


Figure 78: ***E. coli* genome mapping and blast to NCBI database**

×, fifteen times higher than the average coverage of the MDAsample (Figure 79). The coverage distributions obtained with both methods were significantly different (one way Kruskal-Wallis test, p-value = 0.0017).

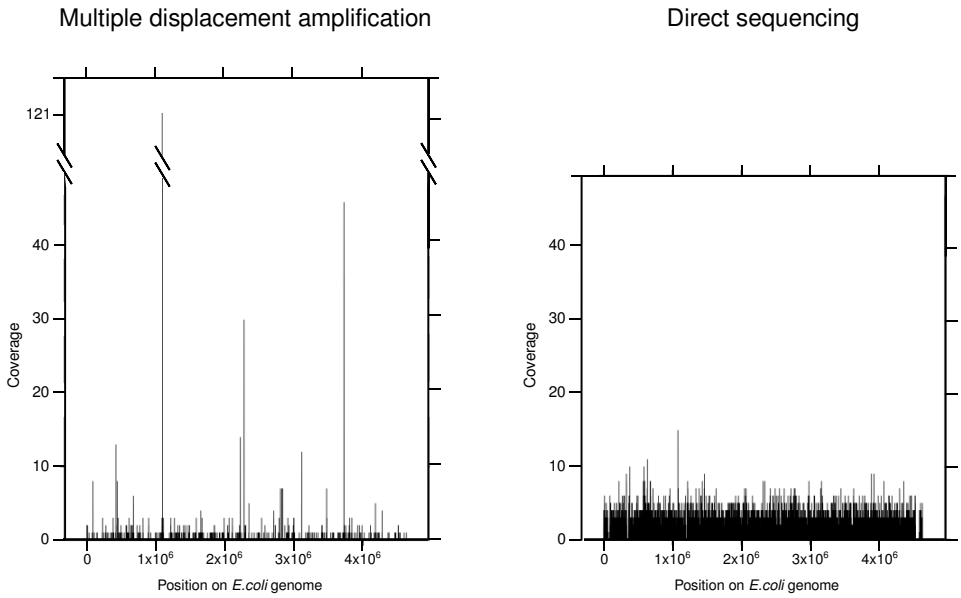


Figure 79: **Distribution of coverage throughout the *E. coli* genome.** The comparison of the genome coverage obtained by MDAsample and DSsample

## 6.4.2 Analysis of unassigned reads

1,460 reads (6.98 % of total Mbp) from the DSsample and 1,423 reads (2.96 % of total Mbp) of MDAsample datasets did not map to the *E. coli* genome but to other species in "nr" database (Figure 78). Approximately one third of these sequences were identified as human and the rest were assigned to other bacteria, mainly *Proteobacteria*. Moreover, in both samples reads, which were not assignable to any organism present in the "nr" database, were also found. More precisely, 94.2 and 96.54 % of the MDAsample and 11.35 and 13.38 % of the DSsample were unassigned processed Mbp in their respective runs 1 and 2 (Figure 78). It is worth noticing that the unclassified reads showed the same quality and length ranges as the *E. coli*-mapped reads.

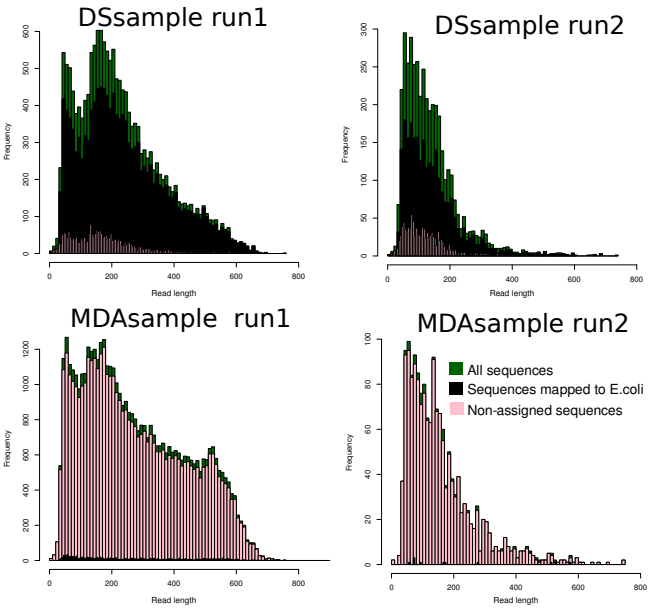


Figure 80: **Read length distributions**

The length, GC content, read quality and complexity was checked in order to investigate the origin of unassigned reads. The results summarized in Table 7 indicate that run 2 performed worse than run 1, but finally both runs confirmed the same results.

The difference between MDAsample and DSsample datasets can be observed here only by lower GC content in the MDAsample. Regarding GC content, it was lower in the unassigned reads of MDAsample (46.1 %) than in the the unassigned reads of DSsample (49.47 %). There was no difference in the read length of the assigned and the unassigned sequences of MDAsample and DSsample (Figure 80).

Table 7: **Sequence quality of MDAsample and DSsample**

| | | Total processed reads | *E.coli* mapped reads | Unassigned reads |
|---|---|---|---|---|
| | | **Median read length** | | |
| **MDAsample** | Run1 | 245.00 | 225.00 | 244.00 |
| | Run2 | 131.00 | 169.00 | 131.00 |
| **DSsample** | Run1 | 203.00 | 214.00 | 159.00 |
| | Run2 | 119.00 | 123.00 | 108.00 |
| | | **GC content** | | |
| **MDAsample** | Run1 | 46.05 | 48.71 | 46.02 |
| | Run2 | 46.15 | 44.96 | 46.19 |
| **DSsample** | Run1 | 48.94 | 48.95 | 49.57 |
| | Run2 | 48.54 | 48.89 | 49.36 |
| | | **Read quality** | | |
| **MDAsample** | Run1 | 35.92 | 35.45 | 35.94 |
| | Run2 | 30.84 | 30.69 | 30.84 |
| **DSsample** | Run1 | 36.18 | 36.21 | 35.90 |
| | Run2 | 31.12 | 31.10 | 31.19 |
| | | **Read complexity** | | |
| **MDAsample** | Run1 | 3.85 | 3.83 | 3.85 |
| | Run2 | 3.73 | 3.77 | 3.73 |
| **DSsample** | Run1 | 3.83 | 3.85 | 3.72 |
| | Run2 | 3.70 | 3.73 | 3.62 |

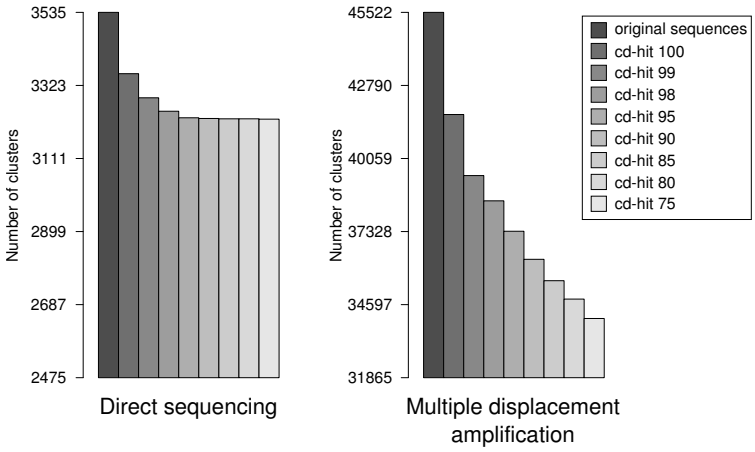


Figure 81: **Clustering of unclassified reads on different sequence identity levels (from 100 to 75 %)**

When unassigned reads from MDAsample were grouped by similarity, an increasing size of clusters was observed, along with a decrease in similarity stringency (from 100 % similarity down to 70 %). On the contrary, the similarity range of unassigned reads of DSsample was not affected by cluster size. Figure 81 shows that the MDAsample was characterized by abrupt clustering, which demonstrates that the MDAsample reads originated by amplification; however, a high number of clusters was still present at 75 % identity level, indicating their uniqueness.

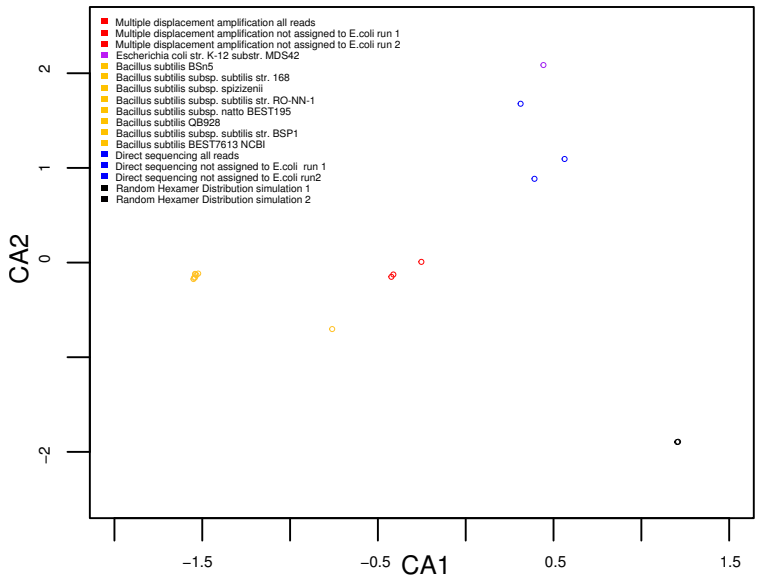


Figure 82: **Correspondence analysis of the hexamer relative abundances tested with *E. coli* and *B. subtilis***

In order to explain the origin of the unassigned reads, the distributions of hexamers in the MDA and the direct sequencing datasets was explored. The Figure 82 shows the comparison of *E. coli*, *B. subtilis* k-mer distributions versus the random hexamer distribution and the distribution of the unassigned reads of MDAsample and DSsample. The taxonomic allocation of the unassigned reads in both methods was obtained using the eigenvalue coordinates for the k-mer relative abundances for each dataset. Unassigned read hexamer distributions of MDAsample as well as DSsample were significantly different from the normal distribution of the artificial genome based on an average purine-pyrimidine ratio of 0.5 (Cramer von Mises test, p-values = $2.99\times10^{-1}$ and $6.69 \times 10^{-8}$, respectively.

In the next step, the analysis was extended to other selected genomes from the public repositories shown in Figure 83, such as: *Agrobacterium radiobacter* K84, *Bradyrhizobium japonicum* USDA 6, *Clostridium perfringens* ATCC 13124, *Delftia acidovorans* SPH-1, *Enterococcus faecium* Aus0004, *Propionibacterium acnes* TypeIA2, *Pseudomonas fluorescens* A506, *Ralstonia pickettii* 12D, *Rhodococcus erythropolis* PR4, *Staphylococcus epidermidis* RP62A and *Stenotrophomonas maltophilia* JV3. These species were selected because they appeared in the list of probable contaminants in samples sequenced in this study by "blastn" analysis on NCBI. In addition to *Bacillus subtilis* which is the origin of $\phi$-polymerase, other species of *Bacillus* were put into analysis: *Bacillus weihenstephanensis* KBAB4 and *Bacillus subtilis* BEST7613. Two substrains of *E. coli* K12 (MG1655 and MDS42) were included, as well. The calculated hexamer distribution of reads from other selected genomes displayed a gamma distribution of hexamers similar to the one observed in the two tested library preparation methods (Cramer von Mises test, p-values ranging from 0.16 to 0.51, depending on the genome). In the Figure 83 is

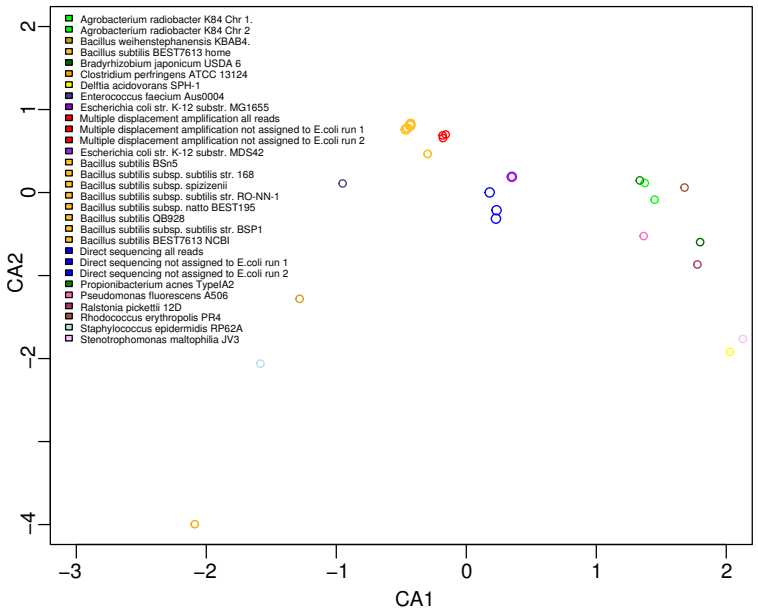


Figure 83: **Correspondence analysis of the hexamer relative abundances iwth *E. coli*, *B. subtilis* and contaminating species**

possible to observe that the MDAsample is close to the *Bacillus subtilis* cluster, while DSsample is close to *E. coli* cluster.

In the next step of analysis, the hierarchical clustering with bootstrap reconciliation of hexamer relative abundance profiles showed that all reads coming from the DSsample were adjacent to the *E. coli* hexamer profiles. Unassigned reads clustered together on the most likely conformation clustering. However, it was not statistically supported by the bootstrap analysis (bootstrap support = 55 %). On the other hand, the distribution of MDAsample unassigned reads was statistically far from *E. coli* distribution, but close to *Bacillus subtilis* genomes (Bootstrap support = 100 %, Figure 84).

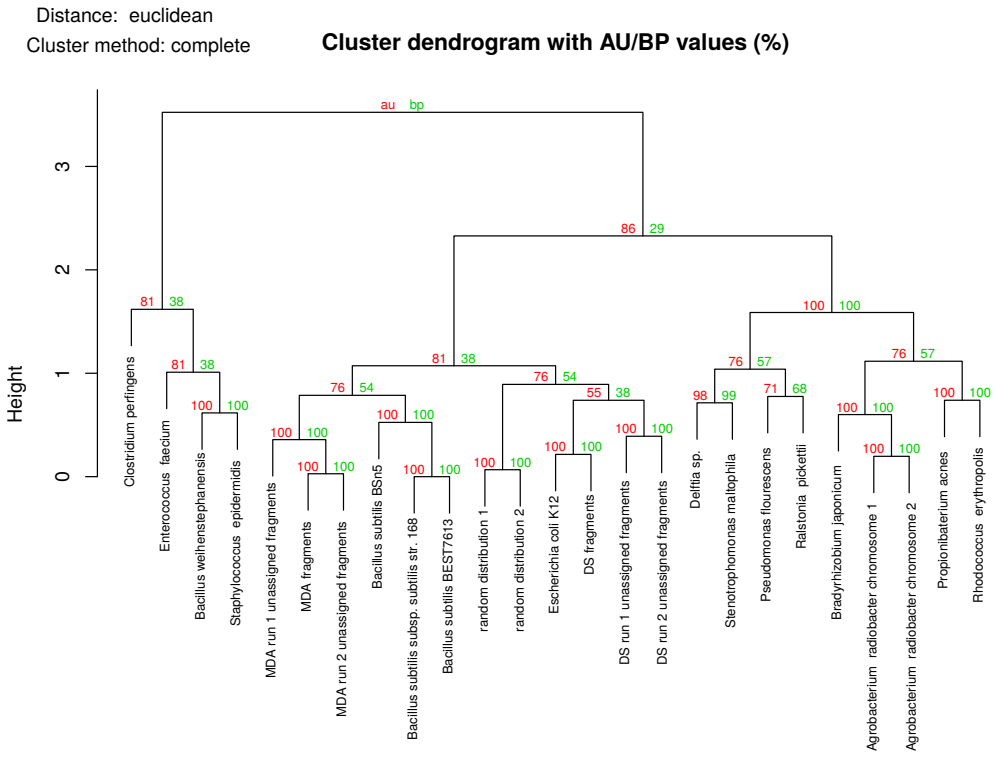


Figure 84: **Clustering analysis of the hexamer abundance distribution**

# 6.5 Discussion

In the standard FLX+ Rapid Shotgun Library preparation protocol, 1 $\mu$g of input DNA is needed. The prepared library must contain $8.4\times10^9$ dsDNA molecules (6,340 pg). It means that losing up to 99.36 % of the initial amount of DNA is permitted. Furthermore, the final amount of the prepared library is diluted up to $10^7$ molecules (7.6 pg), which is the recommended concentration for starting with emPCR titration (Figure 85). This requirement results in an obstacle for sequencing of samples with low DNA content. To overcome this drawback, the most widely used method has been isothermal MDA. However, MDA entails a number of serious problems, which have been reported previously.

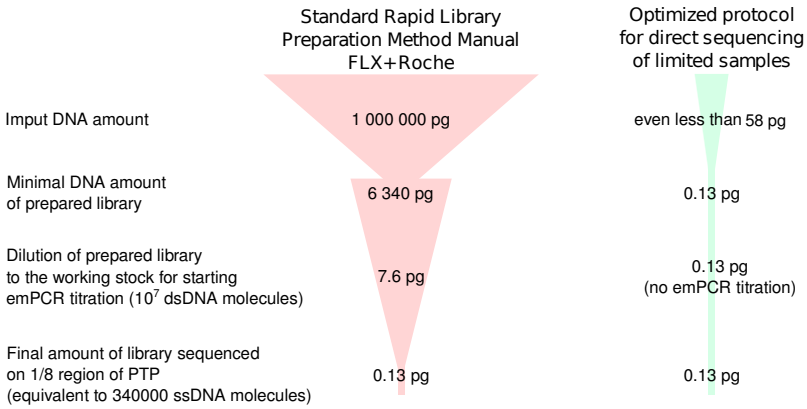


Figure 85: **Required and real amounts of DNA in the sequencing library preparation protocol**

Several authors have already suggested that the next-generation sequencing library preparation protocols can be started with a lower amount of DNA than is the amount required by the standard protocols. They stated that the true limiting factor, in the case of 454 sequencing, is to reach the number of enriched beads required by the platform (Meyer et al., 2008; Zheng et al., 2010; White et al., 2009; Buehler et al., 2010; Lennon et al., 2010). Zheng et al. (2010) in their experiments with low concentrated samples sequencing worked with diluted highly concentrated samples. This work presents a work-flow without diluting a highly concentrated original DNA sample, that the low number is cells is used for the sample prepration including the DNA extration. The amount of size-selected sonicated fragments in this work was definitely lower than 54 pg (theoretically, the DNA content of 10,000 *E. coli* cells), because losses during DNA extraction occur.

This work demonstrates that it is possible to prepare a 454 shotgun library starting with the amount of DNA which is so low that it approximates to the minimal number of molecules required to fill the target PTP region, in this case 340,000 enriched beads for 1/8 PTP plate, equivalent to 0.13 pg of 700 bp fragments (Figure 85). The successful sequencing run was achieved by modification of the steps of the library preparation protocol. Rather than fragmenting the sample in a nebulizer, the samples in this study were sonicated in the same tube in which DNA extraction was performed, thus also avoiding losses due to sample transfer. Small fragments were removed exclusively with AMPure magnetic beads, no purification columns were used. Similar changes have been reported as good alternatives of the standard protocol and they can be used at a large scale (Lennon et al., 2010).

Low concentrated libraries must be appropriately quantified. Minor Groove Binding (MGB) and Locked Nucleic Acid (LNA) probes are surely some of the most sensitive DNA quantification systems (Buh Gasparic et al., 2010). Y adaptors with MGB-Taqman probes designed by Zheng and collaborators were used, because they enable to quantify by qPCR the exact number of amplificable molecules of these minimal libraries (Zheng et al., 2011). Once the exact number of amplificable molecules is calculated, the user can proceed directly to the proper emPCR without the need to perform the previous emPCR titration step and so, a large part of the

library DNA can be saved (Meyer et al., 2008; Zheng et al., 2011; Lennon et al., 2010).

In this work, the performance of the direct sequencing was compared with the widely applied MDA approach used for samples with small amounts of DNA. DSsample provided homogeneous genome coverage throughout most of the genome. In contrast, MDAsample generated regions with a genome coverage as high as 121 ×, leaving almost all of it (97.55 %) uncovered. This observation is in accordance with reports by other authors using MDA, who estimated that more than 40 % of the sequence could be missing, and that the heterogeneous coverage distribution in MDA frequently leads to failure, without being able to complete the target genome by further sequencing efforts either (Marcy et al., 2007b; Zhang et al., 2006; Rodrigue et al., 2009; Woyke et al., 2011). The number of unassigned sequences was considerably lower in DSsample (12.84 %) than in MDAsample (up to 94.24 %). The commercially available MDA reagents have frequently been reported as being contaminated by unwanted DNA. Several authors dealing with MDA contamination concluded that contamination did not come from human DNA or other target genomes, but could originate from hexamer concatenation or from the enzyme preparation process, including host bacteria *Bacillus subtilis* (Spits et al., 2006a; Bredel et al., 2005; Woyke et al., 2011; Jiang et al., 2005; Le Caignec et al., 2006; Iwamoto et al., 2007).

The common question of scientists willing to perform direct sequencing of DNA from bacterial cells is which is the lowest number of cells needed for sequencing ($5^{th}$ Annual Next Generation Sequencing Congress and Single Cell Analysis Congress, London, UK in 2013 and the Single Cell Analysis Conference, Cambridge (MA), USA in 2014). The typical bacterial cell containing 5-16 fg of DNA would never provide sufficient number of molecules for high-throughput sequencing (Huang et al., 2011). It is not possible to recover the complete genome of a single-cell genome without WGA on platforms sequencing fragmented DNA (e.g. Illumina, 454, Solid, Ion Torrent), because when a single-cell genome is sheared into fragments, the shortest fragments must be removed in order to prevent sequencing run failure; it means that many fragments of a single non-enriched genome would be never sequenced. However, third generation sequencing platforms reading single DNA molecules may be used for whole genome sequencing of single-cells not enriched by WGA (Coupland et al., 2012). Due to large limitations of the WGA enrichments, sequencing on the third generation platforms may be promising for single-cell sequencing.

## 6.6 Conclusions

In this work the direct sequencing method was used on the 454 Titanium platform starting from the minimal amounts of input DNA without previous whole genome amplification. This approach could replace MDA in many genome sequencing projects, even in studying previously uncharacterized organisms. Direct sequencing provides unbiased, reliable and reproducible genetic information from any sample with a minimum amount of starting material. In contrast to MDA, which is widely applied to projects dealing with limited amounts of DNA, direct sequencing provides a homogeneous distribution of reads mapped to a reference genome, avoiding low efficiency, chimera formation and amplification problems previously described in MDA.

Direct sequencing is a candidate to replace MDA in most projects in which cells obtained by FACS are sequenced. The direct sequencing method reported in this work is estimated to lower the cost of library preparation and to yield the maximum genetic information while simultaneously reducing sequencing efforts.

Chapter 7

# Viral metagenomics directed by flow cytometry

**Associated original articles:**

Džunková, M., D'Auria, G., Moya, A. (2015) Direct sequencing of human gut virome fractions obtained by flow cytometry. Frontiers in Microbiology 6: 955

MD and GD contributed equally to the work

# 7.1 Introduction

## 7.1.1 Difficulties in shotgun sequencing of viromes

It is estimated that the human gut contains $10^{12}$ of viral particles, formed by approximately 1,000 viral genotypes. About 80 % of them are yet unknown viruses, because they cannot be cultivated (Edwards and Rohwer, 2005). The high-throughput shotgun sequencing opened new possibilities for viral diversity exploration without the need of virus cultivation. The genetic information of novel unculturable viruses may explain viral evolution, disease epidemiology and help to develop effective medical treatment (Ladner et al., 2014; Edwards and Rohwer, 2005). However, the discovery of novel viruses by high-throughput shotgun sequencing by current sequencing platforms encounters several difficulties. The most important are:

- contamination by human or bacterial DNA,
- lack of reference genomes in viral databases,
- low amount of extracted DNA.

**Contamination by human or bacterial DNA**

For virome sequencing, the DNA must be completely free of any contaminants. As the genomes of bacteria or humans outnumber the genome size of an average virus hundreds of times, only one contaminating bacterial or human cell could contaminate the whole viral DNA sample. Despite rigorous efforts to eliminate non-viral particles in environmental samples by filtering or ultracentrifugation in CsCl gradients (Thurber et al., 2009), the majority of assigned sequences still match bacteria and eukaryotic DNA, usually forming up to 70 % of total assigned DNA sequences (Breitbart et al., 2003).

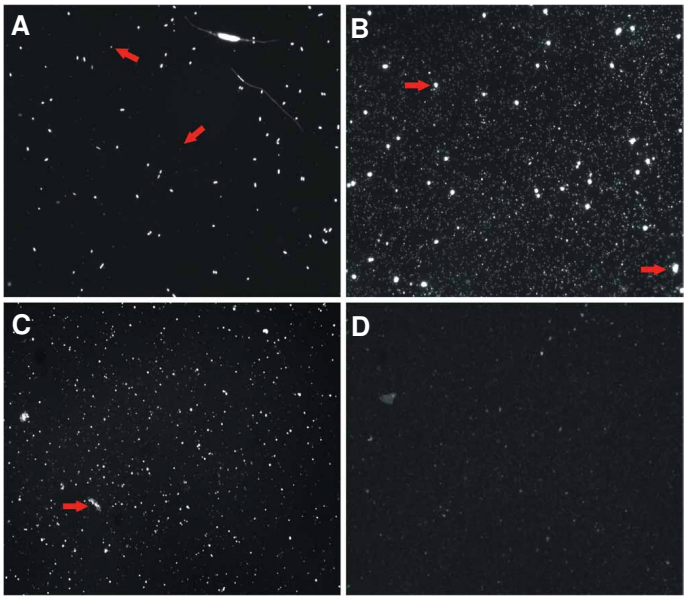


Figure 86: **Fluorescent microscopy fo viral samples.** **Panel A:** Seawater sample with characteristic pinpoint fluorescence. **Panel B:** Concentrated virions and microbial cells (arrow) from 100-kDa tangential-flow filtration retentate. **Panel C:** Virus concentrate after CsCl ultracentrifugation containing contaminating eukaryotic and microbial debris (arrow). **Panel D:** Fluorescence image showing the characteristic milky appearance of a filter overloaded with virus particles. All images were taken at 600x magnification with an oil immersion objective. Author: Thurber et al. (2009)

The purity of a virome should be checked by an epifluorescent microscope (Thurber et al., 2009), as shown in the Figure 86. In non-filtered, non-concentrated sample (Figure 86, panel A) viruses appear as pinpoints of light on unconcentrated water samples. Nuclei and microbial cells are much brighter and larger (Figure

86, panels B and C). These cells appear even after rigorous filtration. If some contaminating particles are still present, the purification might be repeated.

A simple visualization of a viral sample by fluorescent microscopy does not seem to be sufficient for concluding that the sample is free of eukaryotic cells. For example, Breitbart et al. (2003) did not observe any contaminating particles in their fluorescently stained samples of fecal viruses, however, 60 % of assigned sequences belonged to bacteria or eukaryotic organisms.

**Lack of reference genomes in viral databases**

In 2002 Breitbart et al. (2002) published a report about the first marine virome from which approximately 65 % of sequences had no significant similarity to any sequence in the GenBank non-redundant database (Pruitt et al., 2007). However, despite the fact that GenBank database doubled in size in two following years, repeated analyses revealed that most of the viral sequences were still unique (Breitbart et al., 2004) (Figure 87). This problem persists and the newly published viromes from different environments consist of 65-80 % sequences that yield no significant matches against public sequence databases (Vazquez Castellanos et al., 2014). The explanation for this might be the fact that the sequence databases are still incomplete or biased towards the most studied human viruses which can be isolated by culture methods (Venter et al., 2004).

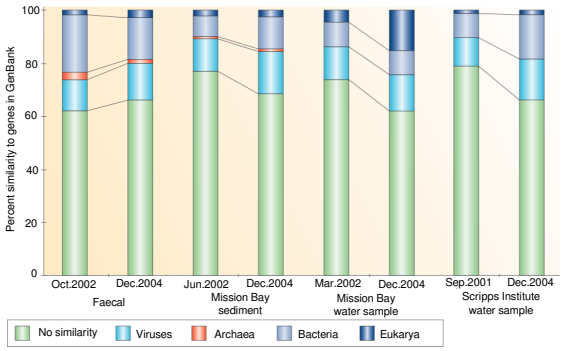


Figure 87: **Comparison of viral metagenomic libraries to the GenBank "nr" database**. Author: Edwards and Rohwer (2005)

However, the whole viral genomes can be recovered from the shotgun sequences, if enormous sequencing efforts are applied. By joining sequence data from previously published viromes, a previously unidentified bacteriophage present in the majority of published human fecal metagenomes was discovered (Dutilh et al., 2014). Its genome encodes proteins that do not have matches to any known sequences in the database, which is why it was not detected before. However, this approach is not applicable for most of studies, where smaller number of sequences or shorter sequences are analyzed.

**Low amount of extracted DNA**

Another limitation in virus discovery is that the high-throughput sequencing platforms require tens of nanograms or even micrograms of DNA, however the DNA yields in virus extractions are usually below 1 ng (Duhaime et al., 2012; Thurber et al., 2009). This requirement resulted to the increasing trend in enrichment of the extracted DNA before sequencing by WGA (Ambrose and Clewley, 2006; Solonenko et al., 2013; Stang et al., 2005; Breitbart et al., 2003, 2008; Pérez-Brocal et al., 2013).

The research group from San Diego State University (M. Breitbart and F. Rohwer as principal authors) used linker-amplified shotgun libraries approach for enrichment of DNA in virome studies very often in their publications (Breitbart et al., 2002, 2003; Edwards and Rohwer, 2005; Breitbart et al., 2004). Amplification with degenerated primers was used by Stang et al. (2005) in the study where cell infected by coxsackievirus B3 and murine adenovirus type 1 were tested. Synthetization of custom degenerated primers for random amplification was the ancestor of WGA methods which are being extensively commercialized and in the

present time is used extensively in virome sequencing (Breitbart et al., 2008; Pérez-Brocal et al., 2013). Another authors prefer to use GenomiPhi (GE Healthcare Life Sciences, Ref. 25-6601-24) which employs rolling circle amplification using phi29 polymerase (Dean et al., 2001; Fire and Xu, 1995). WGA methods, especially those based on rolling circle amplification using phi29, are prone to develop chimeras, GC-content bias and amplification of non-target DNA contamination (Pinard et al., 2006; Lasken and Stockwell, 2007). Moreover, GenomiPhi might also over-amplify certain virus types. Over-amplification of certain regions of viral genomes by GenomiPhi is replicable, so neither the pooling of sample replicates helps to eliminate this bias (Marine et al., 2014).

Nevertheless, the amplification of DNA samples prior to the sequencing is actually not necessary, as the true limiting factor for the sequencing is not the input DNA amount for the sequencing library preparation, but the number of molecules to be loaded on a sequencing plate, as already demonstrated in Chapter 6.

### 7.1.2 FACS of viruses

Previous studies used FC with viral samples coming mainly from water or already known cultivated phages (Chen et al., 2001; Allen et al., 2011; Brussaard, 2004; Li et al., 2010; Brown et al., 2015). However, human gut is a very complex environment, so no FACS of viral particles has been performed yet.

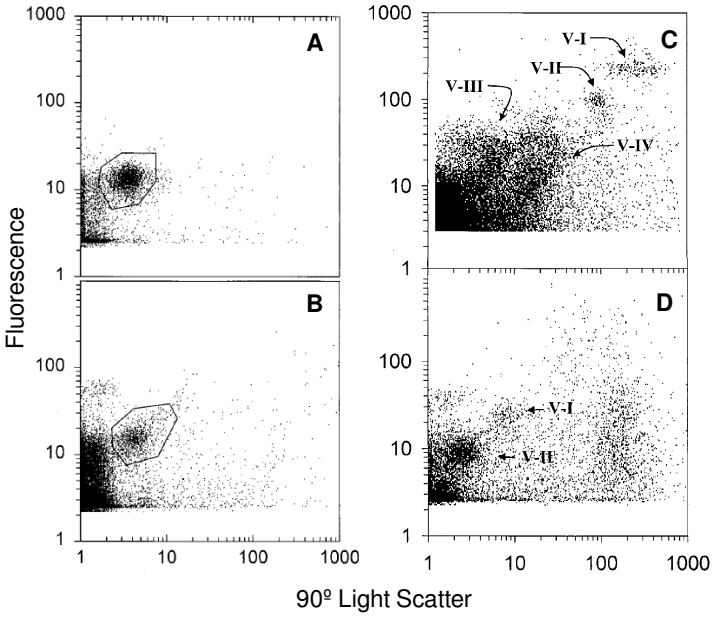


Figure 88: **FC bi-plots of marine viruses. Panel A:** Purified cyanophage P1. **Panel B:** purified cyanophage P49. **Panel C:** Lake Erie sample. **Panel D:** Georgia coastal sample. Author: Chen et al. (2001)

FC has been used for counting viruses from the aquatic communities and activated sludge (Chen et al., 2001; Brussaard, 2004; Li et al., 2010; Brown et al., 2015). However, the viral particles in these studies have not been separated by FACS, neither sequenced. For example, Chen et al. (2001) purified cyanophages P1 and P49 (*Myoviridae*) from marine samples. These phages were stained by SYBR Gold and visualized on FC bi-plots, shown in Figure 88. These two bacteriophages were of different sizes, as their bi-plot showing complexity and fluorescence slightly differ. The water environments (lake or sea samples) contain phages of different sizes, so in the FC bi-plots of water communities several populations of viruses of different sizes can be observed.

Cultured Lambda phages have been separated by FACS in the study of Allen et al. (2011) (Figure 89), enriched by MDA and sequenced. They observed non-uniform coverage variable from 0 × to 2,000 ×. In addition, 38.5 % of the obtained reads could not be mapped to the genome of Lambda phage. They compared these unmapped reads to NCBI "nr" database and found that the contamination consisted from 41.84 % of unassigned reads, 33.71 % of *Pseudomonas*, followed by other bacterial species, such *E. coli*, *Xanthomonas*

*Ralstonia*, *Rhodobacter*, etc, as well as low number of matches to the human genome. This was a report of sequencing of a virus with known genomic sequence, so the exact amount of unmapped reads could be determined and eliminated. However, it is not possible to do this in the case of sequencing of novel unknown viruses, as no reference genome exist.

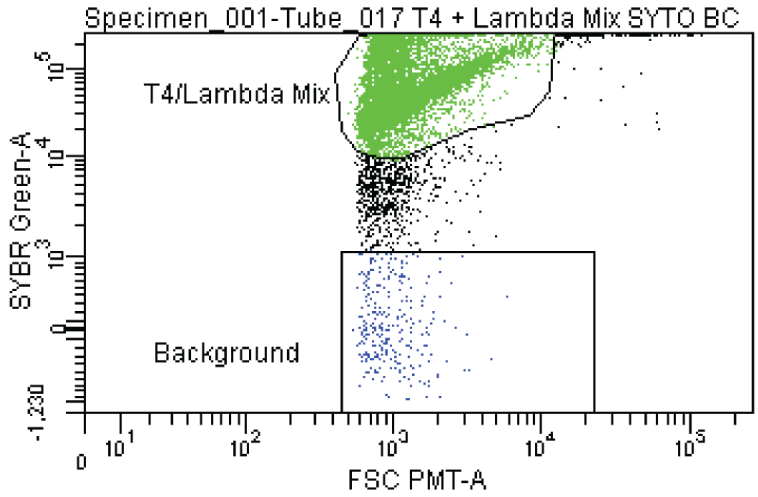


Figure 89: **Flow cytometric bi-plot showing SYBR-stained T4 and lambda phage mixture** Author: Allen et al. (2011)

## 7.2 Objectives

It is estimated that the human gut contain a large number of yet unknown viruses. Due to the lack of reference genomes in the databases and difficulties in sequencing of low DNA content samples, the sequence-based description of novel viruses from the human gut remains difficult.

The objective of the work is to approach the human gut virome by the use of a FC-based approach avoiding any WGA method. Moreover, in this chapter we propose a method for enhancing virome sequence assembly improving the viral sample preparation before sequencing. It is hypothesized that the viral metagenomes can be assembled more efficiently, if the virome samples is purified more deeply, thus human mitochondria and bacterial cells may be eliminated. Therefore, FACS was employed for more precise detection of viral particles.

The DNA will be extracted directly from separated viral samples containing few hundreds of particles. We overcome the DNA limitations obviously encountered when working with low amounts of DNA applying the protocol developed in the previous Chapter 6.

This work represents the first attempt to apply FACS for sorting of viral particles from such an extremely complex environment, as human fecal samples.

# 7.3 Methods

## 7.3.1 Viral sample preparation

**Preparation of phage control**

Three flasks with LB medium were prepared and were let to grow for 4 hours at 37 °C shaking at 250 rpm:

1. flask was inoculated with 200 $\mu$l of overnight culture of *E. coli* ER2738 (New England Biolabs, Ref. E4104S),
2. flask with the same overnight culture and with 1 $\mu$l of M13KE Phage (New England Biolabs, Ref. N0316S),
3. flask with LB was not inoculated as left as a negative control without any bacteria.

The cultures were transferred into 50 ml tubes and processed by the protocol described in the protocol section 11.8 for the fecal samples. The first part of the protocol is the removal of the bacterial pellet by centrifugation. After that, the supernatant is filtered through a series of filters with 5 $\mu$m, 0.8 $\mu$m, 0.45 $\mu$m and 0.2 $\mu$m pores. Filtered buffer TBS and LB medium were prepared as negative controls by the same method and the bacterial controls were the bacterial pellets (*E. coli* and *E. coli* infected by phage). Each sample was split into stained and unstained part. SYBR® Green I stain (Life Technologies, Ref. S-7563) was used for staining of particles containing DNA.

The samples were analyzed by Cytomics FC 500 (Beckman Coulter, Ref. 175487). The cytometer emission filter was 520/30 (FL1) obtaining emission for SYBR® Green I. The trigger was set on side-scatter. The samples containing stained bacterial pellet were used as a control to localize the events with the size of bacterial cells and phage M13KE control was used for detection of area corresponding to the viruses, shown in the Figure 90. FC bi-plots show that filtered culture medium LB and filtered *E. coli* not infected by phage did not contain any bacterial neither viral cells. The particles present in these negative controls have fluorescence equal to the unstained control, indicating that they represent electrical noise of the flow cytometer or are some organic aggregates. In contrast, phage and *E. coli* samples contain fluorescent particles.

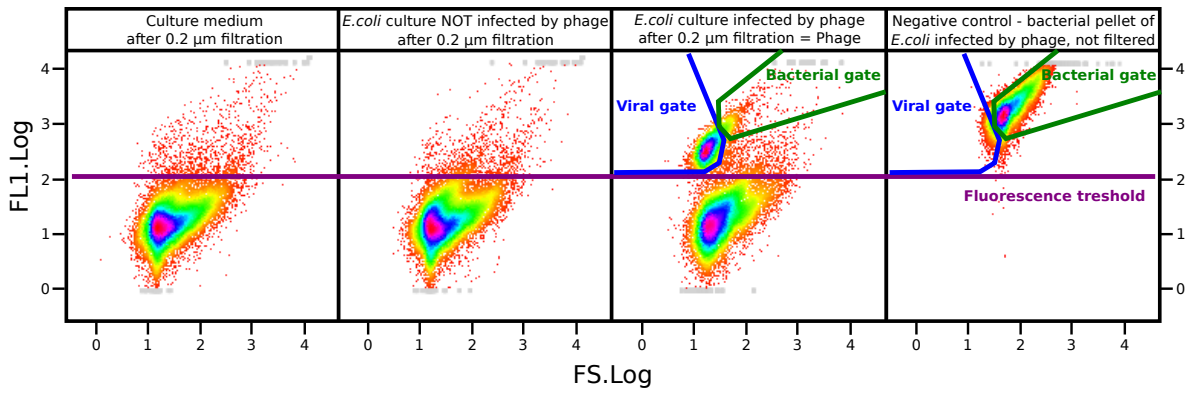


Figure 90: **FC biplots of culture of *E. coli* infected by bacteriophage M13KE.** The fluorescence threshold is set according to the unstained control

### Purification of the viral sample

The fecal sample used in this work was provided by a healthy volunteer. The study was approved by the institutional review board of Valencian Region Foundation for the Promotion of Health and Biomedical Research (FISABIO) - Public Health, and informed consent was obtained. The work-flow the the sample purification is shown in the Figure 91.

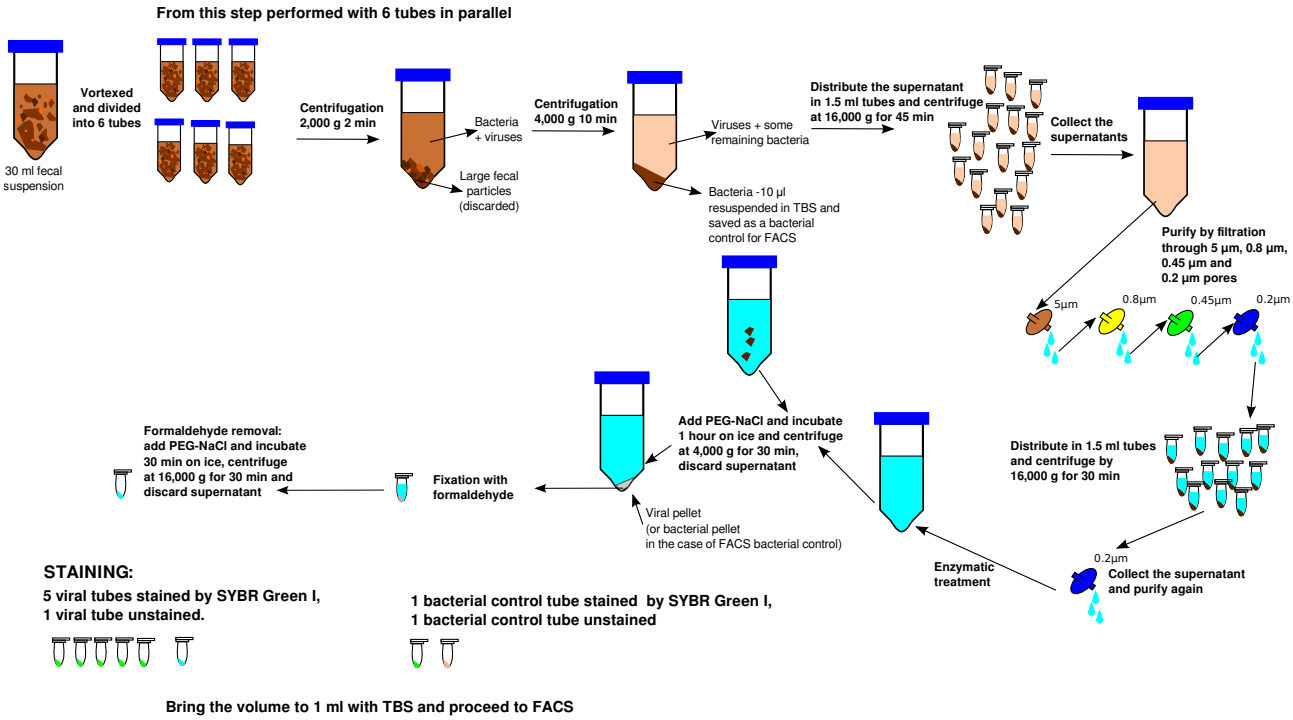


Figure 91: **Laboratory work-flow of fecal virome purification and staining for flow cytometry**

The samples were processed exactly as described in the protocol section 11.8. A small sample from each step of this protocol was kept for flow cytometry control analysis on Cytomics FC 500 (Beckman Coulter, Ref. 175487), which is shown in the Figure 92. Each of these control samples was split into halves and one part was stained with SYBR® Gold I stain (Life Technologies, Ref. S-7563).

The first gate was set according to the bacterial pellet. Figure 92 shows that the number of events in this gate is reducing after each filtration step. In contrast, the number of particles of viral size were increasing after filtration step. After the first 0.2 $\mu$m contained almost no particles with bacterial size. To ensure that no bacterial particles were present, the sample was centrifuged for 40 min in 1.5 ml tubes. After this centrifugation a small pellet of brown color was formed, however, the flow cytometry analysis showed that the pellet was not formed by living organisms, as no fluorescent particles of bacterial size were detected.

FACS was carried out using the MoFlo XDP Cell Sorter (Beckman Coulter, Ref. ML99030). The light sources were the Argon 488 nm (blue) laser (200 mW power) and the 635 nm (red) diode laser (250 mW power). The lasers were aligned using 10 $\mu$m Flow-Check beads (Beckman Coulter, Ref. 6605359) and 3 $\mu$m beads Flow Set (Beckman Coulter, Ref. 6607007).

The area of particles with the smallest size was selected, as shown in the Figure 93. They were named SSV-fraction (small size viruses fraction). The density of events in these area was so low that in order to sort out 314 particles of SSV-fraction (0.016 %), the FACS equipment had to analyze a total of 1,904,265 particles and

the duration of the sorting was 8 hours. The cells were sorted into autoclaved LoBind 1.5 ml tubes (Eppendorf, Ref. 0030 108.051).

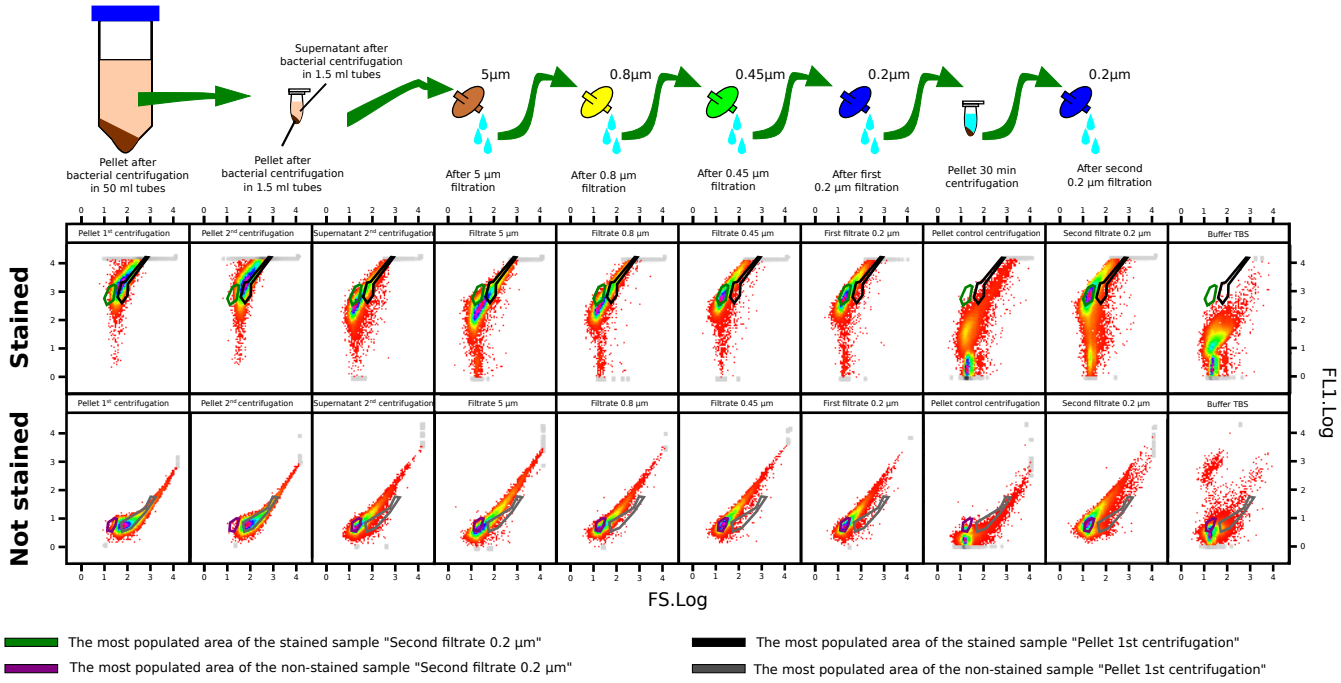


Figure 92: **FC biplots of each of step of virus purification protocol**

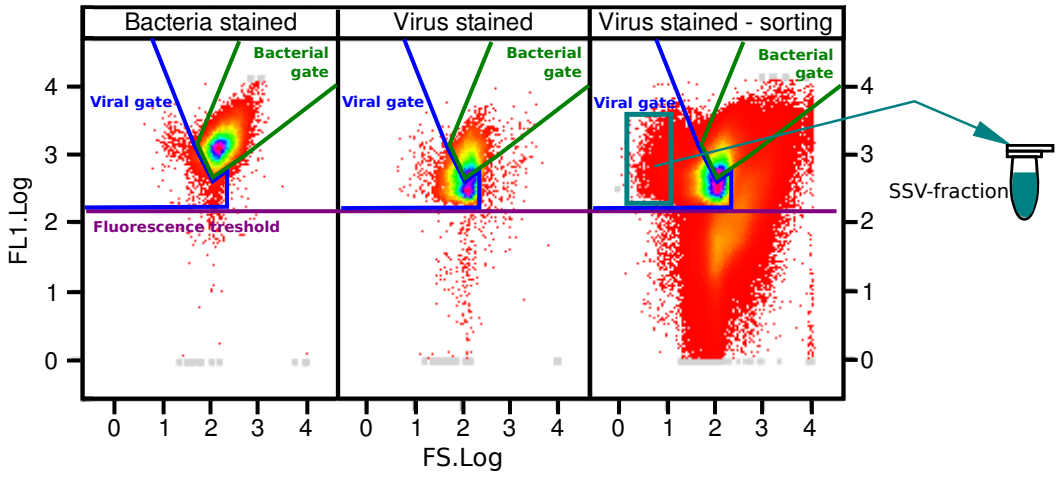


Figure 93: **FACS of the fecal sample**. The area of particles of the smallest size (SSV-fraction) was selected for the sorting

### DNA extraction and sequencing

DNA was extracted according to the protocol by Ausubel et al. (Ausubel et al., 1992) in sterile conditions as described in the protocol section 11.5. For the shotgun library preparation, the standard protocol of the manufacturer (Roche Applied Science) was replaced by the optimized protocol for limited DNA samples described in the protocol section 11.12 and explained in more details in Chapter 6. Shortly, the DNA was

fragmented by sonicator, DNA fragments shorter than 300 bp were removed by Agencourt AMPure Beads XP®(Beckman Coulter, Ref. A63880) and to the size-selected DNA fragments custom 454 adaptors were ligated. The remaining adaptors were removed by repeated purification by Agencourt AMPure Beads XP®. The adaptor Y5 adaptor was used for SSV-fraction library construction. The exact number of molecules present in the 454 shotgun library concentration was determined by qPCR by probes specific for custom "Y" 454 library adaptors, as described by Zheng et al. (2011), shown in details in the protocol section 11.10. The maximal Cp corresponding to the minimal concentration of a library was calculated to be 24.59 (Chapter 6). However, the Cp of the SSV-fraction library was 28.15, meaning that it contained 11,79 × less DNA (28.15 - 24.56 = 3.56; $2^{3.56}$ = 11.79). Therefore, it was amplified by a PCR with low number of cycles and the resulting Cp decreased to 23.79, meaning that the library concentration increased and it was 1.7 × higher than the minimal concentration required for sequencing on 1/8 of a 454 PTP region. The emPCR and sequencing with GS FLX Titanium Sequencing XLR70 Kit (Roche Applied Science, Ref. 05233526001) were performed by the standard protocols on 1/8 of the 454 PTP.

### 7.3.2 Data analysis

#### Sequence processing

The sequences were filtered and trimmed by quality and adaptors were removed by Roche's SFFINFO tool, permitting 3 errors, as shown in the programming section 12.3. Afterwards, the sequences were double-checked for the presence of Y adaptors in the 3' with Biostrings v.2.11 package (Pages et al., 2014) for R programming language (R Development Core Team, 2008), as also adaptors self-ligated dimers might have been sequenced, too. Low complexity reads (entropy < 70), low quality reads (< 25), short reads (< 50bp) and erroneous reads (> 5 % N bases) were removed using PRINSEQ (Schmieder and Edwards, 2011), shown in details in the programming script section 12.6.

Sequences were deposited in EMBL-EBI Sequence Read Archive (SRA) with study number PRJEB7515.

Sequences were assembled with MIRA3 (Chevreux et al., 1999) using de-novo genome accurate 454 settings, permitting to assemble as few as 2 reads per contig. The exact command for MIRA assembly was:

```
1 $ mira --project=virusl --job=denovo,genome,accurate,454 454_SETTINGS -LR:ft=fasta -
    AS:mrpc=2 --notraceinfo
```

#### Sequence annotation

The overview of the bioinformatic analysis performed in this work is shown in the Figure 94. The ORFs (open reading frames) in the larger contigs (>1000 bp) were identified by Glimmer3 (Delcher et al., 1999) by a script written in Perl programming language. The sequences were annotated by InterProScan online search using all available approaches (Quevillon et al., 2005): BlastProDom, Coil, FPrintScan, Gene3D, HAMAP, HMMPanther, HMMPfam, HMMPIR, HMMSmart, HMMTigr, PatternScan and ProfileScan, Seg, SignalPHMM, Superfamily, TMHMM. InterPro combines individual strengths of these different annotation sources and provides comprehensive information about protein families, domains and functional sites. The annotation was performed online using script "iprscan_lwp.pl" available from InterPro website. The maps of ORFs detected in

contigs was constructed using genoPlotR (Guy et al., 2010) package in R programming language (an example is shown in programming script section 12.8).

In addition, the larger contigs (>1,000 bp) were annotated using "blastx" algorithm against "nr" database (Altschul et al., 1990). To decide if a sequence can be classified as virus/phage by "blastx", an approach already used by Law et al. (2013) was used. According to Law et al. (2013), to decide if a sequence belongs to a virus, 100 best matches must be revised. In addition, the same contigs were analyzed by searching in ACLAME database of mobile elements (Leplae et al., 2004).

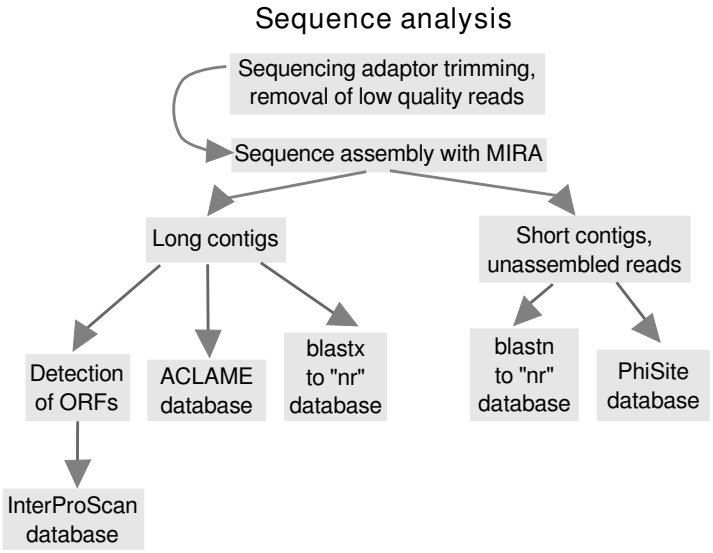


Figure 94: **Workflow diagrams of the data analysis**

Contigs shorter than 1,000 bp and unassembled reads were annotated by "blastn" to "nr" database using megablast algorithm (Altschul et al., 1990). The taxonomy of the best GI matches were retrieved by a script written in the R programming language using "ape" package (Paradis et al., 2004), as shown below:

```
library("ape")
blast <- read.table(file="list-of-GI.txt")
result<-apply(blast, MARGIN=1, FUN=function (x) attr(read.GenBank(x), "species"))
write.table (result, file="result.txt", sep="\t", quote=F)
```

The short contigs and the unassembled reads were also compared to the phiSITE database containing only viral genomes (Klucar et al., 2010).

# 7.4 Results

## 7.4.1 Sequencing results

The sequencing of the SSV-fraction yielded 17.07 Mbp of reads passing quality filters. The reads were assembled into 2,475 contigs; 34 of them were longer than 1,000 bp and had 15.26 x average coverage (maximum coverage 27 x). The largest contig was of 5,313 bp. The details are shown in Table 8. The distribution of contigs length and coverage of all contigs is shown in Figure 95.

Table 8: **Sequencing results and assembly of SSV-fraction**. Description of contigs is shown separately for all contigs and contigs > 1,000 bp and < 1,000 bp

| | All contigs | Contigs > 1000 bp | Contigs <1000 bp |
|---|---|---|---|
| Total Mbp sequenced | 17.07 Mbp | | |
| Number of reads | 60,030 | | |
| Total size of the assembly | 0.66Mbp | | |
| Number of reads assembled | 9,866 | | |
| Largest contig | 5,313 bp | | |
| Number of contigs | 2,475 | 34 | 2441 |
| Average length of contigs | 265.32 bp | 2081.38 bp | 240.03 bp |
| Average coverage of contigs | 3.27 x | 15.26 x | 3.10 x |
| Average number of reads in contigs | 3.99 | 57.06 | 3.25 |

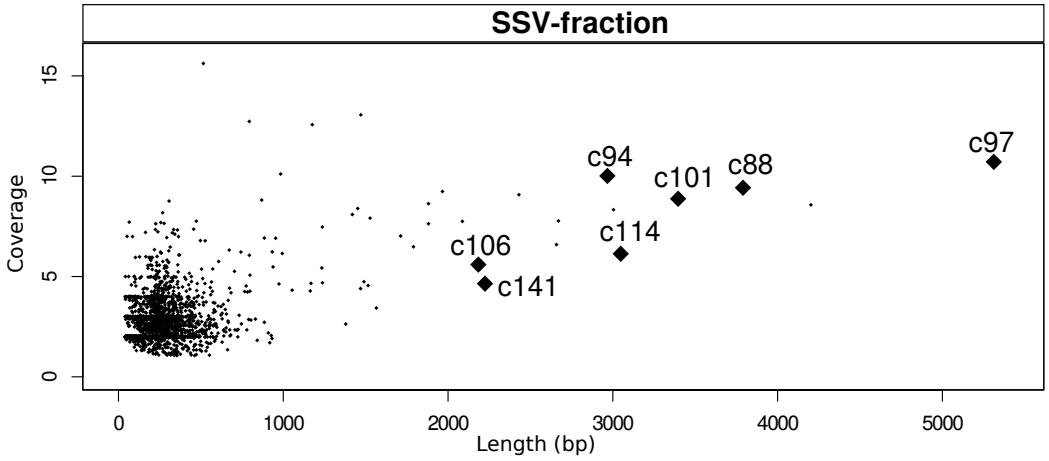


Figure 95: **Length and coverage of contigs assembled in SSV-fraction.** Bigger black spots mark the contigs that had explicit matches to phage related proteins by the thee approaches used in this study ("blastx", ACLAME and InterProScan)

### 7.4.2 Analysis of the large contigs

Thirty-four contigs longer than 1,000 bp contained in total 89 ORFs. InterProScan Sequence Search annotated 62 ORFs, which were present in 28 contigs. Six contigs remained without any annotation. Two of them had no detectable ORFs. InterProScan Sequence Search detected presence of bacteriophages-related proteins, such as: bacteriophage capsid protein, bacteriophage tail protein, virus tail component, translocation-enhancing protein, lambda phage transposase, gene transfer agent portal protein.

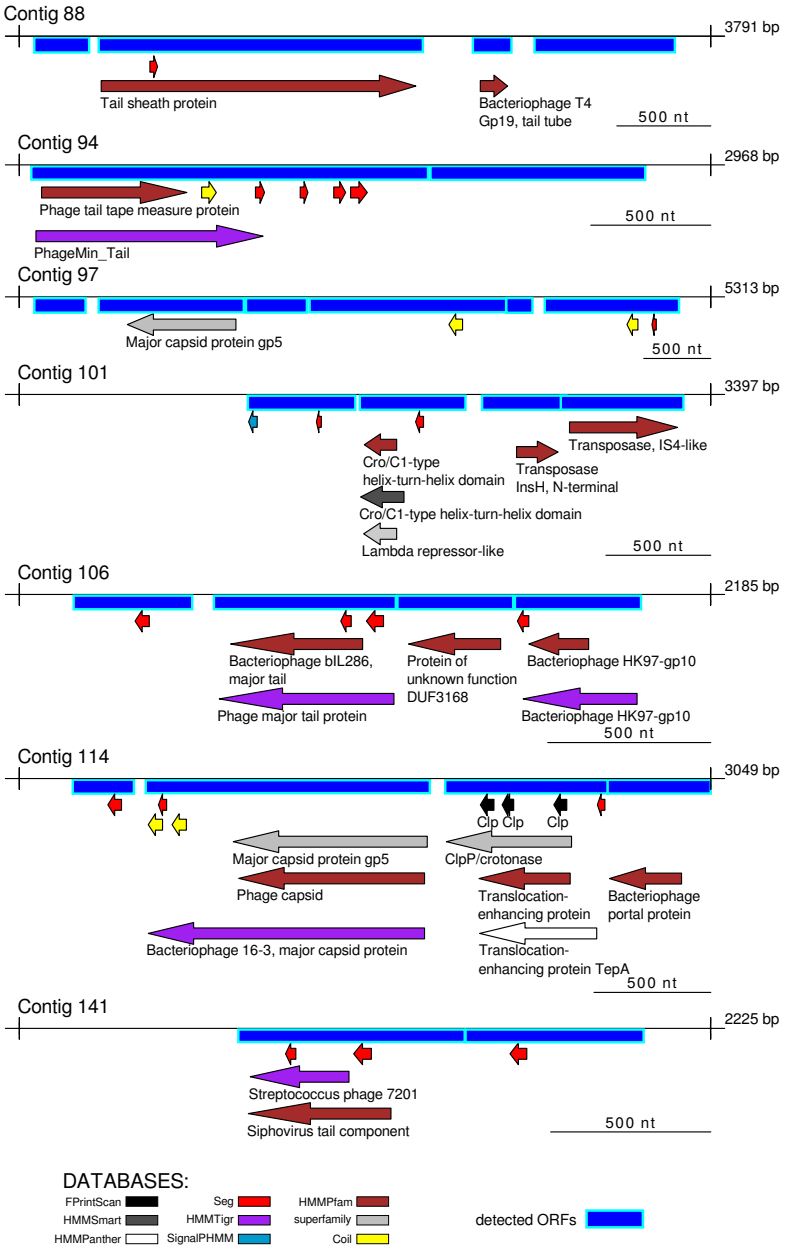


Figure 96: **Visualization of contigs that had explicit matches to phage related proteins by InterProScan.** The remaining contigs with no explicit matches to phage related proteins by InterProScan are shown in Figure 97

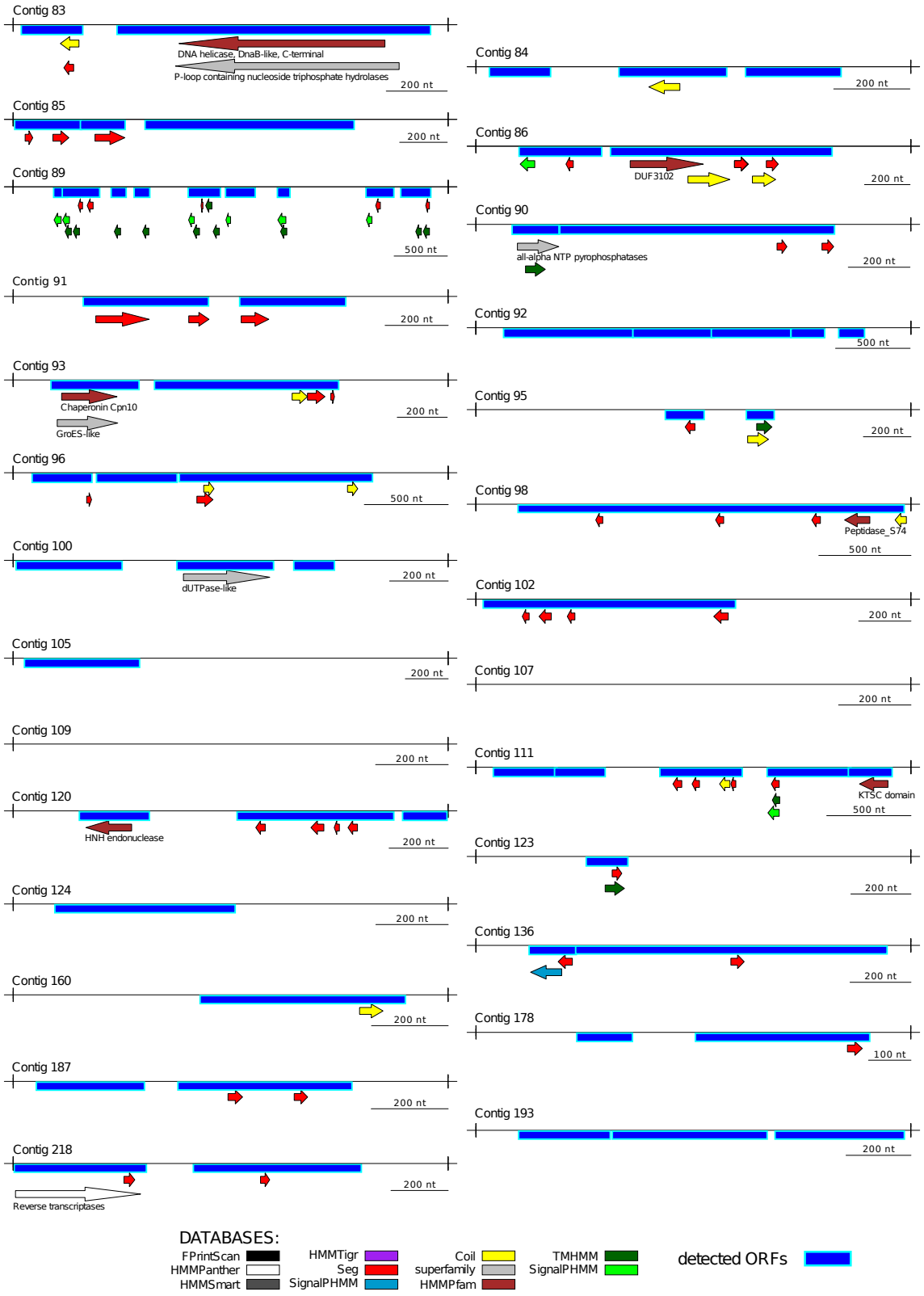


Figure 97: **Visualization of contigs that did not have explicit matches to phage related proteins by InterProScan**

Different annotation approaches gave slightly different results: 16 contigs matched only protein predictors by InterProScan search or low complexity regions "seg", or they did not have any matches at all. However, they were finally annotated as phages by "blastx" or ACLAME approaches. The summary of the proportion of long contigs with explicit matches to bacteriophage proteins by the three tested approaches ("blastx", InterPro and ACLAME) is shown in Figure 98, along with the number of contigs with bacteriophage matches but just one or two databases. In summary, 10 out of 34 long contigs had been unannotated as phages by InterProScan, but they were finally related to bacteriophages by "blastx" and ACLAME. Two more contigs had bacteriophage hits to ACLAME database only (but not "blastx") and 4 more contigs matched potential phages by "blastx" (but not by ACLAME). The visualization of proteins related to bacteriophages identified by InterProScan is shown in Figure 96, while long contigs without any annotation related to phage structural or functional ORFs are shown in the Figure 97.

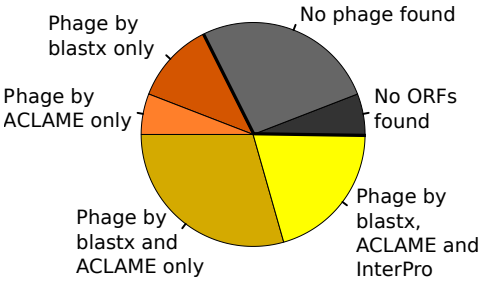


Figure 98: **Proportion of bacteriophage matches**

## 7.4.3 Analysis of unassembled reads

Half (50.54 %) of unassembled sequences and contigs shorter than 1,000 bp could not be assigned by blast to any organism in "nr" database in this study. The most frequent genera detected by "blastn" on NCBI "nr" database were *Bacteroides*, *Alistipes*, *Ruminococcus*, *Bifidobacterium*, *Roseburia*, *Eubacterium*, *Faecalibacterium* and *Odoribacter*. The sample had also matches to the human DNA which probably had some similarities with viral sequences, however none of them matched human mitochondrial or ribosomal DNA The results are shown graphically in the Figure 99, panel A.

The alignment against the phiSITE treated database of viral genomes (Law et al., 2013) showed that short contigs and unassembled reads of the SSV-fraction contained sequences matching phages (110 and 44 matches, respectively, with e-value < 0.00001). The results are shown in Figure 99, panel B.

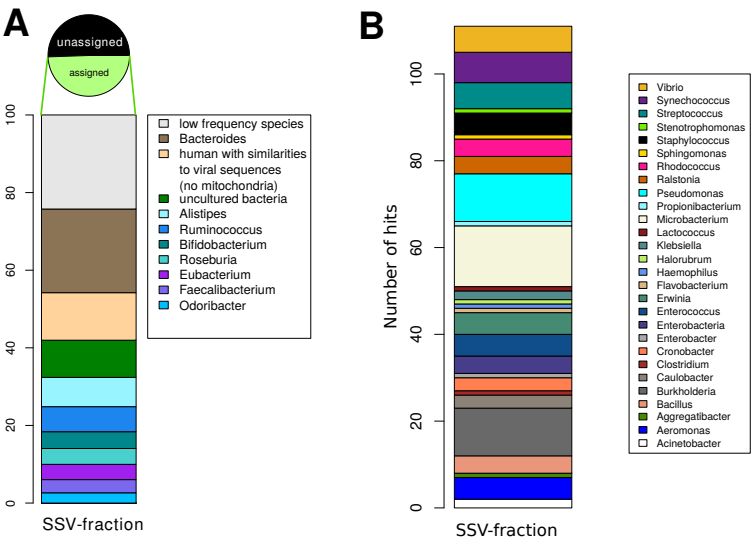


Figure 99: **Analysis of the unassembled reads Panel A:** The most frequent genera detected by "blastn". Composition of species in unassembled sequences and contigs shorter than 1,000 bp detected by "blastn" approach. The upper pie-chart shows the proportion of reads assigned to "nr" database. **Panel B:** Best matches to phiSITE database. All unassembled sequences and contigs shorter than 1,000 bp of SSV-fraction were analyzed. The graphics shows the number of matches to the hosts names

# 7.5 Discussion

FC has been used previously for sorting of cultivated phages and marine viruses (Brussaard, 2004; Chen et al., 2001; Allen et al., 2011; Li et al., 2010; Brown et al., 2015), but this work represents the first cell sorting of human gut virome prepared by common purification methods (filtration through 0.2 $\mu$m pores followed precipitation with PEG-NaCl). The area corresponding to viral particles was identified by comparison with bacterial cells and cultured phages controls, which is a quite common practice in FC of viruses (Li et al., 2010; Brown et al., 2015), as example is shown in the Figure 100. Despite the fact that the samples filtered through 0.2 $\mu$m pores are generally considered "sterile", there are studies that reported size and shape dependent bacterial contamination in filtered freshwater (Hahn, 2004; Wang et al., 2007). Novel uncultured ultra-small bacteria from freshwater with cell size as small as 0.01 - 0.04 mm$^3$ were also detected by FACS (Wang et al., 2009). This underlines the importance of FACS for further exploration of the particles present in a viral samples previously filtered through 0.2 $\mu$m pores.

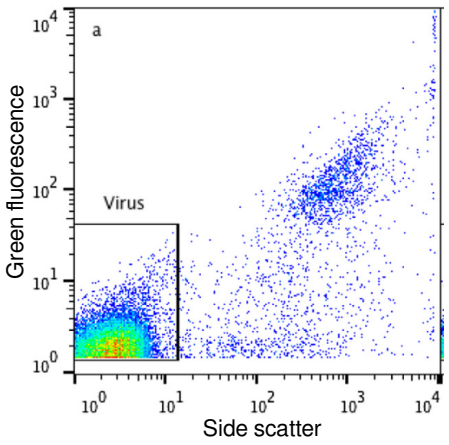


Figure 100: **FC bi-plots of activated sludge.** Author: Brown et al. (2015)

The study of the human gut virome includes generally higher risk of contamination by human DNA. Even one bacterial or human cell accidentally present in the filtered sample can contaminate the whole filtrate as the size of non-viral genomes overreaches viral genome (3.5 kb to > 1 Mb) hundreds or thousands times (Petrov et al., 2010). In our work, the proportion of the human mitochondrial or ribosomal hits in the SSV-fraction was 0.00 %. This is one of the most important achievements of this protocol in terms of optimization of the sequencing efforts. In comparison, in other studies the human contamination could form up to 98 % of all sequences belonging mainly to human ribosomal RNA or mitochondrial DNA (Delcher et al., 1999; Willner et al., 2009).

This study demonstrated that high-throughput shotgun sequencing of as few as 314 virus-like particles is possible without DNA enrichment by WGA. Applying WGA to a viral sample can be very tricky, as the formation of chimeras during WGA could result in miss-identification and over-estimation of viral-like sequences (Pinard et al., 2006; Lasken and Stockwell, 2007). Moreover, as the genome size of viral particles is very variable (Edwards and Rohwer, 2005), some viral species can be over-amplified by WGA and some of them can be omitted (Kim et al., 2008). A sequencing library from SSV-fraction was prepared according to the modified sequencing protocol for ultra-low DNA concentrations presented in details in the Chapter 6. As an alternative, recently developed transposase-based sequencing library preparation protocols can be used, too (Marine et al., 2011). However the bias caused by enzymatic fragmentation in viromes cannot be evaluated, as the viromes are mainly composed of unknown viruses (Edwards and Rohwer, 2005; Reyes et al., 2010; Kristensen et al., 2010).

In the studies of non-fractioned viromes billions of nucleotides are sequenced, but it is almost impossible to assemble these sequences into large viral contigs. In the study of Minot et al. (2013), 56 Gbp was assembled into 478 long contigs. In comparison, 17.07 Mbp were assembled into 34 long contigs in our study, what represents 3,280 fold improvement in comprison with the study of Minot et al. (2013). Our work represent

an approach for improvement of the assembly of the viral genomes by dividing the viral particles into groups according to their size and DNA content, thus each group contains viral particles with similar morphology and genome size. The viral diversity in these groups is reduced in comparison to the non-fractioned viromes and theoretically, these fractions might be composed by viruses of one type only. It is then easier to assemble separately DNA sequences coming from these fractions with reduced diversity than to assemble sequences coming from billions of different organisms present in a non-fractioned virome. The present study explores only one small fraction of the whole fecal virome, but optionally more different viral fractions can be separated by FACS during one sorting session. DNA from these fractions can be sequenced and assembled separately, thus much larger diversity of a virome can be captured.

The sequencing of single viruses is also possible (Allen et al., 2011), however to obtain sufficient genome coverage, it is necessary to enrich their DNA by WGA. The recovery of a whole single viral genome without WGA is not possible on platforms based on sequencing of fragmented DNA (e.g. Illumina, 454, Solid, Ion Torrent), because when a single viral genome is sheared into fragments, the shortest fragments must be removed in order to avoid sequencing run failure, it means that many fragments of a single viral genome will never be sequenced. However, the third generation sequencing platforms reading single DNA molecules can be applied for sequencing of single viral particles (Coupland et al., 2012).

The contigs longer than 1,000 bp in our study possessed mainly genes typical for bacteriophages. This observation is in accordance with the results of many other studies investigating healthy individuals (Breitbart et al., 2003; Minot et al., 2013; Breitbart et al., 2008; Wang et al., 2007; Reyes et al., 2010; Minot et al., 2012; Wagner et al., 2013; Ogilvie et al., 2013), what emphasize the importance of bacteriophages in the human gut. High prevalence of bacteriophages is also notable in conventional metagenomics data sets, which have been estimated to form up to 17 % of microbial DNA recovered from feces (Wang et al., 2007; Reyes et al., 2010; Ogilvie et al., 2013). On the other hand, authors sequencing cDNA from fecal samples of healthy volunteers reported more eukaryotic viruses than bacteriophages, indicating that human viruses in feces might be rather recovered by RNA extraction (Pérez-Brocal et al., 2013; Zhang et al., 2005).

Half (50.54 %) of unassembled sequences could not be assigned by "blastn" to any organism in "nr" database in our study. This is a quite common observation in majority of virome studies, as the sequence databases are biased towards the most studied human viruses and therefore the proportion of the sequences assigned to viruses is reported between 1.5 - 76 % depending on sequence source (DNA/cDNA) and data analysis method (Breitbart et al., 2008; Delcher et al., 1999; Wagner et al., 2013). "Blastn" matches belonged maily to bacteria, concretely *Bacteroides*, *Alistipes*, *Ruminococcus*, *Bifidobacterium*, *Roseburia*, *Eubacterium*, *Faecalibacterium* and *Odoribacter*. These genera were also detected in the viromes of Minot et al. (2013). The presence of bacterial matches in viromes is very common (Finkbeiner et al., 2008; Reyes et al., 2012) and can be explained by the fact that many phages are incorporated in the host genomes and therefore they are presented in the databases as a part of a microbial genome (Ghosh et al., 2008). The reason for extensive presence of bacterial-like genes in viromes might be caused by the presence of prophage-like particles Gene-Transfer Agents (GTA) which are able to mediate horizontal gene transfer. In contrast to common bacteriophages, the amount of GTA is insufficient to encode protein components of the particle itself and it contains random pieces of genome of the producing cell (Wang et al., 2009; Lang et al., 2012). The presence of bacteriophages in the metagenomic samples may be also accessed by clustered regularly interspaced short palindromic repeats analysis, as they serve as a database of fragments derived from phage and plasmid genomes (Kristensen et al., 2010; Stern et al., 2012).

## 7.6 Conclusions

The results indicate that a filtered viral sample contains particles that can be further divided by FACS into fractions according to their size and fluorescence. FACS coupled with the alternative sequencing library preparation protocol omitting artificial DNA enrichment helps to overcome the reported limitations of WGA methods.

Herein presented approach reduces enormously the sequencing force needed for assembling viral sequences into larger contigs (thousands of times when compared to other virome studies). It also eliminates the contamination by human mitochondria. This work demonstrated that the samples containing very low amounts of DNA (as few as 314 viral particles) can be sequenced directly, without WGA, resulting in unbiased and reliable sequences. The sequencing results indicate the presence of novel bacteriophages in the gut of a healthy individual confirming their high diversity which still remains unexplored.

Chapter 8

# General discussion

The human gut contains millions of bacteria and viruses, which have numerous important functions, such as nutrients metabolism and protection against pathogen invasion (Eckburg et al., 2005; Gill et al., 2006). The diversity of the human gut is very individual (Arumugam et al., 2011). A great part of the gut microbes has not been cultured yet, because it is very difficult to imitate the gut environmental conditions in the laboratory. However, the genetic potential of the yet unknown and unculturable microbes can be determined by the metagenomic sequencing (HMPC, 2012). The total DNA of the microbial community can be fragmented, sequenced and aligned to the DNA/protein databases (shotgun metagenome sequencing) (Handelsman, 2004). A general taxonomic diversity overview of a metagenomic sample can be obtained by amplification of the 16S rRNA gene (Morris et al., 2002). However, as the most important genetic differences between strains are found on the whole genome basis, the whole genome sequencing of isolated strains is also very important (Medini et al., 2005).

Antibiotics cause the most important changes of the microbiome composition. They perturb the original microbiome composition, which in some cases may lead to the activation of the opportunistic pathogens, which have been suppressed by the normal bacterial community before antibiotic treatment. After antibiotic treatment, a novel composition of the bacterial community is established and it may be more vulnerable to the overgrowth of opportunistic pathogens. It may lead to the vicious cycle of recurrent intestinal infections (Stecher et al., 2013).

One of such pathogens is *Clostridium difficile*. This pathogen produces high quantities of cytotoxins A and B despite its low prevalence in the gut during infection (CDI) (Kelly et al., 1994; Rupnik et al., 2009). In addition, the healthy gut may be colonized also by the non-toxigenic *C. difficile* and for that reason *C. difficile* usually does not appear as the species differentiating CDI+ and CDI- patients in the conventional metagenomic analyses. There have been numerous attempt to determine which is the microbial composition that makes the human gut vulnerable to the CDI. However, the conclusions of the conventional metagenomics are very elusive (Seekatz and Young, 2014).

The identification of the active bacterial species in CDI is essential for the explanation of the immune recognition mechanisms in dysbiosis during CDI. However, the conventional metagenomic studies cannot determine the taxonomic diversity of the active bacteria, because they take into account also dead and quiescent bacteria as they are also present in the collected fecal samples (Ben-Amor et al., 2005; Peris-Bondia et al., 2011; Maurice et al., 2013). Therefore, the common metagenomic studies cannot reveal whether the activity of the commensal species inhibiting the growth of *C. difficile* decreases after antibiotic treatment. And similarly, it cannot be determined which antibiotic resistant species got activated after initiation of the antibiotic treatment. The detection of the activated antibiotic resistant species is also important, because they may start to produce molecules promoting growth of *C. difficile*.

Moreover, for the explanation of infection processes connected to the dysbiosis, the immune system recognition patterns must be also taken into account. The first line of defense in protecting the intestinal epithelium from pathogens is formed by intestinal secretory immunoglobulin A (SIgA), which coats 25-75 % of all gut bacteria, including the commensal and the pathogenic species (van der Waaij et al., 2004; Palm et al., 2014). The SIgA opsonization of commensals and pathogens results in two different outcomes: the commensal SIgA-coated bacteria are maintained within the gut lumen, while the SIgA-coated pathogens attempting to cross the epithelial barrier are removed (Macpherson et al., 2012; Sansonetti, 2010). It was found that the antibiotic treatment represents the "blooming" opportunity for specialized pathogens which are able to avoid SIgA-opsonization by covering their cell surface by molecules produced by antibiotic resistant species (Ng

et al., 2013; Vimr et al., 2004).

The microbial composition of the active bacterial fraction and of the fraction coated by SIgA can be determined by 16S rDNA gene sequencing of cells selected by fluorescence activated cell sorting (FACS) (Palm et al., 2014; Peris-Bondia et al., 2011; Maurice et al., 2013). FACS physically separates the cells which are fluorescently labeled for selected specific features. Fecal samples from 12 CDI+ and 12 CDI- patients have been processed by FACS in this study. The CDI+ groups contained patients with and also without antibiotic treatment. Similarly, the patients from the CDI- were also taking antibiotics or not. Some patients were under treatment by multiple antibiotics. This patients cohort represented the common clinical practice, in which patients' microbiota are under influence of different factors.

The results of the fluorescent cell counting indicated that the proportion of active bacteria and the bacteria coated by SIgA is very variable. When the patients cohort was divided into group with and without antibiotic treatment, similar proportions of active cells were observed in the both groups. It may be due to the fact that the bacteria susceptible to antibiotics are being replaced by the resistant bacteria which keep maintaining the metabolic functions of the gut. In general, the proportion of the bacteria opsonized by SIgA was lower than the proportion of the active bacteria in the whole cohort, suggesting that not all recently formed bacterial cells can be coated by SIgA immediately.

The analysis of the overall bacterial composition of the individual separated fractions revealed the robust influence of antibiotics on the gut microbiota. The patients' microbiota clustered according to the antibiotics, but not according to the CDI diagnosis. The amounts of toxins quantified by qPCR have been taken into account for analysis of the overall bacterial composition and it was concluded that the effect of antibiotics is even stronger than the influence of the proper *C. difficile* toxins. Gut microbiota modulation by *C. difficile* toxins has been already reported - the toxins may be directly acting on the gut microbiota or the microbiota is changing indirectly due to the inflammation processes in the mucosa disrupted by the *C. difficile* toxins. This is the first work in which the influence of *C. difficile* toxins and antibiotics on microbiota are compared.

FACS showed up to be a helpful tool for determination of dysbiosis patterns in patients with CDI, which could not be discovered by the classical metagenomics. The results of the 16S rDNA sequencing showed that each bacteria genus has a certain portion of cells which belong to the active fraction, while another portion is inactive. The same is true for the bacterial SIgA coating. An example is *Enterococcus* resistant to Vancomycin and Metronidazole which was quickly growing in patients under treatment by these antibiotics, meaning that a great proportion of *Enterococcus* cells were active, while a smaller portion were also dying. This was observed by *in vitro* culture experiments and also by patients' fecal sample analysis. In contrast, in general, a greater part of the most prevalent bacterial species, including *Enterococcus*, was actually inactive in patients without antibiotic treatment.

The comparison of the bacterial proportions in the active and inactive fractions showed that the majority of cells of the beneficial bacteria *Lactobacillales* and *Clostridium* cluster IV are inactive in patients infected by CDI. These bacterial groups have been reported to have inhibitory activity against *C. difficile* (Gao et al., 2010). It suggests that the growth of *C. difficile* may be suppressed in normal conditions by these beneficial bacteria, while the decrease of their activity due to the environmental stress (antibiotics or other factors) induces the "blooming" of *C. difficile*.

The comparison of the proportions of *C. difficile* cells in the fraction opsonized by SIgA with cells in the non-opsonized fraction helped to identify its preferential coating by SIgA in this study. It confirmed that the

intestinal immune system of CDI+ patients recognizes *C. difficile*, meaning that this species is not able to avoid SIgA opsonization, as few specialized pathogens do (Vimr et al., 2004) In the CDI- patients, not *C. difficile* but other bacteria, such as *Fusobacterium*, have been found typically increased in SIgA coated fractions.

The excessive coating of *C. difficile* (*Clostridium* cluster XI) by intestinal SIgA and decreased activity of the beneficial bacteria are the markers of CDI, as they have been observed in the whole CDI+ group, independently on the type of antibiotic treatment taken. These markers have been detected by comparison of the proportions of each bacteria genus in the active and inactive fractions and also in the SIgA-coated and SIgA-not-coated fraction. However, these markers could not be discovered by analysis of the total microbial community, as it is shaped enormously by the antibiotic treatment what lead to the inability to distinguish among gut microbiome of CDI+ and CDI- patients.

Vancomycin and Metronidazole are the most common treatment choice for the initial therapy of primary CDI, but the persistence of spores leads to recurrent infections (Kelly et al., 1994). During the last decade, numerous new resistant and hypervirulent strains have appeared worldwide (He et al., 2013). After antibiotic treatment, the newly established microbial composition may be more vulnerable to CDI or may give the green light for the overgrowth of other pathogens, such as the Vancomycin resistant *Enterococcus* (Willems et al., 2005). Therefore, there is an interest in development of alternative strategies for CDI treatment and prevention. The new treatment agent must have selective inhibitory activity against *C. difficile*, leaving the remaining microbes unaffected. Recently, 8-hydroxyquinoline (8HQ), a simple quinoline alkaloid previously detected in roots of *Sebastiania corniculata*, was demonstrated to be very effective against several bacterial pathogens, including *C. difficile*, while other tested species, such as *Bifidobacteria* were not inhibited (Novakova et al., 2013).

The culture methods commonly used for selectivity testing (e.g. agar dilution or broth microdilution method) do not allow detailed study of the growth dynamics of bacterial populations in co-culture. The selective antibacterial effect of 8HQ has been previously tested *in vitro* only in separate cell cultures (Novakova et al., 2013).

The present study employed fluorescent *in situ* hybridization based on labeling genus specific 16S rRNA sequences for distinguishing between co-cultured *C. difficile* and *Bifidobacterium longum subsp. longum*. Fluorescent cell counting allowed to obtain exact proportions of the two species along time. The selective action of 8HQ towards *C. difficile* was confirmed by counting hybridized cells in different time-points of the growth curve.

The fluorescently hybridized bacterial species can be separated from the total bacterial community by FACS and shotgun sequencing. We applied this approach to one patient with CDI in order to obtain collection of all *C. difficile* cells present it his feces. CDI is a good model infection for such studies, as infections by multiple *C. difficile* strains are being reported very often (Eyre et al., 2012b). The analysis based on ribotyping, toxinotyping or MLST are based on analysis of one isolated colony per patient and are focused to specific genome regions (Griffiths et al., 2010). It has been previously reported that the *C. difficile* strains present in one patient usually differ in thousands of SNPs distributed along the whole genome sequence, thus the conventional colony-PCR-based methods may lead to the false conclusion that patient is infected by only one strain (Eyre et al., 2013b). However, the whole genome sequencing of hundreds of isolated colonies would represent important expenses for routine diagnostic in public health. There is also another important concern: the diagnostics based on the sequencing of isolated colonies may be biased by different growth rate and culture

condition requirements of the different strains, thus there is a need for advanced diagnostic approaches.

Sequencing of *C. difficile* strains collected by FACS has several advantages over the sequencing of microbial culture isolates. The major advantage of the FACS approach used in the present work is that it recovers multiple *C. difficile* strains at their real proportion, independently of their growth rate. Another advantage of FACS is the reduction of the diagnostic time, as there is no need for the microbial culture.

FACS can enrich the microbial sample for the target species. In our study, *C. difficile* proportion increased 129 ×. However, the separated fraction contained contaminating species. The taxonomic diversity of the contaminating bacteria was actually the same as the original fecal sample, what suggest that the contamination comes from the sorting equipment processing the fecal bacteria suspension sample. The proportion of species related to the *C. difficile* was not increased in the contamination what confirmed that the probes were specific for *C. difficile*. More precise cell selection equipment or microfluidic devices may reduce the contamination in the natural *C. difficile* fraction.

The contamination of the FACS-sorted sample impaired the genome coverage analysis, as fragments of many non-*C. difficile* species matched the highly conserved regions, such as 16S rDNA and conjugative transposons of the reference 630 genome. However, apart from these highly covered regions, no other regions with extremely high coverage were detected. This was achieved by direct preparation of the sequencing library from the 10,000 FACS-separated cells, meaning that the cells were not enriched by whole genome amplification (WGA) methods, which is commonly applied to the samples with low DNA concentration. WGA is prone to development of chimeras and GC amplification bias (Lasken and Stockwell, 2007), which would be unacceptable in strains genomes sequencing projects. As no WGA methods were used in this study, it may be concluded that the gaps observed by mapping of the shotgun sequences to the reference genomes were due to their natural absence.

The herein presented approach operates with low genome coverage, which is, however, sufficient for detection of possible SNPs sites within the *C. difficile*-specific genome regions. It may serve as a preliminary screening of fecal samples whether they contain multiple *C. difficile* strains or not. If the presence of SNPs is detected, the strains genomes may be finished by deeper sequencing of the FACS-collected sample or by sequencing of multiple microbial isolates (however, retrieving of these strains by microbial culture is questionable due to the culture conditions bias).

The presence of multiple strains in one patient was confirmed by a PCR amplifying the region within the toxin B gene which contained SNPs detected by mapping of the shotgun sequences. The same PCR was applied to the 11 patients collected within the following three weeks after the collection of the fecal sample of the first patient. The cohort contained patients with 4 possible sequence variants, with 2 sequence variants or with just one sequence variant. No amplicons were obtained from two patients, what may be due to some mismatches not detected by shotgun sequencing, present exactly at the position of the primer annealing sites, thus disabling amplification of some of the sequence types. Therefore, the primers targeting SNPs in one patient may not serve for amplification of the same region in other patients. The shotgun sequencing should be taken as a gold standard for SNPs detection and strains proportion estimation. If only the PCR amplicons analysis is taken into account, it can be concluded that the most prevalent strain in the patient No. 1 was present in different proportions also in three out of next 11 patients collected within the three following weeks at the same hospital department. In total eight different sequence types of the selected region within the toxin B have been detected within the three weeks.

It is difficult to conclude which of the 263 strains genomes available in the online databases was genetically the most similar to the FACS-collected strains of the patient No. 1. Each of the complete *C. difficile* genomes available on the databases contained large gaps (> 5 kbp), which encoded different clade-specific antibiotic resistance genes. The partial genome with the highest number of sequence hits contained also large gaps after the sequence mapping. However, the alignment of the amplicon of the toxin B showed that the variants present in the FACS-collected strains have been previously sequenced by a Chinese team in September 2014. However, the complete genomes of the matching Chinese isolates were not available, thus the presence of these Chinese strains in the patient's sample collected in Boston (MA) could not be confirmed.

As already mentioned above, the number of target cells sorted by FACS for sequencing is usually so low that the FACS-collected samples do not generate the DNA amount required for starting with the sequencing library preparation protocols developed by the next-generation sequencing platforms (e.g. 1 $\mu$g required by Illumina MiSeq and 454 FLX+ for libraries prepared by mechanical fragmentation). The low amount of DNA is usually enriched by WGA. The most commonly used WGA method is Multiple Displacement Amplification (MDA) which employs random hexamers to extend genomic fragments by using the isothermal polymerase from the $\phi$29 phage of *Bacillus subtilis* (Allen et al., 2011; Podar et al., 2007). MDA reaction was found to produce genome coverage bias which is mainly caused by different inter-primer distances, resulting in a low coverage or even unamplified regions. In addition, regions of high GC content could also lead to amplification bias. Finally, MDA reaction is prone to the amplification of template-free hexamer concatenations, to the contamination by alien sequences, and to the formation of chimeric sequences (Lage et al., 2003; Bredel et al., 2005). To overcome the limitations of MDA, a number of protocol improvements or novel bioinformatics approaches have been developed (Woyke et al., 2011; Spits et al., 2006b). However, any of the improvements cannot make artificial amplification completely appropriate for studies of unknown organism or for studies where SNPs and genome rearrangements are of the interest, as there a great risk on working with non-sense sequences.

In fact, the input amount of DNA required for starting with sequencing library preparation is actually overestimated. Most of the input DNA (1 $\mu$g) for 454 sequencing is spent for the titration of the emulsion PCR (emPCR), which involves mixing single-stranded library templates with DNA-capturing sepharose beads in an oil emulsion, expecting thus to capture single sequences. Only about 0.000076 % of the initial DNA amount required for 454 FLX+ library construction is loaded on the sequencing plate, meaning that the majority is lost in the library preparation process or simply stored in a freezer. In the case of MiSeq platform, 0.00162 % of the initial DNA amount required for TrueSeq libraries (mechanical DNA fragmentation) is loaded on the flowcell.

It has been previously shown that the successful quantification of the number of molecules present in the prepared sequencing library is essential for reduction of the amount of starting material needed to sequence a DNA sample. The exact quantification of the number of amplificable molecules present in a library may be performed using Minor Groove Binder Taqman probes (Buh Gasparic et al., 2010; Zheng et al., 2011). The present study demonstrated that if the steps, in which the major DNA losses occur, are substituted by more sparing ones, a library containing the minimal number of molecules required for loading on a sequencing plate can be sequenced successfully. Rather than fragmenting the samples in a nebulizer, they were sonicated in the same tube in which DNA extraction was performed, thus also avoiding losses due to sample transfer. Small fragments were removed exclusively with AMPure magnetic beads and no purification columns were used. By this way the library containing DNA extracted from 10,000 *E. coli* cell (counted by FACS) was

sequenced. The extracted DNA amount was not measurable by the Picogreen assay, but it was definitely lower than 54 pg (the theoretical DNA content of 10,000 *E. coli* cells), because losses during DNA extraction occur. The only concentration control point was the final library quantification by qPCR which confirmed that the constructed library contained the minimal number of DNA molecules required for loading on one 1/8 region of a sequencing plate.

The performance of the direct sequencing was compared with the widely applied MDA approach used for samples with small amounts of DNA. Sample sequenced directly without MDA provided homogeneous genome coverage throughout most of the *E. coli* genome. In contrast, MDA sample generated regions with a extremely high genome coverage, leaving almost all of it uncovered. The number of unassigned sequences was considerably lower in the sample sequenced directly without MDA, while up to 94.24 % of the MDA sample was formed by unknown DNA sequences. By hexamer frequency analysis we concluded that these sequences could originate from hexamer concatenation or from the enzyme preparation process, including host bacteria *Bacillus subtilis*.

The sequences of the sample sequenced directly without MDA, which have been not mapped to the *E. coli* genome (19.41 %), belonged mostly to the species contaminating buffers in the flow cytometer or to the bacteria coming from the human skin. This is an important concern, which was also observed in the separation of *C. difficile* cells by FACS in this work. It seems that contamination is an important issue in the common flow cell sorters and cannot be completely eliminated by bleach which is generally used for equipment cleaning. However, this issue underlines the importance of direct sample sequencing without artificial amplification by MDA. If MDA is applied to a sample with certain proportion of undesired contaminating bacteria, their sequences may be by amplification chimerically attached to the target species sequences. This makes MDA especially risky for sequencing of genomes of unknown organisms separated from their original bacterial community by FACS.

We have demonstrated, that it is possible to sequence DNA coming from as few as 10,000 bacterial cells. The minimal number of cells required for starting with preparation of a sequencing library would depend on the DNA extraction method. However, the study design must take into account that a typical bacterial cell containing 5-16 fg of DNA would never provide a sufficient number of molecules for high-throughput sequencing. It is not possible to recover a complete genome of a single-cell genome without WGA on platforms sequencing fragmented DNA (e.g. Illumina, 454, Solid, Ion Torrent), because when a single-cell genome is sheared into fragments, the shortest fragments must be removed in order to prevent sequencing run failure. It means that many fragments of a single non-enriched genome would be never sequenced.

To address the question which is the minimum number of cells required for sequencing library preparation, a theoretical calculation based on the minimal number of molecules loaded on a sequencing plate was performed in this study. MiSeq Illumina platform generates 25,000,000 reads which correspond to the DNA amount that could be extracted from 3,260 *E. coli* cells if no DNA losses during the DNA extraction occurred. In the case of the 454 FLX+ (1,000,000 reads) it would be 153 cells. However, in the study design, the DNA losses during the extraction protocol and library preparation protocol must be taken into account, too. In contrast, in the Illumina library preparation protocol, the sequencing adaptors are attached by a PCR reaction which actually increases the library concentration. Similarly, the concentration of a 454 library may be increased by a PCR with sequencing adaptor primers. Theoretically, the number of cells for sequencing on the 454 FLX+ platform should be higher than 153 cells (for sequencing on the whole sequencing plate). However, it may be also lower, as the final library can be also amplified by few number of PCR cycles with

library adaptors primers. In addition, the sequencing plate may be divided into smaller regions or numerous samples may be multiplexed and pooled for sequencing on one sequencing plate, meaning that sequencing of multiple samples on one plate would require less bacterial cells. Thus, it is difficult to estimate an exact minimal number of bacterial cells required for a succesful sequencing run on the next-generation sequencing platforms. Third generation sequencing platforms reading single DNA molecules (such as MinION) may be used for direct whole genome sequencing of single bacterial cells.

As the minimal number of bacterial cells required for sequencing has not been exactly defined, we prepared a sequencing run on the 454 FLX+ platform containing DNA from as few as 314 viral particles collected by FACS. We focused on utilization of FACS for human gut viromics, as the sequencing of the viromes prepared by the common purification protocols encounters several difficulties. The fecal samples are usually centrifuged with the objective to remove bacterial fraction. The supernatant is filtered through a series of filters, in which the 0.2 $\mu$m pores are the smallest ones and the obtained filtrate is concentrated by ultracentrifugation (Thurber et al., 2009). However, a high proportion of human and bacterial matches is still being detected in such purified viral samples (Breitbart et al., 2003). Viral DNA extraction results in a low DNA concentration, which does not reach the minimal limit required for sequencing library preparation. Therefore, the viromes are usually enriched by WGA (usually MDA), which is, however, prone to the development of chimeras and amplification bias, as already mentioned above. In addition, as there is a very wide diversity of gut viral species, very extensive sequencing efforts must be made for the assembling of whole viral genomes.

The present work describes an approach to improve human gut virome assembly by employing a more precise preparation of a viral sample before sequencing in which the final viral particles selection is performed by FACS. Particles present in a virome previously filtered through 0.2 $\mu$m pores were stained with a DNA stain and visualized on the flow cytometery bi-plots. One group of viral particles with the smallest size was selected and shotgun sequenced by the optimized sequencing library preparation protocols previously tested with 10,000 *E. coli* cells. The DNA extracted from the FACS-sorted 314 viral particles of the selected fraction was assembled into 34 contigs longer than 1,000 bp with the coverage of over 15 ×. This represents an increase to the number of assembled long contigs per sequenced Gb in comparison with other studies where non-fractioned viromes are sequenced. Seven of these contigs contained open reading frames (ORFs) with explicit matches to proteins related to bacteriophages. The remaining contigs also possessed uncharacterized ORFs with bacteriophage-related domains. The results confirmed the the high diversity of bacteriophages in the healthy human gut.

However, it is also important to mention the presence of unassigned and unassembled sequences in the sequenced virome fraction. About half of the unassembled reads in our study could not be assigned to any organism, which is quite a common observation for the majority of virome studies. The reason for this is that the sequence databases are biased toward the most studied human viruses, and therefore the proportion of the sequences assigned to viruses is very variable and depends on sequence source (DNA/cDNA) and the data analysis method. The bacterial matches are also very common in virome studies and can be explained by the fact that many phages are incorporated in the host genomes and are therefore present on the databases as parts of microbial genomes. The FACS-sorted virome sample presented in this study should be sequenced with more depth in order to finish the complete genomes of these phages and to respond the question, whether the detected bacteriophages in our study contained these unassigned sequences in their genomes or whether these sequences formed the contamination of the flow cytometer equipment, commonly detected in our previous studies.

The results of the present study suggest that the particles, that are present in the filtered viromes, are of very variable sizes and DNA content. The separation of a group of particles with similar size and DNA content actually decreases the viral diversity in the sample and so allow to recover easily large pieces of the viral genomes. Assembly of such a small number of particles results in long contigs without applying large sequences efforts. Moreover, FACS of such a filtrate represents an effective tool for elimination of contamination by human mitochondria and bacteria.

Chapter 9

# General conclusions

1. The comparison of the taxonomic distribution of the two pair of fractions (SIgA-opsonized vs. non-SIgA-opsonized and active vs. not active) allows to determine the dysbiosis patterns in CDI patients. The beneficial bacterial groups, such as *Lactobacillales* and *Clostridium* IV group are mostly inactive in CDI patients. These bacteria might supress the activity of *C. difficile* in healthy individuals in the risk category. The majority of cells of *C. difficile* are opsonized by SIgA during CDI infection. It suggests that *C. difficile* cannot avoid opsonization by SIgA as some specialized pathogens do.
2. *C. difficile* forms as few as 0.0001 % of all intestinal bacteria and is recognized by the immune system as a common pathogen. However, when there is a decrease of beneficial bacteria activity due to the environmental stress caused by antibiotics, it is able to produce high amounts of toxins and cause the infection.
3. 8-hydroxyquinoline is a natural compound which seems to be promising for CDI treatment. Flow cytometry analysis showed that it has selective inhibitory activity against *C. difficile*, while the growth of beneficial *Bifidobacterium longum* grown in co-culture remains unaffected.
4. *C. difficile* infection can be caused by multiple strains. The analysis of single nucleotide polymorphism in genomic sequences obtained from *C. difficile* cells separated directly from feces of a CDI patient by the flow cytometry showed at least three genetic variants of the selected region of the toxin B gene. Three of 11 patients hospitalized at the same department within the following month contained the genetic variants detected in the first patient.
5. Shotgun sequencing of *C. difficile* strains present in one patients collected by flow cytometry may serve as an initial screening for detection of infection by multiple strains as so reduce costs which would be generated by sequencing of hundreds of culture isolates.
6. Despite the cell collection by flow cytometry usually result in low amounts of extracted DNA, these samples can be sequenced by the high-throughput sequencing platforms, if optimized protocols are used. The library prepared by an alternative protocol should contain the minimal number of DNA molecules required for loading on a sequencing plate.
7. The DNA libraries prepared by alternative shotgun protocols generate better sequencing results than libraries prepared from DNA enriched by the whole genome amplification by $\phi$ polymerase. $\phi$ polymerase can generate up to 98 % of unreliable sequences which do not map to the references bacterial genome, which is contrary to the results obtained by the alternative shotgun library preparation protocol.
8. Flow cytometry cell sorting coupled by the use of optimized shotgun sequencing protocols allows to determine the genetic sequence of human viruses. It was shown that a healthy volunteer contains numerous novel bacteriophages.
9. Low number of viral particles collected by flow cytometry improves the genome assembly. Moreover, the contamination of viral filtrates, e.g. human mitochondria and bacteria is reduced.
10. Flow cytometry is a powerful tool for analysis of individual bacterial cells and viral particles. It can be considered as an improving extension for the classical metagenomics, as the cell sorters preselect the bacteria (viruses) with the pre-determined characteristics, so the non-target bacterial cells are eliminated and excluded from the sequencing. The ability to reveal the genetic information of the target group of microorganisms can be very helpful in addressing the biological questions related to the human gut microbiome.

Chapter 10

# Resumen en Castellano

# Introducción

El tracto intestinal humano está poblado por $10^{13}$ - $10^{14}$ bacterias que en conjunto contienen 1,000 veces más genes que el genoma humano (Gill et al., 2006). Varios estudios han confirmado que las bacterias del intestino influyen en la salud del cuerpo humano (Macfarlane et al., 2005; Turnbaugh et al., 2006; Bercik et al., 2011). Además de las bacterias, el intestino humano contiene millones de partículas virales, en su mayoría bacteriófagos. Indirectamente, por lo tanto tambiÃĺn influyen en la salud humana (Minot et al., 2013).

La composición microbiana varia con el individuo. Las especies más numerosas podrían definir tres grupos de individuos: segÃžn predominen *Bacteroides*, *Prevotella* o *Ruminococcus* (Arumugam et al., 2011). No obstatne, las funciones más importantes pueden ser realizadas por especies minoritarias (Lynch and Neufeld, 2015). Durante el dasarrollo, la composición bacteriana en el intestino cambia por efecto de la dieta y el estilo de vida. Los antibióticos provocan fuertes cambios también (Graf et al., 2015).

Es enorme la candidad de información que se ha descubierto en los últimos años sobre las bacterias intestinales, aunque aún quedan muchas cuestiones abiertas. La secuenciación de ADN ha permitido conocer el potencial genético de todas las bacterias en el cuerpo humano sin necesidad de cultivarlas. Se estima que la mitad de las bacterias intestinales no se puede cultivar, pero se puede averiguar su función y aproximar su taxonomía (Morgan et al., 2013).

Hay varios métodos para descifrar el potencial genético de las bacterias:

- Genómica bacteriana: se extrae ADN de las cepas aisladas y se fragmenta con enzimas de restricción o mecánicamente con ultrasonido o ultra presión, ya que los secuenciadores de ADN (Illumina MiSeq o 454 FLX+) no pueden leer la molécula de ADN entera. Las secuencias obtenidas se ensamblan para reconstruir el genoma en su totalidad. El genoma bacteriano se cubre con secuencias solapantes para obtener un ensamblaje correcto.
- Metagenómica: se extrae ADN de todo el conjunto de las bacterias obtenidas directamente de un ambiente. El objetivo es descifrar las secuencias para ver cuáles son las principales rutas metabólicas de ese ambiente e intentar determinar las principales familias bacterianas que son productoras de estos metabolitos. Otra rama de la metagenómica es la transcriptómica, en la que se estudian solo los genes expresados en el momento de recoger las muestras.
- Clasificación taxonómica - La secuenciación del gen 16S rRNA sirve para la identificación de especies bacterianas. El gen se amplifica en la reacción PCR. El producto de la amplificación debe tener el tamaño adecuado para su secuenciación.

Estos métodos de secuenciación de ADN se suelen aplicar a toda la comunidad bacteriana, pero existen métodos de preselección de células bacterianas, como es el caso de la citometría de flujo. La citometría de flujo es una metodología que permite separar fracciones de comunidades microbianas basándose en características tales como el contenido celular de DNA, proteínas en la superficie celular o la taxonomía microbiana.

El citómetro de flujo detecta la fluorescencia emitida por las células marcadas con fluoróforos que indican las características celulares de interés. Las células pueden ser marcadas directamente con un compuesto químico fluorescente o indirectamente con los fluoróforos conjugados con macromoléculas, anticuerpos o sondas (oligonucleótidos). Las células entran al citómetro de flujo en suspensión, se alinean y pasan una detrás de otra a través de uno o varios láseres. Cada partícula desvía la luz en forma diferente y al absorber la

energía de láser, emite diferentes longitudes de onda que se filtran por un sistema de espejos. Las ondas son recogidas por sensores que envían la información de intensidad a un ordenador. Dependiendo del citómetro y de la muestra, el citómetro de flujo puede procesar datos de cientos de miles de células en unos minutos (Picot et al., 2012).

# Objetivos

El ADN de las células con características seleccionadas separadas por la citometría de flujo se pueden secuenciar. Con este método obtendríamos más información que secuenciando la comunidad bacteriana no fraccionada. Esta tesis está enfocada a la metagenómica del intestino humano dirigida por la citometría de flujo. Los objetivos principales de esta tesis son los siguientes:

- **Objetivo 1: Secuenciación de las bacterias activas y cubiertas con inmunoglobulina A secretora en las muestras fecales de pacientes con infección por *Clostridium difficile***
  El objetivo es explorar la diversidad taxonómica de las bacterias activas y opsonizadas por inmunoglobulina A secretora que se separarán por la citometría de flujo. La infección por *C. difficile* está relacionada con el uso de antibióticos de gran espectro. Con el método aplicado en esta tesis se podrá detectar quÃĭ especies se resisten al tratamiento antibiótico, ya que los resultados de los estudios de microbiota total también incluyen las bacterias muertas. La perturbación microbiana puede estar relacionada con cambios en los mecanismos de reconocimiento de bacterias por el sistema inmune, que pueden influir el progreso de la infección. El objetivo 1 de esta tesis es explicar la disbiosis bacteriana que está ocurriendo en el intestino de los pacientes infectados por *C. difficile*.

- **Objetivo 2: Inhibición de *C. difficile* por 8-hidroxiquinoleína**
  La hibridación de células con sondas fluorescentes específicas ayuda a distinguir especies de bacterias distintas en muestras ambientales o en un co-cultivo. El objetivo 2 de esta tesis es estudiar el efecto de 8-hidroxiquinoleína, que es un compuesto antibacteriano con efecto inhibidor selectivo contra *C. difficile*. Se investigará por la citometría de flujo el crecimiento de *C. difficile* y *Bifidobacterium longum* cultivados cuntamente en un medio conteniendo el 8-hidroxiquinoleína .

- **Objetivo 3: Diversidad genética de *C. difficile* separado por citometría de flujo**
  Las células de *C. difficile* marcadas con sondas específicas serán separadas del resto de la comunidad bacteriana intestinal por citometría de flujo. Se secuenciará ADN de todo el conjunto de cepas presentes en heces de un paciente infectado. El objetivo 3 de esta tesis es detectar la infección por múltiples cepas de *C. difficile* en un paciente evitando utilizar los métodos de cultivo tradicionales.

- **Objetivo 4: Adaptación de protocolos de secuenciación masiva a las muestras procedentes de citometría de flujo**
  Las muestras procedentes de citometría de flujo contienen normalmente una cantidad de ADN tan baja que no cumplen con los requisitos de los protocolos de secuenciación masiva. Por eso todo el contenido genético se suele enriquecer con la polimerasa Φ. Sin embargo, esa amplificación es la causa de secuencias quiméricas o falta de regiones enteras. El objetivo 4 de esta tesis es optimizar los protocolos de preparación de las librerías de secuenciación para poder secuenciar muestras procedentes de la citometría de flujo. Los resultados se compararán con los resultados del ADN enriquecido con la polimerasa Φ.

- **Objetivo 5: Virómica del intestino humano dirigida por la citometría de flujo**
  El objetivo 5 de esta tesis es estudiar por citometría de flujo las partículas virales presentes en un filtrado de muestras fecales. Se separará una fracción de partículas con el mismo tamaño y fluorescencia de ADN y se secuenciarán usando el protocolo optimizado en el objetivo 4. Los genes se anotarán y se determinará su origen.

# Métodos

Las células bacterianas procedentes de heces se fijaban con formaldehido y se marcaban con SYTO®62 (Life Lechnologies, Ref. S11344) para distinguir las células de otras partículas de tamaño similar que podían permanecer en las heces después de la purificación bacteriana. Los virus, en el proyecto de secuenciación de viroma, se marcaban con SYBR Green I (Life Technologies, Ref. S-7563). En los otros proyectos, las bacterias activas se marcaban con pironina Y (Sigma-Aldrich, Ref. P9172-1G) que es específico para ARN; las células opsonizadas con inmunoglobulina A secretora se marcaban con anticuerpos conjugados con FITC (Life Technologies, Ref. A24459) y las células de *C. difficile* y *B. longum* se marcaban con sondas conjugadas con fluoróforos de longitudes de emisión diferentes (FITC y Cy5).

Para la separación de células bacterianas o partículas virales se utilizaron los citómetros MoFlo XDP Cell sorter de Beckman Coulter y S3 Cell Sorter de Bio-Rad. En el proyecto de secuenciación de fracciones de bacterias activas y opsonizadas por inmunoglobulinas, se separaron 540,000 células de cada fracción de heces en 12 pacientes infectados por *C. difficile* y 12 pacientes no infectados hospitalizados. En el estudio genómico de *C. difficile* se separaron tan solo 10,000 células de heces de un paciente infectado y en el estudio de viroma se separaron tan solo 314 partículas virales filtradas por poros de tamaño 0.2 $\mu$m de heces en un voluntario sano. En los experimentos donde la separación física no era necesaria, se utilizó el citómetro Cytomics FC 500 de Beckman Coulter para contar las células y para visualizar su fluorescencia.

El ADN se extraía con el método de fenol-cloroformo donde se empleaba bromuro de hexadeciltrimetilamonio, lisozima y proteinasa K (Ausubel et al., 1992). Para estudiar el gen 16S rRNA se amplificaban los regiones V3 y V4 (Klindworth et al., 2013) y los amplicones se trataban según las instrucciones de secuenciación por Illumina. En los estudios genómicos, el ADN se fragmentaba por sonicación o usando el kit Nextera empleando la tagmentación. La secuenciación masiva se llevó a cabo en las plataformas Illumina y 454 FLX+.

En general, las secuencias obtenidas se procesaban con el programa PRINSEQ (Schmieder and Edwards, 2011), que cortaba las secuencias según su calidad y eliminaba secuencias cortas o con baja entropia. En los estudios taxonómicos, los amplicones de 16S rDNA se compararon con la base de datos "Ribosomal database project" (Cole et al., 2009). En los estudios genómicos, las secuencias se compararon con las bases de datos de NCBI usando algoritmos de "blastn" o "blastx" (Altschul et al., 1990) y en el caso de virómica con las bases de datos ACLAME (Leplae et al., 2004) y phiSITE (Klucar et al., 2010). Las secuencias genómicas se ensamblaron con el programa MIRA4 (Chevreux et al., 1999) y los "marcos abierto de lectura" se anotaron en la base de datos InterPro (Hunter et al., 2012). El mapeo de las secuencias genómicas de un genoma en concreto se realizó con los programas SSAHA 2.5.4 (Ning et al., 2001) o Bowtie 2 (Langmead and Salzberg, 2012).

Los resultados se analizaron con los paquetes de programación en R, como por ejemplo "vegan" (Dixon, 2003) para determinar las abundancias bacterianas, "Rsamtools" (Li et al., 2009) para visualizar la cobertura

de genoma determinado con las secuencias obtenidas y "FlowViz" para manejar los datos de citometrá de flujo (Hahne et al., 2009).

## Resultados y conclusiones

La comparación de distribuciones taxonómicas de las dos parejas de fracciones (opsonizadas vs. no opsonizadas y activas vs. inactivas) ha ayudado a determinar las características de disbiosis en pacientes infectados por *C. difficile*. El grupo taxonómico de *C. difficile* estaba preferentemente opsonizado por inmunoglobulina A secretora. En los pacientes no infectados, otras bacterias potencialmente patogénicas también eran opsonizadas por inmunoglobulina A secretora. Los grupos de bacterias beneficiosas, como *Lactobacillales* and *Clostridium* grupo IV eran inactivas en los pacientes infectados. Por las condiciones medioambientales (como tratamiento antibiótico) estas bacterias bajan su actividad lo que promueve la producción de toxinas por *C. difficile* aunque su proporción en el intestino sea muy baja (puede ser tan solo 0.0001 %) y aunque sea reconocido por el sistema inmune. No hubiese sido posible encontrar estos indicadores de disbiosis aplicando los métodos de metagenómica rutinaria en la que se analiza la comunidad bacteriana no fraccionada.

La citometría de flujo es un método para contar las células hibridadas con sondas fluorescentes específicas de especies de interés. Cuando *C. difficile* se ha cultivado en conjunto con *B. longum* en medio sin bacteriocinas, la proporción de las dos especies era similar, oscilaba entre 22.7 y 77.9 % durante toda la curva de crecimiento de 12 horas. En el cultivo con el 8-hidroxiquinoleína el contenido de *C. difficile* bajó después de 4 horas (8.8.-17.5 %). El crecimiento de *B. longum* no se vió afectado por 8-hidroxiquinoleína. Este estudio demuestra que el efecto de 8-hidroxiquinoleína es selectivo contra *C. difficile* y no afecta a las bifidobacterias. Por eso podria servir como tratamiento contra la infección por *C. difficile*.

Las secuencias genómicas de las 10,000 células de *C. difficile* separadas de heces de un paciente infectado se han mapeado al genoma de referencia de la cepa 630. Sin embargo varias regiones específicas para esta cepa faltaban por lo que se puede concluir que el paciente era infectado por otra(s) cepa(s). El estudio del polimorfismo de un solo nucleótido ha detectado dos variantes del mismo nucleótido en varias ocasiones. Los polimorfismos detectados en los genes de toxina A y B se han confirmado por secuenciación de los amplicones de estas regiones. Aunque la cobertura del genoma de referencia no era suficiente para completar el ensamblaje, este método puede servir para detectar las infecciones por cepas múltiples y así reducir los gastos que surgieran si se secuencian las cepas aisladas por el cultivo microbiológico. Además, la separación de células de *C. difficile* por la citometría de flujo no está sesgada por la diferente formas de crecimiento de las cepas.

En los proyectos genómicos de esta tesis queríamos evitar el uso de enriquecimiento con la polimerasa Φ, ya que esta forma secuencias corruptas. Se ha construido una librería de secuenciación que contenía el mínimo número de fragmentos de ADN que se deben cargar en una placa de secuenciación de la plataforma 454 a partir de tan solo 10,000 células de *E. coli* contadas por el citómetro. El optimizado protocolo de la preparación de las librerías de secuenciación empleaba sonicación en lugar de la nebulización y las librerías se cuantificaban por la PCR cuantitativa. El protocolo optimizado daba una cobertura uniforme del genoma de *E. coli*. Los resultados se compararon con la muestra enriquecida con la polimerasa Φ que generó secuencias corruptas (97.8 % se las secuencias) y tan solo 2.45 % del genoma de *E. coli* estuvo cubierto.

En el siguiente proyecto se ha utilizado el protocolo anterior para secuenciar tan solo 314 partículas virales de heces de un voluntario sano. Se han seleccionado las partículas virales con el mismo contenido de ADN y el mismo tamaño. El ensamblaje de las secuencias metagenómicas resultó en 34 contigs con longitud mayor de 1,000 pares de bases. Esto representa un incremento del número de contigs largos por número de lecturas obtenidas. Siete de estos contigs contenían marcos de lecturas abiertas identificados como partes de proteínas de bacteriófagos. Otros contigs largos también tenían cierta similitud con secuencias de los bacteriófagos. Ninguno de los contigs largos contenía genes bacterianos. No se detectó contaminación por mitocondrias humanas. La citometría de flujo aplicada para fraccionar las partículas virales supone muchas ventajas en la investigación del viroma humano. No solo mejora el ensamblaje sino que también reduce la contaminación por células no virales.

En conclusión, esta tesis presenta varios casos en los que la citometría de flujo complementa y aumenta la información biológica que ofrece la metagenómica clásica. Sirve para explicar disbiosis bacteriana en infecciones, para describir las curvas crecimiento de especies mezclados en un cultivo, para detectar la infección por cepas múltiples en un paciente y también sirve para mejorar varios aspectos de los estudios de viroma humano, si se aplican protocolos optimizados de preparación de librerías de secuenciación.

Chapter 11

# Appendix: Laboratory protocols

# 11.1 Amplification of 16S rDNA for Illumina sequencing

1. Prepare the following PCR premix:

   31.75 $\mu$l water

   4 $\mu$l dNTPs 2.5 mM each (Takara, Ref. RR001A)

   5 $\mu$l ExTaq buffer 10x (TakaraRef. RR001A)

   2 $\mu$l 10 mM 16S rDNA forward primer Illumina:

   5' - TCG TCG GCA GCG TCA GAT GTG TAT AAG AGA CAG CCT ACG GGN GGC WGC AG -3'

   2 $\mu$l 10mM 16S rDNA reverse primer Illumina:

   5' - GTC TCG TGG GCT CGG AGA TGT GTA TAA GAG ACA GGA CTA CHV GGG TAT CTA ATC C - 3'

   0.25 $\mu$l ExTaq polymerase 5 U/$\mu$l (Takara, Ref. RR001A)

   5 $\mu$l DNA, extracted according to the protocol in the section 11.5 or water (as a negative control)

2. Incubate the samples in a PCR cycler with the following program:

   Initialization step:

   94 °C 2 min

   Denaturation, annealing and elongation steps: if DNA content is 12.5 ng, perform the PCR with 25 cycles, if it is less increase the number of cycles to 32:

   94 °C 30 sec

   54 °C 30 sec

   72 °C 30 sec

   Final elongation:

   72 °C 10 min

   Final hold at 4 °C

3. Purify the PCR product and prepare the sequencing library according to the manufacturer's instructions in the official Illumina protocol.

## 11.2 Cloning and sequencing by the Sanger method

1. Always work with samples purified from agarose gel.
2. By a bladder knife cut out the DNA band corresponding to the PCR product length.
3. Purify the DNA from the gel using High Pure PCR Product Purification Kit (Roche, Ref. 11732668001 ). At the end, dilute the DNA sample in 30 $\mu$l of water.
4. Ligation reaction:

   6 $\mu$l ligation buffer (Thermo Scientific, Ref. K1231)

   1 $\mu$l blunt enzymes (Thermo Scientific, Ref. K1231)

   3 $\mu$l sample

   Incubate at 70°C for 5 min, place on ice for 5 min.

   Add 1 $\mu$l ligase (Thermo Scientific, Ref. K1231)

   Add 1 $\mu$l vector pJET1.2/blunt (Thermo Scientific, Ref. K1231)

   Incubate at room temperature for 5 min.
5. Proceed to the transformation: Use OneShot® electrocompetent cells (Life Technologies, Ref. C4040-50). Add 2 $\mu$l of the ligation reaction into 50 ml of electrocompetent cells placed on ice and transfer the mixture to electroporation cuvettes 0.1 cm gap (Eppendorf, Ref. 4307 000.569) without introducing bubbles. Transform in Electroporator 2510 (Eppendorf, Ref.12706713) with settings: 3.5 to 4.5 msec, 10 $\mu$F, 600 Ohms, 1,800 Volts.
6. Add 950 $\mu$l of Recovery Medium belonging to One Shot® electrocompetent cells kit to the cuvette and pipet up and down three times to resuspend the cells.
7. Transfer the cells and Recovery Medium to a culture tube.
8. Place the tube in a shaking incubator at 250 rpm for 1 hour at 37°C.
9. Spread 100 $\mu$l of transformation reaction on Petri plates containing selective medium containing 100 $\mu$g/ml of ampicilin.
10. Incubate the plates overnight at 37°C. Only colonies containing insert will grow.
11. Prepare colony PCR premix:

    41.3 $\mu$l water

    5 $\mu$l LA Taq buffer (Takara, Ref. RR002A)

    1 $\mu$l 10mM forward primer

    5’ - CGA CTC ACT ATA GGG AGA GCG GC - 3’

    1 $\mu$l 10mM reverse primer

5’ - AAG AAC ATC GAT TTT CCA TGG CAG - 3’

1.6 $\mu$l dNTPs 2.5 mM each (Takara, Ref. RR002A)

0.1 $\mu$l LA Taq polymerase (Takara, Ref. RR002A)

12. To each tube place 1 colony by a sterilized toothpicker.
13. Colony PCR program:

    Initialization step:

    95 °C 7 min

    Denaturation, annealing and elongation steps in 25 repetitions:

    95 °C 30 sec

    55 °C 30 sec

    72 °C 45 sec

    Final elongation:

    72 °C 8 min

    Final hold at 8 °C
14. Purify the colony PCR with NucleoFast® 96 PCR purification plates (Machinery-Nagel, Ref. 743100.10). In the final step dilute the samples in 50 $\mu$l of water.
15. Prepare Sanger sequencing reaction:

    5 $\mu$l of each sample

    1 $\mu$l primer pJET 10 $\mu$M, either forward or reverse:

    Forward: 5’ - CGA CTC ACT ATA GGG AGA GCG GC - 3’

    Reverse: 5’ - AAG AAC ATC GAT TTT CCA TGG CAG - 3’

    0.4 $\mu$l Big Dye v3.1(Life Technologies, Ref. 4337454)

    1.6 $\mu$l Sequencing Buffer 5× (Life Technologies, Ref. 4337454)
16. Sequencing amplification PCR program:

    Denaturation, annealing and elongation steps in 99 repetitions:

    95 °C 10 sec

    50 °C 5 sec

    60 °C 4 min

    Final hold at 8 °C
17. Proceed to Sanger sequencing.

## 11.3 Collection and fixation of bacterial cells from fecal samples

1. Work with fresh fecal samples, or samples stored at −80 °C.
2. In a 50 ml tube, resuspend 5 ml of the fecal samples in 30 ml of ice cold salt solution (0.9 % NaCl) by vortexing.
3. Centrifuge at 2,000 g for 2 min at 4 °C.
4. Transfer the supernatant to a new 50 ml tube.
5. Centrifuge the cells for 10 minutes at 4,000 g at 4 °C.
6. Remove the supernatant.
7. Resupend the cell pellet in 30 ml of ice cold salt solution containing 3.7 % of formaldehyde.
8. Let the sample incubate on ice for 1 hour.
9. Centrifuge at 4,000 g for 10 min at 4 °C.
10. Discard the supernatant.
11. Resuspend the pellet in 30 ml of ice cold salt solution and centrifuge again by the same conditions.
12. Resuspend the pellet in about 15 ml of salt solution and store at 4 °C for further use. Eventually, the cells can be stored at −20 °C.

## 11.4 Cultivation and fixation of *C. difficile*

1. Prepare Reinforced Clostridial Media (Oxoid, Ref: CM0149) by resuspending 38 g in 1 l of water and autoclave it.
2. After cooling down the media, add 1 ml of L-cystein (Sigma-Aldrich, Ref. C1276-10G) prepared to concentration 0.2g/ml and sterilized by filtration.
3. Transfer 9 ml of the media into anaerobic hungate culture tubes (Chemglass Life Sciences, Ref. CLS-4208) and close the tubes.
4. Prepare one culture tube with indicator of oxigen: Via injection introduce 10 $\mu$l of resazurin (Sigma-Aldrich, Ref. 199303-1G). The culture tube will turn violet. Do not add resazurin to all tubes, as it interferes with fluorescent dyes.
5. Replace the oxigen in the tubes by introducing nitrogen from compressed nitrogen bomb. Conduce the nitrogen from the bomb via plastic tube attached to a needle and allow the release of oxigen from the hungate culture tube via another needle. Let flow the nitrogen inside about 10 seconds and invert the tube several times to mix nitrogen with the media.
6. Wait until the oxigen control tube turns from violet color to original media color (transparent). It takes 30 - 60 minutes.
7. Inject *C. difficile* and cultivate at least 17 hours or more. When the density of cells increases, add 1 ml of 37 % formaldehyde for cell fixation and let incubate at 4 °C for at least 1 hour.
8. Transfer the cells into 50 ml plastic tubes.
9. Add 20 ml of salt solution (0.9 % NaCl).
10. Centrifuge at 4000 g for 10 min at 4 °C.
11. Discard the supernatant.
12. Resuspend the pellet in 30 ml of ice cold salt solution and centrifuge again by the same conditions.
13. Resuspend the pellet at about 15 ml of salt solution and store at 4 °C for further use. Eventually, the cells can be stored at −20 °C.

## 11.5 Extraction of DNA from bacterial samples

1. Perform the extraction in laminar flow cabin and sterilize all the buffers by filtration throught 0.2 $\mu$m pores filters.
2. Work with low amount of bacterial cells, the cell pellet volume should be maximally 5 $\mu$l. The cells should be resuspended in 220 $\mu$l PBS. Preparation of PBS:

   8 g NaCl

   0.2 g KCl

   1.44 g $Na_2HPO_4$

   0.24 g $KH_2PO_4$

   Add 1 liter of water
3. Add 350 $\mu$l lysozyme (Sigma-Aldrich, Ref. L6876-1G)10mg/ml and incubate 30 min at 37 °C.
4. Add 30 $\mu$l of 10 % SDS and incubate 30 min at 50 °C.
5. Add 1.6 $\mu$l of proteinase K at concentration 50mg/ml (Sigma-Aldrich, Ref. P2308-25MG) and continue incubating at 50 °C for 30 min.
6. Add 100 $\mu$l of 5M NaCl and 80 $\mu$l of CTAB (10 % in NaCl) and incubate 15 min at 65 °C.
7. Add 700 $\mu$l phenol:chloroform:isoamylalcohol (Sigma-Aldrich, Ref. P2069-100ML) and vortex for 1 min.
8. Centrifuge for 3 min at maximum speed.
9. Tranfer the supernatant to a new tube containing 700 $\mu$l chloroform and vortex for 1 min.
10. Centrifuge for 5 min at maximum speed.
11. Transfer the supernatant to a new tube containing 220 $\mu$l 5M $NH_4$-acetate and mix by inverting the tube up and down.
12. Add 1 $\mu$l of glycogen (Roche, Ref. 10901393001). Mix by inverting the tube up and down.
13. Add 500 $\mu$l isopropanol and vortex.
14. Incubate for 10 min at room temperature, vortex again and then store for 2-18 hours at −80 °C.
15. Centrifuge 45 min at 4 °C at 13,000 g.
16. Remove supernatant. Add 500 $\mu$l of 70 % ethanol. Vortex and centrifuge at maximum speed 10 min at 4 °C.
17. Discard the supernatant and centrifuge shortly to collect and discard all remaining ethanol.
18. Let remaining ethanol dry out, cca 30 min at room temperature at laminar flow cabin.
19. Resuspend in 100 $\mu$l water and vortex.
20. Store at 4 °C or at −20 °C for long-term storage.

# 11.6 Hybridization of bacteria by specific 16S rDNA probes

1. For hybridization of fecal bacteria, work with cells isolated and fixed according to the protocol 11.3. For hybridization of *C. difficile* as positive/negative controls, cultivate and fix *C. difficile* as described in the section 11.4. The protocol can be adapted for other bacterial species, too.
2. Prepare 1.5 ml tubes with 1 ml of fixed cells with the optical density 600 = 0.5 (equals approximatelly to a pellet of volume 10 $\mu$l after centrifugation). Always prepare one negative control which will undergo the same protocol, but will be not hybridized with fluorescent probes. Moreover, an additional negative sample can be prepared: it will undergo the same hybridization protocol but without flourescent probes and only cellular DNA stain will be added.
3. Centrifuge the samples at 13,000 g for 5 min at 4 °C and remove the supernatant.
4. After centrifugation, add 200 $\mu$l of ice-cold lysozime solution, which consists from:

   100 $\mu$l salt solution (0.9 % NaCl)

   40 $\mu$l 1M Tris-HCl

   60 $\mu$l lysozime (10mg/ml)
5. Incubate at 37 °C for 7 minutes. Put immediatelly on ice.
6. Add 1 ml of ice cold salt solution, vortex and centrifuge at 13,000 g for 5 min at 4 °C and repeat twice. After the third centrifugation, do not add salt solution.
7. Prepare hybridization solution (100 $\mu$l per sample):

   12.9 $\mu$l water

   40 $\mu$l formamide

   2 $\mu$l 1M Tris-HCl

   45 $\mu$l 2M NaCl

   0.1 $\mu$l 10 % SDS
8. Prepare wash solution for probe removal (1 ml per sample):

   529 $\mu$l water

   20 $\mu$l 1M Tris-HCl

   450 $\mu$l 2M NaCl

   1 $\mu$l 10 % SDS
9. Preheat the wash solution to 56 °C.
10. Add 100 $\mu$l of hybridization solution containing 10 $\mu$l of probe (the final concentration of probe will be 0.5 $\mu$g/ml) to the positive samples. Do not add any probes to the negative samples.

11. Incubate the samples at 54 °C for 3 hours. Cover the thermoblock by an aluminium foil or perform it at dark. Allow thermoblock shaking, if possible.
12. After 3 hours, add 1 ml of preheated wash solution and rise the temperature to 56 °C. Incubate at 56 °C for 15 minutes. Cover the thermoblock by an aluminium foil.
13. Centrifuge at 13,000 g for 5 minutes.
14. Discard the supernatant and add 1 ml of salt solution. Vortex. Repeat the centrifugation and discard the supernatant.
15. After the second centrifugation, resuspend the cell pellet in 1 ml of salt solution.
16. If staining of livining cells is required, add 10 $\mu$l of SYTO®62 at concentration 50 $\mu$M (Invitrogen, Ref. S11344).
17. In the flow cytometer, set the negative gates according to the negative control (without probes) and the second negative control stained with SYTO®62 only. The fluorescent area should be determined by comparison with the stained bacterial culture, but the sorting gate should be adjusted according to the comparison with the non-hybridized fecal sample, too.
18. Sort at least 10,000 fluorescent cells.

## 11.7 Positive control preparation for quantification of 454 libraries by qPCR

1. Work with bacterial DNA extracted according to the protocol in the section 11.5 and perform the PCR of your choice resulting in a product of about 300-600 bp length.
2. Load the whole PCR product on a 1.4 % gel and run the gel electrophoresis.
3. By a bladder knife cut out the DNA band corresponding to the PCR product length.
4. Purify the DNA from the gel using High Pure PCR Product Purification Kit (Roche, Ref. 11732668001). At the end, dilute the DNA sample in 20 $\mu$l of water.
5. Prepare the following mixture in 0.2 ml tubes placed on ice:

   1 $\mu$l dNTP 25 $\mu$M each (Thermo-Scientific, Ref. R0181)

   2.5 $\mu$l ligation buffer (New England Biolabs, Ref. M0202S)

   2.5 $\mu$l ATP (Agilent, Ref. 200340-81)

   2 $\mu$l Mg free buffer (New England Biolabs, Ref. M0320S)

   2 $\mu$l Quick blunting enzyme (New England Biolabs, Ref. E1201L)

   0.5 $\mu$l Klenow Fragment (3' $\rightarrow$ 5' exo-) (New England Biolabs, Ref. M0212S)

   0.5 $\mu$l Taq polymerase (New England Biolabs, Ref. M0320S)
6. Pipet 12 $\mu$l of the sample directly into the to the prepared mix in 0.2 ml tubes. Add 12 $\mu$l of water to the negative control.
7. Incubate the samples in PCR cycler with heated lid with the following program:

   12 °C 15 min

   37 °C 15 min

   72 °C 15 min
8. Add 1 $\mu$l of a Y adaptor with MID tags according to Zheng et al. (2011) at concentration 100 $\mu$M, e.g. adaptor Y3:

   Y3:

   5'- C*C*A* T*C*T* CAT CCC TGC GTG TCT CCG ACG ACT ACA CT*A* C*T*C* G*T -3'

   5'-p C*G*A* G*T*A GTG TGA CAC GCA ACA GGG GAT AGA CAA GGC ACA CAG GG*G* A*T*A* G*G -3'

   Asterisks (*) indicate a phosphorothioate-modified bond, p indicates a phosphorylation. Newly synthetized primers must be joined in a PCR cycler by a program in which temperature decreases 0.1 °C each second from 95 °C to 20 °C .
9. Add 1 $\mu$l of T4 DNA ligase (New England Biolabs, Ref. M0202S) and mix by pipetting up and down shortly.

10. Incubate at 12 °C overnight in a PCR cycler.
11. After incubation, bring the sample volume to 50 $\mu$l with water. Then remove possible self-ligated adaptors with Agencourt AMPure Beads XP ® (Beckman Coulter, Ref. A63880) as described in the section 11.9.
12. Prepare premix for PCR with emPCR primers:

    1 $\mu$l of the sample purified by magnetic beads.

    1 $\mu$l of forward emPCR primer:

    5'- CCA TCT CAT CCC TGC GTG TC -3'

    1 $\mu$l of reverse emPCR primer:

    5'- CCT ATC CCC TGT GTG CCT TG -3'

    9.5 $\mu$l of water

    12.5 $\mu$l GoTaq Green polymerase (Promega, Ref. M791A)
13. Incubate the samples in a PCR cycler with the following program:

    Initialization step:

    94 °C 2 min

    Denaturation, annealing and elongation steps in 30 repetitions:

    94 °C 30 sec

    60 °C 1 min

    72 °C 2 min

    Final elongation:

    72 °C 8 min

    Final hold at 4 °C
14. Load the whole volume on a 1.4 % gel.
15. Extract the PCR product band from the agarose gel and clone as described in the protocol section 11.2.
16. After confirmation by Sanger sequencing that the colony PCR product is inserted correctly and its exact size is known, amplify the rest of colony PCR product by PCR with emPCR primers as described above.
17. Purify the sample by Agencourt AMPure Beads XP® (Beckman Coulter, Ref. A63880) as described in the protocol section 11.9.
18. Quantify the purified PCR product by the Picogreen assay (Life Technologies, Ref.P11496).

## 11.8 Purification of human gut virome

1. Divide 30 ml of a fecal sample of a healthy volunteer into equal parts into six 50 ml tubes.
2. Resuspended the fecal samples in 30 ml of TBS (composed from 50 mM Tris, 150 mM NaCl).
3. Centrifuge the 50 ml tubes with resuspended fecal samples at 2,000 g for 2 min at 4 °C. In this stage the supernatants contain both bacteria and virus.
4. Centrifuge the supernatants at 4,000 g for 10 min at 4 °C twice.
5. Transfer 10 $\mu$l of the formed bacterial pellet to a fresh 50 ml tube and resuspend it in 16 ml of fresh TBS. It will be a control sample containing bacterial pellet only.
6. Collect the supernatants and distribute them into 1.5 ml tubes.
7. Centrifuge at 16,000 g for 45 min at 4 °C. The resulting pellet will still contain some remaining bacteria.
8. Collect the supernatant and pool the resulting supernatants and filter them consecutively per 5 $\mu$m, 0.8 $\mu$m, 0.45 $\mu$m and per 0.2 $\mu$m filters (Sartorius, Ref. 17594K).
9. To ensure that the last filtrate do not contain any non-viral particles, distribute it into 1.5 ml tubes and centrifuge at 16,000 g, for 30 min at 4 °C.
10. Pool the resulting supernatant (cca 16 ml) and filter again per 0.2 $\mu$m directly into 50 ml tubes.
11. In order to digest any uncapsulated DNA or RNA of non-viral origin, add the following enzymes:

    5 $\mu$l Turbo DNAse 2U/$\mu$l (Life Technologies, Ref. AM2238)

    0.2 $\mu$l bensoase (Novagen, Ref. 70746-4)

    2 $\mu$l RNAse A 20mg/ml (Roche, Ref. 10109142001)
12. Incubated for 1 hour at 37 °C and inactivate by incubation at 75 °C for 15 min.
13. Concentrate the viral particles by adding 4 ml of 2.5 M NaCl/20 % PEG-8000 (w/v, PEG-NaCl) to the filtered supernatant. The same volume of PEG-NaCl must be also added to the bacterial control sample, which was prepared in a previous step by adding 16 ml of TBS to the bacterial pellet.
14. Vortex the tubes and store for 1 hours on ice.
15. Centrifuge the tubes at 4,000 g for 30 min.
16. Resuspend the concentarted particles in 900 $\mu$l of TBS and fix by adding 100 $\mu$l of 37 % formaldehyde.
17. Incubate for 1 hour at 4 °C.
18. Add 200 $\mu$l of PEG-NaCl to each sample and incubate on ice for 30 min.
19. Centrifuge at 16,000 g for 30 min.
20. Discard the supernatant and resuspend the pellet in 990 $\mu$l of TBS.
21. Add 10 $\mu$l of 10 x diluted SYBR Green I nucleic stain (Life Technologies, Ref. S-7563) and heat at 80 °C for 10 min and cool down. Proceed to the cell sorting within 2 hours.

## 11.9 Purification of samples by magnetic beads

1. The Agencourt AMPure Beads XP® (Beckman Coulter, Ref. A63880) can be used for removal of fragment of any length by adjusting beads:sample volume ratio. For removal primers or small DNA fragments of length less than 400 bp, use beads:sample volume ratio 0.8:1. Establish the correct ratio by testing different volumes with a DNA ladder marker.
2. Vortex and incubate for 3 minutes at room temperature.
3. Place on magnetic particle concentrator (MPC, Life Technologies, Ref. 12321D). Wait 2 minutes.
4. Remove supernatant, do not touch the beads.
5. Add 500 $\mu$l of freshly prepared 70 % ethanol. Move the MPC up and down for 1 minute.
6. Remove supernatant. Add 500 $\mu$l of freshly prepared 70 % ethanol. Move the MPC up and down for 1 minute.
7. Remove supernatant. Remove the tubes from MPC and spin them shortly on microcentrifuge. Place back to MPC and wait for 30 seconds.
8. Remove carefully by a pipette all remaining etanol.
9. Open the tubes and place them in termoblock for 3 minutes incubation at 37 °C. Check if the bead pellet is completely dry (reminds dry soil).
10. Resuspend the bead pellet in any volume, depending on the pellet size and the following step.
11. Place the tube with beads on MPC and wait for 30 seconds.
12. Transfer the supernatant containing the selected DNA fragments into a fresh tube.

# 11.10 qPCR quantification of DNA fragments in 454 libraries

1. Each sample must be quantified in 2-3 replicates. Prepare the PCR premixes for positive qiantification control and for a negative control, too.

   10 $\mu$l of KAPA PROBE FAST qPCR Master Mix (2×) (Kapa Biosystems, Ref. KK4701)

   1.4 $\mu$l of forward emPCR primer:

   5'- CCA TCT CAT CCC TGC GTG TC -3'

   1.4 $\mu$l of reverse emPCR primer:

   5'- CCT ATC CCC TGT GTG CCT TG -3'

   1.2 $\mu$l of MGB-TaqMan probe 10 mM

   5'- 6-FAM - CTA TCC CCT GTT GCG TGT C - MGB -3' (synthetized by Life Technologies, Ref. 4316033)

   5 $\mu$l water

   1 $\mu$l of DNA

2. Quantify the DNA in the samples in a LightCycler 480 Instrument II (Roche, Ref. 05015278001) with the following program:

   Initialization step:

   95 °C 10 min

   Denaturation, annealing and elongation steps in 40 repetitions:

   95 °C 30 sec

   60 °C 15 sec

   68 °C 1 min

   Cooling down to 4 °C

3. Look at the Cp value for each sample and by comparing with Cp of the quantification control, calculate if your sample contains enough molecules for the selected region size of a 454 sequencing plate. First, calculate from the standard quantification curve the number of cycles in which no molecules would be present. As the length of the standard sample amplicon consider the amplicon length plus ligated adaptor A (41 bp) and adaptor B (50 bp).

$$\text{Number of molecules} = \frac{Concentration\ of\ each\ dilution \times Avogadro\ constant\ 6.023{\times}10^{23}}{10^9 \times Length\ of\ the\ standard\ sample\ amplicon\ (bp) \times Average\ weight\ of\ a\ base\ pair\ 650}$$

$$Logarithm = log_{10}(\text{Number of molecules})$$

Afterwards, slope and intercept (Point 0) of arrays in Cp values (y-axis) and in the Logarithm values (x-axis) must be calculated.

$$\text{Slope} = \frac{\sum(x-\overline{x}).(y-\overline{y})}{\sum(x-\overline{x})^2} \qquad Point\ 0 = \overline{y} - Slope.\overline{x}$$

4. For determination, whether the sample contains sufficient DNA amount for sequencing, the the minimal number of molecules required for loading on a picotiter plate must be calculated. Single 1/2 region requires 2,000,000 ssDNA molecules, single 1/4 region 790,000 ssDNA molecules, single 1/8 region 340,000 ssDNA molecules, single 1/16 region 125,000 ssDNA molecules. However, these regions may be further divided, if samples are multiplexed by MIDs. The number of molecules required is divided by the library volume, giving the number of ssDNA molecules per $\mu$l. This number must be further divided by 2, as the sample containes dsDNA molecules before PCR. Afterwards, the minimal quired Cp for selected sequencing size is calculated:

$$\text{Minimal required Cp} = log_{10}\left(\frac{Molecules\ in\ 1\mu l\ of\ sample\ in\ qPCR}{Sample\ volume}\right) . Slope + Point\ 0$$

5. The real Cp of the quantified sample must be lower than the calculated minimal Cp for the library (the concentration must be higher). The number of molecules per $\mu$l in the quantified sample can be calculated by the following equation:

$$\text{ssDNA molecules}/\mu\text{l} = 10^{\left(\frac{sample\ Cp - Point\ 0}{Slope}\right)}.2$$

Volume of the tested sample needed for performing the emPCR of the selected size may be calculated by the following equation:

$$\text{Volume of the sample for emPCR} = \frac{Number\ of\ beads\ required\ per\ sample}{ssDNA\ molecules\ /\ \mu l}$$

6. **Optional:** If the sample does not reach the minimal number of molecules required for sequencing, go back to the library sample and prepare PCR with emPCR primers and GoTaq Green polymerase as described previously, but in reduced volume, meaning that you have to aliquot your cca 46 $\mu$l of the sample into 23 PCR tubes.

   1 $\mu$l of primer emPCR-F:

   5'- CCA TCT CAT CCC TGC GTG TC -3'

   1$\mu$l of primer emPCR-R:

   5'- CCT ATC CCC TGT GTG CCT TG -3'

   1 $\mu$l of water 5 $\mu$l GoTaq Green polymerase (Promega, Ref. M7112)

   2 $\mu$l of sample

   Amplify your sample with low number of cycles, maximally 6 cycles:

   Initialization step:

   94°C 2 min

Denaturation, annealing and elongation steps in maximally 6 repetitions:

94 °C 30 sec

60 °C 1 min

72 °C 2 min

Final elongation:

72 °C 8 min

Final hold at 4 °C

Pool the volumes of all PCR reactions and purify the pooled sample with Agencourt AMPure Beads XP® as described previously in protocol 11.9 . At the end resuspend the beads in 50 $\mu$l of water and repeat the quantification by qPCR.

## 11.11 qPCR quantification of *C. difficile* genes toxin A, toxin B, specific 16S rDNA

1. As a positive control fix the *C. difficile* culture as described in the protocol 11.4.
2. Extract the DNA from the *C. difficile* culture and the bacterial samples for quantification as described in the protocol 11.5.
3. Quantify the sample by the Picogreen assay (Life Technologies, Ref.P11496). Adjust the volumes of the samples to have the same DNA concentration.
4. Prepare 10× dilutions of *C. difficile* sample.
5. Prepare a qPCR reaction with 16S rDNA primers as described in the section 11.1. Eventually, another 16S rDNA primers pairs can be used instead.

   12.5 $\mu$l Kapa SYBR® mix 2 × from the qPCR kit (Kapa, Ref. kk4610)

   1 $\mu$l 10 mM 16S rDNA forward primer

   1 $\mu$l 10mM 16S rDNA reverse primer

   9.5 $\mu$l water

   1 $\mu$l DNA / water
6. Run the qPCR with the following program in a LightCycler 480 Instrument II (Roche, Ref. 05015278001) selecting the fluorescence length of the SYBR® fluorophore.

   Initialization step:

   94 °C 3 min

   Denaturation, annealing and elongation steps in 40 repetitions:

   95 °C 30 sec

   55 °C 30 sec

   72 °C 30 sec

   Cool down to 40 °C
7. Adjust the DNA concentration by water, so that all samples will have the equal DNA concentration as the positive *C. difficile* control.
8. Use the samples with equal number of 16S rDNA molecules for quantification of specific *C. difficile* 16S rDNA sequences. Prepare the following mixture:

   12.5 $\mu$l qPCR mastermix with fluorescein (Qiagen, Ref. 330540)

   1 $\mu$l of *C. difficile* specific 16S rDNA primers (Qiagen, Ref. BPID00110AF)

   5 ng of DNA adjusted with water to the final reation volume of 25 $\mu$l

9. Use the following program selecting light absorption-emission spectra for fluorescein 465-510 nm.

   Initialization step:

   94 °C 10 min

   Denaturation, annealing and elongation steps in 40 repetitions:

   95 °C 15 sec

   60 °C 2 min

   Cool down to 40 °C

10. Quantify by comparison with the standard curve created with *C. difficile* dilutions.

11. The same quantification can be repeated for toxin A (Qiagen, Ref. BPVF00464AF) and toxin B (Qiagen, Ref. BPVF00463AF)

## 11.12 Shotgun 454 libraries for limited DNA samples

1. Work with DNA extracted according to the protocol 11.5. Bring the sample volume to 100 $\mu$l.
2. Shear the DNA using a Raypa UCI-50 sonicator. Sonicate at 2 °C for 3 minutes at maximum intensity, obtaining a fragment distribution of 200-1000 bp. The 2 °C temperature of water can be reached by adding ice to the water. Remove all ice before sonication.
3. Remove DNA fragments shorter than 400 bp by magnetic beads Agencourt AMPure Beads XP® (Beckman Coulter, Ref. A63880) as described in the section 11.9. In the last step of the purification protocol resuspend the bead pellet in 12 $\mu$l of water and introduce directly to the already prepared blunting mixture.
4. The blunting enzyme mix must be prepared in 0.2 ml tubes placed on ice:

   1 $\mu$l dNTP 25 $\mu$M each (Thermo-Scientific, Ref. R0181)

   2.5 $\mu$l ligation buffer (New England Biolabs, Ref. M0202S)

   2.5 $\mu$l ATP (Agilent, Ref. 200340-81)

   2 $\mu$l Mg free buffer (New England Biolabs, Ref. M0320S)

   2 $\mu$l Quick blunting enzyme (New England Biolabs, Ref. E1201L)

   0.5 $\mu$l Klenow Fragment (3' → 5' exo-) (New England Biolabs, Ref. M0212S)

   0.5 $\mu$l Taq polymerase (New England Biolabs, Ref. M0320S)

   Prepare one extra tube as a negative control.
5. Incubate the samples in a PCR cycler with heated lid with the following program:

   12 °C 15 min

   37 °C 15 min

   72 °C 15 min
6. Add 1 $\mu$l of a Y adaptor with MID tags according to Zheng et al. (2011) at concentration 100 $\mu$M, for example adaptors:

   Y3:

   5'- C*C*A* T*C*T* CAT CCC TGC GTG TCT CCG ACG ACT ACA CT*A* C*T*C* G*T -3'

   5'-p C*G*A* G*T*A GTG TGA CAC GCA ACA GGG GAT AGA CAA GGC ACA CAG GG*G* A*T*A* G*G -3'

   Y5:

   5'- C*C*A* T*C*T* CAT CCC TGC GTG TCT CCG ACG ACT ACG AG*T* A*G*A* C*T -3'

   5'-p G*T*C* T*A*C TCG TGA CAC GCA ACA GGG GAT AGA CAA GGC ACA CAG GG*G* A*T*A* G*G -3'

Asterisks (*) indicate a phosphorothioate-modified bond, p indicates a phosphorylation. A newly synthetized primers must be joined in a PCR cycler by a program in which temperature decreases 0.1 °C each second from 95 °C to 20 °C .

7. Add 1 $\mu$l of T4 DNA ligase (New England Biolabs, Ref. M0202S) and mix by pipetting up and down shortly.
8. Incubate at 12 °C overnight in a PCR cycler.
9. After incubation, remove possible self-ligated adaptors with Agencourt AMPure Beads XP (Beckman Coulter, Ref. A63880) as described in the section 11.9. In the last step, dilute the beads pellet in 50 $\mu$l of water.
10. Repeat the whole purification with beads 4 more times using the same beads:sample volume ratio. Finaly dilute in 50 $\mu$l of water.
11. Check the library quality by control PCR. Prepare PCR premix:

    1 $\mu$l of sample

    1 $\mu$l of emPCR forward primer:

    5'- CCA TCT CAT CCC TGC GTG TC -3'

    1 $\mu$l of emPCR reverse primer:

    5'- CCT ATC CCC TGT GTG CCT TG -3'

    9.5 $\mu$l of water

    12.5 $\mu$l GoTaq Green polymerase

    Also prepare one extra tube for negative control without DNA.
12. Incubate the samples in a PCR cycler with the following program:

    Initialization step:

    94 °C 2 min

    Denaturation, annealing and elongation steps in 25 repetitions:

    94 °C 30 sec

    60 °C 1 min

    72 °C 2 min

    Final elongation:

    72 °C 8 min

    Final hold at 4 °C
13. Visualize in a 0.8 % agarose gel. Make sure that no self-ligated adaptors are present - no band of about 100 bp should be visible. If yes, the whole purification with magnetic beads must be repeated at least one more time. If no self-ligated adaptors are visible on the gel, you can continue to the quantification by qPCR described in the protocol section 11.10.

## 11.13 Staining of bacterial DNA and RNA

1. For staining of bacterial DNA use bacterial cells fixed according to the protocol in the section 11.3.
2. Prepare 1ml of fixed cells with the optical density 600 = 0.5 (equals approximatelly to 10 $\mu$l of bacterial pellet after centrifugation). Always prepare one negative control which will undergo the same protocol, but will not be stained. For combined staining of RNA and DNA, prepare 4 replicates:

   DNA staining + RNA staining

   DNA staining

   RNA staining

   Negative sample without staining
3. For DNA staining, add 10 $\mu$l of SYTO®62 at concentration 50 $\mu$M (Life Lechnologies, Ref. S11344).
4. For RNA staining, add 10 $\mu$l of pyronin Y at concentration 0.1 mM (Sigma-Aldrich, Ref. P9172-1G).
5. Incubate at dark at 4 °C for at least 1 hour and proceed to flow cytometry.

## 11.14 Staining of IgA coated cells

1. For staining of bacterial DNA use bacterial cells fixed according to the protocol in the section 11.3.
2. Prepare 1ml of fixed cells with the optical density 600 = 0.5 (equals approximatelly to 10 $\mu$l of bacterial pellet after centrifugation) for each of the 4 replicates:

   IgA human + DNA staining

   IgA mouse + DNA staining

   DNA staining only

   Negative sample without any staining
3. For DNA staining, add 10 $\mu$l of SYTO®62 at concentration 50 $\mu$M (Invitrogen, Ref. S11344).
4. For IgA mouse staining, add 10 $\mu$l anti-mouse IgA labelled with FITC (Life Technologies, Ref. M31001)
5. For human IgA staining, add 10 $\mu$l of anti-Human IgA Secondary Antibody, FITC conjugate (Life Technologies, Ref. A24459).

Chapter 12

# Appendix: Programming scripts

## 12.1 Bayesian networks and extraction of Markov blankets

The script operates with a table containing fold-change values obtained by comparison of the positive and negative fraction pairs in the programming script in the section 12.4. A metadata table is needed, too. The two tables should have the same sample names.

```
library(made4)
library(bnlearn)
library(Rgraphviz)
fold <- read.table(file="fold.txt", sep="\t", header=TRUE)
head(fold)
#  Sample Act.pos.Bifidobacterium Act.pos.Clostridium.IV Act.pos.Coprococcus
#1 CDIneg01               0.000000              0.000000            0.000000
#2 CDIneg02               0.000000              3.466313            0.000000
#3 CDIneg03               0.000000              4.440353            0.000000
#4 CDIneg04               3.279490              8.031787            0.000000
#5 CDIneg05               3.970326              0.000000            0.000000
#6 CDIneg06               0.000000              0.000000            2.233341
rownames(fold) <- as.character(fold$Sample)
fold <- fold[, 2:ncol(fold)]
meta <- as.data.frame(read.table(file="metadatajoined.csv", sep=",", header=TRUE))
head(meta)
#  Sample MD.CDI MD.ATBagainstCDI MD.ATBpromotingCDI MD.ATBneutralCDI
#1 CDIneg01     no              yes                 no               no
#2 CDIneg02     no              yes                yes               no
#3 CDIneg03     no              yes                yes              yes
#4 CDIneg04     no              yes                yes              yes
#5 CDIneg05     no               no                 no               no
#6 CDIneg06     no               no                 no               no
rownames(meta) <- as.character(meta$Sample)
meta<-meta[ ,2:ncol(meta)]
meta <- meta[rownames(fold), ]
#replace the negative values by neg, the positive values by pos and the 0 by Zero
fold.filt<-fold
fold.filt[fold.filt<0] <- -1
fold.filt[fold.filt>0] <- 1
for(i in 1:ncol(fold.filt)) fold.filt[, i] <- as.character(fold.filt[, i])
fold.filt[fold.filt=="-1"] <- "neg"
fold.filt[fold.filt=="1"] <- "pos"
fold.filt[fold.filt=="0"] <- "Zero"
data <- cbind(fold.filt, meta)
save(data, file="data.RData")
load(file="data.RData")
write.table(data, file="databnlearn.txt", quote=F, sep="\t")
dat.bn<-read.table(file="databnlearn.txt", sep="\t")
```

```
#define the colors of the nodes corresponding to the medical variables
nodeColor <- rep("white", ncol(dat.bn))
nodeColor[grep("MD.", colnames(dat.bn))] <- "yellow"
nodeColor[grep("IgA.pos.", colnames(dat.bn))] <- "lightcoral"
nodeColor[grep("Act.pos.", colnames(dat.bn))] <- "plum2"
nodeColor[grep("IgA.neg.", colnames(dat.bn))] <- "lightskyblue"
nodeColor[grep("Act.neg.", colnames(dat.bn))] <- "mediumspringgreen"
names(nodeColor) <- colnames(dat.bn)
bn.res <- hc(dat.bn)
# remove singleton nodes
cond <- unlist(lapply(bn.res$nodes, FUN=function(x) if(length(x$parents)==0&length(x$
    children)==0) return(FALSE) else return(TRUE) ))
bn.res$nodes <- bn.res$nodes[cond]
graph.res <- graphviz.plot(bn.res)
attrs <- list(node=list(shape="ellipse", fixedsize=FALSE))
eAttrs <- list()
nAttrs <- list()
eAttrs.names <- apply(arcs(bn.res), MARGIN=1, FUN=function(x) paste(x, collapse="~"))
eAttrs$arrowhead <- rep("none", length(eAttrs.names))
names(eAttrs$arrowhead) <- eAttrs.names
eAttrs$dir <- rep("none", length(eAttrs.names))
names(eAttrs$dir) <- eAttrs.names
nAttrs.names <- nodes(bn.res)
nAttrs$fillcolor <- nodeColor[nAttrs.names]
names(nAttrs$fillcolor) <- nAttrs.names
nAttrs$color <- rep("gray48", length(nAttrs.names))
names(nAttrs$color) <- nAttrs.names
eAttrs$color <- rep("gray48", length(eAttrs.names))
names(eAttrs$color) <- eAttrs.names
#create the pdf with the network
pdf(file="bayesian.network.pdf", width=21, height=21)
plot(graph.res, edgeAttrs=eAttrs, attrs=attrs, nodeAttrs=nAttrs, cex=100)
dev.off()
```

Extraction of Markov blankets, in this case node of the medical variable CDI is shown here:

```
library(bnlearn)
library(Rgraphviz)
#define function for plotting a graph
myPLot <- function(myGraph, filename){
  attrs <- list(node=list(shape="ellipse", fixedsize=FALSE))
  eAttrs <- list()
  nAttrs <- list()

  myarcs.l <- strsplit(names(myGraph@edgeData@data), split="[|]")
  myarcs <- c()
  for(i in 1:length(myarcs.l)) myarcs <- rbind(myarcs, myarcs.l[[i]])

```

```
  eAttrs.names <- apply(myarcs, MARGIN=1, FUN=function(x) paste(x, collapse="~"))
  nAttrs.names <- nodes(myGraph)

  eAttrs$arrowhead <- rep("none", length(eAttrs.names))
  names(eAttrs$arrowhead) <- eAttrs.names

  eAttrs$dir <- rep("none", length(eAttrs.names))
  names(eAttrs$dir) <- eAttrs.names

  eAttrs$color <- rep("gray48", length(eAttrs.names))
  names(eAttrs$color) <- eAttrs.names

  nAttrs$fillcolor <- nodeColor[nAttrs.names]
  names(nAttrs$fillcolor) <- nAttrs.names

  nAttrs$color <- rep("gray48", length(nAttrs.names))
  names(nAttrs$color) <- nAttrs.names

  pdf(file=filename)
  plot(myGraph, edgeAttrs=eAttrs, nodeAttrs=nAttrs, attrs=attrs)
  dev.off()
}
dat.bn<-read.table(file="databnlearn.txt", sep="\t")
#define color of the nodes correspondign to the medical variables
nodeColor <- rep("yellow", ncol(dat.bn))
nodeColor[grep("MD.", colnames(dat.bn))] <- "yellow"
nodeColor[grep("IgA.pos.", colnames(dat.bn))] <- "lightcoral"
nodeColor[grep("Act.pos.", colnames(dat.bn))] <- "plum2"
nodeColor[grep("IgA.neg.", colnames(dat.bn))] <- "lightskyblue"
nodeColor[grep("Act.neg.", colnames(dat.bn))] <- "mediumspringgreen"
names(nodeColor) <- colnames(dat.bn)
bn.res <- hc(dat.bn)
# remove singleton nodes
cond <- unlist(lapply(bn.res$nodes, FUN=function(x) if(length(x$parents)==0&length(x$
    children)==0) return(FALSE) else return(TRUE) ))
bn.res$nodes <- bn.res$nodes[cond]
graph.res <- graphviz.plot(bn.res)
#select the node name
myNode <- c("MD.CDI")
mySet <- c(myNode, bn.res$nodes[[myNode]]$mb)
myGraph <- subGraph(mySet, graph.res)
#plot the graph using predefined function mygraph
myPLot(myGraph, filename="node.MD.CDI.pdf")
```

## 12.2 Canonical correspondence analysis with "envfit" function

The script works with a table containing proportions (in %) of bacterial genera in samples and also with a metadata table. The two tables should contain the same sample names.

```
library(vegan)
abund <- read.table(file="taxonomy-in-percentage.txt", sep="\t", header=TRUE)
head(abund)
#               Acidaminococcus Actinomyces Akkermansia  Alistipes Anaerococcus
#ActnegCDIneg01               0 0.000000000   0.0000000 0.00000000            0
#ActnegCDIneg02               0 0.009369024   6.2414232 2.24691236            0
#ActnegCDIneg03               0 0.001981776   0.3353164 0.00000000            0
#ActnegCDIneg04               0 0.000000000   0.0000000 0.00000000            0
#ActnegCDIneg05               0 0.000000000   0.0000000 0.01940015            0
#ActnegCDIneg06               0 0.001973060   3.2926423 0.13495729            0

metadata <- read.csv2(file="metadata.csv", sep=",", header=TRUE)
head(metadata)
#         Sample MD.Fraction MD.CD MD.CDIrec MD.int MD.chemotherapy NV.CD16S NV.toxA NV.toxB  NV.againstCDI NV.cephalofluoroprot  NV.penicillinenutral
#1 ActnegCDIneg01    ActiveNeg   neg        no     no               no        0       0          0          14000                   0                     0
#2 ActnegCDIneg02    ActiveNeg   neg        no     no               no        0       0          0           7000               54000                     0
#3 ActnegCDIneg03    ActiveNeg   neg        no     no               no   0.0002       0          0           6000               12000                  6000
#4 ActnegCDIneg04    ActiveNeg   neg        no     no              yes   0.0008       0          0          21000               36000                 51500
#5 ActnegCDIneg05    ActiveNeg   neg        no     no               no        0       0          0             0                   0                     0
#6 ActnegCDIneg06    ActiveNeg   neg        no     no               no   0.0002       0          0             0                   0                     0

#joining metagata and bacterial proportions files
for(i in 1:ncol(metadata)) metadata[, i] <- as.character(metadata[, i])
rownames(metadata) <- metadata$Sample
metadata <- metadata[rownames(abund), ]
#selection one of the four fractions
group <- "ActivePos"
ind <- which(metadata$MD.Fraction==group)
abund.t <- abund[ind, ]
metadata.t <- metadata[ind, ]
abund.t <- abund.t[, which(apply(abund.t, MARGIN=2, FUN=function(x) if(sum(x)>=0.001) return(TRUE) else return(FALSE))==TRUE)]
#selection of the variables to be tested
```

```
33 dataTemp <- cbind(abund.t, NV.CD16S=as.numeric(metadata.t$NV.CD16S), NV.toxA=as.numeric(
       metadata.t$NV.toxA), NV.toxB=as.numeric(metadata.t$NV.toxB), NV.againstCDI2=as.
       numeric(metadata.t$NV.againstCDI2), NV.cephalofluoroprot=as.numeric(metadata.t$NV.
       cephalofluoroprot), NV.penicillinenutral=as.numeric(metadata.t$NV.penicillinenutral),
        MD.againstCDI=as.factor(metadata.t$MD.againstCDI), MD.cephalofluoroprot=as.factor(
       metadata.t$MD.cephalofluoroprot), MD.penicillinenutral=as.factor(metadata.t$MD.
       penicillinenutral),  MD.CD=as.factor(metadata.t$MD.CD))
34 # canonical correspondence analysis
35 res.cca <- cca(abund.t ~ NV.CD16S + NV.toxA + NV.toxB + NV.againstCDI2 + NV.
       cephalofluoroprot + NV.penicillinenutral + MD.cephalofluoroprot + MD.
       penicillinenutral + MD.againstCDI + MD.CD,  data=dataTemp)
36 pct.var <- format(summary(res.cca)$concont[[1]][2,1:2]*100, digits=4)
37 #plot the results, change the name of the plot according to the selected fraction
38 pdf(file=paste("ActivePos-test-ud", group, "pdf", sep="."))
39 res.cca.plot <- plot(res.cca, type="none", xlab=paste("CCA1", paste("(", pct.var[1], "%",
        ")", sep=""), sep=" "),
40           ylab=paste("CCA2", paste("(", pct.var[2], "%", ")", sep=""), sep=" "))
41 my.levels <- rownames(res.cca.plot$centroids)
42 my.samples <- rownames(res.cca.plot$sites)
43 text(x=res.cca.plot$sites[c(1:12),1], y=res.cca.plot$sites[c(1:12),2], col="blue", cex
       =0.5)
44 text(x=res.cca.plot$sites[c(13:24),1], y=res.cca.plot$sites[c(13:24),2], col="red", cex
       =0.5)
45 indF1 <- grep("MD.CD", rownames(res.cca.plot$centroids))
46   text(x=res.cca.plot$centroids[indF1, 1], y=res.cca.plot$centroids[indF1, 2], col="grey"
         , cex=0.7, labels=rownames(res.cca.plot$centroids)[indF1])
47   arrows(x0=0, y0=0, x1=res.cca.plot$centroids[indF1, 1], y1=res.cca.plot$centroids[indF1
         , 2], col="red", length=0)
48
49 plot(envfit(res.cca, dataTemp),p.max=0.01,col="black", cex=0.7)
50 dev.off()
51 #print which variables are significantly influencing the ordination of samples
52 a<-envfit(res.cca, dataTemp)
53 a
54 #print which numerical variables are significant
55  b<-a$vectors
56  pval<-b$pval
57  e<-scores(a, display= "vectors")
58  d<-cbind(pval, e)
59  f<-as.data.frame(d)
60  indexplus<-f$pval<0.01
61  f2<-f[indexplus, ]
62 f2
```

## 12.3 Checking for presence of 454 adaptors

Extraction of sequences with the selected MID is performed by sffinfo tool; in this case it is the adaptor Y5 with sequence 5'- ACGAGTAGACT -3':

```
$ sfffile -o sequences-without-adaptors.sff ACGAGTAGACT/3@original-sequences.sff
$ sffinfo -s sequence-without-adaptors.sff > sample.fna
$ sffinfo -q sequences-without-adaptors.sff > sample.qual
```

Afterwards, the sequences are checked for presence of an adaptor in the end of a sequence and for the dimeric forms of the adaptors, for adaptorY5.fasta:

```
>adaptorY5
GTCTACTCGTGACACGCAACAGGGGATAGACAAGGCACACAGGGGATAGG
```

```
$formatdb -i sample.fna -p F -o F -n sample_gd -t sample_gd
$formatdb -i adaptorY5.fasta -p F -n adaptorY5
$blastall -p blastn -i sample.fna -d  adaptorY5 -o sample.blout -e 0.001 -m 8
```

The parts of sequences, in which remaining adaptors were found, are trimmed by a R script, which uses the sample.blout table as a template for trimming.

```
library(Biostrings)
blast.query <- read.DNAStringSet("sample.fna","fasta")
# The names of blast.query are modified:
names(blast.query) <- unlist(lapply(strsplit(names(blast.query), split=" "), FUN=function
    (x) x[1]))
blast.out <- read.table(file="sample.blout")
# The data is adapted according to the output format:
colnames(blast.out) <- c("qseqid", "sseqid", "identity", "alignmentLength", "
    numberofmismatches", "numberofgapopenings",
      "qstart", "qend", "sstart", "send", "evalue", "bitscore")
blast.out$qseqid <- as.character(blast.out$qseqid)
blast.out$sseqid <- as.character(blast.out$sseqid)
# Only queries with identity more than 80% is kept.
blast.out <- blast.out[which(blast.out$identity>=80), ]
blast.out <- blast.out[which(blast.out$qstart<blast.out$qend), ]
# If more aligments are identified, only the longest is kept.
blast.out.l <- by(data=blast.out, INDICES=blast.out$qseqid, FUN=function(x){
    qstart <- x$qstart
    qend <- x$qend
    width <- abs(qend-qstart)
    ind <- which(width==max(width))[1]
    return(x[ind, ])
  }, simplify=TRUE)
blast.out <- c()
for(i in 1:length(blast.out.l)) blast.out <- rbind(blast.out, blast.out.l[[i]])
```

```
# The sequences from blast.out$qseqid in blast.query are cut according to the values in "qstart" and "qend"
query.in <- as.character(blast.query)
names(query.in) <- names(blast.query)
blast.out$seq <- query.in[blast.out$qseqid]
query.out <- apply(blast.out, MARGIN=1, FUN=function(x) substr(x[13], start=1, stop=(as.numeric(x[7])-1)))
names(query.out) <- blast.out$qseqid
# Detection of selfligated adaptor dimers
query.out <- query.out[which(query.out!="")]
query.out <- DNAStringSet(query.out)
write.XStringSet(query.out, file="sample.tagCleaned.by.blast.fna")
```

Afterwards, join the cut sequences with the sequences which have not been modified:

```
$ cat sample-extract.out.fas sample.tagCleaned.by.blast.fna >> sample-noadaptor.fasta
```

## 12.4 Fold-change comparison of genera proportions in bacterial fractions pairs

```
library(gtools)
library(edgeR)
test<-read.table(file="contigency-genus.txt", sep="\t", header=T)
#the table must contain real counts of reads for each genera
#              X ActnegCDIneg01 ActnegCDIneg02 ActnegCDIneg03 ActnegCDIneg04
# 1 Acidaminococcus             0             0             0             0
# 2     Actinomyces             0            17             5             0
# 3     Akkermansia             0         11325           846             0
# 4       Alistipes             0          4077             0             0
# 5    Anaerococcus             0             0             0             0
# 6    Anaerostipes             1           187            83             0
#set the biological coefficient of variation
bcv <- 0.3
# This is an example for active-F sample CDI01, repeat this with more samples
Act.CDIneg01<-test[,c("ActnegCDIneg01", "ActposCDIneg01")]
y<-DGEList(counts=Act.CDIneg01, group=1:2)
et <- exactTest(y, dispersion=bcv^2)
ettable<-et$table
test$Act.CDIneg01pvalue<-ettable$PValue
test$Act.CDIneg01logFC<-ettable$logFC
indexpos<-test$Act.CDIneg01pvalue<0.01 & test$Act.CDIneg01logFC>0
Act.pos.CDIneg01<-test[indexpos, ]
sel<-c("X", "Act.CDIneg01logFC")
Act.pos.CDIneg01.sel<-Act.pos.CDIneg01[,sel]
x<-colnames(Act.pos.CDIneg01.sel)
colnames(Act.pos.CDIneg01.sel)<-replace(x, x=="Act.CDIneg01logFC", "Act.CDIneg01")
indexneg<-test$Act.CDIneg01pvalue<0.01 & test$Act.CDIneg01logFC<0
Act.neg.CDIneg01<-test[indexneg, ]
sel<-c("X", "Act.CDIneg01logFC")
Act.neg.CDIneg01.sel<-Act.neg.CDIneg01[,sel]
x<-colnames(Act.neg.CDIneg01.sel)
colnames(Act.neg.CDIneg01.sel)<-replace(x, x=="Act.CDIneg01logFC", "Act.CDIneg01")
ActCDIneg01<-rbind(Act.neg.CDIneg01.sel, Act.pos.CDIneg01.sel)
#join all the fold-change lists, here is an example for five samples:
list.of.data.frames <- list(ActCDIneg01, ActCDIneg02, ActCDIneg03, ActCDIneg04,
    ActCDIneg05)
merged.data.frame <- Reduce(function(...) merge(..., all=T), list.of.data.frames)
merged <- t(merged.data.frame[,1:ncol(merged.data.frame)])
write.table(merged, file="edgeR.txt", sep="\t", quote=F, col.names=F)
#open the table and replace NA for 0
#Create a heatmap without clustering
library(RColorBrewer)
library(gplots)
```

```
43 foldchanged <- read.table ("edgeR.txt", header=TRUE, row.names=1, sep="\t")
44 rownames(foldchanged)
45     colors = c(seq(-15,-0.000001,length=3),seq(-0.000001,0.000001,length=2),seq
       (0.000001,15,length=3))
46     my_palette <- colorRampPalette(c("blue", "white", "red"))(n = 7)
47 lwid = c(0.5,3)
48 lhei = c(0.5,3)
49 pdf("edgeR.pdf",  width=20, height=10)
50 heatmap.2(as.matrix(foldchanged), col=my_palette,
51         breaks=colors, dendrogram = "none", Rowv = FALSE, Colv = FALSE, density.info="
           none", trace="none",
52           symm=F,symkey=F,symbreaks=T, scale="none", cexRow=1, cexCol=1, lwid = lwid,
               lhei = lhei, mar=c(18,22))
53 dev.off()
```

## 12.5 Mapping of reads on a reference genome

**Bowtie2:**

The fastq of filtered sequences (CDall50.fastq) is mapped to the complete genome of *C. difficile* 630 strain sequenced in the Sanger Institute. The result is converted to the .bam format.

```
$bowtie2-build complete_reference_CD630.sanger.fasta complete630refsanger
$samtools faidx complete_reference_CD630.sanger.fasta
$bowtie2 -x complete630refsanger -U CDall50.fastq -S CD50.630sanger.bowtieveryfast.sam --
    very-fast
$samtools view -bt complete_reference_CD630.sanger.fasta.fai CD50.630sanger.
    bowtieveryfast.sam -o $CD50.630sanger.bowtieveryfast
$samtools sort CD50.630sanger.bowtieveryfast CD50.630sanger.bowtieveryfastsorted
$samtools index CD50.630sanger.bowtieveryfastsorted.bam
```

**Samtools:**

At the beginning change the reference sequence in format .fasta into fasta.fai format and then perform the mapping.

```
$ samtools faidx reference.fasta
$ samtools view -bt reference.fasta.fai sample.sam -o sample-output
$ samtools sort sample-output sample-sorted
$ samtools index sample-sorted.bam
```

## 12.6 Sequence processing by Prinseq

The sequences in sample.fastq file are filtered for entropy (>70), quality in 10 bp windows (>25), sequence length (>50) and N bases (<5):

```
$perl prinseq-lite.pl -verbose -fastq sample.fastq -lc_method entropy
-lc_threshold 70 -trim_qual_right 25 -trim_qual_window 10
-trim_qual_type mean -trim_qual_rule lt -min_len 50
-ns_max_p 5 -out_good sample-outfile -out_bad sample-outfilebad
```

By the following command, the sequences of length of length +/- 1 bp of the expected amplicon length are filtered, in this example the length of amplicon of the selected region of the toxin gene B is 411 bp:

```
$perl prinseq-lite.pl -fastq amplicon.join.fq -out_format 3 -min_len 410
-max_len 412 -ns_max_n 0
```

## 12.7 Setting a polygonal gate for FC plots

This example works with .fcs files, however teher is a variety of FC equipments which may have different file extensions, such as .lmd. Therefore, the pattern of column names of the .fcs/.lmd files must be checked before starting the analysis and it must be modified in the script.

```
library (flowCore)
library (flowViz)
#read all the .fcs files in the folder in alphabetic order:
PATTERN<-".fcs"
ALTNAM<-TRUE
TRANS<-FALSE
COLPATT<-"SSC.A|FSC.A|PerCP.Cy5.5.A|PE.A"
PATH<-"."
fs.fast<-read.flowSet(path=PATH, alter.names=ALTNAM, transformation=TRANS, pattern=
    PATTERN, column.pattern=COLPATT)
#set the polygonal gate for area of bacterial size in side scatter - forward scatter bi-
    plot:
sqrcut <- matrix(c(299,299,399,899,799, 1,499,899,899,1),ncol=2,nrow=5)
  colnames(sqrcut) <- c("SSC.A","FSC.A")
  pgtriangle<- polygonGate(filterId="nonDebris", .gate= sqrcut)
fsfilt<-Subset(fs.fast, pgtriangle)
# draw a gate for bacteria with low RNA content and low DNA content in PE - PerCP.Cy5 bi-
    plot, visualizing fluorescence of pyronins on y-axis (PE.A) and fluorescence of SYTO
    62 on x-axis (PerCP.Cy5.5.A):
sqrcut <-matrix(c(0,0,560,560,0,0,630,630,0,0),ncol=2,nrow=5)
     colnames(sqrcut) <- c("PE.A","PerCP.Cy5.5.A")
     neggate <- polygonGate(filter= sqrcut)
png (file = "pyronin-syto62-negative-gate.png", width=800, height=400)
xyplot(`PE.A` ~ `PerCP.Cy5.5.A`, data=fsfilt, smooth=FALSE, colramp=rainbow, filter=
    neggate)
dev.off()
#count the bacteria within this "negative" gate:
sqrcut <- matrix(c(0,0,560,560,0,0,630,630,0,0),ncol=2,nrow=5)
     colnames(sqrcut) <- c("PE.A","PerCP.Cy5.5.A")
    neggate<- polygonGate(filter= sqrcut)
resultneg<- filter(fsfilt, neggate)
summary(resultneg)
summary(result)
```

## 12.8 Visualization of annotated ORFs in a contig

This is an example for the contig83 which contains 5 annotated ORFs.

```
library(genePlotR)
df1 <- data.frame(name = c("contig83"), start = c(1), end = c(1471), strand = c(1), col = c("blue"))
dna_seg1 <- dna_seg(df1)
df2 <- data.frame(name = c("start", "contig83-1", "contig83-2", "end"), start = c(0, 29, 382, 1470), end = c(1, 235,1440, 1471), strand = c(1, -1, -1,1),
col = c("black", "blue", "blue", "black"))
df3 <- data.frame(name = c("start", "seg", "coiled-coil", "P-loop containing nucleoside triphosphate hydrolases", "DnaB_C", "end"), start = c(0,172,160,549,561,1470), end = c(1,205,223,1305,1257, 1471), strand = c(1,-1,-1,-1, -1, 1), col = c("black","red", "yellow","grey", "brown", "black"))
dna_seg1 <- dna_seg(df1)
dna_seg2 <- dna_seg(df2)
dna_seg3 <- dna_seg(df3)
dna_segs <- list(dna_seg1, dna_seg2, dna_seg3)
pdf (file = "contig83.pdf")
plot_gene_map (dna_segs = dna_segs)
dev.off()
```

## 12.9 Visualization of the whole genome coverage

This script works with .bam format of mapping which may be obtained by conversion of the .sam format into .bam format.

```
library(Rsamtools)
require(ShortRead)
require(chipseq)
bamName="sample.bam"
#==========retrieve headers -reference genome and length
ft<- scanBamHeader(bamName)[[1]][["targets"]]
print(ft)
#======== Define ScanBam parameters
what <- scanBamWhat()
which <- GRanges(names(ft), IRanges(1, ft))
print(which)
param <- ScanBamParam(which=which, what=what)
#========== Read Bam
bam <- scanBam(bamName, param = param)
IRanges   <- IRanges(start = bam[[1]][["pos"]], width=bam[[1]][["qwidth"]])
 Cov       <- coverage(IRanges)
 Peaks     <- slice(Cov, 0)
png(file="sample.png",  width = 480, height = 480)
coverageplot(Peaks, main=names(bam)[1], ylim=c(0, 50))
dev.off()
max(as.vector(Peaks[[1]]))
```

Chapter 13

# Appendix: Abstracts of other publications not related to the thesis

# Human monoclonal antibodies to *Clostridium difficile* toxins (MK-3415A) mediate gut microbiome restoration

**Džunková, M., D'Auria, G., Moya, A., Kelly, C., Chen, X.**

**Submitted**

The increasing incidence of *Clostridium difficile* infection (CDI) demonstrates that the current antibiotic treatment approaches are inadequate, as they disrupt the normal gut microbiome protecting against CDI recurrence. Human monoclonal antibody MK-3415A to *C. difficile toxin* A and toxin B has been shown to reduce significantly the recurrence of CDI in mice and humans, but its mechanisms in preventing recurrent CDI is not well understood.

Experimental mice have been pretreated by Clindamycin and infected by *C. difficile*. We compared the bacterial diversity of the gut microbiome of CDI mice treated with MK-3425A, non-treated mice, mice treated with Vancomycin (standard antibiotic treatment of CDI) and mice treated with Vancomycin combined with MK-3415A.

*C. difficile* infection simulation resulted in the prevalence of *Enterobacter* species. Sixty % of mice of the vehicle group died after two days and their microbiome was almost exclusively formed by *Enterobacter*. MK-3415A achieved to decrease *Enterobacter* levels and to restore *Blautia*, *Akkermansia* and *Lactobacillus* levels which had been the most important components of the original mice microbiota. Vancomycin treated mice had short life span, which was in contrast to the mice treated by MK-3415A antibody combined with Vancomycin. Vancomycin treatment decreased bacterial diversity with predominant *Enterobacter* and *Akkermansia*, while *Staphylococcus* expanded after the Vancomycin treatment finished. In contrast, mice treated by Vancomycin combined with MK-3415A also experienced decreased bacterial diversity during the Vancomycin treatment, however, they were able to recover their initial *Blautia* and *Lactobacillus* proportions, even though episodes of *Staphylococcus* overgrowth were being detected during the last experiment days.

In conclusion, the antibody MK-3415A facilitates the normalization of the gut microbiota. In contrast, Vancomycin decreases bacterial diversity and reduces the proportions of the most common species of the normal microbiota, what increases the risk of expansion of opportunistic pathogens or disease recurrence.

# Genome of *Lactobacillus plantarum* strain 19L3 as starter culture for "Slovenská bryndza" ovine cheese

**D'Auria, G., Džunková, M., Moya, A., Tomáška, M., Kolšta, M., Kmet, V.**

**Genome Announcements (2014) 2: e00292-14**

The genome sequence of *Lactobacillus plantarum* isolated from ovine cheese is presented here. This bacterium is proposed as a starter strain, named 19L3, for "Slovenská bryndza" cheese, a traditional Slovak cheese fulfilling European Food Safety Authority (EFSA) requirements.

# Estudios de epidemiología molecular sobre población inmigrante en España

**González-Candelas, F., Bracho, M.A., Comas, I., D'Auria, G., Džunková, M., García, R., Gosalbes, M.J., Isaac, S., Latorre, A., López-Labrador, F.X., Patiño Galindo, J.A., Palero, F., Pérez-Brocal, V., Pérez-Cobas, A.E., Sánchez Busó, L., Silva, F.J., Vázquez Castellanos, J., Moya, A.**

**Revista Española de Salud Pública (2014) 88: 121-130**

Fundamentos: La epidemiología molecular es una nueva disciplina que permite la integración de la información sobre la variabilidad genética de patógenos infecciosos con su difusión en la población y subgrupos de la misma incluyendo, por ejemplo, las mutaciones de resistencia a antibióticos y antivirales. El objetivo es conocer qué posibles diferencias existe en las características genéticas de los agentes infecciosos que afectan a las poblaciones inmigrante y autóctoctona en España.

Métodos: Se revisaron artículos originales publicados entre 1998-2013, con las palabras clave "epidemiología molecular", "tipado molecular", "secuenciación", "inmigrante", "España".

Resultados: De un total de 267 artículos identificados inicialmente, 50 pasaron los diferentes filtros establecidos. De ellos, 36 analizan las infecciones por *Mycobacterium tuberculosis* y VIH, seguidos de los que analizan infecciones por *Staphylococcus aureus* (3) y el Virus de la Hepatitis B (3).

Conclusiones: Los objetivos principales de estos trabajos fueron el tipado del patógeno y la determinación de la frecuencia de mutaciones de resistencia. Los estudios más frecuentes correspondieron a cohortes retrospectivas, seguidos por los estudios ecológicos y los ensayos clínicos. En general los estudios son descriptivos y su ámbito por el tipo y tamaño de muestra es bastante restringido. En varios se determina que las cepas o variantes del patógeno encontradas en inmigrantes tienen su origen más probable en sus países de origen, si bien otros también ponen de manifiesto la transmisión desde la población autóctona a la inmigrante.

# Hybrid sequencing approach applied to human fecal metagenomic clone libraries revealed clones with potential biotechnological applications

**Džunková, M., D'Auria, G., Pérez-Villarroya, D., Moya, A.**

**PLoS One (2012) 7: e47654**

Natural environments represent an incredible source of microbial genetic diversity. Discovery of novel biomolecules involves biotechnological methods that often require the design and implementation of biochemical assays to screen clone libraries. However, when an assay is applied to thousands of clones, one may eventually end up with very few positive clones which, in most of the cases, have to be "domesticated" for downstream characterization and application, and this makes screening both laborious and expensive. The negative clones, which are not considered by the selected assay, may also have biotechnological potential; however, unfortunately they would remain unexplored. Knowledge of the clone sequences provides important clues about potential biotechnological application of the clones in the library; however, the sequencing of clones one-by-one would be very time-consuming and expensive.

In this study, we characterized the first metagenomic clone library from the feces of a healthy human volunteer, using a method based on 454 pyrosequencing coupled with a clone-by-clone Sanger end-sequencing. Instead of whole individual clone sequencing, we sequenced 358 clones in a pool. The medium-large insert (7-15 kb) cloning strategy allowed us to assemble these clones correctly, and to assign the clone ends to maintain the link between the position of a living clone in the library and the annotated contig from the 454 assembly. Finally, we found several open reading frames (ORFs) with previously described potential medical application.

The proposed approach allows planning ad-hoc biochemical assays for the clones of interest, and the appropriate sub-cloning strategy for gene expression in suitable vectors/hosts.

# Intraspecific sequence comparisons reveal similar rates of non-collinear gene insertion in the B and D genomes of bread wheat

**Bartoš, J., Vlcek, C., Choulet, F., Džunková, M., Cviková, K., Šafár, J., Šimková, H., Paces, J., Strnad, H., Sourdille, P., Bergès, H., Cattonaro, F., Feuillet, C., Doležel, J.**

**BMC Plant Biology (2012) 12: 155**

Background

Polyploidization is considered one of the main mechanisms of plant genome evolution. The presence of multiple copies of the same gene reduces selection pressure and permits sub-functionalization and neo-functionalization leading to plant diversification, adaptation and speciation. In bread wheat, polyploidization and the prevalence of transposable elements resulted in massive gene duplication and movement. As a result, the number of genes which are non-collinear to genomes of related species seems markedly increased in wheat.

Results

We used new-generation sequencing (NGS) to generate sequence of a Mb-sized region from wheat chromosome arm 3DS. Sequence assembly of 24 BAC clones resulted in two scaffolds of 1,264,820 and 333,768 bases. The sequence was annotated and compared to the homoeologous region on wheat chromosome 3B and orthologous loci of *Brachypodium distachyon* and rice. Among 39 coding sequences in the 3DS scaffolds, 32 have a homoeolog on chromosome 3B. In contrast, only fifteen and fourteen orthologs were identified in the corresponding regions in rice and Brachypodium, respectively. Interestingly, five pseudogenes were identified among the non-collinear coding sequences at the 3B locus, while none was found at the 3DS locus.

Conclusion

Direct comparison of two Mb-sized regions of the B and D genomes of bread wheat revealed similar rates of non-collinear gene insertion in both genomes with a majority of gene duplications occurring before their divergence. Relatively low proportion of pseudogenes was identified among non-collinear coding sequences. Our data suggest that the pseudogenes did not originate from insertion of non-functional copies, but were formed later during the evolution of hexaploid wheat. Some evidence was found for gene erosion along the B genome locus.

# Characterisation of the Amaranth Genetic Resources in the Czech Gene Bank

**Janovská, D., Hlásná Čepková, P., Džunková, M.**

**In book: Genetic Diversity in Plants (2012), Publisher: In tech, Editors: Mahmut Caliskan, pp.457-478. ISBN: 978-953-51-0185-7**

Amaranth is mostly named as a crop of the future. Due to very good contents of protein, oil and many components with positive effects to humans, it is one of the promising crops. In the Czech Republic, there was interest of amaranth growing in the fields and the consumption of amaranth products is increasing as well. Most of grain raw material is imported to the Czech Republic from other countries, but there is increasing demand of Czech amaranth production. For amaranth cultivation it is necessary to know, what species could be grown. Because amaranth is not native in Europe, we have to receive seeds from other sides. In Czech legislation act about invasive weeds exists. Several amaranth species are included in this Act.

In order to avoid cultivation of weedy amaranths, it is necessary to know the characteristics of the cultivated species and do not confuse them. Due to vegetable and weedy amaranth have black seed colour, it is impossible to use this trait as a marker. Amaranth glutelins were the best tool for the amaranth species identification, because they showed high polymorphism not only in position of bands but also in their intensity.

The method used here was based on the data concerning the relative intensity and the position of the bands in the glutelin spectra obtained by the chip capillary electrophoresis what resulted in the exact similarity calculation of the protein fraction spectra and thus in the segregation of the cultivated grain species, the monoecious wild species and the dioecious wild species into three separate clusters. Each of the grain amaranth species was characterized by one dark band in the polymorphic region (54 - 65 kDa), while the hybrids possessed more bands of different relative intensity.

The study brought several new contributions to the amaranth genetic research and is a very useful tool for species identification before cultivation in the field conditions. Unfortunately, this method is not so sensitive for individual amaranth genotype identification. We work on it in our current tasks.

# Glutelin protein fraction as a tool for clear identification of *Amaranth* accessions

**Džunková, M., Janovská, D., Hlásná Čepková, P., Prohasková, A., Kolář, M.**

**Journal of Cereal Science (2011) 53: 198-205**

In order to simplify the identification of amaranth accessions in gene banks or seed laboratories, a comprehensive method based on band position and relative band intensity data from the glutelin patterns of the chip microfluidic electrophoresis was developed. Chip electrophoresis protein fraction patterns were compared with the patterns obtained by the classical SDS-PAGE method. Fifty-nine amaranth accessions (*Amaranthus australis*, *Amaranthus cannabinus*, *Amaranthus deflexus*, *Amaranthus retroflexus*, *Amaranthus tuberculatus*, *Amaranthus wrightii* and 53 unknown accessions of the grain species *Amaranthus caudatus*, *Amaranthus cruentus* and *Amaranthus hypochondriacus*) were analysed.

Detailed pattern description of each group is provided here in the form of simplified pattern codes in the glutelin polymorphic area, enabling the identification of hybrid accessions and wild species. Inflorescence type and colour, weight of a thousand seeds, and seed colour were tested as additional phenotypic markers. The clustering within the grain amaranths group was related only to the different inflorescence types generally used to discriminate amaranth species. Statistical analysis of pattern similarities resulted in the segregation of the cultivated grain species, the monoecious wild species, and the dioecious wild species into three separate clusters.

Chapter 14

# Bibliography

# Bibliography


Abulencia, C. B., Wyborski, D. L., Garcia, J. A., Podar, M., Chen, W., Chang, S. H., Chang, H. W., Watson, D., Brodie, E. L., et al. 2006. Environmental whole-genome amplification to access microbial populations in contaminated sediments. *Applied and Environmental Microbiology*, 72(5):3291–3301. Available from: http://dx.doi.org/10.1128/aem.72.5.3291-3301.2006.

Al-Nassir, W. N., Sethi, A. K., Li, Y., Pultz, M. J., Riggs, M. M., and Donskey, C. J. 2008. Both oral metronidazole and oral vancomycin promote persistent overgrowth of vancomycin-resistant enterococci during treatment of Clostridium difficile-associated disease. *Antimicrobial Agents and Chemotherapy*, 52(7):2403–2406. Available from: http://dx.doi.org/10.1128/aac.00090-08.

Allen, L. Z., Ishoey, T., Novotny, M. A., McLean, J. S., Lasken, R. S., and Williamson, S. J. 2011. Single virus genomics: A new tool for virus discovery. *PLoS ONE*, 6(3):e17722+. Available from: http://dx.doi.org/10.1371/journal.pone.0017722.

Altschul, S. F., Gish, W., Miller, W., Myers, E. W., and Lipman, D. J. 1990. Basic local alignment search tool. *Journal of Molecular Biology*, 215(3):403–410. Available from: http://dx.doi.org/10.1006/jmbi.1990.9999.

Amann, R. and Fuchs, B. M. 2008. Single-cell identification in microbial communities by improved fluorescence in situ hybridization techniques. *Nature Reviews Microbiology*, 6(5):339–348. Available from: http://dx.doi.org/10.1038/nrmicro1888.

Ambrose, H. E. and Clewley, J. P. 2006. Virus discovery by sequence-independent genome amplification. *Rev. Med. Virol.*, 16(6):365–383. Available from: http://dx.doi.org/10.1002/rmv.515.

Andrews, J. M. 2001. Determination of minimum inhibitory concentrations. *The Journal of Antimicrobial Chemotherapy*, 48 Suppl 1(suppl 1):5–16. Available from: http://dx.doi.org/10.1093/jac/48.suppl_1.5.

Aronesty, E. 2013. Comparison of sequencing utility programs. *Comparison of Sequencing Utility Programs*, 7:1–8. Available from: http://benthamopen.com/ABSTRACT/TOBIOIJ-7-1.

Arthur, J. C., Perez-Chanona, E., Mühlbauer, M., Tomkovich, S., Uronis, J. M., Fan, T.-J., Campbell, B. J., Abujamel, T., Dogan, B., et al. 2012. Intestinal inflammation targets Cancer-Inducing activity of the microbiota. *Science*, 338(6103):120–123. Available from: http://dx.doi.org/10.1126/science.1224820.

Arumugam, M., Raes, J., Pelletier, E., Le Paslier, D., Yamada, T., Mende, D. R., Fernandes, G. R., Tap, J., Bruls, T., et al. 2011. Enterotypes of the human gut microbiome. *Nature*, 473(7346):174–180. Available from: http://dx.doi.org/10.1038/nature09944.

Ashelford, K. E., Weightman, A. J., and Fry, J. C. 2002. PRIMROSE: a computer program for generating and estimating the phylogenetic range of 16S rRNA oligonucleotide probes and primers in conjunction with the RDP-II database. *Nucleic Acids Research*, 30(15):3481–3489. Available from: http://dx.doi.org/10.1093/nar/gkf450.

Atarashi, K., Tanoue, T., Shima, T., Imaoka, A., Kuwahara, T., Momose, Y., Cheng, G., Yamasaki, S., Saito, T., et al. 2011. Induction of colonic regulatory T cells by indigenous Clostridium species. *Science*, 331(6015):337–341. Available from: http://dx.doi.org/10.1126/science.1198469.

Ausubel, F. M., Brent, R., Kingston, R. E., Moore, D. D., Seidman, J. G., and Struhl, K. 1992. Current Protocols in Molecular Biology. Pp. 2.1.1–2.4.5. Available from: http://eu.wiley.com/WileyCDA/WileyTitle/productCd-047150338X.html.

Barketi-Klai, A., Hoys, S., Lambert-Bordes, S., Collignon, A., and Kansau, I. 2011. Role of fibronectin binding protein A in Clostridium difficile intestinal colonization. *Journal of Medical Microbiology*, 60(8):jmm.0.029553–0–1161. Available from: http://dx.doi.org/10.1099/jmm.0.029553-0.

Barnett, J. M., Cuchens, M. A., and Buchanan, W. 1984. Automated immunofluorescent speciation of oral bacteria using flow cytometry. *Journal of Dental Research*, 63(8):1040–1042. Available from: http://view.ncbi.nlm.nih.gov/pubmed/6205030.

Bartlett, J. G., Chang, T. W., Gurwith, M., Gorbach, S. L., and Onderdonk, A. B. 1978. Antibiotic-associated pseudomembranous colitis due to toxin-producing clostridia. *The New England Journal of Medicine*, 298(10):531–534. Available from: http://view.ncbi.nlm.nih.gov/pubmed/625309.

Beeching, N. J., Jones, R., and Gazzard, B. 2011. 4 gastrointestinal opportunistic infections. *HIV Medicine*, 12:43–54. Available from: http://dx.doi.org/10.1111/j.1468-1293.2011.00944_5.x.

Ben-Amor, K., Heilig, H., Smidt, H., Vaughan, E. E., Abee, T., and de Vos, W. M. 2005. Genetic diversity of viable, injured, and dead fecal bacteria assessed by fluorescence-activated cell sorting and 16S rRNA gene analysis. *Applied and Environmental Microbiology*, 71(8):4679–4689. Available from: http://dx.doi.org/10.1128/aem.71.8.4679-4689.2005.

Bercik, P., Denou, E., Collins, J., Jackson, W., Lu, J., Jury, J., Deng, Y., Blennerhassett, P., Macri, J., et al. 2011. The intestinal microbiota affect central levels of brain-derived neurotropic factor and behavior in mice. *Gastroenterology*, 141(2). Available from: http://dx.doi.org/10.1053/j.gastro.2011.04.052.

Berdy, J. 2005. Bioactive microbial metabolites. *The Journal of Antibiotics*, 58(1):1–26. Available from: http://dx.doi.org/10.1038/ja.2005.1.

Bhatt, A. S., Freeman, S. S., Herrera, A. F., Pedamallu, C. S., Gevers, D., Duke, F., Jung, J., Michaud, M., Walker, B. J., et al. 2013. Sequence-based discovery of Bradyrhizobium enterica in cord colitis syndrome. *New England Journal of Medicine*, 369(6):517–528. Available from: http://dx.doi.org/10.1056/nejmoa1211115.

Bidet, P., Barbut, F., Lalande, V., Burghoffer, B., and Petit, J. C. 1999. Development of a new PCR-ribotyping method for clostridium difficile based on ribosomal RNA gene sequencing. *FEMS Microbiology Letters*, 175(2):261–266. Available from: http://view.ncbi.nlm.nih.gov/pubmed/10386377.

Binga, E. K., Lasken, R. S., and Neufeld, J. D. 2008. Something from (almost) nothing: the impact of multiple displacement amplification on microbial ecology. *The ISME Journal*, 2(3):233–241. Available from: http://dx.doi.org/10.1038/ismej.2008.10.

Birnboim, H. C. and Doly, J. 1979. A rapid alkaline extraction procedure for screening recombinant plasmid DNA. *Nucleic Acids Research*, 7(6):1513–1523. Available from: http://dx.doi.org/10.1093/nar/7.6.1513.

Blainey, P. C. 2013. The future is now: single-cell genomics of bacteria and archaea. *FEMS Microbiology Reviews*, 37(3):407–427. Available from: http://dx.doi.org/10.1111/1574-6976.12015.

Bodilis, J., Nsigue-Meilo, S., Besaury, L., and Quillet, L. 2012. Variable copy number, intra-genomic heterogeneities and lateral transfers of the 16S rRNA gene in pseudomonas. *PLoS ONE*, 7(4). Available from: http://view.ncbi.nlm.nih.gov/pubmed/22545126.

Boisvert, S., Raymond, F., Godzaridis, E., Laviolette, F., and Corbeil, J. 2012. Ray meta: scalable de novo metagenome assembly and profiling. *Genome Biology*, 13(12):R122+. Available from: http://dx.doi.org/10.1186/gb-2012-13-12-r122.

Bonner, W. A., Hulett, H. R., Sweet, R. G., and Herzenberg, L. A. 1972. Fluorescence activated cell sorting. *The Review of Scientific Instruments*, 43(3):404–409. Available from: http://view.ncbi.nlm.nih.gov/pubmed/5013444.

Borenfreund, E. and Puerner, J. A. 1985. Toxicity determined in vitro by morphological alterations and neutral red absorption. *Toxicology Letters*, 24(2-3):119–124. Available from: http://dx.doi.org/10.1016/0378-4274(85)90046-3.

Borody, T. J. and Khoruts, A. 2012. Fecal microbiota transplantation and emerging applications. *Nature Reviews. Gastroenterology and Hepatology*, 9(2):88–96. Available from: http://dx.doi.org/10.1038/nrgastro.2011.244.

Bouskra, D., Brazillon, C., Barard, M., Werts, C., Varona, R., Boneca, I. G., and Eberl, G. A. 2008. Lymphoid tissue genesis induced by commensals through NOD1 regulates intestinal homeostasis. *Nature*, 456(7221):507–510. Available from: http://dx.doi.org/10.1038/nature07450.

Braun, V., Hundsberger, T., Leukel, P., Sauerborn, M., and von Eichel-Streiber, C. 1996. Definition of the single integration site of the pathogenicity locus in Clostridium difficile. *Gene*, 181(1-2):29–38. Available from: http://view.ncbi.nlm.nih.gov/pubmed/8973304.

Bredel, M., Bredel, C., Juric, D., Kim, Y., Vogel, H., Harsh, G. R., Recht, L. D., Pollack, J. R., and Sikic, B. I. 2005. Amplification of whole tumor genomes and gene-by-gene mapping of genomic aberrations from limited sources of fresh-frozen and paraffin-embedded DNA. *The Journal of Molecular Diagnostics*, 7(2):171–182. Available from: http://dx.doi.org/10.1016/s1525-1578(10)60543-0.

Breitbart, M., Felts, B., Kelley, S., Mahaffy, J. M., Nulton, J., Salamon, P., and Rohwer, F. 2004. Diversity and population structure of a near-shore marine-sediment viral community. *Proceedings. Biological Sciences / The Royal Society*, 271(1539):565–574. Available from: http://dx.doi.org/10.1098/rspb.2003.2628.

Breitbart, M., Haynes, M., Kelley, S., Angly, F., Edwards, R. A., Felts, B., Mahaffy, J. M., Mueller, J., Nulton, J., et al. 2008. Viral diversity and dynamics in an infant gut. *Research in Microbiology*, 159(5):367–373. Available from: http://dx.doi.org/10.1016/j.resmic.2008.04.006.

Breitbart, M., Hewson, I., Felts, B., Mahaffy, J. M., Nulton, J., Salamon, P., and Rohwer, F. 2003. Metagenomic analyses of an uncultured viral community from human feces. *Journal of Bacteriology*, 185(20):6220–6223. Available from: http://dx.doi.org/10.1128/jb.185.20.6220.

Breitbart, M., Salamon, P., Andresen, B., Mahaffy, J. M., Segall, A. M., Mead, D., Azam, F., and Rohwer, F. 2002. Genomic analysis of uncultured marine viral communities. *Proceedings of the National Academy of Sciences of the United States of America*, 99(22):14250–14255. Available from: http://dx.doi.org/10.1073/pnas.202488399.

Bressan, M., Trinsoutrot Gattin, I., Desaire, S., Castel, L., Gangneux, C., and Laval, K. 2015. A rapid flow cytometry method to assess bacterial abundance in agricultural soil. *Applied Soil Ecology*, 88:60–68. Available from: http://dx.doi.org/10.1016/j.apsoil.2014.12.007.

Brouwer, M. S. M., Roberts, A. P., Hussain, H., Williams, R. J., Allan, E., and Mullany, P. 2013. Horizontal gene transfer converts non-toxigenic clostridium difficile strains into toxin producers. *Nature Communications*, 4. Available from: http://dx.doi.org/10.1038/ncomms3601.

Brouwer, M. S. M., Warburton, P. J., Roberts, A. P., Mullany, P., and Allan, E. 2011. Genetic organisation, mobility and predicted functions of genes on integrated, mobile genetic elements in sequenced strains of Clostridium difficile. *PLoS ONE*, 6(8):e23014+.

Brown, M. R., Camézuli, S., Davenport, R. J., Petelenz-Kurdziel, E., Øvreås, L., and Curtis, T. P. 2015. Flow cytometric quantification of viruses in activated sludge. *Water Research*, 68:414–422. Available from: http://dx.doi.org/10.1016/j.watres.2014.10.018.

Brown, S. P., Le Chat, L., De Paepe, M., and Taddei, F. 2006. Ecology of microbial invasions: amplification allows virus carriers to invade more rapidly when rare. *Current Biology*, 16(20):2048–2052. Available from: http://view.ncbi.nlm.nih.gov/pubmed/17055985.

Brussaard, C. P. D. 2004. Optimization of procedures for counting viruses by flow cytometry. *Applied and Environmental Microbiology*, 70(3):1506–1513. Available from: http://dx.doi.org/10.1128/aem.70.3.1506-1513.2004.

Buehler, B., Hogrefe, H. H., Scott, G., Ravi, H., Pabón-Peña, C., O'Brien, S., Formosa, R., and Happe, S. 2010. Rapid quantification of DNA libraries for next-generation sequencing. *Methods*, 50(4):S15–S18. Available from: http://dx.doi.org/10.1016/j.ymeth.2010.01.004.

Buffie, C. G., Bucci, V., Stein, R. R., McKenney, P. T., Ling, L., Gobourne, A., No, D., Liu, H., Kinnebrew, M., et al. 2014. Precision microbiome reconstitution restores bile acid mediated resistance to clostridium difficile. *Nature*, 517(7533):205–208. Available from: http://dx.doi.org/10.1038/nature13828.

Buh Gasparic, M., Tengs, T., La Paz, J. L. L., Holst-Jensen, A., Pla, M., Esteve, T., Zel, J., and Gruden, K. 2010. Comparison of nine different real-time PCR chemistries for qualitative and quantitative applications in GMO detection. *Analytical and bioanalytical chemistry*, 396(6):2023–2029. Available from: http://dx.doi.org/10.1007/s00216-009-3418-0.

Calabi, E., Ward, S., Wren, B., Paxton, T., Panico, M., Morris, H., Dell, A., Dougan, G., and Fairweather, N. 2001. Molecular characterization of the surface layer proteins from Clostridium difficile. *Molecular Microbiology*, 40(5):1187–1199. Available from: http://view.ncbi.nlm.nih.gov/pubmed/11401722.

Cario, E. 2013. Microbiota and innate immunity in intestinal inflammation and neoplasia. *Current Opinion in Gastroenterology*, 29(1):85–91. Available from: http://view.ncbi.nlm.nih.gov/pubmed/23207600.

Carter, G. P., Lyras, D., Allen, D. L., Mackin, K. E., Howarth, P. M., O'Connor, J. R., and Rood, J. I. 2007. Binary toxin production in Clostridium difficile is regulated by CdtR, a LytTR family response regulator. *Journal of Bacteriology*, 189(20):7290–7301. Available from: http://dx.doi.org/10.1128/jb.00731-07.

Carter, G. P., Rood, J. I., and Lyras, D. 2012. The role of toxin a and toxin b in the virulence of clostridium difficile. *Trends in Microbiology*, 20(1):21–29. Available from: http://dx.doi.org/10.1016/j.tim.2011.11.003.

Chalfie, M., Tu, Y., Euskirchen, G., Ward, W. W., and Prasher, D. C. 1994. Green fluorescent protein as a marker for gene expression. *Science*, 263(5148):802–805. Available from: http://dx.doi.org/10.1126/science.8303295.

ChapetónMontes, D., Candela, T., Collignon, A., and Janoir, C. 2011. Localization of the Clostridium difficile cysteine protease Cwp84 and insights into its maturation process. *Journal of Bacteriology*, 193(19):5314–5321. Available from: http://dx.doi.org/10.1128/jb.00326-11.

Chen, F., Lu, J.-r., Binder, B. J., Liu, Y.-c., and Hodson, R. E. 2001. Application of Digital Image Analysis and Flow Cytometry To Enumerate Marine Viruses Stained with SYBR Gold. *Applied and Environmental Microbiology*, 67(2):539–545. Available from: http://dx.doi.org/10.1128/aem.67.2.539-545.2001.

Chevreux, B., Wetter, T., and Suhai, S. 1999. Genome sequence assembly using trace signals and additional sequence information. In *Computer Science and Biology: Proceedings of the German Conference on Bioinformatics (GCB)*, volume 99, Pp. 45–56. Available from: http://mira-assembler.sourceforge.net/docs/DefinitiveGuideToMIRA.html.

Chobot, V., Drage, S., and Hadacek, F. 2011. Redox properties of 8-quinolinol and implications for its mode of action. *Natural Product Communications*, 6(5):597–602. Available from: http://view.ncbi.nlm.nih.gov/pubmed/21615015.

Clabots, C. R., Johnson, S., Bettin, K. M., Mathie, P. A., Mulligan, M. E., Schaberg, D. R., Peterson, L. R., and Gerding, D. N. 1993. Development of a rapid and efficient restriction endonuclease analysis typing system for clostridium difficile and correlation with other typing systems. *Journal of Clinical Microbiology*, 31(7):1870–1875. Available from: http://www.ncbi.nlm.nih.gov/pmc/articles/PMC265648/.

Claesson, M. J., Jeffery, I. B., Conde, S., Power, S. E., O'Connor, E. M., Cusack, S., Harris, H. M. B., Coakley, M., Lakshminarayanan, B., et al. 2012. Gut microbiota composition correlates with diet and health in the elderly. *Nature*, 488(7410):178–184. Available from: http://dx.doi.org/10.1038/nature11319.

Clarke, S. F., Murphy, E. F., Nilaweera, K., Ross, P. R., Shanahan, F., O'Toole, P. W., and Cotter, P. D. 2012. The gut microbiota and its relationship to diet and obesity: new insights. *Gut Microbes*, 3(3):186–202. Available from: http://view.ncbi.nlm.nih.gov/pubmed/22572830.

Coconnier, M. H., Liévin, V., Bernet-Camard, M. F., Hudault, S., and Servin, A. L. 1997. Antibacterial effect of the adhering human lactobacillus acidophilus strain LB. *Antimicrobial Agents and Chemotherapy*, 41(5):1046–1052. Available from: http://www.ncbi.nlm.nih.gov/pmc/articles/PMC163848/.

Cole, J. R., Wang, Q., Cardenas, E., Fish, J., Chai, B., Farris, R. J., Kulam-Syed-Mohideen, A. S., McGarrell, D. M., Marsh, T., et al. 2009. The Ribosomal Database Project: improved alignments and new tools for rRNA analysis. *Nucleic Acids Research*, 37(Database issue):D141–D145. Available from: http://dx.doi.org/10.1093/nar/gkn879.

Collins, M. D., Lawson, P. A., Willems, A., Cordoba, J. J., Fernandez-Garayzabal, J., Garcia, P., Cai, J., Hippe, H., and Farrow, J. A. 1994. The phylogeny of the genus Clostridium: proposal of five new genera and eleven new species combinations. *International Journal of Systematic Bacteriology*, 44(4):812–826. Available from: http://dx.doi.org/10.1099/00207713-44-4-812.

Coons, A. H., Creech, H. J., and Jones, R. N. 1941. Immunological properties of an antibody containing a fluorescent group. *Experimental Biology and Medicine*, 47(2):200–202. Available from: http://dx.doi.org/10.3181/00379727-47-13084p.

Coons, A. H. and Kaplan, M. H. 1950. Localization of antigen in tissue cells; improvements in a method for the detection of antigen by means of fluorescent antibody. *The Journal of Experimental Medicine*, 91(1):1–13. Available from: http://view.ncbi.nlm.nih.gov/pubmed/15395569.

Coupland, P., Chandra, T., Quail, M., Reik, W., and Swerdlow, H. 2012. Direct sequencing of small genomes on the Pacific Biosciences RS without library preparation. *BioTechniques*, 53(6):365–372. Available from: http://dx.doi.org/10.2144/000113962.

Curry, S. R., Marsh, J. W., Muto, C. A., O'Leary, M. M., Pasculle, A. W., and Harrison, L. H. 2007. tcdC genotypes associated with severe TcdC truncation in an epidemic clone and other strains of clostridium difficile. *Journal of Clinical Microbiology*, 45(1):215–221. Available from: http://view.ncbi.nlm.nih.gov/pubmed/17035492.

David, L. A., Maurice, C. F., Carmody, R. N., Gootenberg, D. B., Button, J. E., Wolfe, B. E., Ling, A. V., Devlin, A. S., Varma, Y., et al. 2014. Diet rapidly and reproducibly alters the human gut microbiome. *Nature*, 505(7484):559–563. Available from: http://dx.doi.org/10.1038/nature12820.

De La Cochetière, M. F., Durand, T., Lalande, V., Petit, J. C., Potel, G., and Beaugerie, L. 2008. Effect of antibiotic therapy on human fecal microbiota and the relation to the development of Clostridium difficile. *Microbial Ecology*, 56(3):395–402. Available from: http://view.ncbi.nlm.nih.gov/pubmed/18209965.

de la Riva, L., Willing, S. E., Tate, E. W., and Fairweather, N. F. 2011. Roles of cysteine proteases Cwp84 and Cwp13 in biogenesis of the cell wall of Clostridium difficile. *Journal of Bacteriology*, 193(13):3276–3285. Available from: http://dx.doi.org/10.1128/jb.00248-11.

De Paepe, M., Hutinet, G., Son, O., Amarir-Bouhram, J., Schbath, S., and Petit, M.-A. A. 2014a. Temperate phages acquire DNA from defective prophages by relaxed homologous recombination: the role of rad52-like recombinases. *PLoS Genetics*, 10(3). Available from: http://view.ncbi.nlm.nih.gov/pubmed/24603854.

De Paepe, M., Leclerc, M., Tinsley, C. R., and Petit, M.-A. A. 2014b. Bacteriophages: an underestimated role in human and animal health? *Frontiers in Cellular and Infection Microbiology*, 4. Available from: http://view.ncbi.nlm.nih.gov/pubmed/24734220.

Dean, F. B., Hosono, S., Fang, L., Wu, X., Faruqi, A. F., Bray-Ward, P., Sun, Z., Zong, Q., Du, Y., et al. 2002. Comprehensive human genome amplification using multiple displacement amplification. *Proceedings of the National Academy of Sciences of the United States of America*, 99(8):5261–5266. Available from: http://dx.doi.org/10.1073/pnas.082089499.

Dean, F. B., Nelson, J. R., Giesler, T. L., and Lasken, R. S. 2001. Rapid amplification of plasmid and phage DNA using Phi 29 DNA polymerase and multiply-primed rolling circle amplification. *Genome Research*, 11(6):1095–1099. Available from: http://dx.doi.org/10.1101/gr.180501.

del Giorgio, P. A., Prairie, Y. T., and Bird, D. F. 1997. Coupling between rates of bacterial production and the abundance of metabolically active bacteria in lakes, enumerated using CTC reduction and flow cytometry. *Microbial Ecology*, 34(2):144–154. Available from: http://dx.doi.org/10.1007/s002489900044.

Delcher, A. L., Harmon, D., Kasif, S., White, O., and Salzberg, S. L. 1999. Improved microbial gene identification with GLIMMER. *Nucleic Acids Research*, 27(23):4636–4641. Available from: http://dx.doi.org/10.1093/nar/27.23.4636.

Demarest, S. J., Hariharan, M., Elia, M., Salbato, J., Jin, P., Bird, C., Short, J. M., Kimmel, B. E., Dudley, M., Woodnutt, G., and Hansen, G. 2010. Neutralization of Clostridium difficile toxin A using antibody combinations. *mAbs*, 2(2):190–198. Available from: http://www.ncbi.nlm.nih.gov/pmc/articles/PMC2840238/.

Dennehy, P. H. 2000. Transmission of rotavirus and other enteric pathogens in the home. *The Pediatric Infectious Disease Journal*, 19(10 Suppl). Available from: http://view.ncbi.nlm.nih.gov/pubmed/11052397.

Didelot, X., Eyre, D., Cule, M., Ip, C., Ansari, M., Griffiths, D., Vaughan, A., O'Connor, L., Golubchik, T., et al. 2012. Microevolutionary analysis of Clostridium difficile genomes to investigate transmission. *Genome Biology*, 13(12):R118+. Available from: http://dx.doi.org/10.1186/gb-2012-13-12-r118.

Dietrich, M. A., Truax, R. E., French, D. D., Lea, D. F., Stear, M. J., and Newman, M. J. 1991. Measurement of antibody binding to intact bacteria using flow cytometric techniques. *Journal of Microbiological Methods*, 13(4):281–291. Available from: http://dx.doi.org/10.1016/0167-7012(91)90065-x.

Dingle, K. E., Didelot, X., Ansari, M. A., Eyre, D. W., Vaughan, A., Griffiths, D., Ip, C. L. C., Batty, E. M., Golubchik, T., et al. 2013. Recombinational switching of the Clostridium difficile S-Layer and a novel glycosylation gene cluster revealed by large-scale whole-genome sequencing. *Journal of Infectious Diseases*, 207(4):675–686. Available from: http://dx.doi.org/10.1093/infdis/jis734.

Dingle, K. E., Elliott, B., Robinson, E., Griffiths, D., Eyre, D. W., Stoesser, N., Vaughan, A., Golubchik, T., Fawley, W. N., et al. 2014. Evolutionary history of the clostridium difficile pathogenicity locus. *Genome Biology and Evolution*, 6(1):36–52. Available from: http://dx.doi.org/10.1093/gbe/evt204.

Dingle, K. E., Griffiths, D., Didelot, X., Evans, J., Vaughan, A., Kachrimanidou, M., Stoesser, N., Jolley, K. A., Golubchik, T., et al. 2011. Clinical Clostridium difficile: clonality and pathogenicity locus diversity. *PLoS ONE*, 6(5):e19993+. Available from: http://dx.doi.org/10.1371/journal.pone.0019993.

Dixon, P. 2003. VEGAN, a package of r functions for community ecology. *Journal of Vegetation Science*, 14(6):927–930. Available from: http://dx.doi.org/10.1111/j.1654-1103.2003.tb02228.x.

Dodsworth, J. A., Blainey, P. C., Murugapiran, S. K., Swingley, W. D., Ross, C. A., Tringe, S. G., Chain, P. S. G., Scholz, M. B., Lo, C.-C., et al. 2013. Single-cell and metagenomic analyses indicate a fermentative and saccharolytic lifestyle for members of the OP9 lineage. *Nature Communications*, 4:1854+. Available from: http://dx.doi.org/10.1038/ncomms2884.

Drudy, D., Kyne, L., O'Mahony, R., and Fanning, S. 2007. gyrA mutations in fluoroquinolone-resistant Clostridium difficile PCR-027. *Emerging Infectious Diseases*, 13(3):504–505. Available from: http://dx.doi.org/10.3201/eid1303.060771.

Du, P., Cao, B., Wang, J., Li, W., Jia, H., Zhang, W., Lu, J., Li, Z., Yu, H., Chen, C., and Cheng, Y. 2014. Sequence variation in tcdA and tcdB of clostridium difficile: ST37 with truncated tcdA is a potential epidemic strain in china. *Journal of Clinical Microbiology*, 52(9):3264–3270. Available from: http://dx.doi.org/10.1128/jcm.03487-13.

Duhaime, M. B., Deng, L., Poulos, B. T., and Sullivan, M. B. 2012. Towards quantitative metagenomics of wild viruses and other ultra-low concentration DNA samples: a rigorous assessment and optimization of the linker amplification method. *Environmental Microbiology*, 14(9):2526–2537. Available from: http://dx.doi.org/10.1111/j.1462-2920.2012.02791.x.

DuRand, M. D., Olson, R. J., and Chisholm, S. W. 2001. Phytoplankton population dynamics at the bermuda atlantic time-series station in the sargasso sea. *Deep Sea Research Part II: Topical Studies in Oceanography*, 48(8-9):1983–2003. Available from: http://dx.doi.org/10.1016/s0967-0645(00)00166-1.

Durbán, A., Abellán, J. J., Jiménez-Hernández, N., Artacho, A., Garrigues, V., Ortiz, V., Ponce, J., Latorre, A., and Moya, A. 2013. Instability of the faecal microbiota in diarrhoea-predominant irritable bowel syndrome. *FEMS Microbiology and Ecology*, 86(3):581–589. Available from: http://view.ncbi.nlm.nih.gov/pubmed/23889283.

Durbán, A., Abellán, J. J., Jiménez-Hernández, N., Ponce, M., Ponce, J., Sala, T., D'Auria, G., Latorre, A., and Moya, A. 2011. Assessing gut microbial diversity from feces and rectal mucosa. *Microbial ecology*, 61(1):123–133. Available from: http://view.ncbi.nlm.nih.gov/pubmed/20734040.

Dutilh, B. E., Cassman, N., McNair, K., Sanchez, S. E., Silva, G. G. Z., Boling, L., Barr, J. J., Speth, D. R., Seguritan, V., et al. 2014. A highly abundant bacteriophage discovered in the unknown sequences of human faecal metagenomes. *Nature Communications*, 5. Available from: http://dx.doi.org/10.1038/ncomms5498.

Eckburg, P. B., Bik, E. M., Bernstein, C. N., Purdom, E., Dethlefsen, L., Sargent, M., Gill, S. R., Nelson, K. E., and Relman, D. A. 2005. Diversity of the human intestinal microbial flora. *Science*, 308(5728):1635–1638. Available from: http://dx.doi.org/10.1126/science.1110591.

Edgar, R. C. 2010. Search and clustering orders of magnitude faster than BLAST. *Bioinformatics*, 26(19):2460–2461. Available from: http://dx.doi.org/10.1093/bioinformatics/btq461.

Edwards, R. A. and Rohwer, F. 2005. Viral metagenomics. *Nature Reviews Microbiology*, 3(6):504–510. Available from: http://dx.doi.org/10.1038/nrmicro1163.

Ekimov, A. I., Efros, A., and Onushchenko, A. A. 1985. Quantum size effect in semiconductor microcrystals. *Solid State Communications*, 56(11):921–924. Available from: http://dx.doi.org/10.1016/s0038-1098(85)80025-9.

Elliott, B., Dingle, K. E., Didelot, X., Crook, D. W., and Riley, T. V. 2014. The complexity and diversity of the pathogenicity locus in Clostridium difficile clade 5. *Genome Biology and Evolution*, 6(12):3159–3170. Available from: http://dx.doi.org/10.1093/gbe/evu248.

Endt, K., Stecher, B., Chaffron, S., Slack, E., Tchitchek, N., Benecke, A., Van Maele, L., Sirard, J.-C. C., Mueller, A. J., et al. 2010. The microbiota mediates pathogen clearance from the gut lumen after non-typhoidal salmonella diarrhea. *PLoS Pathogens*, 6(9):e1001097+. Available from: http://dx.doi.org/10.1371/journal.ppat.1001097.

Evans, M. E., Pollack, M., Hardegen, N. J., Koles, N. L., Guelde, G., and Chia, J. K. S. 1990. Fluorescence-activated cell sorter analysis of binding by lipopolysaccharide-specific monoclonal antibodies to gram-negative bacteria. *Journal of Infectious Diseases*, 162(1):148–155. Available from: http://dx.doi.org/10.1093/infdis/162.1.148.

Eyre, D. W., Cule, M. L., Griffiths, D., Crook, D. W., Peto, T. E. A., Walker, A. S., and Wilson, D. J. 2013a. Detection of mixed infection from bacterial whole genome sequence data allows assessment of its role in Clostridium difficile transmission. *PLoS Computational Biology*, 9(5):e1003059+. Available from: http://dx.doi.org/10.1371/journal.pcbi.1003059.

Eyre, D. W., Cule, M. L., Wilson, D. J., Griffiths, D., Vaughan, A., O'Connor, L., Ip, C. L. C., Golubchik, T., Batty, E. M., et al. 2013b. Diverse sources of C. difficile infection identified on whole-genome sequencing. *New England Journal of Medicine*, 369(13):1195–1205. Available from: http://dx.doi.org/10.1056/nejmoa1216064.

Eyre, D. W., Golubchik, T., Gordon, N. C., Bowden, R., Piazza, P., Batty, E. M., Ip, C. L. C., Wilson, D. J., Didelot, X., et al. 2012a. A pilot study of rapid benchtop sequencing of Staphylococcus aureus and Clostridium difficile for outbreak detection and surveillance. *BMJ Open*, 2(3):e001124+. Available from: http://dx.doi.org/10.1136/bmjopen-2012-001124.

Eyre, D. W., Walker, A. S., Griffiths, D., Wilcox, M. H., Wyllie, D. H., Dingle, K. E., Crook, D. W., and Peto, T. E. 2012b. Clostridium difficile mixed infection and reinfection. *Journal of Clinical Microbiology*, 50(1):142–144. Available from: http://view.ncbi.nlm.nih.gov/pubmed/22075589.

Fedorak, R. N. 2010. Probiotics in the management of ulcerative colitis. *Gastroenterology & Hepatology*, 6(11):688–690. Available from: http://www.ncbi.nlm.nih.gov/pmc/articles/PMC3033537/.

Fei, N. and Zhao, L. 2012. An opportunistic pathogen isolated from the gut of an obese human causes obesity in germfree mice. *The ISME Journal*, 7(4):880–884. Available from: http://dx.doi.org/10.1038/ismej.2012.153.

Finkbeiner, S. R., Allred, A. F., Tarr, P. I., Klein, E. J., Kirkwood, C. D., and Wang, D. 2008. Metagenomic Analysis of Human Diarrhea: Viral Detection and Discovery. *PLoS Pathog*, 4(2):e1000011+. Available from: http://dx.doi.org/10.1371/journal.ppat.1000011.

Fire, A. and Xu, S. Q. 1995. Rolling replication of short DNA circles. *Proceedings of the National Academy of Sciences of the United States of America*, 92(10):4641–4645. Available from: http://www.pnas.org/content/92/10/4641.abstract.

Focà, A., Liberto, M. C., Quirino, A., Marascio, N., Zicca, E., and Pavia, G. 2015. Gut inflammation and immunity: What is the role of the human gut virome? *Mediators of Inflammation*, Pp. 326032+. Available from: http://www.hindawi.com/journals/mi/2015/326032/.

Franks, A. H., Harmsen, H. J., Raangs, G. C., Jansen, G. J., Schut, F., and Welling, G. W. 1998. Variations of bacterial populations in human feces measured by fluorescent in situ hybridization with group-specific 16S rRNA-targeted oligonucleotide probes. *Applied and Environmental Microbiology*, 64(9):3336–3345. Available from: http://aem.asm.org/content/64/9/3336.abstract.

Franzosa, E. A., Morgan, X. C., Segata, N., Waldron, L., Reyes, J., Earl, A. M., Giannoukos, G., Boylan, M. R., Ciulla, D., et al. 2014. Relating the metatranscriptome and metagenome of the human gut. *Proceedings of the National Academy of Sciences of the United States of America*, 111(22):E2329–E2338. Available from: http://dx.doi.org/10.1073/pnas.1319284111.

Fraser, R. S. and Creanor, J. 1975. The mechanism of inhibition of ribonucleic acid synthesis by 8-hydroxyquinoline and the antibiotic lomofungin. *The Biochemical journal*, 147(3):401–410. Available from: http://view.ncbi.nlm.nih.gov/pubmed/810137.

Frias-Lopez, J., Shi, Y., Tyson, G. W., Coleman, M. L., Schuster, S. C., Chisholm, S. W., and DeLong, E. F. 2008. Microbial community gene expression in ocean surface waters. *Proceedings of the National Academy of Sciences of the United States of America*, 105(10):3805–3810. Available from: http://dx.doi.org/10.1073/pnas.0708897105.

Fuchs, B. M., Wallner, G., Beisker, W., Schwippl, I., Ludwig, W., and Amann, R. 1998. Flow cytometric analysis of the in situ accessibility of escherichia coli 16S rRNA for fluorescently labeled oligonucleotide probes. *Applied and Environmental Microbiology*, 64(12):4973–4982. Available from: http://aem.asm.org/cgi/content/abstract/64/12/4973.

Fulwyler, M. J. 1965. Electronic separation of biological cells by volume. *Science*, 150(3698):910–911. Available from: http://dx.doi.org/10.1126/science.150.3698.910.

Galdeano, C. M. and Perdigón, G. 2006. The probiotic bacterium Lactobacillus casei induces activation of the gut mucosal immune system through innate immunity. *Clinical and Vaccine Immunology*, 13(2):219–226. Available from: http://view.ncbi.nlm.nih.gov/pubmed/16467329.

Gao, X. W., Mubasher, M., Fang, C. Y., Reifer, C., and Miller, L. E. 2010. Dose-response efficacy of a proprietary probiotic formula of Lactobacillus acidophilus cl1285 and Lactobacillus casei lbc80r for antibiotic-associated diarrhea and Clostridium difficile-associated diarrhea prophylaxis in adult patients. *American Journal of Gastroenterology*, 105(7):1636–1641. Available from: http://dx.doi.org/10.1038/ajg.2010.11.

Geric, B., Rupnik, M., Gerding, D. N., Grabnar, M., and Johnson, S. 2004. Distribution of Clostridium difficile variant toxinotypes and strains with binary toxin genes among clinical isolates in an american hospital. *Journal of Medical Microbiology*, 53(Pt 9):887–894. Available from: http://view.ncbi.nlm.nih.gov/pubmed/15314196.

Ghosh, D., Roy, K., Williamson, K. E., White, D. C., Wommack, K. E., Sublette, K. L., and Radosevich, M. 2008. Prevalence of lysogeny among soil bacteria and presence of 16S rRNA and trzN genes in viral-community DNA. *Applied and Environmental Microbiology*, 74(2):495–502. Available from: http://dx.doi.org/10.1128/aem.01435-07.

Ghoshal, U. C., Shukla, R., Ghoshal, U., Gwee, K.-A. A., Ng, S. C., and Quigley, E. M. 2012. The gut microbiota and irritable bowel syndrome: friend or foe? *International Journal of Inflammation*, 2012. Available from: http://view.ncbi.nlm.nih.gov/pubmed/22577594.

Gill, S. R., Pop, M., Deboy, R. T., Eckburg, P. B., Turnbaugh, P. J., Samuel, B. S., Gordon, J. I., Relman, D. A., Fraser-Liggett, C. M., and Nelson, K. E. 2006. Metagenomic analysis of the human distal gut microbiome. *Science*, 312(5778):1355–1359. Available from: http://dx.doi.org/10.1126/science.1124234.

Glass, R. I., Parashar, U. D., and Estes, M. K. 2009. Norovirus gastroenteritis. *New England Journal of Medicine*, 361(18):1776–1785. Available from: http://dx.doi.org/10.1056/nejmra0804575.

Goodman, A. L., Kallstrom, G., Faith, J. J., Reyes, A., Moore, A., Dantas, G., and Gordon, J. I. 2011. Extensive personal human gut microbiota culture collections characterized and manipulated in gnotobiotic mice. *Proceedings of the National Academy of Sciences of the United States of America*, 108(15):6252–6257. Available from: http://dx.doi.org/10.1073/pnas.1102938108.

Goorhuis, A., Bakker, D., Corver, J., Debast, S. B., Harmanus, C., Notermans, D. W., Bergwerff, A. A., Dekker, F. W., and Kuijper, E. J. *Clinical Infectious Diseases*.

Gosalbes, M. J., Llop, S., Vallès, Y., Moya, A., Ballester, F., and Francino, M. P. 2013. Meconium microbiota types dominated by lactic acid or enteric bacteria are differentially associated with maternal eczema and respiratory problems in infants. *Clinical and Experimental Allergy*, 43(2):198–211. Available from: http://view.ncbi.nlm.nih.gov/pubmed/23331561.

Graf, D., Di Cagno, R., Fåk, F., Flint, H. J., Nyman, M., Saarela, M., and Watzl, B. 2015. Contribution of diet to the composition of the human gut microbiota. *Microbial ecology in health and disease*, 26. Available from: http://view.ncbi.nlm.nih.gov/pubmed/25656825.

Gregory, J. C., Buffa, J. A., Org, E., Wang, Z., Levison, B. S., Zhu, W., Wagner, M. A., Bennett, B. J., Li, L., DiDonato, J. A., Lusis, A. J., and Hazen, S. L. 2014. Transmission of atherosclerosis susceptibility with gut microbial transplantation. *Journal of Biological Chemistry*, Pp. jbc.M114.618249+. Available from: http://dx.doi.org/10.1074/jbc.m114.618249.

Griffiths, D., Fawley, W., Kachrimanidou, M., Bowden, R., Crook, D. W., Fung, R., Golubchik, T., Harding, R. M., Jeffery, K. J. M., et al. 2010. Multilocus sequence typing of Clostridium difficile. *Journal of Clinical Microbiology*, 48(3):770–778. Available from: http://dx.doi.org/10.1128/jcm.01796-09.

Guinane, C. M. and Cotter, P. D. 2013. Role of the gut microbiota in health and chronic gastrointestinal disease: understanding a hidden metabolic organ. *Therapeutic Advances in Gastroenterology*, 6(4):295–308. Available from: http://dx.doi.org/10.1177/1756283x13482996.

Gunasekera, T. S., Attfield, P. V., and Veal, D. A. 2000. A flow cytometry method for rapid detection and enumeration of total bacteria in milk. *Applied and Environmental Microbiology*, 66(3):1228–1232. Available from: http://dx.doi.org/10.1128/aem.66.3.1228-1232.2000.

Günther, S., Trutnau, M., Kleinsteuber, S., Hause, G., Bley, T., Röske, I., Harms, H., and Müller, S. 2009. Dynamics of Polyphosphate-Accumulating bacteria in wastewater treatment plant microbial communities detected via DAPI (4âĂš,6âĂš-Diamidino-2-Phenylindole) and tetracycline labeling. *Applied and Environmental Microbiology*, 75(7):2111–2121. Available from: http://dx.doi.org/10.1128/aem.01540-08.

Guy, L., Kultima, J. R., and Andersson, S. G. E. 2010. genoPlotR: comparative gene and genome visualization in R. *Bioinformatics*, 26(18):2334–2335. Available from: http://dx.doi.org/10.1093/bioinformatics/btq413.

Hahn, M. W. 2004. Broad diversity of viable bacteria in 'sterile' (0.2 $\mu$m) filtered water. *Research in Microbiology*, 155(8):688–691. Available from: http://dx.doi.org/10.1016/j.resmic.2004.05.003.

Hahne, F., LeMeur, N., Brinkman, R., Ellis, B., Haaland, P., Sarkar, D., Spidlen, J., Strain, E., and Gentleman, R. 2009. flowCore: a Bioconductor package for high throughput flow cytometry. *BMC Bioinformatics*, 10(1):106+. Available from: http://dx.doi.org/10.1186/1471-2105-10-106.

Haiser, H. J. and Turnbaugh, P. J. 2013. Developing a metagenomic view of xenobiotic metabolism. *Pharmacological Research*, 69(1):21–31. Available from: http://dx.doi.org/10.1016/j.phrs.2012.07.009.

Hammond, G. A. and Johnson, J. L. 1995. The toxigenic element of Clostridium difficile strain VPI 10463. *Microbial Pathogenesis*, 19(4):203–213. Available from: http://dx.doi.org/10.1016/s0882-4010(95)90263-5.

Handelsman, J. 2004. Metagenomics: application of genomics to uncultured microorganisms. *Microbiology and Molecular Biology Reviews*, 68(4):669–685. Available from: http://dx.doi.org/10.1128/mmbr.68.4.669-685.2004.

Hapfelmeier, S., Lawson, M. A., Slack, E., Kirundi, J. K., Stoel, M., Heikenwalder, M., Cahenzli, J., Velykoredko, Y., Balmer, M. L., et al. 2010. Reversible microbial colonization of germ-free mice reveals the dynamics of IgA immune responses. *Science*, 328(5986):1705–1709. Available from: http://dx.doi.org/10.1126/science.1188454.

He, J., Sakaguchi, K., and Suzuki, T. 2012. Acquired tolerance to oxidative stress in bifidobacterium longum 105-A via expression of a catalase gene. *Applied and environmental microbiology*, 78(8):2988–2990. Available from: http://dx.doi.org/10.1128/aem.07093-11, doi:10.1128/aem.07093-11.

He, M., Miyajima, F., Roberts, P., Ellison, L., Pickard, D. J., Martin, M. J., Connor, T. R., Harris, S. R., Fairley, D., et al. 2013. Emergence and global spread of epidemic healthcare-associated Clostridium difficile. *Nature Genetics*, 45(1):109–113. Available from: http://dx.doi.org/10.1038/ng.2478.

He, M., Sebaihia, M., Lawley, T. D., Stabler, R. A., Dawson, L. F., Martin, M. J., Holt, K. E., Seth-Smith, H. M. B., Quail, M. A., Rance, R., et al. 2010. Evolutionary dynamics of Clostridium difficile over short and long time scales. *Proceedings of the National Academy of Sciences of the United States of America*, 107(16):7527–7532. Available from: http://dx.doi.org/10.1073/pnas.0914322107.

Héchard, Y., Jayat, C., Letellier, F., Julien, R., Cenatiempo, Y., and Ratinaud, M. H. 1992. On-line visualization of the competitive behavior of antagonistic bacteria. *Applied and Environmental Microbiology*, 58(11):3784–3786. Available from: http://view.ncbi.nlm.nih.gov/pubmed/1482199.

Heeg, D., Burns, D. A., Cartman, S. T., and Minton, N. P. 2012. Spores of clostridium difficile clinical isolates display a diverse germination response to bile salts. *PloS one*, 7(2). Available from: http://view.ncbi.nlm.nih.gov/pubmed/22384234.

Heijtz, R. D., Wang, S., Anuar, F., Qian, Y., Björkholm, B., Samuelsson, A., Hibberd, M. L., Forssberg, H., and Pettersson, S. 2011. Normal gut microbiota modulates brain development and behavior. *Proceedings of the National Academy of Sciences of the United States of America*, 108(7):3047–3052. Available from: http://dx.doi.org/10.1073/pnas.1010529108.

Hennequin, C., Janoir, C., Barc, M.-C. C., Collignon, A., and Karjalainen, T. 2003. Identification and characterization of a fibronectin-binding protein from Clostridium difficile. *Microbiology (Reading, England)*, 149(Pt 10):2779–2787. Available from: http://view.ncbi.nlm.nih.gov/pubmed/14523111.

HMPC 2012. Structure, function and diversity of the healthy human microbiome. *Nature*, 486(7402):207–214. Available from: http://dx.doi.org/10.1038/nature11234.

Hooper, L. V. and Gordon, J. I. 2001. Commensal Host-Bacterial relationships in the gut. *Science*, 292(5519):1115–1118. Available from: http://dx.doi.org/10.1126/science.1058709.

Hooper, L. V., Wong, M. H., Thelin, A., Hansson, L., Falk, P. G., and Gordon, J. I. 2001. Molecular analysis of commensal host-microbial relationships in the intestine. *Science*, 291(5505):881–884. Available from: http://dx.doi.org/10.1126/science.291.5505.881.

Hosono, S., Faruqi, A. F., Dean, F. B., Du, Y., Sun, Z., Wu, X., Du, J., Kingsmore, S. F., Egholm, M., and Lasken, R. S. 2003. Unbiased whole-genome amplification directly from clinical samples. *Genome Research*, 13(5):954–964. Available from: http://dx.doi.org/10.1101/gr.816903.

Hsiao, E. Y., McBride, S. W., Hsien, S., Sharon, G., Hyde, E. R., McCue, T., Codelli, J. A., Chow, J., Reisman, S. E., et al. 2013. Microbiota modulate behavioral and physiological abnormalities associated with neurodevelopmental disorders. *Cell*, 155(7):1451–1463. Available from: http://dx.doi.org/10.1016/j.cell.2013.11.024.

Huang, J., Zheng, Z., Andersson, A. F., Engstrand, L., and Ye, W. 2011. Rapid screening of complex DNA samples by single-molecule amplification and sequencing. *PLoS ONE*, 6(5):e19723+. Available from: http://dx.doi.org/10.1371/journal.pone.0019723.

Hunter, S., Jones, P., Mitchell, A., Apweiler, R., Attwood, T. K., Bateman, A., Bernard, T., Binns, D., et al. 2012. InterPro in 2011: new developments in the family and domain prediction database. *Nucleic Acids Research*, 40(Database issue):D306–D312. Available from: http://dx.doi.org/10.1093/nar/gkr948.

Huson, D. H., Auch, A. F., Qi, J., and Schuster, S. C. 2007. MEGAN analysis of metagenomic data. *Genome Research*, 17(3):377–386. Available from: http://dx.doi.org/10.1101/gr.5969107.

Hutchison, C. A., Smith, H. O., Pfannkoch, C., and Venter, J. C. 2005. Cell-free cloning using phi29 DNA polymerase. *Proceedings of the National Academy of Sciences of the United States of America*, 102(48):17332–17336. Available from: http://dx.doi.org/10.1073/pnas.0508809102.

Inoue, J., Shigemori, Y., and Mikawa, T. 2006. Improvements of rolling circle amplification (RCA) efficiency and accuracy using thermus thermophilus SSB mutant protein. *Nucleic Acids Research*, 34(9). Available from: http://view.ncbi.nlm.nih.gov/pubmed/16707659.

Ishoey, T., Woyke, T., Stepanauskas, R., Novotny, M., and Lasken, R. S. 2008. Genomic sequencing of single microbial cells from environmental samples. *Current Opinion in Microbiology*, 11(3):198–204. Available from: http://dx.doi.org/10.1016/j.mib.2008.05.006.

Iwamoto, K., Bundo, M., Ueda, J., Nakano, Y., Ukai, W., Hashimoto, E., Saito, T., and Kato, T. 2007. Detection of chromosomal structural alterations in single cells by snp arrays: A systematic survey of amplification bias and optimized workflow. *PLoS ONE*, 2(12):e1306+. Available from: http://dx.doi.org/10.1371/journal.pone.0001306.

Janoir, C., Péchiné, S., Grosdidier, C., and Collignon, A. 2007. Cwp84, a surface-associated protein of Clostridium difficile, is a cysteine protease with degrading activity on extracellular matrix proteins. *Journal of Bacteriology*, 189(20):7174–7180. Available from: http://dx.doi.org/10.1128/jb.00578-07.

Janvilisri, T., Scaria, J., Thompson, A. D., Nicholson, A., Limbago, B. M., Arroyo, L. G., Songer, J. G., Gröhn, Y. T., and Chang, Y.-F. F. 2009. Microarray identification of Clostridium difficile core components and divergent regions associated with host origin. *Journal of Bacteriology*, 191(12):3881–3891. Available from: http://dx.doi.org/10.1128/jb.00222-09.

Jeon, J.-H., Lee, C.-H., and Lee, H.-S. 2009. Antimicrobial activities of 2-Methyl-8-Hydroxyquinoline and its derivatives against human intestinal bacteria. *Journal of the Korean Society for Applied Biological Chemistry*, 52(2):202–205. Available from: http://dx.doi.org/10.3839/jksabc.2009.037.

Jiang, Z., Zhang, X., Deka, R., and Jin, L. 2005. Genome amplification of single sperm using multiple displacement amplification. *Nucleic Acids Research*, 33(10):e91. Available from: http://dx.doi.org/10.1093/nar/gni089.

Kalisky, T. and Quake, S. R. 2011. Single-cell genomics. *Nature Methods*, 8(4):311–314. Available from: http://dx.doi.org/10.1038/nmeth0411-311.

Kamentsky, L. A. and Melamed, M. R. 1967. Spectrophotometric cell sorter. *Science*, 156(3780):1364–1365. Available from: http://dx.doi.org/10.1126/science.156.3780.1364.

Karpińska, G., Mazurek, A. P., and Dobrowolski, J. C. 2010. On tautomerism and substituent effect in 8-hydroxyquinoline-derived medicine molecules. *Journal of Molecular Structure*, 961(1-3):101–106. Available from: http://dx.doi.org/10.1016/j.theochem.2010.09.006.

Kawamoto, S., Maruya, M., Kato, L. M., Suda, W., Atarashi, K., Doi, Y., Tsutsui, Y., Qin, H., Honda, K., et al. 2014. Foxp3(+) t cells regulate immunoglobulin a selection and facilitate diversification of bacterial species responsible for immune homeostasis. *Immunity*, 41(1):152–165. Available from: http://view.ncbi.nlm.nih.gov/pubmed/25017466.

Kawamoto, S., Tran, T. H., Maruya, M., Suzuki, K., Doi, Y., Tsutsui, Y., Kato, L. M., and Fagarasan, S. 2012. The inhibitory receptor pd-1 regulates iga selection and bacterial composition in the gut. *Science*, 336(6080):485–489. Available from: http://dx.doi.org/10.1126/science.1217718.

Kelly, C. P. and Kyne, L. 2011. The host immune response to Clostridium difficile. *Journal of Medical Microbiology*, 60(8):1070–1079. Available from: http://dx.doi.org/10.1099/jmm.0.030015-0.

Kelly, C. P., Pothoulakis, C., and LaMont, J. T. 1994. Clostridium difficile colitis. *New England Journal of Medicine*, 330(4):257–262. Available from: http://dx.doi.org/10.1056/nejm199401273300406.

Kim, K.-H. H., Chang, H.-W. W., Nam, Y.-D. D., Roh, S. W. W., Kim, M.-S. S., Sung, Y., Jeon, C. O. O., Oh, H.-M. M., and Bae, J.-W. W. 2008. Amplification of uncultured single-stranded DNA viruses from rice paddy soil. *Applied and Environmental Microbiology*, 74(19):5975–5985. Available from: http://dx.doi.org/10.1128/aem.01275-08.

Klaassen, C. H., van Haren, H. A., and Horrevorts, A. M. 2002. Molecular fingerprinting of clostridium difficile isolates: pulsed-field gel electrophoresis versus amplified fragment length polymorphism. *Journal of Clinical Microbiology*, 40(1):101–104. Available from: http://www.ncbi.nlm.nih.gov/pmc/articles/PMC120100/.

Klein, C. A., Schmidt-Kittler, O., Schardt, J. A., Pantel, K., Speicher, M. R., and Riethmüller, G. 1999. Comparative genomic hybridization, loss of heterozygosity, and DNA sequence analysis of single cells. *Proceedings of the National Academy of Sciences of the United States of America*, 96(8):4494–4499. Available from: http://dx.doi.org/10.1073/pnas.96.8.4494.

Klindworth, A., Pruesse, E., Schweer, T., Peplies, J., Quast, C., Horn, M., and Glöckner, F. O. O. 2013. Evaluation of general 16S ribosomal RNA gene PCR primers for classical and next-generation sequencing-based diversity studies. *Nucleic Acids Research*, 41(1):e1. Available from: http://dx.doi.org/10.1093/nar/gks808.

Klucar, L., Stano, M., and Hajduk, M. 2010. phiSITE: database of gene regulation in bacteriophages. *Nucleic Acids Research*, 38(suppl 1):D366–D370. Available from: http://dx.doi.org/10.1093/nar/gkp911.

Knecht, H., Neulinger, S. C., Heinsen, F. A., Knecht, C., Schilhabel, A., Schmitz, R. A., Zimmermann, A., dos Santos, V. M., Ferrer, M., et al. 2014. Effects of beta-lactam antibiotics and fluoroquinolones on human gut microbiota in relation to Clostridium difficile associated diarrhea. *PLoS ONE*, 9(2):e89417+. Available from: http://dx.doi.org/10.1371/journal.pone.0089417.

Knierim, E., Lucke, B., Schwarz, J. M. M., Schuelke, M., and Seelow, D. 2011. Systematic comparison of three methods for fragmentation of long-range PCR products for next generation sequencing. *PLoS ONE*, 6(11):e28240+. Available from: http://dx.doi.org/10.1371/journal.pone.0028240.

Koboldt, D. C., Zhang, Q., Larson, D. E., Shen, D., McLellan, M. D., Lin, L., Miller, C. A., Mardis, E. R., Ding, L., and Wilson, R. K. 2012. VarScan 2: Somatic mutation and copy number alteration discovery in cancer by exome sequencing. *Genome Research*, 22(3):568–576. Available from: http://dx.doi.org/10.1101/gr.129684.111.

Koenig, J. E., Spor, A., Scalfone, N., Fricker, A. D., Stombaugh, J., Knight, R., Angenent, L. T., and Ley, R. E. 2011. Succession of microbial consortia in the developing infant gut microbiome. *Proceedings of the National Academy of Sciences of the United States of America*, 108(S1):4578–4585. Available from: http://dx.doi.org/10.1073/pnas.1000081107.

Koo, H. L., Van, J. N., Zhao, M., Ye, X., Revell, P. A., Jiang, Z.-D. D., Grimes, C. Z., Koo, D. C., Lasco, T., et al. 2014. Real-time polymerase chain reaction detection of asymptomatic Clostridium difficile colonization and rising C. difficile-associated disease rates. *Infection control and hospital epidemiology : the official journal of the Society of Hospital Epidemiologists of America*, 35(6):667–673. Available from: http://view.ncbi.nlm.nih.gov/pubmed/24799643.

Kostic, A. D., Gevers, D., Pedamallu, C. S. S., Michaud, M., Duke, F., Earl, A. M., Ojesina, A. I., Jung, J., Bass, A. J., et al. 2012. Genomic analysis identifies association of fusobacterium with colorectal carcinoma. *Genome Research*, 22(2):292–298. Available from: http://dx.doi.org/10.1101/gr.126573.111.

Kristensen, D. M., Mushegian, A. R., Dolja, V. V., and Koonin, E. V. 2010. New dimensions of the virus world discovered through metagenomics. *Trends in Microbiology*, 18(1):11–19. Available from: http://dx.doi.org/10.1016/j.tim.2009.11.003.

Kuijper, E. J., Barbut, F., Brazier, J. S., Kleinkauf, N., Eckmanns, T., Lambert, M. L., Drudy, D., Fitzpatrick, F., Wiuff, C., Brown, D. J., et al. 2008. Update of clostridium difficile infection due to PCR ribotype 027 in europe, 2008. *Euro Surveillance*, 13(31). Available from: http://view.ncbi.nlm.nih.gov/pubmed/18761903.

Kunin, V., Engelbrektson, A., Ochman, H., and Hugenholtz, P. 2010. Wrinkles in the rare biosphere: pyrosequencing errors can lead to artificial inflation of diversity estimates. *Environmental Microbiology*, 12(1):118–123. Available from: http://dx.doi.org/10.1111/j.1462-2920.2009.02051.x.

Kuroda, M., Serizawa, M., Okutani, A., Sekizuka, T., Banno, S., and Inoue, S. 2010. Genome-wide single nucleotide polymorphism typing method for identification of Bacillus anthracis species and strains among B. cereus group species. *Journal of Clinical Microbiology*, 48(8):2821–2829. Available from: http://view.ncbi.nlm.nih.gov/pubmed/20554827.

Kyne, L., Warny, M., Qamar, A., and Kelly, C. P. 2000. Asymptomatic carriage of Clostridium difficile and serum levels of IgG antibody against toxin A. *New England Journal of Medicine*, 342(6):390–397. Available from: http://dx.doi.org/10.1056/nejm200002103420604.

Ladner, J. T., Beitzel, B., Chain, P. S. G., Davenport, M. G., Donaldson, E., Frieman, M., Kugelman, J., Kuhn, J. H., O'Rear, J., et al. 2014. Standards for sequencing viral genomes in the era of high-throughput sequencing. *mBio*, 5(3):e01360–14+. Available from: http://dx.doi.org/10.1128/mbio.01360-14.

Lage, J. M., Leamon, J. H., Pejovic, T., Hamann, S., Lacey, M., Dillon, D., Segraves, R., Vossbrinck, B., González, A., et al. 2003. Whole genome analysis of genetic alterations in small DNA samples using hyperbranched strand displacement amplification and array-CGH. *Genome Research*, 13(2):294–307. Available from: http://dx.doi.org/10.1101/gr.377203.

Lang, A. S., Zhaxybayeva, O., and Beatty, J. T. 2012. Gene transfer agents: phage-like elements of genetic exchange. *Nature Reviews. Microbiology*, 10(7):472–482. Available from: http://view.ncbi.nlm.nih.gov/pubmed/22683880.

Langmead, B. and Salzberg, S. L. 2012. Fast gapped-read alignment with bowtie 2. *Nature Methods*, 9(4):357–359. Available from: http://dx.doi.org/10.1038/nmeth.1923.

Lasken, R. S. 2013. Single-cell sequencing in its prime. *Nature Biotechnology*, 31(3):211–212. Available from: http://dx.doi.org/10.1038/nbt.2523.

Lasken, R. S. and Stockwell, T. B. 2007. Mechanism of chimera formation during the multiple displacement amplification reaction. *BMC Biotechnology*, 7:19+. Available from: http://dx.doi.org/10.1186/1472-6750-7-19.

Law, J., Jovel, J., Patterson, J., Ford, G., O'keefe, S., Wang, W., Meng, B., Song, D., Zhang, Y., et al. 2013. Identification of hepatotropic viruses from plasma using deep sequencing: A next generation diagnostic tool. *PLoS ONE*, 8(4):e60595+. Available from: http://dx.doi.org/10.1371/journal.pone.0060595.

Lawlor, G. and Moss, A. C. 2010. Cytomegalovirus in inflammatory bowel disease: pathogen or innocent bystander? *Inflammatory Bowel Diseases*, 16(9):1620–1627. Available from: http://view.ncbi.nlm.nih.gov/pubmed/20232408.

Le Caignec, C., Spits, C., Sermon, K., De Rycke, M., Thienpont, B., Debrock, S., Staessen, C., Moreau, Y., Fryns, J.-P., et al. 2006. Single-cell chromosomal imbalances detection by array CGH. *Nucleic Acids Research*, 34(9):e68. Available from: http://dx.doi.org/10.1093/nar/gkl1336.

Lennon, N., Lintner, R., Anderson, S., Alvarez, P., Barry, A., Brockman, W., Daza, R., Erlich, R., Giannoukos, G., et al. 2010. A scalable, fully automated process for construction of sequence-ready barcoded libraries for 454. *Genome Biology*, 11(2):R15+. Available from: http://dx.doi.org/10.1186/gb-2010-11-2-r15.

Lepage, P., Colombet, J., Marteau, P., Sime-Ngando, T., Doré, J., and Leclerc, M. 2008. Dysbiosis in inflammatory bowel disease: a role for bacteriophages? *Gut*, 57(3):424–425. Available from: http://view.ncbi.nlm.nih.gov/pubmed/18268057.

Lepage, P., Häsler, R., Spehlmann, M. E., Rehman, A., Zvirbliene, A., Begun, A., Ott, S., Kupcinskas, L., Doré, J., Raedler, A., and Schreiber, S. 2011. Twin study indicates loss of interaction between microbiota and mucosa of patients with ulcerative colitis. *Gastroenterology*, 141(1):227–236. Available from: http://dx.doi.org/10.1053/j.gastro.2011.04.011.

Leplae, R., Hebrant, A., Wodak, S. J., and Toussaint, A. 2004. ACLAME: a CLAssification of Mobile genetic Elements. *Nucleic Acids Research*, 32:D45–D49. Available from: http://dx.doi.org/10.1093/nar/gkh084.

Leung, K., Zahn, H., Leaver, T., Konwar, K. M., Hanson, N. W., Pagé, A. P., Lo, C.-C., Chain, P. S., Hallam, S. J., and Hansen, C. L. 2012. A programmable droplet-based microfluidic device applied to multiparameter analysis of single microbes and microbial communities. *Proceedings of the National Academy of Sciences of the United States of America*, 109(20):7665–7670. Available from: http://dx.doi.org/10.1073/pnas.1106752109.

Ley, R. E. 2014. Harnessing microbiota to kill a pathogen: The sweet tooth of Clostridium difficile. *Nature Medicine*, 20(3):248–249. Available from: http://dx.doi.org/10.1038/nm.3494.

Li, D., He, M., and Jiang, S. C. 2010. Detection of infectious adenoviruses in environmental waters by fluorescence-activated cell sorting assay. *Applied and Environmental Microbiology*, 76(5):1442–1448. Available from: http://dx.doi.org/10.1128/aem.01937-09.

Li, H., Handsaker, B., Wysoker, A., Fennell, T., Ruan, J., Homer, N., Marth, G., Abecasis, G., Durbin, R., and 1000 Genome Project Data Processing Subgroup 2009. The sequence alignment/map format and SAMtools. *Bioinformatics*, 25(16):2078–2079. Available from: http://dx.doi.org/10.1093/bioinformatics/btp352.

Li, K., Bihan, M., Yooseph, S., and Methé, B. A. 2012. Analyses of the microbial diversity across the human microbiome. *PLoS ONE*, 7(6):e32118+. Available from: http://dx.doi.org/10.1371/journal.pone.0032118.

Li, W. and Godzik, A. 2006. Cd-hit: a fast program for clustering and comparing large sets of protein or nucleotide sequences. *Bioinformatics*, 22(13):1658–1659. Available from: http://dx.doi.org/10.1093/bioinformatics/btl158.

Lin, Y.-P. P., Kuo, C.-J. J., Koleci, X., McDonough, S. P., and Chang, Y.-F. F. 2011. Manganese binds to Clostridium difficile Fbp68 and is essential for fibronectin binding. *The Journal of Biological Chemistry*, 286(5):3957–3969. Available from: http://dx.doi.org/10.1074/jbc.m110.184523.

Ling, Z., Liu, X., Jia, X., Cheng, Y., Luo, Y., Yuan, L., Wang, Y., Zhao, C., Guo, S., et al. 2014. Impacts of infection with different toxigenic Clostridium difficile strains on faecal microbiota in children. *Scientific Reports*, 4(7485). Available from: http://www.nature.com/srep/2014/141215/srep07485/full/srep07485.html.

Liu, C., Bayer, A., Cosgrove, S. E., Daum, R. S., Fridkin, S. K., Gorwitz, R. J., Kaplan, S. L., Karchmer, A. W., Levine, D. P., et al. 2011. Clinical practice guidelines by the infectious diseases society of america for the treatment of methicillin-resistant Staphylococcus aureus infections in adults and children. *Clinical Infectious Diseases*, 52(3):ciq146+. Available from: http://dx.doi.org/10.1093/cid/ciq146.

Llano-Sotelo, B., Azucena, E. F., Kotra, L. P., Mobashery, S., and Chow, C. S. 2002. Aminoglycosides modified by resistance enzymes display diminished binding to the bacterial ribosomal aminoacyl-tRNA site. *Chemistry & biology*, 9(4):455–463. Available from: http://view.ncbi.nlm.nih.gov/pubmed/11983334.

Loftus, E. V. 2004. Clinical epidemiology of inflammatory bowel disease: Incidence, prevalence, and environmental influences. *Gastroenterology*, 126(6):1504–1517. Available from: http://view.ncbi.nlm.nih.gov/pubmed/15168363.

Lopetuso, L. R., Scaldaferri, F., Petito, V., and Gasbarrini, A. 2013. Commensal Clostridia: leading players in the maintenance of gut homeostasis. *Gut pathogens*, 5(1). Available from: http://view.ncbi.nlm.nih.gov/pubmed/23941657.

López-Amorós, R., Castel, S., Comas-Riu, J., and Vives-Rego, J. 1997. Assessment of E. coli and Salmonella viability and starvation by confocal laser microscopy and flow cytometry using rhodamine 123, DiBAC4(3), propidium iodide, and CTC. *Cytometry*, 29(4):298–305. Available from: http://view.ncbi.nlm.nih.gov/pubmed/9415412.

Lu, S., Zong, C., Fan, W., Yang, M., Li, J., Chapman, A. R., Zhu, P., Hu, X., Xu, L., et al. 2012. Probing meiotic recombination and aneuploidy of single sperm cells by whole-genome sequencing. *Science*, 338(6114):1627–1630. Available from: http://dx.doi.org/10.1126/science.1229112.

Lutgendorff, F., Akkermans, L. M., and Söderholm, J. D. 2008. The role of microbiota and probiotics in stress-induced gastro-intestinal damage. *Current Molecular Medicine*, 8(4):282–298. Available from: http://view.ncbi.nlm.nih.gov/pubmed/18537636.

Lynch, M. D. J. and Neufeld, J. D. 2015. Ecology and exploration of the rare biosphere. *Nature Reviews Microbiology*, 13(4):217–229. Available from: http://dx.doi.org/10.1038/nrmicro3400.

Macfarlane, S., Woodmansey, E. J., and Macfarlane, G. T. 2005. Colonization of mucin by human intestinal bacteria and establishment of biofilm communities in a two-stage continuous culture system. *Applied and Environmental Microbiology*, 71(11):7483–7492. Available from: http://dx.doi.org/10.1128/aem.71.11.7483-7492.2005.

Macpherson, A. J., Gatto, D., Sainsbury, E., Harriman, G. R., Hengartner, H., and Zinkernagel, R. M. 2000. A primitive T cell-independent mechanism of intestinal mucosal IgA responses to commensal bacteria. *Science*, 288(5474):2222–2226. Available from: http://view.ncbi.nlm.nih.gov/pubmed/10864873.

Macpherson, A. J., Geuking, M. B., Slack, E., Hapfelmeier, S., and McCoy, K. D. 2012. The habitat, double life, citizenship, and forgetfulness of IgA. *Immunological reviews*, 245(1):132–146. Available from: http://view.ncbi.nlm.nih.gov/pubmed/22168417.

Manichanh, C., Borruel, N., Casellas, F., and Guarner, F. 2012. The gut microbiota in IBD. *Nature Reviews. Gastroenterology & Hepatology*, 9(10):599–608. Available from: http://view.ncbi.nlm.nih.gov/pubmed/22907164.

Marcy, Y., Ishoey, T., Lasken, R. S., Stockwell, T. B., Walenz, B. P., Halpern, A. L., Beeson, K. Y., Goldberg, S. M. D., and Quake, S. R. 2007a. Nanoliter reactors improve multiple displacement amplification of genomes from single cells. *PLoS Genetics*, 3(9):e155–1708. Available from: http://dx.doi.org/10.1371/journal.pgen.0030155.

Marcy, Y., Ouverney, C., Bik, E. M., Lösekann, T., Ivanova, N., Martin, H. G., Szeto, E., Platt, D., Hugenholtz, P., et al. 2007b. Dissecting biological "dark matter" with single-cell genetic analysis of rare and uncultivated TM7 microbes from the human mouth. *Proceedings of the National Academy of Sciences of the United States of America*, 104(29):11889–11894. Available from: http://dx.doi.org/10.1073/pnas.0704662104.

Marie, D., Brussaard, C. P. D., Thyrhaug, R., Bratbak, G., and Vaulot, D. 1999. Enumeration of marine viruses in culture and natural samples by flow cytometry. *Applied and Environmental Microbiology*, 65(1):45–52. Available from: http://www.ncbi.nlm.nih.gov/pmc/articles/PMC90981/.

Marine, R., McCarren, C., Vorrasane, V., Nasko, D., Crowgey, E., Polson, S. W., and Wommack, K. E. 2014. Caught in the middle with multiple displacement amplification: the myth of pooling for avoiding multiple displacement amplification bias in a metagenome. *Microbiome*, 2(1). Available from: http://dx.doi.org/10.1186/2049-2618-2-3.

Marine, R., Polson, S. W., Ravel, J., Hatfull, G., Russell, D., Sullivan, M., Syed, F., Dumas, M., and Wommack, K. E. 2011. Evaluation of a transposase protocol for rapid generation of shotgun high-throughput sequencing libraries from nanogram quantities of DNA. *Applied and Environmental Microbiology*, 77(22):8071–8079. Available from: http://dx.doi.org/10.1128/aem.05610-11.

Martin, C. E., Weishaupt, M. W., and Seeberger, P. H. 2011. Progress toward developing a carbohydrate-conjugate vaccine against Clostridium difficile ribotype 027: synthesis of the cell-surface polysaccharide PS-I repeating unit. *Chemical Communications*, 47(37):10260–10262. Available from: http://dx.doi.org/10.1039/c1cc13614c.

Martinez-Garcia, M., Brazel, D., Poulton, N. J., Swan, B. K., Gomez, M. L., Masland, D., Sieracki, M. E., and Stepanauskas, R. 2011. Unveiling in situ interactions between marine protists and bacteria through single cell sequencing. *The ISME Journal*, 6(3):703–707. Available from: http://dx.doi.org/10.1038/ismej.2011.126.

Matsuda, K., Tsuji, H., Asahara, T., Takahashi, T., Kubota, H., Nagata, S., Yamashiro, Y., and Nomoto, K. 2012. Sensitive quantification of Clostridium difficile cells by reverse transcription-quantitative PCR targeting rRNA molecules. *Applied and Environmental Microbiology*, 78(15):5111–5118. Available from: http://dx.doi.org/10.1128/aem.07990-11.

Maurice, C. F. F., Haiser, H. J. J., and Turnbaugh, P. J. J. 2013. Xenobiotics shape the physiology and gene expression of the active human gut microbiome. *Cell*, 152(1-2):39–50. Available from: http://dx.doi.org/10.1016/j.cell.2012.10.052.

Mazmanian, S. K., Liu, C. H., Tzianabos, A. O., and Kasper, D. L. 2005. An immunomodulatory molecule of symbiotic bacteria directs maturation of the host immune system. *Cell*, 122(1):107–118. Available from: http://dx.doi.org/10.1016/j.cell.2005.05.007.

McEllistrem, M. C., Carman, R. J., Gerding, D. N., Genheimer, C. W., and Zheng, L. 2005. A hospital outbreak of Clostridium difficile disease associated with isolates carrying binary toxin genes. *Clinical Infectious Diseases*, 40(2):265–272. Available from: http://dx.doi.org/10.1086/427113.

McGuckin, M. A., LindÃ©n, S. K., Sutton, P., and Florin, T. H. 2011. Mucin dynamics and enteric pathogens. *Nature Reviews Microbiology*, 9(4):265–278. Available from: http://dx.doi.org/10.1038/nrmicro2538.

Medini, D., Donati, C., Tettelin, H., Masignani, V., and Rappuoli, R. 2005. The microbial pan-genome. *Current Opinion in Genetics & Development*, 15(6):589–594. Available from: http://dx.doi.org/10.1016/j.gde.2005.09.006.

Mehlig, M., Moos, M., Braun, V., Kalt, B., Mahony, D. E., and von Eichel-Streiber, C. 2001. Variant toxin B and a functional toxin A produced by Clostridium difficile C34. *FEMS Microbiology Letters*, 198(2):171–176. Available from: http://view.ncbi.nlm.nih.gov/pubmed/11430410.

Merenstein, D., El-Nachef, N., and Lynch, S. V. 2014. Fecal microbial therapy: promises and pitfalls. *Journal of Pediatric Gastroenterology and Nutrition*, 59(2):157–161. Available from: http://view.ncbi.nlm.nih.gov/pubmed/24796803.

Merrigan, M. M., Sambol, S. P., Johnson, S., and Gerding, D. N. 2003. Prevention of fatal Clostridium difficile-associated disease during continuous administration of clindamycin in hamsters. *The Journal of Infectious Diseases*, 188(12):1922–1927. Available from: http://view.ncbi.nlm.nih.gov/pubmed/14673773.

Meyer, M., Briggs, A. W., Maricic, T., Höber, B., Höffner, B., Krause, J., Weihmann, A., Pääbo, S., and Hofreiter, M. 2008. From micrograms to picograms: quantitative PCR reduces the material demands of high-throughput sequencing. *Nucleic Acids Research*, 36(1):e5. Available from: http://dx.doi.org/10.1093/nar/gkm1095.

Mills, S., Serrano, L. M., Griffin, C., O'Connor, P. M., Schaad, G., Bruining, C., Hill, C., Ross, R. P., and Meijer, W. C. 2011. Inhibitory activity of Lactobacillus plantarum LMG p-26358 against Listeria innocua when used as an adjunct starter in the manufacture of cheese. *Microbial Cell Factories*, 10 Suppl 1. Available from: http://view.ncbi.nlm.nih.gov/pubmed/21995443.

Mills, S., Shanahan, F., Stanton, C., Hill, C., Coffey, A., and Ross, R. P. 2013. Movers and shakers: influence of bacteriophages in shaping the mammalian gut microbiota. *Gut Microbes*, 4(1):4–16. Available from: http://view.ncbi.nlm.nih.gov/pubmed/23022738.

Minot, S., Bryson, A., Chehoud, C., Wu, G. D., Lewis, J. D., and Bushman, F. D. 2013. Rapid evolution of the human gut virome. *Proceedings of the National Academy of Sciences of the United States of America*, 110(30):12450–12455. Available from: http://dx.doi.org/10.1073/pnas.1300833110.

Minot, S., Grunberg, S., Wu, G. D., Lewis, J. D., and Bushman, F. D. 2012. Hypervariable loci in the human gut virome. *Proceedings of the National Academy of Sciences of the United States of America*, 109(10):3962–3966. Available from: http://dx.doi.org/10.1073/pnas.1119061109.

Minot, S., Sinha, R., Chen, J., Li, H., Keilbaugh, S. A., Wu, G. D., Lewis, J. D., and Bushman, F. D. 2011. The human gut virome: inter-individual variation and dynamic response to diet. *Genome Research*, 21(10):1616–1625. Available from: http://dx.doi.org/10.1101/gr.122705.111.

Modi, S. R., Lee, H. H., Spina, C. S., and Collins, J. J. 2013. Antibiotic treatment expands the resistance reservoir and ecological network of the phage metagenome. *Nature*, 499(7457):219–222. Available from: http://dx.doi.org/10.1038/nature12212.

Morgan, M., Anders, S., Lawrence, M., Aboyoun, P., Pagès, H., and Gentleman, R. 2009. Shortread: a bioconductor package for input, quality assessment and exploration of high-throughput sequence data. *Bioinformatics*, 25:2607–2608. Available from: http://dx.doi.org10.1093/bioinformatics/btp450.

Morgan, M., Pagès, H., Obenchain, V., and Hayden, N. 2015. Rsamtools: Binary alignment (bam), fasta, variant call (bcf), and tabix file import. R package version 1.18.3. Available from: http://bioconductor.org/packages/release/bioc/html/Rsamtools.html.

Morgan, X. C., Segata, N., and Huttenhower, C. 2013. Biodiversity and functional genomics in the human microbiome. *Trends in Genetics*, 29(1):51–58. Available from: http://dx.doi.org/10.1016/j.tig.2012.09.005.

Morris, R. M., Rappé, M. S., Connon, S. A., Vergin, K. L., Siebold, W. A., Carlson, C. A., and Giovannoni, S. J. 2002. SAR11 clade dominates ocean surface bacterioplankton communities. *Nature*, 420(6917):806–810. Available from: http://view.ncbi.nlm.nih.gov/pubmed/12490947.

Moya, A., Peretó, J., Gil, R., and Latorre, A. 2008. Learning how to live together: genomic insights into prokaryote-animal symbioses. *Nature Reviews. Genetics*, 9(3):218–229. Available from: http://dx.doi.org/10.1038/nrg2319.

Mullane, K. M., Miller, M. A., Weiss, K., Lentnek, A., Golan, Y., Sears, P. S., Shue, Y.-K., Louie, T. J., and Gorbach, S. L. 2011. Efficacy of fidaxomicin versus vancomycin as therapy for Clostridium difficile infection in individuals taking concomitant antibiotics for other concurrent infections. *Clinical Infectious Diseases*, 53(5):440–447. Available from: http://dx.doi.org/10.1093/cid/cir404.

Müller, S. and Babel, W. 2003. Analysis of bacterial DNA patterns–an approach for controlling biotechnological processes. *Journal of Microbiological Methods*, 55(3):851–858. Available from: http://view.ncbi.nlm.nih.gov/pubmed/14607431.

Müller, S. and Nebe-von Caron, G. 2010. Functional single-cell analyses: flow cytometry and cell sorting of microbial populations and communities. *FEMS Microbiology Reviews*, 34(4):554–587. Available from: http://dx.doi.org/10.1111/j.1574-6976.2010.00214.x.

Murphy, E. F., Cotter, P. D., Healy, S., Marques, T. M., O'Sullivan, O., Fouhy, F., Clarke, S. F., O'Toole, P. W., Quigley, E. M., et al. 2010. Composition and energy harvesting capacity of the gut microbiota: relationship to diet, obesity and time in mouse models. *Gut*, 59(12):1635–1642. Available from: http://dx.doi.org/10.1136/gut.2010.215665.

Ng, K. M., Ferreyra, J. A., Higginbottom, S. K., Lynch, J. B., Kashyap, P. C., Gopinath, S., Naidu, N., Choudhury, B., Weimer, B. C., et al. 2013. Microbiota-liberated host sugars facilitate post-antibiotic expansion of enteric pathogens. *Nature*, 502(7469):96–99. Available from: http://dx.doi.org/10.1038/nature12503.

Ning, Z., Cox, A. J., and Mullikin, J. C. 2001. SSAHA: a fast search method for large DNA databases. *Genome Research*, 11(10):1725–1729. Available from: http://dx.doi.org/10.1101/gr.194201.

Norman, J. M., Handley, S. A., Baldridge, M. T., Droit, L., Liu, C. Y., Keller, B. C., Kambal, A., Monaco, C. L., Zhao, G., et al. 2015. Disease-specific alterations in the enteric virome in inflammatory bowel disease. *Cell*, 160(3):447–460. Available from: http://dx.doi.org/10.1016/j.cell.2015.01.002.

Novakova, J., Vlkova, E., Bonusova, B., Rada, V., and Kokoska, L. 2013. In vitro selective inhibitory effect of 8-hydroxyquinoline against bifidobacteria and clostridia. *Anaerobe*, 22:134–136. Available from: http://view.ncbi.nlm.nih.gov/pubmed/23770542.

Novo, D. J., Perlmutter, N. G., Hunt, R. H., and Shapiro, H. M. 2000. Multiparameter flow cytometric analysis of antibiotic effects on membrane potential, membrane permeability, and bacterial counts of Staphylococcus aureus and Micrococcus luteus. *Antimicrobial Agents and Chemotherapy*, 44(4):827–834. Available from: http://www.ncbi.nlm.nih.gov/pmc/articles/PMC89778/.

Ogilvie, L. A., Bowler, L. D., Caplin, J., Dedi, C., Diston, D., Cheek, E., Taylor, H., Ebdon, J. E., and Jones, B. V. 2013. Genome signature-based dissection of human gut metagenomes to extract subliminal viral sequences. *Nature Communications*, 4. Available from: http://view.ncbi.nlm.nih.gov/pubmed/24036533.

Ohman, L. and Simrén, M. 2013. Intestinal microbiota and its role in irritable bowel syndrome (IBS). *Current Gastroenterology Reports*, 15(5). Available from: http://view.ncbi.nlm.nih.gov/pubmed/23580243.

Okubo, K., Hori, N., Matoba, R., Niiyama, T., Fukushima, A., Kojima, Y., and Matsubara, K. 1992. Large scale cDNA sequencing for analysis of quantitative and qualitative aspects of gene expression. *Nature Genetics*, 2(3):173–179. Available from: http://dx.doi.org/10.1038/ng1192-173.

Ozaki, E., Kato, H., Kita, H., Karasawa, T., Maegawa, T., Koino, Y., Matsumoto, K., Takada, T., Nomoto, K., et al. 2004. Clostridium difficile colonization in healthy adults: transient colonization and correlation with enterococcal colonization. *Journal of Medical Microbiology*, 53(Pt 2):167–172. Available from: http://view.ncbi.nlm.nih.gov/pubmed/14729940.

Pabst, O. 2012. New concepts in the generation and functions of IgA. *Nature Reviews Immunology*, 12(12):821–832. Available from: http://dx.doi.org/10.1038/nri3322.

Pachmann, K. 2015. Current and potential use of MAINTRAC method for cancer diagnosis and prediction of metastasis. *Expert Review of Molecular Diagnostics*, 15(5):597–605. Available from: http://dx.doi.org/10.1586/14737159.2015.1032260.

Paez, J. G., Lin, M., Beroukhim, R., Lee, J. C., Zhao, X., Richter, D. J., Gabriel, S., Herman, P., Sasaki, H., et al. 2004. Genome coverage and sequence fidelity of phi29 polymerase-based multiple strand displacement whole genome amplification. *Nucleic Acids Research*, 32(9):e71. Available from: http://dx.doi.org/10.1093/nar/gnh069.

Pages, H., Aboyoun, P., Gentleman, R., and DebRoy, S. 2014. *Biostrings: String objects representing biological sequences, and matching algorithms*. R package version 2.26.3.

Palm, N. W., de Zoete, M. R., Cullen, T. W., Barry, N. A., Stefanowski, J., Hao, L., Degnan, P. H., Hu, J., Peter, I., et al. 2014. Immunoglobulin a coating identifies colitogenic bacteria in inflammatory bowel disease. *Cell*, 158(5):1000–1010. Available from: http://dx.doi.org/10.1016/j.cell.2014.08.006.

Pan, X., Urban, A. E., Palejev, D., Schulz, V., Grubert, F., Hu, Y., Snyder, M., and Weissman, S. M. 2008. A procedure for highly specific, sensitive, and unbiased whole-genome amplification. *Proceedings of the National Academy of Sciences of the United States of America*, 105(40):15499–15504. Available from: http://dx.doi.org/10.1073/pnas.0808028105.

Paradis, E., Claude, J., and Strimmer, K. 2004. APE: Analyses of phylogenetics and evolution in R language. *Bioinformatics*, 20(2):289–290. Available from: http://dx.doi.org/10.1093/bioinformatics/btg412.

Parsons, R. J., Breitbart, M., Lomas, M. W., and Carlson, C. A. 2012. Ocean time-series reveals recurring seasonal patterns of virioplankton dynamics in the northwestern Sargasso Sea. *The ISME journal*, 6(2):273–284. Available from: http://view.ncbi.nlm.nih.gov/pubmed/21833038.

Pearl, J. 1988. *Probabilistic Reasoning in Intelligent Systems: Networks of Plausible Inference*. San Francisco, CA, USA: Morgan Kaufmann Publishers Inc. Available from: http://portal.acm.org/citation.cfm?id=52121.

Peltier, J., Courtin, P., El Meouche, I., Lemée, L., Chapot-Chartier, M.-P. P., and Pons, J.-L. L. 2011. Clostridium difficile has an original peptidoglycan structure with a high level of N-acetylglucosamine deacetylation and mainly 3-3 cross-links. *The Journal of Biological Chemistry*, 286(33):29053–29062. Available from: http://view.ncbi.nlm.nih.gov/pubmed/21685382.

Pépin, J., Valiquette, L., Alary, M.-E. E., Villemure, P., Pelletier, A., Forget, K., Pépin, K., and Chouinard, D. 2004. Clostridium difficile-associated diarrhea in a region of quebec from 1991 to 2003: a changing pattern of disease severity. *CMAJ*, 171(5):466–472. Available from: http://view.ncbi.nlm.nih.gov/pubmed/15337727.

Pérez-Brocal, V., García-López, R., Vázquez-Castellanos, J. F., Nos, P., Beltrán, B., Latorre, A., and Moya, A. 2013. Study of the viral and microbial communities associated with Crohn's disease: a metagenomic approach. *Clinical and Translational Gastroenterology*, 4(6):e36+. Available from: http://dx.doi.org/10.1038/ctg.2013.9.

Pérez-Cobas, A. E., Gosalbes, M. J., Friedrichs, A., Knecht, H., Artacho, A., Eismann, K., Otto, W., Rojo, D., Bargiela, R., et al. 2012. Gut microbiota disturbance during antibiotic therapy: a multi-omic approach. *Gut*, Pp. gutjnl–2012–303184+. Available from: http://dx.doi.org/10.1136/gutjnl-2012-303184.

Peris-Bondia, F., Latorre, A., Artacho, A., Moya, A., and D'Auria, G. 2011. The active human gut microbiota differs from the total microbiota. *PLoS ONE*, 6(7). Available from: http://view.ncbi.nlm.nih.gov/pubmed/21829462.

Perkins, T. T., Kingsley, R. A., Fookes, M. C., Gardner, P. P., James, K. D., Yu, L., Assefa, S. A., He, M., Croucher, N. J., et al. 2009. A strand-specific RNA-Seq analysis of the transcriptome of the typhoid bacillus Salmonella typhi. *PLoS Genetics*, 5(7):e1000569+. Available from: http://dx.doi.org/10.1371/journal.pgen.1000569.

Peterson, D. A., McNulty, N. P., Guruge, J. L., and Gordon, J. I. 2007. Iga response to symbiotic bacteria as a mediator of gut homeostasis. *Cell Host & Microbe*, 2(5):328–339. Available from: http://dx.doi.org/10.1016/j.chom.2007.09.013.

Petrov, V. M., Ratnayaka, S., Nolan, J. M., Miller, E. S., and Karam, J. D. 2010. Genomes of the T4-related bacteriophages as windows on microbial genome evolution. *Virology Journal*, 7. Available from: http://view.ncbi.nlm.nih.gov/pubmed/21029436.

Picot, J., Guerin, C. L., Le Van Kim, C., and Boulanger, C. M. 2012. Flow cytometry: retrospective, fundamentals and recent instrumentation. *Cytotechnology*, 64(2):109–130. Available from: http://dx.doi.org/10.1007/s10616-011-9415-0.

Pinard, R., de Winter, A., Sarkis, G., Gerstein, M., Tartaro, K., Plant, R., Egholm, M., Rothberg, J., and Leamon, J. 2006. Assessment of whole genome amplification-induced bias through high-throughput, massively parallel whole genome sequencing. *BMC Genomics*, 7(1):216+. Available from: http://dx.doi.org/10.1186/1471-2164-7-216.

Podar, M., Abulencia, C. B., Walcher, M., Hutchison, D., Zengler, K., Garcia, J. A., Holland, T., Cotton, D., Hauser, L., and Keller, M. 2007. Targeted access to the genomes of low-abundance organisms in complex microbial communities. *Applied and Environmental Microbiology*, 73(10):3205–3214. Available from: http://dx.doi.org/10.1128/aem.02985-06.

Popoff, M. R., Rubin, E. J., Gill, D. M., and Boquet, P. 1988. Actin-specific ADP-ribosyltransferase produced by a Clostridium difficile strain. *Infection and Immunity*, 56(9):2299–2306. Available from: http://view.ncbi.nlm.nih.gov/pubmed/3137166.

Pruesse, E., Quast, C., Knittel, K., Fuchs, B. M., Ludwig, W., Peplies, J., and Glöckner, F. O. O. 2007. SILVA: a comprehensive online resource for quality checked and aligned ribosomal RNA sequence data compatible with ARB. *Nucleic Acids Research*, 35(21):7188–7196. Available from: http://dx.doi.org/10.1093/nar/gkm864.

Pruitt, K. D., Tatusova, T., and Maglott, D. R. 2007. NCBI reference sequences (RefSeq): a curated non-redundant sequence database of genomes, transcripts and proteins. *Nucleic Acids Research*, 35(suppl 1):D61–D65. Available from: http://dx.doi.org/10.1093/nar/gkl842.

Qin, J., Li, R., Raes, J., Arumugam, M., Burgdorf, K. S., Manichanh, C., Nielsen, T., Pons, N., Levenez, F., et al. 2010. A human gut microbial gene catalogue established by metagenomic sequencing. *Nature*, 464(7285):59–65. Available from: http://dx.doi.org/10.1038/nature08821.

Quevillon, E., Silventoinen, V., Pillai, S., Harte, N., Mulder, N., Apweiler, R., and Lopez, R. 2005. InterProScan: protein domains identifier. *Nucleic Acids Research*, 33(suppl 2):W116–W120. Available from: http://dx.doi.org/10.1093/nar/gki442.

R Development Core Team 2008. *R: A Language and Environment for Statistical Computing*. R Foundation for Statistical Computing, Vienna, Austria. ISBN 3-900051-07-0. Available from: http://www.R-project.org.

Rada, V. and Petr, J. 2000. A new selective medium for the isolation of glucose non-fermenting bifidobacteria from hen caeca. *Journal of Microbiological Methods*, 43(2):127–132. Available from: http://view.ncbi.nlm.nih.gov/pubmed/11121611.

Raghunathan, A., Ferguson, H. R., Bornarth, C. J., Song, W., Driscoll, M., and Lasken, R. S. 2005. Genomic DNA amplification from a single bacterium. *Applied and Environmental Microbiology*, 71(6):3342–3347. Available from: http://dx.doi.org/10.1128/aem.71.6.3342-3347.2005.

Rakoff-Nahoum, S. and Medzhitov, R. 2008. Innate immune recognition of the indigenous microbial flora. *Mucosal Immunology*, 1(1s):S10–S14. Available from: http://dx.doi.org/10.1038/mi.2008.49.

Rasheed, Z., Rangwala, H., and Barbara, D. 2013. 16S rRNA metagenome clustering and diversity estimation using locality sensitive hashing. *BMC Systems Biology*, 7(S4):S11+. Available from: http://dx.doi.org/10.1186/1752-0509-7-s4-s11.

Reinhardt, C., Bergentall, M., Greiner, T. U., Schaffner, F., Ostergren-Lunden, G., Petersen, L. C., Ruf, W., and Backhed, F. 2012. Tissue factor and PAR1 promote microbiota-induced intestinal vascular remodelling. *Nature*, 483(7391):627–631. Available from: http://dx.doi.org/10.1038/nature10893.

Renner, E. D. 1994. Development and clinical evaluation of an amplified flow cytometric fluoroimmunoassay for Clostridium difficile toxin A. *Cytometry*, 18(2):103–108. Available from: http://view.ncbi.nlm.nih.gov/pubmed/7924698.

Reyes, A., Haynes, M., Hanson, N., Angly, F. E., Heath, A. C., Rohwer, F., and Gordon, J. I. 2010. Viruses in the faecal microbiota of monozygotic twins and their mothers. *Nature*, 466(7304):334–338. Available from: http://dx.doi.org/10.1038/nature09199.

Reyes, A., Semenkovich, N. P., Whiteson, K., Rohwer, F., and Gordon, J. I. 2012. Going viral: next-generation sequencing applied to phage populations in the human gut. *Nature Reviews. Microbiology*, 10(9):607–617. Available from: http://view.ncbi.nlm.nih.gov/pubmed/22864264.

Reynolds, C. B., Emerson, J. E., de la Riva, L., Fagan, R. P., and Fairweather, N. F. 2011. The Clostridium difficile cell wall protein cwpv is antigenically variable between strains, but exhibits conserved aggregation-promoting function. *PLoS Pathog*, 7(4):e1002024+. Available from: http://dx.doi.org/10.1371/journal.ppat.1002024.

Roberts, R. J. and Murray, K. 1976. Restriction endonuclease. *Critical Reviews in Biochemistry and Molecular Biology*, 4(2):123–164. Available from: http://dx.doi.org/10.3109/10409237609105456.

Robinson, J. T., Thorvaldsdottir, H., Winckler, W., Guttman, M., Lander, E. S., Getz, G., and Mesirov, J. P. 2011. Integrative genomics viewer. *Nature Biotechnology*, 29(1):24–26. Available from: http://dx.doi.org/10.1038/nbt.1754.

Rodrigue, S., Malmstrom, R. R., Berlin, A. M., Birren, B. W., Henn, M. R., and Chisholm, S. W. 2009. Whole genome amplification and de novo assembly of single bacterial cells. *PLoS ONE*, 4(9):e6864+. Available from: http://dx.doi.org/10.1371/journal.pone.0006864.

Rohwer, F. 2003. Global phage diversity. *Cell*, 113(2):141+. Available from: http://dx.doi.org/10.1016/s0092-8674(03)00276-9.

Rojo, D., Gosalbes, M. J., Ferrari, R., Perez-Cobas, A. E., Hernandez, E., Oltra, R., Buesa, J., Latorre, A., Barbas, C., et al. 2015. Clostridium difficile heterogeneously impacts intestinal community architecture but drives stable metabolome responses. *The ISME Journal*. Available from: http://dx.doi.org/10.1038/ismej.2015.32.

Rolfe, R. D., Helebian, S., and Finegold, S. M. 1981. Bacterial interference between clostridium difficile and normal fecal flora. *Journal of Infectious Diseases*, 143(3):470–475. Available from: http://dx.doi.org/10.1093/infdis/143.3.470.

Ronaghi, M., Uhlén, M., and Nyrén, P. 1998. A sequencing method based on real-time pyrophosphate. *Science*, 281(5375):363–365. Available from: http://dx.doi.org/10.1126/science.281.5375.363.

Rupnik, M. 2008. Heterogeneity of large clostridial toxins: importance of Clostridium difficile toxinotypes. *FEMS Microbiology Reviews*, 32(3):541–555. Available from: http://dx.doi.org/10.1111/j.1574-6976.2008.00110.x.

Rupnik, M. 2010. Clostridium difficile toxinotyping. *Methods in Molecular Biology*, 646:67–76. Available from: http://view.ncbi.nlm.nih.gov/pubmed/20597003.

Rupnik, M., Brazier, J. S., Duerden, B. I., Grabnar, M., and Stubbs, S. L. J. 2001. Comparison of toxinotyping and PCR ribotyping of Clostridium difficile strains and description of novel toxinotypes. *Microbiology*, 147(2):439–447. Available from: http://mic.sgmjournals.org/content/147/2/439.abstract.

Rupnik, M., Wilcox, M. H., and Gerding, D. N. 2009. Clostridium difficile infection: new developments in epidemiology and pathogenesis. *Nature Reviews. Microbiology*, 7(7):526–536. Available from: http://dx.doi.org/10.1038/nrmicro2164.

Sambrook, J. and Russell, D. W. 2006a. Fragmentation of DNA by nebulization. *Cold Spring Harbor Protocols*, 2006(4):pdb.prot4539+. Available from: http://dx.doi.org/10.1101/pdb.prot4539.

Sambrook, J. and Russell, D. W. 2006b. Fragmentation of DNA by sonication. *CSH protocols*, 2006(4). Available from: http://view.ncbi.nlm.nih.gov/pubmed/22485919.

Sansonetti, P. J. 2010. To be or not to be a pathogen: that is the mucosally relevant question. *Mucosal Immunology*, 4(1):8–14. Available from: http://dx.doi.org/10.1038/mi.2010.77.

Sarkar, D., Gentleman, R., Lawrence, M., and Yao, Z. 2015. *chipseq: A package for analyzing chipseq data*. R package version 1.16.0.

Savage, D. C. 1977. Microbial ecology of the gastrointestinal tract. *Annual Review of Microbiology*, 31(1):107–133. Available from: http://dx.doi.org/10.1146/annurev.mi.31.100177.000543.

Schmieder, R. and Edwards, R. 2011. Quality control and preprocessing of metagenomic datasets. *Bioinformatics*, 27(6):863–864. Available from: http://dx.doi.org/10.1093/bioinformatics/btr026.

Schnorr, S. L., Candela, M., Rampelli, S., Centanni, M., Consolandi, C., Basaglia, G., Turroni, S., Biagi, E., Peano, C., et al. 2014. Gut microbiome of the hadza hunter-gatherers. *Nature Communications*, 5. Available from: http://dx.doi.org/10.1038/ncomms4654.

Schönhuber, W., Fuchs, B., Juretschko, S., and Amann, R. 1997. Improved sensitivity of whole-cell hybridization by the combination of horseradish peroxidase-labeled oligonucleotides and tyramide signal amplification. *Applied and Environmental Microbiology*, 63(8):3268–3273. Available from: http://aem.asm.org/content/63/8/3268.abstract.

Schubert, A. M., Rogers, M. A., Ring, C., Mogle, J., Petrosino, J. P., Young, V. B., Aronoff, D. M., and Schloss, P. D. 2014. Microbiome data distinguish patients with clostridium difficile infection and non-C. difficile-associated diarrhea from healthy controls. *mBio*, 5(3). Available from: http://dx.doi.org/10.1128/mbio.01021-14, doi:10.1128/mbio.01021-14.

Schwan, C., Stecher, B., Tzivelekidis, T., van Ham, M., Rohde, M., Hardt, W.-D. D., Wehland, J., and Aktories, K. 2009. Clostridium difficile toxin CDT induces formation of microtubule-based protrusions and increases adherence of bacteria. *PLoS Pathogens*, 5(10):e1000626+. Available from: http://dx.doi.org/10.1371/journal.ppat.1000626.

Sebaihia, M., Wren, B. W., Mullany, P., Fairweather, N. F., Minton, N., Stabler, R., Thomson, N. R., Roberts, A. P., Cerdeño Tárraga, A. M., et al. 2006. The multidrug-resistant human pathogen Clostridium difficile has a highly mobile, mosaic genome. *Nature Genetics*, 38(7):779–786. Available from: http://dx.doi.org/10.1038/ng1830.

Seekatz, A. M. and Young, V. B. 2014. Clostridium difficile and the microbiota. *The Journal of Clinical Investigation*, 124(10):4182–4189. Available from: http://view.ncbi.nlm.nih.gov/pubmed/25036699.

Segata, N., Izard, J., Waldron, L., Gevers, D., Miropolsky, L., Garrett, W. S., and Huttenhower, C. 2011. Metagenomic biomarker discovery and explanation. *Genome Biology*, 12(6):R60+. Available from: http://dx.doi.org/10.1186/gb-2011-12-6-r60.

Selinger, C. P., Bell, A., Cairns, A., Lockett, M., Sebastian, S., and Haslam, N. 2013. Probiotic VSL#3 prevents antibiotic-associated diarrhoea in a double-blind, randomized, placebo-controlled clinical trial. *Journal of Hospital Infection*, 84(2):159–165. Available from: http://dx.doi.org/10.1016/j.jhin.2013.02.019.

Sherr, E. B., Sherr, B. F., and Verity, P. G. 2002. Distribution and relation of total bacteria, active bacteria, bacterivory, and volume of organic detritus in atlantic continental shelf waters off cape hatteras NC, USA. *Deep Sea Research Part II: Topical Studies in Oceanography*, 49(20):4571–4585. Available from: http://dx.doi.org/10.1016/s0967-0645(02)00129-7.

Silva, F., Ferreira, S., Queiroz, J. a. A., and Domingues, F. C. 2011. Coriander (Coriandrum sativum L.) essential oil: its antibacterial activity and mode of action evaluated by flow cytometry. *Journal of Medical Microbiology*, 60(10):1479–1486. Available from: http://dx.doi.org/10.1099/jmm.0.034157-0.

Sims, D., Sudbery, I., Ilott, N. E., Heger, A., and Ponting, C. P. 2014. Sequencing depth and coverage: key considerations in genomic analyses. *Nature Reviews. Genetics*, 15(2):121–132. Available from: http://dx.doi.org/10.1038/nrg3642.

Sjögren, K., Engdahl, C., Henning, P., Lerner, U. H., Tremaroli, V., Lagerquist, M. K., Bäckhed, F., and Ohlsson, C. 2012. The gut microbiota regulates bone mass in mice. *Journal of Bone and Mineral Research*, 27(6):1357–1367. Available from: http://dx.doi.org/10.1002/jbmr.1588.

Skarstad, K., Steen, H. B., and Boye, E. 1983. Cell cycle parameters of slowly growing Escherichia coli B/r studied by flow cytometry. *Journal of Bacteriology*, 154(2):656–662. Available from: http://www.ncbi.nlm.nih.gov/pmc/articles/PMC217513/.

Skraban, J., Dzeroski, S., Zenko, B., Mongus, D., Gangl, S., and Rupnik, M. 2013. Gut microbiota patterns associated with colonization of different Clostridium difficile ribotypes. *PLoS ONE*, 8(2):e58005+. Available from: http://dx.doi.org/10.1371/journal.pone.0058005.

Solonenko, S., Espinoza, J. I., Alberti, A., Cruaud, C., Hallam, S., Konstantinidis, K., Tyson, G., Wincker, P., and Sullivan, M. 2013. Sequencing platform and library preparation choices impact viral metagenomes. *BMC Genomics*, 14(1):320+. Available from: http://dx.doi.org/10.1186/1471-2164-14-320.

Sommer, F. and Bäckhed, F. 2013. The gut microbiota–masters of host development and physiology. *Nature Reviews. Microbiology*, 11(4):227–238. Available from: http://view.ncbi.nlm.nih.gov/pubmed/23435359.

Song, K. P., Ow, S. E., Chang, S. Y., and Bai, X. L. 1999. Sequence analysis of a new open reading frame located in the pathogenicity locus of Clostridium difficile strain 8864. *FEMS Microbiology Letters*, 180(2):241–248. Available from: http://view.ncbi.nlm.nih.gov/pubmed/10556718.

Song, Y., Garg, S., Girotra, M., Maddox, C., von Rosenvinge, E. C., Dutta, A., Dutta, S., and Fricke, W. F. 2013. Microbiota dynamics in patients treated with fecal microbiota transplantation for recurrent Clostridium difficile infection. *PLoS ONE*, 8(11):e81330+. Available from: http://dx.doi.org/10.1371/journal.pone.0081330.

Sorek, R. and Cossart, P. 2010. Prokaryotic transcriptomics: a new view on regulation, physiology and pathogenicity. *Nature Reviews. Genetics*, 11(1):9–16. Available from: http://dx.doi.org/10.1038/nrg2695.

Sorg, J. A. and Sonenshein, A. L. 2009. Chenodeoxycholate is an inhibitor of clostridium difficile spore germination. *Journal of bacteriology*, 191(3):1115–1117. Available from: http://view.ncbi.nlm.nih.gov/pubmed/19060152.

Spits, C., Le Caignec, C., De Rycke, M., Van Haute, L., Van Steirteghem, A., Liebaers, I., and Sermon, K. 2006a. Optimization and evaluation of single-cell whole-genome multiple displacement amplification. *Human Mutation*, 27(5):496–503. Available from: http://dx.doi.org/10.1002/humu.20324.

Spits, C., Le Caignec, C., De Rycke, M., Van Haute, L., Van Steirteghem, A., Liebaers, I., and Sermon, K. 2006b. Whole-genome multiple displacement amplification from single cells. *Nature Protocols*, 1(4):1965–1970. Available from: http://dx.doi.org/10.1038/nprot.2006.326.

Stabler, R., He, M., Dawson, L., Martin, M., Valiente, E., Corton, C., Lawley, T., Sebaihia, M., Quail, M., et al. 2009. Comparative genome and phenotypic analysis of Clostridium difficile 027 strains provides insight into the evolution of a hypervirulent bacterium. *Genome Biology*, 10(9):R102+. Available from: http://dx.doi.org/10.1186/gb-2009-10-9-r102.

Stabler, R. A., Gerding, D. N., Songer, J. G., Drudy, D., Brazier, J. S., Trinh, H. T., Witney, A. A., Hinds, J., and Wren, B. W. 2006. Comparative phylogenomics of Clostridium difficile reveals clade specificity and microevolution of hypervirulent strains. *Journal of Bacteriology*, 188(20):7297–7305. Available from: http://dx.doi.org/10.1128/jb.00664-06.

Stang, A., Korn, K., Wildner, O., and Uberla, K. 2005. Characterization of virus isolates by particle-associated nucleic acid PCR. *Journal of Clinical Microbiology*, 43(2):716–720. Available from: http://dx.doi.org/10.1128/jcm.43.2.716-720.2005.

Stecher, B. and Hardt, W.-D. D. 2008. The role of microbiota in infectious disease. *Trends in Microbiology*, 16(3):107–114. Available from: http://dx.doi.org/10.1016/j.tim.2007.12.008.

Stecher, B., Maier, L., and Hardt, W.-D. 2013. 'Blooming' in the gut: how dysbiosis might contribute to pathogen evolution. *Nature Reviews Microbiology*, 11(4):277–284. Available from: http://dx.doi.org/10.1038/nrmicro2989.

Stepanauskas, R. and Sieracki, M. E. 2007. Matching phylogeny and metabolism in the uncultured marine bacteria, one cell at a time. *Proceedings of the National Academy of Sciences of the United States of America*, 104(21):9052–9057. Available from: http://dx.doi.org/10.1073/pnas.0700496104.

Stern, A., Mick, E., Tirosh, I., Sagy, O., and Sorek, R. 2012. CRISPR targeting reveals a reservoir of common phages associated with the human gut microbiome. *Genome Research*, 22(10):1985–1994. Available from: http://dx.doi.org/10.1101/gr.138297.112.

Strateva, T. and Yordanov, D. 2009. Pseudomonas aeruginosa - a phenomenon of bacterial resistance. *Journal of Medical Microbiology*, 58(Pt 9):1133–1148. Available from: http://dx.doi.org/10.1099/jmm.0.009142-0.

Stubbs, S., Rupnik, M., Gibert, M., Brazier, J., Duerden, B., and Popoff, M. 2000. Production of actin-specific ADP-ribosyltransferase (binary toxin) by strains of Clostridium difficile. *FEMS Microbiology Letters*, 186(2):307–312. Available from: http://dx.doi.org/10.1111/j.1574-6968.2000.tb09122.x.

Sutera, V., Caspar, Y., Boisset, S., and Maurin, M. 2014. A new dye uptake assay to test the activity of antibiotics against intracellular Francisella tularensis. *Frontiers in Cellular and Infection Microbiology*, 4. Available from: http://view.ncbi.nlm.nih.gov/pubmed/24672776.

Suzuki, R. and Shimodaira, H. 2014. *pvclust: Hierarchical Clustering with P-Values via Multiscale Bootstrap Resampling*. R package version 1.3-2. Available from: http://CRAN.R-project.org/package=pvclust.

Swan, B. K., Martinez-Garcia, M., Preston, C. M., Sczyrba, A., Woyke, T., Lamy, D., Reinthaler, T., Poulton, N. J., Dashiell, et al. 2011. Potential for chemolithoautotrophy among ubiquitous bacteria lineages in the dark ocean. *Science*, 333(6047):1296–1300. Available from: http://dx.doi.org/10.1126/science.1203690.

Syed, F., Grunenwald, H., and Caruccio, N. 2009. Next-generation sequencing library preparation: simultaneous fragmentation and tagging using in vitro transposition. *Nature Methods*, 6(11). Available from: http://dx.doi.org/10.1038/nmeth.f.272.

Tanner, H. E., Hardy, K. J., and Hawkey, P. M. 2010. Coexistence of multiple multilocus variable-number tandem-repeat analysis subtypes of Clostridium difficile PCR ribotype 027 strains within fecal specimens. *Journal of Clinical Microbiology*, 48(3):985–987. Available from: http://dx.doi.org/10.1128/jcm.02012-09.

Tasteyre, A., Barc, M. C., Collignon, A., Boureau, H., and Karjalainen, T. 2001. Role of FliC and FliD flagellar proteins of Clostridium difficile in adherence and gut colonization. *Infection and Immunity*, 69(12):7937–7940. Available from: http://dx.doi.org/10.1128/iai.69.12.7937-7940.2001.

Tasteyre, A., Karjalainen, T., Avesani, V., Delmée, M., Collignon, A., Bourlioux, P., and Barc, M. C. 2000. Phenotypic and genotypic diversity of the flagellin gene (fliC) among Clostridium difficile isolates from different serogroups. *Journal of Clinical Microbiology*, 38(9):3179–3186. Available from: http://view.ncbi.nlm.nih.gov/pubmed/10970353.

Tatusova, T., Ciufo, S., Fedorov, B., O'Neill, K., and Tolstoy, I. 2014. RefSeq microbial genomes database: new representation and annotation strategy. *Nucleic Acids Research*, 42(Database issue). Available from: http://view.ncbi.nlm.nih.gov/pubmed/24316578.

Tazzari, P. L. L., Ricci, F., Carnicelli, D., Caprioli, A., Tozzi, A. E., Rizzoni, G., Conte, R., and Brigotti, M. 2004. Flow cytometry detection of Shiga toxins in the blood from children with hemolytic uremic syndrome. *Cytometry. Part B, Clinical cytometry*, 61(1):40–44. Available from: http://view.ncbi.nlm.nih.gov/pubmed/15351981.

Teeling, H., Waldmann, J., Lombardot, T., Bauer, M., and Glöckner, F. O. O. 2004. TETRA: a web-service and a stand-alone program for the analysis and comparison of tetranucleotide usage patterns in DNA sequences. *BMC Bioinformatics*, 5(1):163+. Available from: http://dx.doi.org/10.1186/1471-2105-5-163.

Telenius, H., Carter, N. P., Bebb, C. E., Nordenskjöld, M., Ponder, B. A., and Tunnacliffe, A. 1992. Degenerate oligonucleotide-primed PCR: general amplification of target DNA by a single degenerate primer. *Genomics*, 13(3):718–725. Available from: http://view.ncbi.nlm.nih.gov/pubmed/1639399.

Theriot, C. M., Koenigsknecht, M. J., Carlson, P. E., Hatton, G. E., Nelson, A. M., Li, B., Huffnagle, G. B., Z Li, J., and Young, V. B. 2014. Antibiotic-induced shifts in the mouse gut microbiome and metabolome increase susceptibility to Clostridium difficile infection. *Nature Communications*, 5. Available from: http://view.ncbi.nlm.nih.gov/pubmed/24445449.

Thurber, R. V., Haynes, M., Breitbart, M., Wegley, L., and Rohwer, F. 2009. Laboratory procedures to generate viral metagenomes. *Nature Protocols*, 4(4):470–483. Available from: http://dx.doi.org/10.1038/nprot.2009.10.

Tonooka, T., Sakata, S., Kitahara, M., Hanai, M., Ishizeki, S., Takada, M., Sakamoto, M., and Benno, Y. 2005. Detection and quantification of four species of the genus Clostridium in infant feces. *Microbiology and Immunology*, 49(11):987–992. Available from: http://view.ncbi.nlm.nih.gov/pubmed/16301809.

Trompette, A., Gollwitzer, E. S., Yadava, K., Sichelstiel, A. K., Sprenger, N., Ngom-Bru, C., Blanchard, C., Junt, T., Nicod, L. P., et al. 2014. Gut microbiota metabolism of dietary fiber influences allergic airway disease and hematopoiesis. *Nature Medicine*, 20(2):159–166. Available from: http://dx.doi.org/10.1038/nm.3444.

Troutt, A. B., McHeyzer-Williams, M. G., Pulendran, B., and Nossal, G. J. 1992. Ligation-anchored PCR: a simple amplification technique with single-sided specificity. *Proceedings of the National Academy of Sciences of the United States of America*, 89(20):9823–9825. Available from: http://dx.doi.org/10.1073/pnas.89.20.9823.

Turnbaugh, P. J., Ley, R. E., Mahowald, M. A., Magrini, V., Mardis, E. R., and Gordon, J. I. 2006. An obesity-associated gut microbiome with increased capacity for energy harvest. *Nature*, 444(7122):1027–1031. Available from: http://dx.doi.org/10.1038/nature05414.

Twine, S. M., Reid, C. W., Aubry, A., McMullin, D. R., Fulton, K. M., Austin, J., and Logan, S. M. 2009. Motility and flagellar glycosylation in Clostridium difficile. *Journal of Bacteriology*, 191(22):7050–7062. Available from: http://dx.doi.org/10.1128/jb.00861-09.

Ueckert, J. E., Nebe von Caron, G., Bos, A. P., and ter Steeg, P. F. 1997. Flow cytometric analysis of Lactobacillus plantarum to monitor lag times, cell division and injury. *Letters in Applied Microbiology*, 25(4):295–299. Available from: http://view.ncbi.nlm.nih.gov/pubmed/9351280.

van den Berg, R. J., Ameen, H. A. A., Furusawa, T., Claas, E. C. C., van der Vorm, E. R., and Kuijper, E. J. 2005. Coexistence of multiple PCR-ribotype strains of Clostridium difficile in faecal samples limits epidemiological studies. *Journal of Medical Microbiology*, 54(Pt 2):173–179. Available from: http://view.ncbi.nlm.nih.gov/pubmed/15673513.

van den Berg, R. J., Schaap, I., Templeton, K. E., Klaassen, C. H., and Kuijper, E. J. 2007. Typing and subtyping of Clostridium difficile isolates by using multiple-locus variable-number tandem-repeat analysis. *Journal of Clinical Microbiology*, 45(3):1024–1028. Available from: http://dx.doi.org/10.1128/jcm.02023-06.

van der Waaij, L. A., Kroese, F. G., Visser, A., Nelis, G. F., Westerveld, B. D., Jansen, P. L., and Hunter, J. O. 2004. Immunoglobulin coating of faecal bacteria in inflammatory bowel disease. *European journal of gastroenterology & hepatology*, 16(7):669–674. Available from: http://view.ncbi.nlm.nih.gov/pubmed/15201580.

van Eijk, E., Anvar, S. Y. Y., Browne, H. P., Leung, W. Y. Y., Frank, J., Schmitz, A. M., Roberts, A. P., and Smits, W. K. K. 2015. Complete genome sequence of the Clostridium difficile laboratory strain 630 delta erm reveals differences from strain 630, including translocation of the mobile element CTn5. *BMC genomics*, 16(1):31+. Available from: http://dx.doi.org/10.1186/s12864-015-1252-7.

Van Wey, A. S., Cookson, A. L., Roy, N. C., McNabb, W. C., Soboleva, T. K., and Shorten, P. R. 2011. Bacterial biofilms associated with food particles in the human large bowel. *Molecular nutrition & food research*, 55(7):969–978. Available from: http://view.ncbi.nlm.nih.gov/pubmed/21638777.

Varga, J. J., Nguyen, V., O'Brien, D. K., Rodgers, K., Walker, R. A., and Melville, S. B. 2006. Type IV pili-dependent gliding motility in the Gram-positive pathogen Clostridium perfringens and other Clostridia. *Molecular Microbiology*, 62(3):680–694. Available from: http://view.ncbi.nlm.nih.gov/pubmed/16999833.

Vazquez Castellanos, J., Garcia Lopez, R., Perez Brocal, V., Pignatelli, M., and Moya, A. 2014. Comparison of different assembly and annotation tools on analysis of simulated viral metagenomic communities in the gut. *BMC Genomics*, 15(1):37+. Available from: http://dx.doi.org/10.1186/1471-2164-15-37.

Vazquez-Castellanos, J. F., Serrano-Villar, S., Latorre, A., Artacho, A., Ferrus, M. L., Madrid, N., Vallejo, A., Sainz, T., Martinez-Botas, J., et al. 2014. Altered metabolism of gut microbiota contributes to chronic immune activation in HIV-infected individuals. *Mucosal Immunology*. Available from: http://dx.doi.org/10.1038/mi.2014.107.

Vedantam, G., Clark, A., Chu, M., McQuade, R., Mallozzi, M., and Viswanathan, V. K. 2012. Clostridium difficile infection: toxins and non-toxin virulence factors, and their contributions to disease establishment and host response. *Gut Microbes*, 3(2):121–134. Available from: http://view.ncbi.nlm.nih.gov/pubmed/22555464.

Venter, J. C., Remington, K., Heidelberg, J. F., Halpern, A. L., Rusch, D., Eisen, J. A., Wu, D., Paulsen, I., Nelson, K. E., et al. 2004. Environmental genome shotgun sequencing of the Sargasso Sea. *Science*, 304(5667):66–74. Available from: http://dx.doi.org/10.1126/science.1093857.

Vestvik, N., Rønneseth, A., Kalgraff, C. A. K., Winther-Larsen, H. C., Wergeland, H. I., and Haugland, G. T. 2013. Francisella noatunensis subsp. noatunensis replicates within atlantic cod (Gadus morhua L.) leucocytes and inhibits respiratory burst activity. *Fish & Shellfish Immunology*, 35(3):725–733. Available from: http://dx.doi.org/10.1016/j.fsi.2013.06.002.

Vieites, J. M., Guazzaroni, M.-E., Beloqui, A., Golyshin, P. N., and Ferrer, M. 2009. Metagenomics approaches in systems microbiology. *FEMS Microbiology Reviews*, 33(1):236–255. Available from: http://dx.doi.org/10.1111/j.1574-6976.2008.00152.x.

Vimr, E. R., Kalivoda, K. A., Deszo, E. L., and Steenbergen, S. M. 2004. Diversity of microbial sialic acid metabolism. *Microbiology and Molecular Biology Reviews*, 68(1):132–153. Available from: http://dx.doi.org/10.1128/mmbr.68.1.132-153.2004.

Vives-Rego, J., Lebaron, P., and Caron, G. N.-v. 2000. Current and future applications of flow cytometry in aquatic microbiology. *FEMS Microbiology Reviews*, 24(4):429–448. Available from: http://dx.doi.org/10.1111/j.1574-6976.2000.tb00549.x.

Vlková, E., Nevoral, J., Jencikova, B., Kopecný, J., Godefrooij, J., Trojanová, I., and Rada, V. 2005. Detection of infant faecal bifidobacteria by enzymatic methods. *Journal of Microbiological Methods*, 60(3):365–373. Available from: http://view.ncbi.nlm.nih.gov/pubmed/15649538.

Vlček, v. and Pačes, V. 1986. Nucleotide sequence of the late region of Bacillus phage phi29 completes the 19285-bp sequence of phi29 genome. Comparison with the homologous sequence of phage PZA. *Gene*, 46(2-3):215–225. Available from: http://dx.doi.org/10.1016/0378-1119(86)90406-3.

von Eiff, C., Herrmann, M., and Peters, G. 1995. Antimicrobial susceptibilities of Stomatococcus mucilaginosus and of Micrococcus spp. *Antimicrobial Agents and Chemotherapy*, 39(1):268–270. Available from: http://view.ncbi.nlm.nih.gov/pubmed/7695321.

von Nussbaum, F., Brands, M., Hinzen, B., Weigand, S., and Häbich, D. 2006. Antibacterial natural products in medicinal chemistry-exodus or revival? *Angewandte Chemie International Edition*, 45(31):5072–5129. Available from: http://dx.doi.org/10.1002/anie.200600350.

Wagner, J., Maksimovic, J., Farries, G., Sim, W. H., Bishop, R. F., Cameron, D. J., Catto-Smith, A. G., and Kirkwood, C. D. 2013. Bacteriophages in gut samples from pediatric Crohn's disease patients: metagenomic analysis using 454 pyrosequencing. *Inflammatory Bowel Diseases*, 19(8):1598–1608. Available from: http://view.ncbi.nlm.nih.gov/pubmed/23749273.

Wagner, R. 1994. The regulation of ribosomal RNA synthesis and bacterial cell growth. *Archives of Microbiology*, 161(2):100–109. Available from: http://dx.doi.org/10.1007/bf00276469.

Waligora, A. J., Hennequin, C., Mullany, P., Bourlioux, P., Collignon, A., and Karjalainen, T. 2001. Characterization of a cell surface protein of Clostridium difficile with adhesive properties. *Infection and Immunity*, 69(4):2144–2153. Available from: http://dx.doi.org/10.1128/iai.69.4.2144-2153.2001.

Walker, A. S., Eyre, D. W., Wyllie, D. H., Dingle, K. E., Harding, R. M., O'Connor, L., Griffiths, D., Vaughan, A., Finney, J., et al. 2012. Characterisation of Clostridium difficile hospital ward-based transmission using extensive epidemiological data and molecular typing. *PLoS Medicine*, 9(2):e1001172+. Available from: http://dx.doi.org/10.1371/journal.pmed.1001172.

Waller, A. S., Yamada, T., Kristensen, D. M., Kultima, J. R., Sunagawa, S., Koonin, E. V., and Bork, P. 2014. Classification and quantification of bacteriophage taxa in human gut metagenomes. *The ISME Journal*, 8(7):1391–1402. Available from: http://dx.doi.org/10.1038/ismej.2014.30.

Wang, Y., Hammes, F., Boon, N., Chami, M., and Egli, T. 2009. Isolation and characterization of low nucleic acid (LNA)-content bacteria. *The ISME Journal*, 3(8):889–902. Available from: http://dx.doi.org/10.1038/ismej.2009.46.

Wang, Y., Hammes, F., Boon, N., and Egli, T. 2007. Quantification of the filterability of freshwater bacteria through 0.45, 0.22, and 0.1 $\mu$m pore size filters and shape-dependent enrichment of filterable bacterial communities. *Environmental Science and Technology*, 41(20):7080–7086. Available from: http://dx.doi.org/10.1021/es0707198.

White, R., Blainey, P., Fan, H. C., and Quake, S. 2009. Digital PCR provides sensitive and absolute calibration for high throughput sequencing. *BMC Genomics*, 10(1):116+. Available from: http://dx.doi.org/10.1186/1471-2164-10-116.

Wickham, H. 2009. *ggplot2: elegant graphics for data analysis*. Springer New York. Available from: http://had.co.nz/ggplot2/book.

Willems, R. J., Top, J., van Santen, M., Robinson, D. A., Coque, T. M., Baquero, F., Grundmann, H., and Bonten, M. J. 2005. Global spread of vancomycin-resistant Enterococcus faecium from distinct nosocomial genetic complex. *Emerging Infectious Diseases*, 11(6):821–828. Available from: http://view.ncbi.nlm.nih.gov/pubmed/15963275.

Williamson, S. J., Allen, L. Z., Lorenzi, H. A., Fadrosh, D. W., Brami, D., Thiagarajan, M., McCrow, J. P., Tovchigrechko, A., Yooseph, S., and Venter, J. C. 2012. Metagenomic exploration of viruses throughout the Indian Ocean. *PLoS ONE*, 7(10):e42047+. Available from: http://dx.doi.org/10.1371/journal.pone.0042047.

Willner, D., Furlan, M., Haynes, M., Schmieder, R., Angly, F. E., Silva, J., Tammadoni, S., Nosrat, B., Conrad, D., and Rohwer, F. 2009. Metagenomic analysis of respiratory tract DNA viral communities in cystic fibrosis and non-cystic fibrosis individuals. *PLoS ONE*, 4(10):e7370+. Available from: http://dx.doi.org/10.1371/journal.pone.0007370.

Woese, C. R. and Fox, G. E. 1977. Phylogenetic structure of the prokaryotic domain: the primary kingdoms. *Proceedings of the National Academy of Sciences of the United States of America*, 74(11):5088–5090. Available from: http://dx.doi.org/10.1073/pnas.74.11.5088.

Wong, K. H. H., Jin, Y., and Moqtaderi, Z. 2013. Multiplex Illumina sequencing using DNA barcoding. *Current protocols in molecular biology / edited by Frederick M. Ausubel ... [et al.]*, Chapter 7. Available from: http://view.ncbi.nlm.nih.gov/pubmed/23288465.

Wooley, J. C., Godzik, A., and Friedberg, I. 2010. A primer on metagenomics. *PLoS Computational Biology*, 6(2):e1000667+. Available from: http://dx.doi.org/10.1371/journal.pcbi.1000667.

Wostmann, B. S. 1981. The germfree animal in nutritional studies. *Annual Review of Nutrition*, 1:257–279. Available from: http://view.ncbi.nlm.nih.gov/pubmed/6764717.

Woyke, T., Sczyrba, A., Lee, J., Rinke, C., Tighe, D., Clingenpeel, S., Malmstrom, R., Stepanauskas, R., and Cheng, J.-F. 2011. Decontamination of MDA reagents for single cell whole genome amplification. *PLoS ONE*, 6(10):e26161+. Available from: http://dx.doi.org/10.1371/journal.pone.0026161.

Wu, G. D., Chen, J., Hoffmann, C., Bittinger, K., Chen, Y.-Y., Keilbaugh, S. A., Bewtra, M., Knights, D., Walters, W. A., et al. 2011. Linking long-term dietary patterns with gut microbial enterotypes. *Science*, 334(6052):105–108. Available from: http://dx.doi.org/10.1126/science.1208344.

Xiao, Y., Gordon, A., and Yakovlev, A. 2006. A C++ Program for the Cramér-Von Mises Two-sample test. *Journal of Statistical Software*, 17(8):1–15. Available from: http://www.jstatsoft.org/v17/i08.

Xiong, J., Hynes, M. F., Ye, H., Chen, H., Yang, Y., M'zali, F., and Hawkey, P. M. 2006. bla(IMP-9) and its association with large plasmids carried by Pseudomonas aeruginosa isolates from the People's Republic of China. *Antimicrobial Agents and Chemotherapy*, 50(1):355–358. Available from: http://dx.doi.org/10.1128/aac.50.1.355-358.2006.

Yano, J. M., Yu, K., Donaldson, G. P., Shastri, G. G., Ann, P., Ma, L., Nagler, C. R., Ismagilov, R. F., Mazmanian, S. K., and Hsiao, E. Y. 2015. Indigenous bacteria from the gut microbiota regulate host serotonin biosynthesis. *Cell*, 161(2):264–276. Available from: http://dx.doi.org/10.1016/j.cell.2015.02.047.

Yoon, H. S., Price, D. C., Stepanauskas, R., Rajah, V. D., Sieracki, M. E., Wilson, W. H., Yang, E. C., Duffy, S., and Bhattacharya, D. 2011. Single-cell genomics reveals organismal interactions in uncultivated marine protists. *Science*, 332(6030):714–717. Available from: http://dx.doi.org/10.1126/science.1203163.

Youngster, I., Russell, G. H., Pindar, C., Ziv-Baran, T., Sauk, J., and Hohmann, E. L. 2014. Oral, capsulized, frozen fecal microbiota transplantation for relapsing clostridium difficile infection. *JAMA*, 312(17):1772–1778. Available from: http://view.ncbi.nlm.nih.gov/pubmed/25322359.

Zhang, K., Martiny, A. C., Reppas, N. B., Barry, K. W., Malek, J., Chisholm, S. W., and Church, G. M. 2006. Sequencing genomes from single cells by polymerase cloning. *Nature Biotechnology*, 24(6):680–686. Available from: http://dx.doi.org/10.1038/nbt1214.

Zhang, T., Breitbart, M., Lee, W. H., Run, J.-Q., Wei, C. L., Soh, S. W., Hibberd, M. L., Liu, E. T., Rohwer, F., and Ruan, Y. 2005. Rna viral community in human feces: Prevalence of plant pathogenic viruses. *PLoS Biology*, 4(1):e3+. Available from: http://dx.doi.org/10.1371/journal.pbio.0040003.

Zheng, Z., Advani, A., Melefors, O., Glavas, S., Nordström, H., Ye, W., Engstrand, L., and Andersson, A. F. 2010. Titration-free massively parallel pyrosequencing using trace amounts of starting material. *Nucleic Acids Research*, 38(13):e137. Available from: http://dx.doi.org/10.1093/nar/gkq332.

Zheng, Z., Advani, A., Melefors, O., Glavas, S., Nordstrom, H., Ye, W., Engstrand, L., and Andersson, A. F. 2011. Titration-free 454 sequencing using Y adapters. *Nature Protocols*, 6(9):1367–1376. Available from: http://dx.doi.org/10.1038/nprot.2011.369.

Zhulidov, P. A., Bogdanova, E. A., Shcheglov, A. S., Vagner, L. L., Khaspekov, G. L., Kozhemyako, V. B., Matz, M. V., Meleshkevitch, E., Moroz, L. L., et al. 2004. Simple cdna normalization using Kamchatka crab duplex-specific nuclease. *Nucleic Acids Research*, 32(3):e37+. Available from: http://dx.doi.org/10.1093/nar/gnh031.

Zong, C., Lu, S., Chapman, A. R., and Xie, X. S. 2012. Genome-wide detection of single-nucleotide and copy-number variations of a single human cell. *Science*, 338(6114):1622–1626. Available from: http://dx.doi.org/10.1126/science.1229164.

Chapter 15

# Glossary

# Glossary

**8HQ** 8-Hydroxyquinoline. It is an organic compound, a monoprotic bidentate chelating agent. 74, 75, 77, 80, 81

**ATP** Adenosine 5'-Triphosphate. It is a substrate for many ATP-dependent enzyme systems, as DNA ligation. 186, 195

**CD** Crohn's disease. It is a form of the inflammatory bowel disease. 28, 29

**CDI** *Clostridium difficile* infection. This disease is actually an inflammation of the large intestine. *C. difficile* releases toxins that may cause bloating and diarrhea, with abdominal pain, which may become severe. 50, 51, 56, 66, 72, 80, 89, 91

**Cp** The number of cycles which are needed to generate enough molecules that have enough fluorescence to be detected by the qPCR system. 144, 190

**CTAB** Cetyltrimethylammonium bromide. It is a cationic surfactant used in the extraction of DNA. 183

**dNTP** 2'-Deoxynucleotide Triphosphates mix containing deoxyadenosine triphosphate (dATP), deoxyguanosine triphosphate (dGTP), deoxycytidine triphosphate (dCTP), deoxythymidine triphosphate (dTTP). 186, 195

**emPCR** Emulsion PCR. It isolates individual DNA molecules along with primer-coated beads in aqueous droplets within an oil phase. The PCR then coats each bead with clonal copies of the DNA molecule followed by immobilization for later DNA sequencing. 117, 121, 130

**FACS** Fluorescent activated cell sorting. It is a specialized type of flow cytometry. It provides a method for sorting a heterogeneous mixture of biological cells into two or more containers, one cell at a time, based upon the specific light scattering and fluorescent characteristics of each cell. 41, 50, 52, 91, 98, 104, 107, 110, 117, 132, 138, 140, 142, 152

**FC** Flow cytometry. It is a laser-based, biophysical technology employed in cell counting, cell sorting, biomarker detection and protein engineering, by suspending cells in a stream of fluid and passing them by an electronic detection apparatus. It allows simultaneous multiparametric analysis of the physical and chemical characteristics of up to thousands of particles per second. 33, 34, 41, 53, 70, 74, 76, 77, 81, 93, 138, 140, 150

**FISH** Fluorescence in situ hybridization. It is a cytogenetic technique that is used to detect and localize the presence or absence of specific DNA sequences on chromosomes. FISH uses fluorescent probes that bind to only complementary parts of the genome. Fluorescence microscopy or flow cytometry can be used to find out where the fluorescent probe is bound to the chromosomes. 31, 35, 36, 74, 76

**GI** Gastrointestinal tract. 25

**IBD** Inflammatory bowel disease. 29

**Klenow Fragment** Klenow Fragment (3'→ 5' exo-) is an N-terminal truncation of DNA Polymerase I which retains polymerase activity, but has lost the 5'→ 3' exonuclease activity and has mutations (D355A, E357A) which abolish the 3'→5' exonuclease activity. 186, 195

**LB** Lysogeny broth. It is a nutritionally rich medium, which is primarily used for the growth of bacteria, consiting usually from 10 g tryptone, 5 g yeast extract and 10 g NaCl per liter of water. 118, 141

**MDA** Multiple Displacement Amplification. It is a non-PCR based DNA amplification technique for whole genome amplification. This method can rapidly amplify minute amounts of DNA samples to a reasonable quantity for genomic analysis. The reaction starts by annealing random hexamer primers to the template: DNA synthesis is carried out by a high fidelity enzyme, preferentially phi29 DNA polymerase, at a constant temperature. 116–118, 130, 132, 138

**MGB** Minor groove binder probes are DNA probes with conjugated minor groove binder groups form extremely stable duplexes with single-stranded DNA targets, allowing shorter probes to be used for hybridization based assays. 116, 120, 190

**MIC** Minimum inhibitory concentration. It is the lowest concentration of an antimicrobial that will inhibit the visible growth of a microorganism after overnight incubation. 75, 77, 80

**MID** Multiplex identifiers tags. They allow identifying multiple libraries so that they may be multiplexed for sequencing on one sequencing plate. 120, 125, 186, 191, 207

**MLST** Multilocus sequence typing. 89, 91

**ORF** Open reading frame. An open reading frame is essentially the same as genes. They are also referred to as protein-coding regions. ORFs are identified in genomes by several algorithms, most of which search for stretches of DNA sequence without stop codons. 27, 144, 147

**OTU** Operational Taxonomic Units. Operational definition of a species or group of species often used when only DNA sequence data is available. 62

**PBS** Phosphate-buffered saline. A buffer commonly used in biological research. The osmolarity and ion concentrations of the solutions match those of the human body (isotonic). 183

**PEG** Polyethylene glycol. It is a polyether compound, a hydrophilic polymer, with many applications from industrial manufacturing to medicine. 150, 188

**PTP** Pico titer plate. The sequencing plate of 454 sequencing platform. 120, 130

**qPCR** Quantitative PCR. It is a real-time polymerase chain reaction, which is used to amplify and simultaneously detect or quantify a targeted DNA molecule. For the DNA quantification can be employed (1) non-specific fluorescent dyes that intercalate with any double-stranded DNA or (2) sequence-specific oligonucleotides that are labelled with a fluorescent reporter which permits detection only after hybridization with its complementary sequence. 98, 116, 117, 120, 130

**SDS** Sodium dodecyl suphate. It is an anionic surfactant used in many cleaning and hygiene products. 76, 183

**SNP** Single Nucleotide Polymorphisms. It a DNA sequence variation occurring commonly within a population in which a single nucleotide - A, T, C or G - in the genome differs. 89, 107

**TBS** Tris-buffered saline. It is a buffer used in some biochemical techniques to maintain the pH within a relatively narrow range. TBS has many uses because it is isotonic and non-toxic. 141, 188

**UC** Ulcerative colitis. It is a form of inflammatory bowel disease. Ulcerative colitis is a form of colitis, a disease of the colon, that includes characteristic ulcers, or open sores. The main symptom of active disease is usually constant diarrhea mixed with blood, of gradual onset. 29

**WGA** Whole genome amplification. It is a way of increasing the amount of limited DNA samples where DNA quantities are limited but many analyses or high amounts of input DNA are required. 117, 131, 137, 140, 150, 152

VNIVERSITAT DE VALÈNCIA

Valencia, 2016